2019

The hippocampus and entorhinal cortex map events across space and time

BOSTON UNIVERSITY

SCHOOL OF MEDICINE

Dissertation

THE HIPPOCAMPUS AND ENTORHINAL CORTEX MAP EVENTS ACROSS SPACE AND TIME

by

JOHN HODGETTS BLADON

B.A., Bates College, 2010
M.A. Boston University School of Medicine, 2013

Submitted in partial fulfillment of the

requirements for the degree of

Doctor of Philosophy

2019

Approved by

First Reader _____

Marc Howard, Ph.D.
Professor of Psychological and Brain Sciences

Second Reader _____

Chantal Stern, Ph.D.
Professor of Psychological and Brain Sciences

Third Reader _____

Steve Ramirez, Ph.D.
Assistant Professor of Psychological and Brain Sciences

Failure is success in progress.

-Albert Einstein

DEDICATION

I would like to dedicate this work to my greatest mentor, the late Dr. Howard Eichenbaum.

You are one of my greatest role models.

ACKNOWLEDGMENTS

First, I would like to thank my wife Eliza Bladon. You have supported me through this process in so many ways; it is for you what I achieve. I would also like to thank Marc Howard and Mike Hasselmo for their mentorship and their help with interpreting the complicated datasets that comprise this dissertation. I would also like to thank my current and past peers Chris K, Nat K, Dan O, Dan S, Ryan P, Will M, Sam L, Sam M, Catherine M, and Dave S for all the things you do to make the Eichenbaum lab a stimulating and productive place. Not many labs are afforded this level of camaraderie, expertise, and academic rigor. Last and certainly not least, I would like to thank the team of undergraduate students I have worked with over the years. You are truly the unsung heroes of research, and you inspire me more than you know.

THE HIPPOCAMPUS AND ENTORHINAL CORTEX MAP EVENTS ACROSS SPACE AND TIME

JOHN HODGETTS BLADON

Boston University School of Medicine, 2019

Major Professor: Marc Howard, Ph.D. Professor of Psychological and Brain Sciences

ABSTRACT

The medial temporal lobe supports the encoding of new facts and experiences, and organizes them so that we can infer relationships and make unique associations during new encounters. Evidence from studies on humans and animals suggest that the hippocampus is specifically required for our ability to form these internal representations of the world. The mechanism by which the hippocampus performs this function remains unclear, but electrophysiological recordings in the hippocampus support a general model. One component of this model suggests that the cortex represents places, times, and events separately, and then the hippocampus generates conjunctive representations that connect the three. According to this hypothesis, the hippocampus binds places and events to an existing relational structure. This dissertation explores how item and place associations develop within cortex, and then examines the relational structure that organizes these events within the hippocampus. The first study suggests that contrary to previous models, events and places are bound together outside of the hippocampus in the entorhinal cortex and perirhinal cortex. The second study shows that this relational scaffold may be embodied by a continually changing code that permits both the association and separation

of information across the continuum of time. The final study suggests that the hippocampus and entorhinal cortex contain qualitatively different time codes that may act in a complementary fashion to bind events and places and relate them across time. Overall, these studies support a theory wherein time is encoded in a range of brain regions that also contain conjunctive item and position information. In these regions, conjunctive representations of items, places, and times are organized not only by their perceptual similarity but also their temporal proximity.

TABLE OF CONTENTS

LIST OF TABLES

LIST OF FIGURES

LIST OF ILLUSTRATIONS

LIST OF ABBREVIATIONS

ANOVA ..... Analysis Of Variance

BU ..... Boston University

CA1 ..... Cornu Ammonis 1

CA2 ..... Cornu Ammonis 2

CA3 ..... Cornu Ammonis 3

DG ..... Dentate Gyrus

EC ..... Entorhinal Cortex

dHPC ..... dorsal Hippocampus

fMRI ..... function Magnetic Resonance Imaging

GABA ..... gamma-aminobutyric-acid

Hz ..... Hertz

im ..... Intramuscular

ip ..... Intraperitoneal

kg ..... kilogram

kHz ..... kilohertz

LDA ..... Linear Discriminant Analysis

LEC ..... Lateral Entorhinal Cortex

LED ..... Light Emitting Diode

LTP ..... Long Term Potentiation

MEC ..... Medial Entorhinal Cortex

mg ..... Milligrams

ml ..... Milliliters

ms ..... Milliseconds

MTL ..... Medial Temporal Lobe

NMDA ..... N-methyl-D-aspartate receptor

PHC ..... Parahippocampal Cortex

pp ..... Perforant Pathway

PRC ..... Perirhinal Cortex

PV+ ..... Parvalbumin Positive

ROC ..... Receiver Operating Characteristics

RSA ..... Representational Similarity Analysis

SI ..... Selectivity Index

SOM+ ..... Somatostatin Positive

ta ..... Temporoammonic

µA ..... micro-Amps

µm ..... Microns

vHPC ..... ventral Hippocampus

Chapter 1. General Introduction

1.1 The taxonomy of memory

Our understanding of the world around us is composed of the accumulated knowledge and experience that we have gained throughout our lives. Our worldview and our identity are comprised of these memories that come in the form of associations, skills, facts, and beliefs about the stimuli we constantly experience, as well as autobiographical memories. Our autobiographical memories, also known as episodic memories contain perhaps the most detailed and salient experiences we have and can be consciously conjured in great detail. Indeed it is an incredible feat to perform 'mental time travel' and conjure the myriad details of a past experience from a prompt as simple as the smell of a perfume.

Our long-term memories have historically been described in two basic forms: first are those memories that we consciously recall and can verbalize, such as facts, concepts and past experiences. The second form of memories are those skills and habits that cannot be easily articulated. The first clear evidence towards a dissociation of these two types of long-term memory came after the famous surgery on patient H.M. by William Scoville, and the subsequent study by Brenda Milner (Caparelli et al., 2012). HM received bilateral removal of major portions of his medial temporal lobe, including the anterior hippocampus and rhinal cortices in an attempt to cure intractable epilepsy. After his surgery, H.M. was left frozen in time: he was unable to recall any recent experiences and he was unable learn new factual information. H.M. was, however, spared his ability

to learn new skills such as habit and motor learning (Gabrieli, Corkin, Mickel, & Growdon, 1993).

The importance of medial temporal lobe structures is clear from observations of HM. Every time H.M. shifted his attention his memory was wiped clean, leaving him completely dependent on others for the remainder of his life. Every shift in attention required HM to reorient himself in space, and progress in any activity he had made before the shift was immediately lost. The findings from the case of H.M. formed the questions and theories of memory research for decades, and chiefly led to the belief that the medial temporal lobe is specifically responsible for consciously encoding, retrieving, and organizing those explicit, or declarative memories.

Deficits in this type of memory are rather common in those affected by diseases such as Alzheimer's, Parkinson's disease, dementia, and traumatic brain injury, and are a central reason for why these disorders are so debilitating (Gaugler, James, Johnson, Scholz, & Weuve, 2016). A better understanding of this type of memory has broad implications that span areas from childhood education, all the way to neuropsychiatric disease. In the interest of precision over descriptive accuracy, these memories that are specifically dependent upon the medial temporal lobe will be defined as explicit memories.

The defining features of explicit memory have been described in many ways, and extend far beyond their uniquely verbal form described above. In essence, skill and habit memories are automatic, inflexible, and progressively shaped. Conversely, explicit memory has been described as declarative, symbolic, flexible, hierarchical, detailed, and

relational in form (Cohen et al., 1999; Cohen & Squire, 1980; Collins & Quillian, 1969; Tulving, 1985; Tulving & Madigan, 1970). The organization of explicit memory is still not fully understood, and no one taxonomy accounts for the myriad anatomical, psychological, and physiological observations of the process of remembering the organized facts and details from our past.

1.1.1 Interrogating explicit memory in the lab

The psychological study of explicit memory is broad and comprehensive, but generally involves variations on a common theme. Explicit memory involves an encoding period where 'items' are presented, followed by a mnemonic delay, and then a test period where the subject recalls those past 'items' or experiences. One method for testing explicit memory is called free recall. This test begins with the subject observing a list of items or item pairs. After a prolonged delay that can span minutes to hours to days the subject then recalls items or pairs from the list. These tests are useful in understanding how we organize memories in our mind. Subjects can freely recall large numbers of items, but generally perform better at recalling items towards the beginning of the list (called primacy) and at the end of the list (recency) (Murdock, 1962). Similarly, subjects tend to recall items together that were initially observed close in time (the contiguity effect) (Kahana, 1996). These effects support the theory that the temporal order of stimuli is an important organizer of information in memory. Similarly, subjects will also tend to recall items in groups based on their common features, e.g. pieces of furniture, or different fruits (Bousfield, 1953; G. H. Bower, 1970). Tests of free recall are informative,

in that they provide evidence that our explicit memories are organized based on temporal and conceptual similarity. However, free recall is a test that cannot easily be adapted for study in nonverbal animals, and therefore it is difficult to study the neurological substrate for this type of memory.

In an alternative test of explicit memory, subjects are prompted with a second list of items during the recall phase, and then rate the items on their familiarity. This memory task can be performed on humans, nonhuman primates, and rodents alike, and animal species show order effects such as primacy and recency as well (Kesner, Crutcher, & Beers, 1988). Variations on this test examine more complicated memories, such as those for the relationships between items. For example, one may be presented with a sequence of items during study, and then upon presentation of two of those items during test, asked to retrieve the earlier item in the list. Initial use of these types of recall experiments in animals was instrumental in establishing a congruency in mnemonic abilities between animals and humans.

An initial report observed that the scrub jay could form memories that included not only the identity of different food items, but also where and when they had been cached (Clayton & Dickinson, 1998). Expanding on these results, a variety of groups found that both rats and monkeys would preferentially explore objects, places, and object-place combinations that they had never experienced (Ennaceur & Delacour, 1988; Parkinson, Murray, & Mishkin, 1988). Thus, animals could remember highly detailed configurations items in unique places and times, and would often prefer new item-place-time (also known as ‘what-where-which’) configurations to those recently seen (Eacott &

Norman, 2004; Parkinson et al., 1988). These authors argued that in an operational sense, animals could create memories nearly as specific as those in humans, and the strength of these memories could be behaviorally tested. This laid the groundwork for research into the anatomical underpinnings of the different associations that comprise explicit memory.

The gross and mesoscale anatomy of the medial temporal lobe is conserved across species, so anatomical research on the explicit memory systems in rodents and monkeys began later, but quickly surpassed that in humans (Illustration 1) (Squire, 1992; Witter, 1993). In broad sweeps, the perirhinal cortex (PRC) and postrhinal (POC) (or parahippocampal cortex (PHC)) receive connections from widespread brain regions, and converge upon the medial and lateral entorhinal cortex, respectively. From there, these two anatomically segregated information streams converge directly onto the hippocampal formation. The hippocampus contains a largely unidirectional excitatory loop, where the formation of episodic memories is thought to occur (Illustration 1) (Amaral, 1993). Fiber pathways return back from the hippocampus to the cortex via the same two pathways in a segregated manner. The entorhinal cortex is thought to be the cortical gateway to the hippocampus across species, and the hippocampus is thought to be the nexus of explicit memory formation. This large body of behavioral evidence for researchers to be convinced that animals could generate memories rich enough to be analogous to explicit memory (Griffiths, Dickinson, & Clayton, 1999; Tulving, 2001).

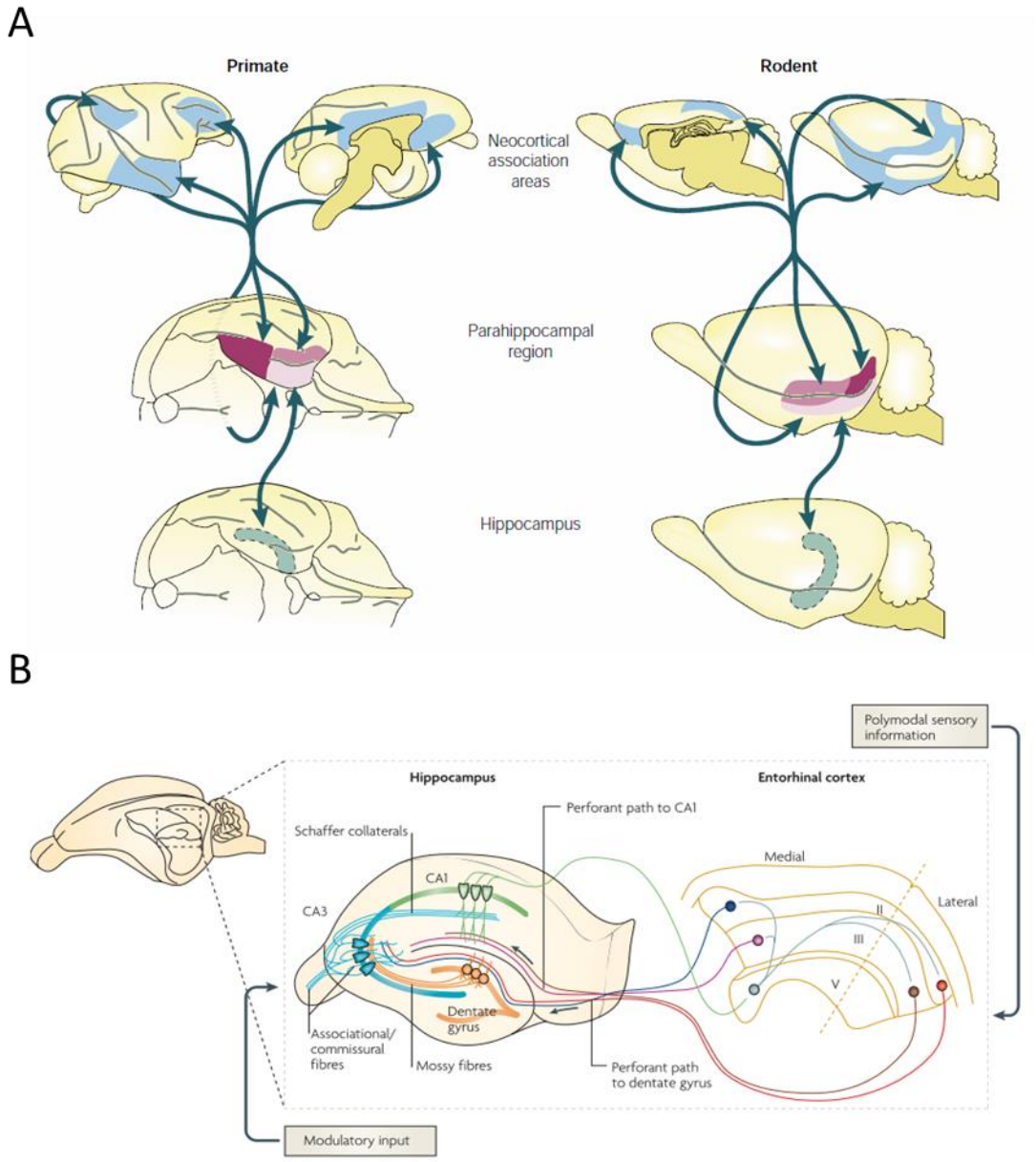

Illustration 1: The extended declarative memory system and the hippocampal trisynaptic loop.

Top: Two cortical processing streams converge upon the medial temporal lobe. Fiber pathways converge from widespread neocortical regions separately into the medial entorhinal cortex and lateral entorhinal cortex. Bottom: The hippocampal trisynaptic loop begins with superficial entorhinal cells innervating the dentate, continues from dentate to ca3, ca3 to ca1, and then returns out to deep layers of the entorhinal cortex. Adapted from (Eichenbaum, 2000; Neves, Cooke, & Bliss, 2008)

1.2 The organization of explicit memory

Following initial reports that explicit memory was anatomically localized, the most viable step forward was the anatomical dissection of the different conceptual components of this type of memory. There are two prominent theories describing the organization of explicit memory, each involving a different dichotomy. One theory on the organization of memory posits that there are two systems that support explicit memory, called semantic memory and episodic memory. In its original theoretical conception, Tulving described episodic memory as that which 'receives and stores information about temporally dated episodes or events, and temporal-spatial relations among these events' (Tulving, 1972). Tulving fervently argued that episodic memory is a distinctly human entity, and therefore unable to be studied in animals (Cheke & Clayton, 2010; Terrace & Metcalfe, 2005). In other words, episodic memory is the memory of specific experiences that happened to us in our past that carry an autobiographical index (Holt, Reiff, & Scheerer, 1961). This is in contrast to semantic memory, which is described as those facts that are not associated with a unique instance in our past.

Alternatively, studies wherein the subject reports their confidence in their memory judgements suggest there are two systems that contribute to item recognition (Fortin, Wright, & Eichenbaum, 2004; Yonelinas, 2002; Yonelinas, Kroll, Dobbins, Lazzara, & Knight, 1998). One system supports vivid recollection of past events in great detail, and can place them in a unique location and time. The other system supports a vague sense of stimulus familiarity, and does not involve the recall of details about that past experience. These systems are similar to episodic memory and semantic memory,

except that in this theory, each system acts in parallel rather than in series (Yonelinas, 2002). One common element of these two theories is that there is a system that supports the memory for the elements of an experience *and* their relationships, whereas the other system supports a weaker memory for the elements alone. The section below first outlines how different types of mnemonic associations can be operationally defined, then covers the brain regions necessary for these categories, and finally covers the anatomical organization of the system these regions comprise.

1.2.1 The anatomical localization of different types of associations

Studies examining the differential contributions of medial temporal lobe sub-regions to different types of explicit memory draw different conclusion depending on the species and behavior. Studies from monkeys performing delayed matching tasks tend to support a hierarchical organization, such that memory for conjunctions is built from item and place memories. Rodent studies suggest parallel independent systems for item, place, and conjunctive memories, and human studies vary widely.

An influential collection of rodent studies leveraged spontaneous exploration to tease apart the anatomical substrates for episodic and semantic memories. These studies showed that PRC lesions specifically block recognition of recently seen objects, POC lesions block memory for the locations of objects, and hippocampal lesions block memory for the association of the two (Eacott & Gaffan, 2011; Norman & Eacott, 2005). This literature supports a modular system wherein the PRC and POC are necessary for semantic associations that comprise items and places, and the hippocampus is required to

bind these events and places into a spatiotemporal context in episodic memory (Eacott & Norman, 2004; Norman & Eacott, 2005). These studies found a triple dissociation of item memory, place memory and item-place memory within the rodent brain. In other words, the recognition of objects was independent from recognition of places, and both were independent of recollection of episodic-like conjunctive memories (Eacott, Machin, & Gaffan, 2001).

A separate body of work performed in monkeys has provided contradictory results and suggests an interdependence of item and item-place memory. These studies are based upon operant tasks wherein the subject is rewarded for discriminating the novel object, location, or object-location from that presented during a previous study period. In these experiments, PRC and POC lesions in monkeys produced deficits in not only item or position memory, but also in item-position conjunctions (Suzuki, Zola-Morgan, Squire, & Amaral, 1993; Zola-Morgan, Squire, Amaral, & Suzuki, 1989). Alternatively, lesions of the hippocampus selectively impaired relational, or episodic-like memory and not item or place memory (Mishkin, 1978; Murray & Mishkin, 1998; Parkinson et al., 1988). These studies used a delayed matching task, rather than spontaneous exploration to conclude that episodic and semantic memory work in serial. One alternative conclusion from these studies is that the rhinal cortices are necessary to act upon and use those conjunctive item-place memories to obtain reward. Despite this alternative, the rodent and monkey work established some conflict in the literature about whether semantic memory and episodic memory acted in parallel or in series. On the other hand,

these two literatures agreed that semantic memory remained intact following lesions restricted to the hippocampal formation.

Observational studies in humans conflicted with both the monkey and the rodent literature. A wide variety of studies on humans with brain damage caused by viral encephalitis, anoxia, or physical injury to medial temporal structures observed that humans exhibit similar impairments in episodic and semantic memory (Squire & Zola, 1998). These studies concluded that episodic and semantic memory are two components of a unitary phenomenon, and are anatomically inseparable. However, a very impactful paper by Faraneh Vargha-Khadem observed spared declarative memory in a group of patients who at a young age received lesions specifically to the hippocampus for medical reasons. Crucially, these patients had episodic deficits, but were spared their ability to encode new semantic information (Vargha-Khadem et al., 1997). As such, these children exhibited normal aptitude in school even though they could not remember the specifics of prior events. This result was inconsistent with the previous human literature and instead agreed with the animal literature, suggesting that at least semantic memory can function independently of episodic memory. This result stoked a contentious debate between researchers about whether episodic and semantic memory were truly independent (DeLong & Heinz, 1997; Eichenbaum, 1998). More recent evidence suggests a double dissociation between episodic like associations and semantic like recognition in humans as well. Recent human cases have recapitulated results in rodents that recognition may be impaired in the event of anterior temporal lobe damage, while recollection may be spared (Bowles et al., 2007).

Functional MRI studies on humans also support an anatomical separation between memory for items, places, and conjunctions (Eichenbaum, Yonelinas, & Ranganath, 2007). These more modern studies show differential activation in rhinal regions and the hippocampus during encoding and retrieval of items and conjunctive associations. Specifically, PRC or anterior temporal cortex activity during event encoding is predictive of later item recognition only whereas PHC and hippocampal activity is predictive of item-context associations (Davachi, Mitchell, & Wagner, 2003; Weis et al., 2004). Further work has implicated the hippocampus specifically during both encoding and retrieval involve a time component, such as for sequences of items (Ross, Brown, & Stern, 2009). These studies support a model consistent across species wherein the PRC supports memory for items, and the hippocampus supports the relationships between them.

1.2.2 Interactions between hippocampus and cortex

While the hippocampal dependent associative memories and rhinal cortex dependent item or place memories can be dissociated from one another, there is a large body of literature describing interactions between the two. This literature focuses on the time-limited dependence of memories on the hippocampus, and the hippocampal dependent ability to navigate semantic structures, or schema.

While it is clear that the hippocampus is necessary to encode new memories, its role diminishes as memories grow older. Rodents with hippocampal lesions show sparing of old memories, and even H.M. was able to recall detailed autobiographical memories from the distant past (Anagnostaras, Maren, & Fanselow, 1999; Caparelli et al., 2012).

These observations appear to contradict theories that suggest relational or conjunctive memory is strictly hippocampal, and reveal cross modal associations may not always require the hippocampus (Kitamura et al., 2017; Wiltgen, Brown, Talton, & Silva, 2004). This well-replicated evidence that the hippocampus is only temporarily necessary for explicit memories supports the classic theory that memory consolidation involves the migration of a memory from the hippocampus to the cortex (McGaugh, 1999). Dubbed systems consolidation, this model describes how episodic memories initially dependent upon the hippocampus slowly lose such dependence. One theory posits that this phenomenon occurs during sleep and quiet daydreaming and may involve transient reactivation of memory engrams (Todorova & Zugaro, 2018; Wiltgen et al., 2004; Zhang, Fell, & Axmacher, 2018).

Conversely, there is a large literature in rodents and in humans showing hippocampal lesions cause deficits in the flexible expression of semantic memory. These observations extend the function of the hippocampus beyond a role in encoding concrete what-where-when associations that comprise individual autobiographical experiences, and implicate a role in the flexible processing and expression of semantic content. Formally known as the relational theory of hippocampal processing, Howard Eichenbaum and Neal Cohen aided in part in conceiving this theory and have provided great empirical evidence in support, using both human and rodents as subjects (Eichenbaum & Cohen, 2014; Konkel, Warren, Duff, Tranel, & Cohen, 2008).

The relational theory of memory fuses neuropsychological observations of item and associative memories with the psychological observations of Piaget on memory

schema. Indeed the notion that all memory is built upon a foundation of preexisting knowledge, or schema is well established in the psychology literature (Piaget, 1952). In this context, schema are the organized neural patterns entering the hippocampus from the cortex and are analogous to recognized semantic items. The proposed role of the hippocampus is to integrate new information into schema via different forms of memory consolidation, is similar to putting new items into context.

A number of existing data points can be reevaluated to support the relational theory. Early studies of rodents who lost the ability to navigate familiar spatial environments following hippocampal lesions supports an inability to integrate new locations into an existing spatial framework (Morris, Garrud, Rawlins, & O'Keefe, 1982). Similarly, human amnesiacs have trouble placing cities on maps even though they can describe their general location, suggesting a more subtle deficit in relational processing (Rosenbaum et al., 2000, 2005). These data that initially supported a deficit in spatial navigation can be reinterpreted to support the relational theory. Furthermore, human fMRI work suggests the hippocampus is specifically involved when subjects experience or imagine novel stimuli or stimulus conformations (Hasselmo & Stern, 2006; Preston, Shrager, Dudukovic, & Gabrieli, 2004; Stern et al., 1996; Zeithamova, Schlichting, & Preston, 2012). More recent supporting evidence from human amnesiacs has come from studies of language processing that outline deficits in multiple source information (Kurczek, Brown-Schmidt, & Duff, 2013). In rodents, hippocampal lesions cause deficits in relational tasks such as transitive inference, temporal order memory, and symmetry (Eichenbaum & Cohen, 2014). In a pair of influential studies, groups from the

Eichenbaum lab showed that rodents were trained on odor pair associations, they could structure the odor sets and make inferences about the relationship between novel pairings (Bunsey & Eichenbaum, 1996; DeVito, Kanter, & Eichenbaum, 2009). Crucially, these experiments showed that in rats and mice the hippocampus was necessary to make inferences about item relationships in a non-spatial domain. Together, these observations suggest that episodic-like associations are slowly shifted out of the hippocampus, but the flexible access to memories is hippocampal-dependent.

The relational theory of memory processing explains a wide range of experimental findings, but also makes predictions about how episodic memories are related. First, redefining semantic content into schema suggest that the information entering the hippocampus may already contain not only items but common spatiotemporal contexts in which they occur. Individual memories can thus be considered pointers along continuous ‘contextual’ axes, and the similarity of these pointers is measured as their closeness along these axes (Nielson, Smith, Sreekumar, Dennis, & Sederberg, 2015). In this way, the neural substrate for an episodic memory, or episode can also reflect its schematic similarity to other memories (Bellmund, Gärdenfors, Moser, & Doeller, 2018; Huth, Nishimoto, Vu, & Gallant, 2012; LaRocque et al., 2013). Second, it is clear that the hippocampus is necessary for processing novel situations, and relating them to others across space and time (Tulving & Markowitsch, 1998). This suggests that the hippocampus may be necessary to act appropriately in novel situations, by rapidly organizing new experiences into existing schema (Kimble & Kimble, 1965; Zeithamova et al., 2012).

1.3 The neurobiological basis of memory

In parallel to the taxonomy of human episodic memory, there exists a more general theory of memory that is described at the cellular and molecular level. In 1920 Richard Semon was the first to describe a memory engram as an indelible physical change in the brain, and hypothesized how it may be encoded and retrieved (Schacter, Eich, & Tulving, 1978). Subsequent attempts dominated the basic anatomy research for decades. At the crux of this debate was whether certain skills, memories, and functions were topographically organized onto the surface of the cortex, or whether these skills and memories were distributed throughout the cortex. While some scientists found evidence for localization using electrical stimulation, others were less successful when using lesion techniques (Lashley, 1929; Penfield & Rasmussen, 1950).

An alternative framing to this debate Hebb hypothesized that the engram of a memory might exist at a finer scale: within the connections between neurons residing in the brain. Hebb suggested that learning occurred when neurons fired together, and the anatomical substrate of memory was a change in the connections between those neurons as a result (Attneave & Hebb, 1950). Subsequently, a variety of researchers found physiological evidence of activity induced synaptic change in model systems (Bliss & Lømo, 1973; For review: Feldman, 2009). A real breakthrough occurred when Eric Kandel showed a direct relationship between synaptic changes and behavioral learning (Brunelli, Castellucci, & Kandel, 1976; Castellucci & Kandel, 1976). This collection of papers revealed that a learned stimulus response relationship coincided with changes in

the connections between neurons responsible for perceiving the stimulus and producing the response. Kandel later showed that modifying the synaptic strength between those neurons was responsible for producing the behavioral association (Castellucci & Kandel, 1976). These separate pieces of evidence led to the synaptic theory of memory and provided a basis for how a pair of cells, one responding to a stimulus, and another generating a response may become associated when that stimulus and response co-occur.

Cellular neuroscience provided a possible mechanism for learning and memory, whereas the cognitive neuroscience literatures pointed to the hippocampus as the locus where this biochemical process ought to be leveraged to subserve declarative memory. The specific hypothesis was that the hippocampus contained firing patterns that somehow embodied the spatial and temporal relations among events that occur in every-day life (Eichenbaum, Otto, & Cohen, 1994; Howard, Fotedar, Datey, & Hasselmo, 2005). These firing patterns would organize in a manner conducive to synaptic learning, so that the elements of episodic memory could be rapidly formed and remembered. The basic principle of this organization was thought to be the same as for the rest of the brain: individual units would have firing fields, and would fire when a stimulus was present providing a window for synaptic plasticity.

Traditional models of firing fields involve a stepwise translation of simple sensory stimuli to more complicated configurations of stimuli, and ultimately to the items and associations that comprise the objects and places with which we interact (Wiesel & Hubel, 1979). A stereotypical model might involve combined inputs from cells that respond to different features of an object onto a single cell that represents the whole

object (Hopfield, 1995). When all features are present, the combined inputs are sufficient to cause that cell to fire. When the post-synaptic cell fires as a result of the combined input from the presynaptic cells firing, the active synapses are strengthened and those features are then associated with that object. In a similar vein, inactive inputs corresponding to features not associated with that object are diminished, and outputs from active feature cells to other inactive object cells are also diminished. These models have been incredibly effective at describing the signaling cascades in primary cortices, and have been successfully employed as an *in-silico* model of learning and memory.

1.4 Memory mechanisms in the medial temporal lobe

While circuits across the brain exhibit firing fields and synaptic plasticity, the hippocampus and surrounding regions exhibit unique forms of plasticity and firing properties in support of episodic memory function. The hippocampus exhibits some of the most rapid and sometimes transient forms of synaptic plasticity and reorganization, some of the most intricate laminar organization, and some of the most complex tuning curve parameters yet described in the brain. These characteristics all work together to allow for continuous encoding of experience in the most detailed form.

The hippocampus has been long studied for its easily inducible synaptic plasticity in highly specific and organized synaptic pathways (Bliss & Lømo, 1973). Indeed long term potentiation was first discovered in the hippocampus, and provided a proof of concept for information storage on a behaviorally-relevant timescale. The hippocampus also contains some of the only neurons in the mammalian brain to undergo neurogenesis,

supplying the circuit continuously with new opportunities for synaptic plasticity to occur (Kempermann, Jessberger, Steiner, & Kronenberg, 2004). Along with a continual supply of new neurons, synapses in the hippocampus are thought to be highly dynamic. A recent study found that dendritic spines in the hippocampus undergo 100% turnover in a matter of weeks, in contrast with the cortex, which is thought to contain a significant proportion of dendritic spines that are virtually static (Attardo, Fitzgerald, & Schnitzer, 2015; Holtmaat et al., 2005).

Along with its unique cellular characteristics, the hippocampus exhibits a unique network organization suggestive of a role in episodic memory. John O'Keefe was the first to examine firing patterns in the hippocampus of freely moving subjects *in vivo*. He was able to do this through development of a technology allowing for extracellular unit recordings from freely moving rodents. In his rats, O'Keefe found hippocampal neurons that only fired when the animal occupied a specific location in the testing arena. These cells appeared to have firing fields centered on a specific 'place' and thus were dubbed 'place cells'. In this seminal report, O'Keefe also described other cells, dubbed 'misplace cells' whose firing fields seemed to select for certain events occurring in a specific place, either the surprising removal, or insertion of a cue. While ascribing cells to a specific function is convenient, it is more prudent to describe the firing fields displayed by these cells instead. Therefore, 'place fields' will be used to describe this intricate organization of action potentials (O'Keefe & Burgess, 1996). These highly selective firing fields served as a crucial link to connect cognitive abilities in vertebrates down to cellular and molecular changes in the brain.

This laid the groundwork for models that describe how information cascades converging on the hippocampus generate highly specific patterns of activity contributing to the synaptic learning that underlies the association of stimuli to a unique spatial context. Under one hypothesis, place fields may represent the spatial context within which events may occur. Thus, a place field may coincidently occur with an object field responding when an object is placed there, and through rapid plasticity, that object is bound to a place. Item place associations are two of the three necessary components of an episodic memory, the third being time.

A second breakthrough in our understanding of how episodic associations may be formed came when Pastalkova published a paper that described hippocampal firing fields that organized in time (Pastalkova, Itskov, Amarasingham, & Buzsáki, 2008). These cells, later dubbed ‘time cells’ exhibit firing fields at specific moments after an event, marking how long ago that event took place (Eichenbaum, 2014; Macdonald, Lepage, Eden, & Eichenbaum, 2011). Much like place fields, time cells provide an obvious substrate for tracking when experiences occur, and provides a potential mechanism for ordering events across time. Together with the discovery of place fields, these studies reveal a cellular code in the hippocampus for a combined spatiotemporal context that could function to generate episodic associations between events. This theory makes intuitive sense, but as the following sections will show, the physiological and anatomical organization of memory in vertebrates goes far beyond the simple firing fields and fire together, wire together plasticity rules initially discovered in invertebrates.

1.5 Anatomy of the medial temporal lobe

Place fields exist in all hippocampal subregions of the declarative memory network, and similarly specific firing fields can be found in neighboring cortex. The declarative memory system includes multiple medial temporal lobe structures, subcortical structures including the septum and thalamic relays and their connections, and some prefrontal areas. Within these structures, there is a computational mechanism for rapidly encoding information, and transforming it into a crystallized, durable form.

As discussed above, cellular activity can promote the changes in synaptic connections between neurons that underlie memory. Therefore, the organization of synaptic connections is the basis for memory organization itself. The section below outlines the pathways that are crucial for episodic memory, and describes the importance of the connections between nodes in the episodic memory loop. It is these cells, and more specifically their synapses that are thought to be the substrate for episodic and semantic memory. Thus, it is the firing fields generated by these cells that support and modify synapses to encode new episodic memories.

1.5.1 Segregated processing streams converging on the hippocampus

A large body of anatomical tractography research has identified a general direction of flow in this system that arise from two general processing streams that converge in the hippocampus proper, and then project back out to the same two pathways (van Strien, Cappaert, & Witter, 2009). These two processing streams carry qualitatively different information in that the medial processing stream carries information about spatial configurations and orientations, whereas the lateral processing stream carries

information about objects and their perceptible features and relationships. These two processing streams converge in the hippocampus and initiate what is canonically called the trisynaptic loop. The trisynaptic loop begins with the entorhinal projections into granule cells in the dentate gyrus. Dentate Granule cells then send their axons to CA3, and then CA3 cells send projections that converge with those from the EC to CA1, thus ending the trisynaptic loop. CA1 cells project chiefly out to the subiculum and then to widespread areas of the cortex (Blatt & Rosene, 1998). Within this trisynaptic framework there exist even more intricate topologies that are discussed below.

The medial processing stream is a convergence of fibers from temporal, parietal and occipital cortices that enters the POC and then the medial entorhinal cortex. The lateral processing stream is a bundle of fibers originating from ventral temporal and frontal association areas as well as unimodal olfactory regions in the rat, or unimodal visual regions in the monkey to the PRC and then to the lateral entorhinal cortex (Burwell, Witter, & Amaral, 1995; Witter et al., 2000). The medial and lateral entorhinal cortices exhibit exquisite organization, and show clearly converging and diverging inputs into the hippocampus.

The medial and lateral entorhinal cortices together give rise to the two main cortical inputs to the hippocampus: the perforant pathway (pp) arising from layer 2 cells, and the temporoammonic pathway (ta) arising from layer 3 cells. These connections are topographically organized, or are ‘lamellar’ such that the cells at a specific dorsoventral level in the medial and lateral entorhinal cortex project the same dorsoventral level (or rostrocaudal level in primates) in the hippocampus (Amaral & Witter, 1989; Sloviter &

Lømo, 2012). In contrast, the MEC and LEC send axons to separate layers and levels of the hippocampus within this framework. The medial pp axons ramify in the inner third of the dentate molecular layer at the distal dendrite, whereas lateral pp axons ramify in the outer third of the dentate molecular layer at intermediate dendrites of dentate granule cells (van Groen, Miettinen, & Kadish, 2003). Moreover, the medial and lateral inputs exhibit distinct synaptic receptor classes, such as the mu opioid receptor (Breindl, Derrick, Rodriguez, & Martinez, 1994). The lateral ta pathway sends more axons to the distal (closer to the subiculum) region of CA1, and more heavily innervates cells residing in the superficial cell layer, whereas the Medial ta pathway sends more axons to the proximal region of CA1, and more heavily innervates cells residing in the deep layer (Masurkar et al., 2017). These anatomical similarities and differences suggest that the types of information conveyed by these axons are qualitatively different, but are both integrated within the hippocampus. Further clues to how these types of information differ within the entorhinal cortices are found in the electrophysiological properties and laminar distribution of cells in each of these regions. The most obvious differences between these regions may be the noticeably denser packing of cells in layer 2 of the LEC over the MEC (Amaral & Witter, 1989).

1.5.2 The hippocampus proper

The hippocampus proper is necessary for the retrieval of episodic memories as characterized by the joint representation of what, where, and when information. The hippocampus is made up of three principal regions each with unique properties that suggest they perform complementary computational functions. The dentate gyrus exhibits

sparse coding and neurogenesis that suggest a function called pattern separation: CA3 exhibits denser coding and recurrent connectivity that suggests pattern completion: and CA1 exhibits highly organized temporal dynamics in its firing fields that reflects multiplexing of inputs and suggests a role in integrating information from two sources (J. K. Leutgeb, Leutgeb, Moser, & Moser, 2007; S. Leutgeb & Leutgeb, 2007; Neunuebel & Knierim, 2014).

The dentate gyrus receives its major input from the pp, comprising the first node in trisynaptic loop from the entorhinal cortex. The dentate gyrus is comprised chiefly of excitatory granule cells and mossy cells, and inhibitory basket cells (Amaral, Scharfman, & Lavenex, 2007). Granule cells extend dendrites throughout the molecular layer, and send axons through the stratum lucidum to CA3 (Senzai & Buzsáki, 2017). Dentate granule cells receive lateral pp input to their distal dendrites, and medial pp input to their intermediate dendrites. A computationally relevant feature of the dentate gyrus is the extreme sparsity of its activity. Granule cells of the dentate rarely fire action potentials, suggesting they are responsive only to very specific elements of experience. This is achieved by a unique inhibitory environment wherein inhibitory interneurons and longitudinal association fibers have extremely efficacious clamping influence on granule activity. Dentate granule cells express unique GABAergic receptor subtypes on their distal, intermediate and proximal dendrites that result in shunting inhibition of inputs to their dendritic tree (J. D. Foster, Kitchen, Bettler, & Chen, 2013). Conversely, mossy cells residing in the hilus are highly active, ramify on local interneurons, and are thought to act in an inhibitory feedback loop that may help tune the sparsity of granule cell firing

fields (Amaral et al., 2007). Feedback along the dentate gyrus via mossy cells extends through a longitudinal fasciculus projecting almost the full longitudinal extent of the dentate, suggesting that the dentate is capable of behaving as a singular unit (Scharfman & Myers, 2013). A second unique and incredibly important feature of the dentate is that dentate granule cells are continually generated throughout life (Kempermann et al., 2004). Young granule cells progress through multiple developmental stages, including those marked by intracellular chloride balance, and later preferential excitability by lateral pp input (Collie et al., 2018; Dieni, Chancey, & Overstreet-Wadiche, 2013; Kempermann et al., 2004). Interestingly, cell populations are not recycled, but rather the number of granule cells continually increases throughout life. Neurogenesis is thought to aid in the function of pattern separation as continual dendritic growth offers a constant opportunity for the creation of new synaptic connections, and therefore new constellations of connectivity (Kitamura et al., 2009). Without new synapses, one could easily imagine that the pathways carved into the brain by experience become worn, and with no new naïve cells, there ceases to be an opportunity to break this mold. Indeed disrupting neurogenesis in the dentate causes episodic memory deficits in animals (Akers et al., 2014; Goodman et al., 2010). These two properties suggest that dentate granule cells may respond only to very specific inputs, and cells are continually available to integrate new information. These temporally transient and thematically sparse firing patterns match the nature of episodic memories. Episodic memories are incredibly specific, and we continue to create new memories throughout our lifetime.

Dentate granule cells send axons that terminate in the stratum lucidum onto the proximal dendrites of CA3 pyramidal neurons. The synaptic contacts between dentate granule cells and CA3 pyramidal cells are notably efficacious, and are so dubbed ‘detonator synapses’ (Henze, Wittner, & Buzsáki, 2002). CA3 neurons also receive inputs from the entorhinal cortex via the pp as well as direct feedforward excitation from other CA3 pyramidal cells. Entorhinal axons ramify on the distal dendrites of CA3 in a similar manner to dentate in that the lateral pp axons ramify on the more apical dendrites of CA3 cells (Witter, 2007). The activity of CA3 pyramidal cells is markedly different from that of dentate granule cells in that these cells have a much higher basal firing rate (GoodSmith et al., 2017). However the representation of experience in CA3 is still sparser than that in CA1 (Stefan Leutgeb, 2004). A higher firing rate together with the prominence of feedforward excitation in CA3 both suggest that a sparse, or degraded input can generate a dense and stable activation pattern. CA3 thus is suggested to perform pattern completion, the complementary function to the dentate (Neunuebel & Knierim, 2014).

Within the hippocampus there is a balance between feedforward excitation and excitation from the dentate versus external input from the entorhinal cortex. This balance is mediated by cholinergic tone, such that when acetylcholine is high, inputs from dentate CA3 recurrent fibers are repressed (Hasselmo & Schnell, 1994; Hasselmo, Schnell, & Barkai, 1995). This is thought to allow for cortical inputs, especially those from the LEC to dominate, and may correspond to encoding phases of memory (Kahle & Cotman, 1989). Conversely when cholinergic tone is low, dentate and CA3 recurrents may be

potentiated, allowing for stored patterns in the dentate and CA3 to propagate through the trisynaptic loop (Winson & Abzug, 1978). This dynamic weighting of pathways is thought to be a mechanism for rapid storage and retrieval of episodic information, as acetylcholine release changes from memory encoding to retrieval (Hasselmo, 1999; Teles-Grilo Ruivo & Mellor, 2013).

CA3 axons send collaterals (called Schaffer collaterals) to the CA1 area of the hippocampus, comprising the third synapse of the trisynaptic loop. Schaffer collaterals ramify onto the proximal dendrites of CA1 neurons in the stratum radiatum, whereas inputs from the entorhinal cortex traveling through the ta pathway innervate the distal dendritic tree of CA1 neurons. These synapses occur in the stratum lacunosum moleculare, so named for its high degree of vascularization. There is further segregation of ta fibers such that the LEC inputs prefer to innervate CA1 neurons that are more distal to CA3, and that reside in the more superficial cell layer, whereas MEC inputs prefer to innervate proximal, deeper CA1 neurons. This highly organized topology of afferents suggests there is integration of a wide range of inputs at the level of CA1 (Masurkar et al., 2017).

CA1 pyramidal cells send axon collaterals chiefly to the subiculum, but also to widespread regions of the cortex (Blatt & Rosene, 1998). From the subiculum, the major output then projects to the entorhinal cortex and in turn back down the spatial and non-spatial cortical processing streams. In this way, the hippocampal formation receives highly processed information from two sources, manipulates that information through an intricately organized feed-forward loop, and then feeds back on those same cortical

systems, presumably modifying the input traces in a way that sub-serves declarative memory formation.

The fimbria is a lemniscus of fibers that courses the length of the hippocampus and continues on as the fornix to connect the two hippocampi, and each directly to subcortical structures. Commonly known as Papez circuit, these fibers arise from all hippocampal subfields and travel through the fimbria/fornix to the contralateral hippocampus, and insert into the diencephalon via the mammillary bodies (Vann, 2013). Collaterals from those fibers continue in a loop to innervate subcortical structures including areas in the thalamus and hypothalamus (Wyss, Swanson, & Cowan, 1979). The connections to the septum are of specific interest, wherein inhibitory GABAergic, and excitatory glutamatergic and cholinergic fibers from subcortical structures innervate the hippocampus through the fornix as well. Modulation of septal activity has marked effects on hippocampal network activity, such as gating hippocampal output, and modulating local oscillations (Brandon et al., 2011; Haam, Zhou, Cui, & Yakel, 2018; Villette et al., 2010).

1.6 Physiology of the medial temporal lobe

As mentioned before, the firing patterns of hippocampal cells were initially thought to be a substrate for spatial navigation. While initial research focused on dorsal CA1 unit firing during spatial navigation, the studies outlined below make clear that unit activity across the MTL can be correlated to various aspects of experience and memory. The sections below will outline how firing fields in the medial temporal lobe reflect

processing of spatial locations, objects and non-spatial stimuli, object-position associations, abstract contextual designations, the temporal order of future and past events, and finally time itself. This research suggests that the medial temporal lobes contain a code that reflects the myriad stimuli one may experience, and the spatial and temporal relationships between them, that supports episodic memory.

1.6.1 Spatially tuned firing fields in the hippocampus

The spatial firing characteristics of hippocampal cells are most easily studied, as their observation requires no behavioral manipulations and minimal behavioral monitoring. Indeed, studies on the spatial specificity of hippocampal unit activity have provided a wealth of information as to how hippocampal neurons organize their firing fields. While initially discovered in CA1, place fields have been found throughout the hippocampus, and examination of the environmental and physiological factors that modulate place fields is a focus of continuing research (McNaughton, Barnes, & O'Keefe, 1984; O'Keefe & Dostrovsky, 1971; Rangel et al., 2014).

Place fields are generally studied under the backdrop of spatial navigation as an animal traverses a linear track or wanders an open field in search of randomly placed food. In this situation place fields are incidentally recorded, and appear to represent nothing else but the current position and bearing of the rat (O'Keefe, 1976). While 'place cells' are increasingly studied in more mnemonically relevant situations, their inception and much of their characterization has been in rats and mice performing this relatively passive paradigm.

Place fields represent the myriad of stimuli across modalities that comprise a location in an environment. As such, the removal of a single modality is insufficient to fully disrupt place field representations. Place fields persist in blind rats (Save, Cressant, Thinus-Blanc, & Poucet, 1998), in the dark and without auditory cues (Save, Nerad, & Poucet, 2000), in zero gravity (Knierim, McNaughton, & Poe, 2000), in and even virtual reality (Harvey, Collman, Dombeck, & Tank, 2009). Similarly, lesions to the prefrontal cortex (Kyd & Bilkey, 2005), thalamus, post-subiculum, entorhinal cortex (Brun et al., 2008; L. Lu et al., 2013; Van Cauter, Poucet, & Save, 2008), PRC (Lee & Park, 2013), mammillary bodies (Sharp & Koester, 2008), fornix (Miller & Best, 1980), CA3 (Nakashiba, Young, McHugh, Buhl, & Tonegawa, 2008), and medial septum (Stefan Leutgeb & Mizumori, 1999) are insufficient alone to abolish place. Together these studies show that while no one region or sensory modality is necessary for place fields, a wide range of stimuli and processing streams contribute to their existence.

Place fields take time to organize, and may take multiple visits to a place for fields to develop. Place field formation is thought to be a rapid event that involves both intracellular and circuit level mechanics that are modulated by attention. When the animal attentively scans a new environment, presumably in an attempt to orient themselves, place fields are more likely to develop (Monaco, Rao, Roth, & Knierim, 2014). Recent work examining the formation of place fields reveals a complicated interplay between intracellular phenomena and network influences that occur prior to organized spiking activity. Specifically, novelty and attention promote parvalbumin (PV+) cell firing and depresses somatostatin (SOM+) cell firing (Sheffield, Adoff, &

Dombeck, 2017). As PV+ cells are thought to clamp somatic potentials, and SOM+ cells dendritic potentials, this suggests a shift in network state towards current integration in the dendritic compartment (Abbas et al., 2018; Amilhon et al., 2015). This likely increases the probability of what are called dendritic plateau potentials in the hippocampus. CA1 place field formation is usually preceded by dendritic plateau potentials, which require both NMDA receptors and sustained calcium influx. This suggests place field formation involves a mechanism that extends the time window for synaptic plasticity (Bittner, Milstein, Grienberger, Romani, & Magee, 2017). Sheffield went on to show that this may be a mechanism by which specific dendritic branches are chosen above others, as the dendrites exhibiting plateau potentials drive stable place field activity (Sheffield et al., 2017). This choice process likely involves interneurons, as their activity is thought to strongly suppress sparsely active inputs and effectively threshold inputs (Grienberger, Milstein, Bittner, Romani, & Magee, 2017; Wagatsuma et al., 2017). These results together suggest a model wherein inputs converging on specific dendrites are selected to generate new place fields by a shift in interneuron dynamics. These inputs generate dendritic plateau potentials that selectively increases the efficacy of those inputs, so that subsequent visits to that place elicits firing field activity.

A closer examination of the inputs to CA1 during field formation revealed that these plateau potentials are often generated by finely timed inputs from EC and CA3 (Bittner et al., 2015). Both SOM and PV interneurons are thought to organize inputs within the fine timescale of oscillations in the local field potential (LFP) (Royer et al., 2012). Interneuron spiking is thought to generate local oscillations in the hippocampal

LFP, which influences pyramidal firing through phasic and compartmentalized inhibition (Amilhon et al., 2015). The theta rhythm is a well-documented and prominent oscillation occurring in the local field potential at 7-12 Hz (Buzsáki, 2002). A recent report perturbing SOM+ interneurons suggests a central role of these cells in controlling both the power and timing of ca1 afferents to specific phases of theta rhythm (Lovett-Barron et al., 2012). This suggests an alternative mechanism for organizing inputs and supporting place fields supported by network oscillations.

Both spatial coordination via plateau potentials, and temporal coordination via oscillatory coupling may synergistically act to generate new place fields. Interestingly, place fields can be generated in the absence of NMDA receptor activity, however they show lower long term stability (Kentros, 1998). Thus, while network coordination may be sufficient to generate place fields, NMDA dependent synaptic plasticity is required for long term stability of place fields, and consequently memory for context.

Once established, cell firing during passes through a place field exhibit a stereotyped pattern that is characterized by bursting activity that occurs at a specific relationship to theta (O'Keefe & Recce, 1993). Place fields in CA1 and CA3 both phase-lock to the theta rhythm in the LFP (Schomburg et al., 2014). The existence of this rhythm, as well as the selectivity of pyramidal cells to a specific phase of the rhythm suggests interneuron networks aid in both generation of and maintenance of place fields.

Both the amplitude of the theta rhythm as well as the firing of place fields tend to be dependent on the animals behavior. Theta power and place field firing are elevated when the animal is moving faster, and this is not a mere product of visual flow (X. Lu &

Bilkey, 2010). This observation suggests that these cells are important when animals are integrating changing sensory inputs. Further supporting this theory, place fields representing neighboring positions fire in rapid sequences, called ‘theta sequences’ that recapitulate the relationship between the places they represent in real time (D. J. Foster & Wilson, 2007). This relationship is promoted through a complex interaction with the theta rhythm. Specifically, as an animal moves through a place field, that cells spikes occur at progressively earlier phases of the theta rhythm (Skaggs, McNaughton, Wilson, & Barnes, 1996). This is called phase precession, and precedes the fine organization of adjacent place fields. When theta is disrupted, place fields cease to exhibit this finely timed relationship, and recently formed place fields display unreliable spike time relationships with their neighbors (Feng, Silva, & Foster, 2015). Indeed, theta is hypothesized to support segregated encoding and retrieval functions in the hippocampus, as well as in organizing ensemble activity across space and time (Hasselmo & Stern, 2014). Overall, these characteristics of place fields suggest they form relationships between each other that is based on the temporal relationships between the places they represent. In other words, place firing may represent pointers along a dimension that are linked to their neighbors like a chain or net.

When examining ensembles of place fields across different behaviors and environments, studies have shown that place field ensembles can change as a coherent unit, or in a disjointed fashion. Individual place fields generally anchor to prominent environmental cues much like we do when orienting ourselves in space. In some circumstances, rotation of prominent visual cues can cause an ensemble of place fields to

rotate coherently as though the entire map were guided by these cues. Interestingly, these maps are generally insensitive to the relocation of local objects in the enclosure (Cressant, Muller, & Poucet, 1997). Place maps are also sensitive to the geometry of an environment, and undergo changes that may correlate to when the animal senses difference. In a pair of similar experiments, animals were place in an environment as it transitioned from a square into a circle. In one experiment the animals were familiar with both the square and the circle geometries, having previously built separate hippocampal representations for each enclosure. As the animal was introduced to varying intermediates between a square and circle, the hippocampal place representation mapped either to the square or to the circle, but not a morph between the two (Wills, 2005). Similarly, when mice mistakenly confuse their orientation in a symmetric room, their place maps are coherently flipped as well (Keinath, Julian, Epstein, & Muzzio, 2017; Kinsky, Sullivan, Mau, Hasselmo, & Eichenbaum, 2018). Finally, one study found that when rats confused one room with another, they generated identical place maps in each environment (Grieves, Jenkins, Harland, Wood, & Dudchenko, 2016). These data suggest that ensembles of place fields can maintain coherence across very similar situations.

Other environmental manipulations cause ensembles of place fields to change in a disjointed fashion. In an interesting replication of the above circle-square experiment, animals were exposed to a progressively morphing enclosure, rather than random intermediates between a circle and square (J. K. Leutgeb et al., 2005). In this experiment, hippocampal place maps slowly morphed with the environment, with different fields changing at different moments. A separate study found similar results by cleverly rotating

proximal and distal cues out of register. This experiment revealed not a dichotomy, but rather a spectrum of shifting fields such that some followed local cues, some followed distal cues, and many showed a graded shift reflecting an intermediate between the two. This was in stark contrast to head direction cells, that all rotated coherently from trial to trial (Knierim, 2002). However in both of these experiments, the difference between the environments and the referenced context were obvious, and thus the animals may have recognized this was a new place built from familiar components. These studies suggest that the hippocampal representation can 'remap' in a dynamic fashion that may reflect the similarity of that context to multiple reference points.

Together, the observations of both coherent shifts in place maps as well as disjointed remapping suggests a dynamic mechanism that reflects a dynamic representation of context memory. When the environment is similar enough to what might be held in memory, the map may behave as an attractor network, overcoming differences. On the other hand when the current environment is clearly new, the hippocampal map may include features that are similar to old maps, but the relationships between nodes in the new representation may reflect the unique conformation of the current situation.

1.6.2 Hippocampal firing fields are sufficient for memory

The data on remapping suggest that place maps are the substrate for ones memory of a spatial environment. Indeed a large body of research using a wide range of techniques has provided evidence for a causal role in place field firing and the memory of the events occurring in that place. One amazing body of work has leveraged the action of

immediate early genes to label active cells and provide evidence of a ‘hippocampal engram’ for an environment (X. Liu et al., 2012). In these studies, cells exhibiting firing field activity are “tagged’ by leveraging the action of immediate early genes expressed after a cell exhibits a high firing rates. This in theory captures all the cells that exhibited place field activity in that chamber (Morgan & Curran, 1989; Shen & Greenberg, 1990). When these tagged cells are then reactivated in a different environment using optogenetics, animals respond as if they were still in the tagged chamber. Scientists have been able to tag both aversive and appetitive experiences, and have shown that the activity of these hippocampal ensembles represents not just the place or stimulus alone, but the conjunctive representation of these stimuli and the place they occurred (Redondo et al., 2014). Thus, the activity of a hippocampal ensemble provides information to the animal about where they are and what experiences may have happened there in the past. Following up on this hypothesis, one study associated reward via medial forebrain bundle stimulation with the firing of a single place field during sleep (de Lavilléon, Lacroix, Rondi-Reig, & Benchenane, 2015). When the animal was put back into the environment in which that cell fired, the animal preferred the place in which that cell had fired earlier. Remarkably, the action of a single hippocampal neuron provides sufficient information for an animal to know their precise location in space, and to prefer that location when it is artificially linked to reward.

1.6.3 Hippocampal firing fields lock to non-spatial stimuli

Hippocampal units also generate firing fields that are centered on a variety of nonspatial cues, such as odors, tones, objects, and even tastes that are organized in a similar manner to place fields (Aronov, Nevers, & Tank, 2017; Herzog et al., 2019; Komorowski, Manns, & Eichenbaum, 2009; Otto & Eichenbaum, 1992; Terada, Sakurai, Nakahara, & Fujisawa, 2017). Generally units will respond to one or more stimuli of a set, and often times they will respond in a graded fashion firing maximally to one item, and less so for others (Otto & Eichenbaum, 1992). These firing fields generally lock to the onset of the stimulus, and generally sustain firing when the animal attends to that stimulus (Terada et al., 2017). In one interesting investigation, hippocampal units were found to respond with firing fields that tiled a spectrum of sound frequencies as an animal navigated to a target frequency to obtain reward. In other words, individual units would respond when a specific tone was heard, and as that tone changed pitch, the cells firing rate field diminished. This study provided evidence that the hippocampus may map non-spatial dimensions in the same way that it maps place: by generating firing fields that center on pointers along that dimension. Much like place fields, stimulus responsive cells exhibit both theta locking and phase precession (Aronov et al., 2017; Terada et al., 2017). This provides evidence that hippocampal ensembles may map non-spatial stimuli onto a continuum of relatedness by organizing the spectrum of stimuli onto a series of overlapping firing fields.

1.6.4 Hippocampal firing fields depend on "context"

Aside from generating firing fields centered on non-spatial stimuli, non-spatial changes to an environment can trigger remapping of hippocampal spatial representations (Bulkin, Law, & Smith, 2016; Smith & Mizumori, 2006; Stark, Reagh, Yassa, & Stark, 2018). For example, changing non-spatial features such as the ambient odor, the presence of an overhead light, or even the specific task the animal is performing can induce remapping in hippocampal representations. Indeed some studies have induced two completely independent spatial maps of the exact same space by generating two behavioral paradigms in the same place (Markus et al., 1995). These results led researchers to suggest that hippocampal place fields contain a code for more than just space, but a general notion of context.

Context can be a sweepingly broad definition, causing one review to make the confusing claim that that context must be both stable across time, but also be continually changing (Stark et al., 2018). One review generated a more concrete definition of context as a constellation of spatial and situational factors that designate one behaviorally relevant setting from another (Smith & Mizumori, 2006). Alternatively, if interpreted through a relational theory lens, context can be defined as the schematic similarity between episodic experiences. Under this interpretation, context involves the overall semantic similarity between one experience to another, and therefore is expressed on a spectrum, rather than as unrelated entities (Huth et al., 2012).

1.6.5 Coding of recent past and future plans

Animals may also hold different representations of the same place that depend on either past or planned trajectories. Route dependent place fields have been observed both preceding, as well as following divergent navigational behaviors (Ferbinteanu & Shapiro, 2003). Classically, place field 'splitting' has been observed during mnemonic delays during delayed non-match to place tasks (Wood, Dudchenko, Robitsek, & Eichenbaum, 2000). Splitting is not restricted to space however, as during odor sequence learning tasks, hippocampal cells may respond only to an odor if it follows another odor (Allen, Salz, McKenzie, & Fortin, 2016). More generally, place fields are sensitive to sequences of events as they play out in time. Conceptually, successful navigation depends on, and episodic memory is organized into an ordered sequence of events. This dependence of hippocampal firing patterns on the sequential elements of an experience supports the notion that hippocampal activity patterns reflect the index of not only places and things, but also the sequence of places and things that comprises an episode.

1.6.6 Hippocampal firing fields code temporal context

Initial reports of the hippocampal map suggested the hippocampus generates temporally stable representations within a given context. A static representation of space provides a stable foundation onto which to bind experiences (O'Keefe & Dostrovsky, 1971). Prolonged stability can be found in individual hippocampal firing fields for up to months of time. In contrast, studies examining cross-temporal discriminations indicate instability is a key feature of the hippocampal representation. The rate of change in the overall hippocampal representation across time correlates to ones' ability to recall the

relative order of events both humans and in animals (Jenkins & Ranganath, 2016; Manns, Howard, & Eichenbaum, 2007). Constant flux may appear in direct conflict with a stable schematic foundation onto which experiences may be assimilated. However, a large body of empirical work outlines multiple mechanisms by which the hippocampus can exhibit both a stable representation and one that is constantly changing across time.

In a group of studies done in the Leutgeb lab, Emily Mankin recorded from a variety of hippocampal and cortical regions over the course of weeks. Mankin found that as time wore on, the hippocampal map morphed in some regions more than others. Specifically, this study observed that in general, CA1 place fields ‘drifted’ over the course of weeks when compared to CA3, which were stable over that lag. Crucially, even though individual units drifted across time, the ensemble always discriminate between different enclosures (Mankin et al., 2012; Mankin, Diehl, Sparks, Leutgeb, & Leutgeb, 2015). Thus, this study found that hippocampal ensembles could track both changes within a context across time while holding a stable representation of the differences between spatial contexts. A separate study observed dentate activity across extended time exhibited similar changes, and revealed this time code to be impacted by neurogenesis (Rangel et al., 2014). These results are corroborated by a study that used a different methodology. In this study, the active cell ensemble in the dentate was labeled using the tet-tag technology previously mentioned in unique environments separated by hours or days. The overlap in the active ensemble was lower between environments experienced across greater time lags, and this was correlated to a behavioral readout of perceived similarity between those experiences (Cai et al., 2016).

Together these studies corroborate the role of the dentate in separating experiences (pattern separation), of CA3 in representing consistencies across time (pattern completion), and of CA1 in mapping both commonalities and differences. Furthermore, these studies suggest that the hippocampal map includes a representation of a slowly changing context. However they do not explain how individual units express such a code, and whether this code exists across the continuum of time scales.

1.6.7 Hippocampal time cells

While the above studies have examined temporal modulation of firing fields under the backdrop of space or events, other studies have managed to isolate time more specifically. Time cells, introduced in the last section, are those with firing fields that occur at precise delays after an event. While time cells have been observed during delays in which position is not fixed, time cells are most widely studied as animals run in place so as to fix other environmental features (Gill, Mizumori, & Smith, 2011; Pastalkova et al., 2008). This affords behavioral control so that time fields can be attributed to no external cues, and thus only the passage of time. Time cells have also been found in head-fixed preparations and are thus not dependent on treadmill movement (Macdonald, Carrow, Place, & Eichenbaum, 2013). Time fields have been found in the dorsal hippocampus in both CA1 and CA3 and arise regardless of the need to associate events prior to the delay with those following (Salz et al., 2016). This organization of firing fields around time is of specific relevance to relational theories of hippocampal function because it provides a viable structure for relating events across time (Kitamura, Macdonald, & Tonegawa, 2015; Villette, Malvache, Tressard, Dupuy, & Cossart, 2015).

Indeed time cells can be considered as pointers that identify an experience, and because of their relationship to other cells can provide a pathway to relate thematically similar or temporally close experiences.

1.7 Spatial and non-spatial correlates of entorhinal activity

Place fields are thought to arise from inputs from a variety of cortical regions that together represent the spatial and non-spatial context of the animal (Stefan Leutgeb, Leutgeb, Moser, & Moser, 2005; Solstad, Moser, & Einevoll, 2006). The firing properties of hippocampal firing fields are organized across a variety of dimensions, and reflect the overall schematic organization of ongoing experience. In order to understand how this schematic landscape is generated and how it is organized, research has examined the properties of cells that innervate the hippocampus. Indeed these properties must either be generated within the hippocampus, or are passed on to the hippocampus from surrounding cortex (Eichenbaum, 2014). This search has led to the cataloging of firing fields in the medial and lateral entorhinal cortices.

As outlined above in the anatomy section, the medial and lateral entorhinal cortices are terminal nodes in two segregated processing streams. The MEC receives input from brain regions responsible for spatial orientation and movement related perception, whereas the LEC receives input from regions that join multimodal inputs to define the features that comprise objects and creatures. From these two regions, spatial and non-spatial information converge onto cells at all stages of the hippocampal trisynaptic loop.

1.7.1 The medial entorhinal cortex

The response properties of MEC cells are in accordance with its ascribed spatial function. Within the MEC, units may respond to boundaries, head directions, and other physical determinants of space. Cells that respond when a rat encounters a physical boundary such as a wall are called border cells (Solstad, Boccara, Kropff, Moser, & Moser, 2008). Head direction cells fire only when the rat is facing a specific topographic direction, and are located throughout the spatial processing stream (Burgalossi et al., 2011). Grid cells show incredible spatial modulation such that they contain firing fields that are organized in a grid like lattice across an open enclosure (Hafting, Fyhn, Molden, Moser, & Moser, 2005). Groups of grid cells form modules, such that within a module the spacing and orientation between each cells firing fields but not their locations are coherent across the population (Stensola et al., 2012). Moreover, individual units within the MEC may exhibit conjunctive head direction, velocity, and grid selectivity (Sargolini et al., 2006). These observations have reinforced the theory that the MEC specifically processes spatial information, but a lack MEC involvement in non-spatial processing has not been reported. Thus, it remains unclear whether the MEC can exhibit object-selective activity.

1.7.2 The lateral entorhinal cortex

LEC unit activity has been less well describe in the literature, however reports are consistent with its role in processing non-spatial information. In contrast to the MEC, the LEC exhibits poor spatial selectivity in open environments (Hargreaves, Rao, Lee, & Knierim, 2005). A similar dichotomy between the Medial and lateral entorhinal cortices

was described by Jim Knierim and colleagues, wherein LEC ensembles track local cues whereas MEC ensembles track distal cues (Neunuebel, Yoganarasimha, Rao, & Knierim, 2013). In line with a local object framework, firing fields can be observed in the LEC at the location of objects within an enclosure (Wang et al., 2018). When space is controlled, object and odor responsive fields are well documented in the LEC and show a wide range of responses. Some units in the LEC may respond to a single odor or object, others may respond to only new, or misplaced objects, and yet other cells may respond to multiple objects in a graded fashion (Young, Otto, Fox, & Eichenbaum, 1997). One class of cells in the LEC that has intrigued memory researchers is the object trace cell that exhibits firing fields in the locations where objects have been removed (Tsao, Moser, & Moser, 2013). This suggests that the LEC may process spatial information, but only where there is relevant non-spatial information. Together these data suggest that units in LEC generate firing fields centered on local objects, but also exhibit mnemonically relevant activity patterns that might include space.

1.7.3 Time in the MEC and LEC

As outlined above, hippocampal units organize activity across mnemonic delays by generating firing fields that are sequentially active. There are two strong hypotheses for how such a sequence of firing fields becomes bound to a sequence of events. On the one hand, pre-organized recurrent activity may generate a template onto which external stimuli may be bound and later recalled. On the other, a slowly evolving time code elsewhere in the brain provides the input necessary for the generation of time cell like pointers along the dimension of time (Eichenbaum, 2014).

While the MEC is the most likely candidate for the source of spatial information in the hippocampus, and the LEC for non-spatial, it remains unclear how these inputs generate hippocampal firing fields sensitive to the conjunction of space, events, and time all together. The existing literature has suggested largely non-overlapping functions of the medial and lateral entorhinal cortex (Van Cauter et al., 2013). Aside from spatial and non-spatial processing, studies have shown that the MEC is capable of organizing firing fields over short delays, whereas the LEC is capable of organizing firing activity across extended time (Kraus et al., 2015; Tsao et al., 2018). Aside from examining different time scales, these studies also describe different firing characteristics of single units. MEC units observed across a mnemonic delay appeared to have multi-peaked firing fields that centered on moments during the delay. Conversely, LEC units observed over minutes and hours exhibited slowly decaying, or slowly firing rates across time. These studies leave open the question of whether the LEC also represents time at a finer scale, and whether it does so via sequences similar to those exhibited in the dorsal hippocampus and MEC.

Chapter 2. Complementary Functional Organization of Neuronal Activity Patterns in the Perirhinal, Lateral Entorhinal, and Medial Entorhinal Cortices[a]

2.1 Abstract

Abstract: It is commonly conceived that the cortical areas of the hippocampal region are functionally divided into the perirhinal cortex (PRC) and the lateral entorhinal cortex (LEC) that selectively process object information and the medial entorhinal cortex (MEC) that selectively processes spatial information. Contrary to this notion, in rats performing a task that demands both object and spatial information processing, single neurons in PRC, LEC, and MEC, including those in both superficial and deep cortical areas and in grid, border, and head direction cells of MEC, have a highly similar range of selectivity to object and spatial dimensions of the task. By contrast, representational similarity analysis of population activity reveals a key distinction in the organization of information in these areas, such that PRC and LEC populations prioritize object over location information whereas MEC populations prioritize location over object information. These findings bring to the hippocampal system a growing emphasis on

---

[a] This chapter was published in Journal of Neuroscience as the following manuscript:
Keene, C. S., Bladon, J., McKenzie, S., Liu, C. D., O'Keefe, J., & Eichenbaum, H. B. (2016). Complementary Functional Organization of Neuronal Activity Patterns in the Perirhinal, Lateral Entorhinal, and Medial Entorhinal Cortices. The Journal of Neuroscience, 36(13), 3660–3675. https://doi.org/10.1523/JNEUROSCI.4368-15.2016
All contributing authors including Christopher S. Keene have given expressed consent for its inclusion in this dissertation. Author Contributions: CSK & HBE designed the experiment, CSK, JHB, CDF & JO acquired the data, CSK, JHB & HBE analyzed data with help from SM, and CSK, JHB & HBE wrote the manuscript.

population analyses as a powerful tool for characterizing neural representations supporting cognition and memory.

2.2 Introduction:

A main theme in the functional anatomy of the medial temporal lobe (MTL) memory system has emphasized input pathways composed of extensions of the classic "what" and "where" streams that converge within the MTL (Davachi, 2006; Diana, Yonelinas, & Ranganath, 2007; Eichenbaum et al., 2007; Strange, Witter, Lein, & Moser, 2014). One pathway involves inputs from sensory and association areas that enter the MTL via the perirhinal cortex (PRC) and then the lateral entorhinal cortex (LEC) where information about objects and events is represented (Amaral & Witter, 1989; Burwell & Amaral, 1998; Burwell et al., 1995; Kerr, Agster, Furtak, & Burwell, 2007; van Strien et al., 2009). The other pathway involves inputs from spatial processing areas that enter the MTL via the parahippocampal (in primates; postrhinal in rodents) cortex (PHC) and then the medial entorhinal cortex (MEC) where information about spatial context is represented. While there are connections between the PRC-LEC and PHC-MEC areas, most emphasize that the two streams converge primarily within the hippocampus where objects and events are represented in spatial context. This simple model has recently been challenged by reconsiderations of the functional distinctions between LEC and MEC that suggest a mixture of object and spatial processing functions in these areas (Knierim, Neunuebel, & Deshmukh, 2013; Morrissey & Takehara-Nishiuchi, 2014; Sasaki, Leutgeb, & Leutgeb, 2015).

Here we examine object versus spatial coding in PRC, LEC, and MEC, respectively, as embodied in this model. Studies on MEC have highlighted "grid cell" neurons that fire with spatial periodicity throughout an environmental context (Hafting et al., 2005), as well as neurons that encode head direction and spatial borders (Moser et al., 2014; Sargolini et al., 2006). Notably, the observation of prominent spatial coding is almost exclusively from studies of animals foraging in an open field in the absence of salient non-spatial stimuli or task demands. By contrast, LEC neurons exhibit little spatial specificity in this behavioral situation (Hargreaves et al., 2005) and PRC neurons exhibit none (Deshmukh, Johnson, & Knierim, 2012). Conversely, in experiments where animals perform object recognition or discrimination tasks, PRC and LEC neurons fire during the presentation of specific odor (in rats) or visual (in monkeys) cues, during maintenance of non-spatial memories, or associated with behavioral responses, but firing patterns associated with the animals' location in space were not examined (Ahn & Lee, 2015; Brown & Banks, 2015; Igarashi, Lu, Colgin, Moser, & Moser, 2014; Suzuki, Miller, & Desimone, 1997; Young et al., 1997). Some recent studies have identified activity in PRC and LEC neurons associated with objects or visual patterns in particular places as animals explore an open field (Deshmukh et al., 2012; Deshmukh & Knierim, 2011; Tsao et al., 2013) or traverse a circular path in a maze (Neunuebel et al., 2013). In these studies the objects and visual cues were not associated with specific behaviors or rewards and the only behavioral demand was movement through the environment in which these cues were positioned. So, it is unclear whether the objects and visual cues

were encoded as specific non-spatial stimuli independent of their locations or as among the stimuli composing distinct spatial representations of a changing environment.

In the present study we examined the activity patterns of PRC, LEC, and MEC neurons and neuronal populations in animals performing a task in which they were required to use the current spatial context to associate objects with reward or non-reward at multiple locations within each context. This task demanded the animals to attend to the environmental cues and to the objects independent of their location in an environment, as well as to employ the spatial context to guide retrieval of object-reward associations.

2.3 Materials and methods

Subjects.

Subjects were 10 Long-Evans rats (Charles River) weighing between 300-325 grams at the start of the experiment. All animals were single housed and maintained on a 12 h light/dark cycle (lights on 8:00 A.M. to 8:00 P.M.). Behavioral training and testing were conducted exclusively during the light phase. Animals were maintained at a minimum 85% of their ad libitum feeding body weight and had ad libitum access to water in the home cage. Procedures were conducted according to the requirements set by the National Institutes of Health (NIH) and Boston University Institutional Animal Care and Use Committee.

Materials and apparatus.

The behavioral training environment was a custom-built apparatus (160 l x 60 w x 40 h cm) consisting of two 40 cm x 40 cm boxes connected by a central alley. The training apparatus was surrounded by black curtains which limited the availability of distal cues. Each context was composed of unique visual and tactile cues. The objects consisted of identical terra cotta pots (10 cm high with an internal diameter of 9 cm), with unique digging media and odors (e.g., purple beads with grapefruit scent). To prevent the animal being guided by the smell of the Froot Loop, the pots and digging media were sprinkled with crushed Froot Loops. An open field environment (1 m x 1m) was used to examine spatial firing patterns of cells following behavioral training.

Behavioral task.

Rats were trained to perform the complete behavioral paradigm through successive stages. Initially, rats were trained to dig for a reward (one-quarter Froot Loop) buried in a pot filled with unscented sand. Once rats reliably retrieved buried rewards, they were trained on a simple odor discrimination task in their home cages. Two pots filled with sand each scented with a distinct odor (aloe and cloves) were simultaneously presented to the rat in pseudorandomized left or right positions. The aloe-scented pot was always rewarded, while the cloves-scented pot was never rewarded. Simple odor discrimination continued until the rats reached a criterion of 80% correct across 20 consecutive trials. Upon reaching criterion, rats were habituated to the testing apparatus during a 30 min exploration period with Froot Loops scattered throughout the environment and all context dividers removed. Following habituation, behavioral training in the complete task ensued.

The behavioral training environment consisted of two chambers composed of unique visual and tactile cues on the floors and walls connected by a central alleyway that allowed rats to shuttle between them, with access restricted to one context per trial (Figure 1). The objects consisted of identical terra cotta pots with unique digging media and odors (e.g., purple beads with grapefruit scent), which could be presented in either of two pseudorandomized positions for a given trial where the rat was restricted to a single context. Rewards in the form of one-quarter Froot Loop (Kellogg's) were buried in the rewarded pot on each trial. After reaching behavioral criterion, 10 rats were implanted with microdrives targeting PRC, LEC, or MEC (five PRC, four LEC, and four MEC with 3 microdrives yielding both PRC and LEC data in the same rats). Following recovery, neuronal activity in perirhinal or entorhinal cortex was monitored in rats during the retrieval of memories where two distinct environmental contexts (1 and 2) predicted different reward expectations for behavioral responses to two distinct objects (A and B) presented in either of two positions within each context. It is important to note that context, but not position within a context, was predictive of object-reward associations. When presented at either position in Context 1, choosing object A was rewarded and choosing object B was not rewarded, whereas in Context 2, choosing object B was rewarded and not A (Figure 1). Positions within a context shared the same object-reward association, whereas comparisons across context reflected opposing object-reward associations. Each session consisted of two contexts with two paired odor/digging media combinations, but new sets of contexts and stimuli were introduced throughout training in the same order across all rats. After each behavioral training session, rats were allowed

to explore an open field environment while foraging for Froot Loops which was later used to examine spatial firing patterns of cells in MEC.

Each session consisted of 90 trials, 45 in each context. In a typical trial, the animal was allowed to enter and explore one of the contexts in the absence of objects for 10 seconds. At the end of this context exploration period, a divider was inserted in the middle of the context restricting the rat to one half of the context while two pots (Objects A and B) with unique digging media and odors were placed in the corners behind the divider. The divider was then removed, allowing the rat to approach the pots where it could choose to dig in the pot or refrain from digging and sample the other pot. The beginning of object sampling was defined as the moment in time when the rat's nose crossed the threshold of the pot rim. Object position within each context was pseudo-randomized, and no object occurred in the same location for more than three consecutive trials. After most trials, the animal moved into the opposite context via the alleyway. However, on 9 trials for each session, the animal remained in the same context for an additional trial to prevent utilization of a strict alternation strategy. On these trials, the pots were removed, the rat remained in the same context, and the context exploration period began, after which the divider was inserted and testing resumed as previously described. Prior to drive implantation, rats were trained to criterion, which was defined as correct performance on 70% of trials in each context over a 20 trial block. Following implantation, rats were re-trained to criterion and given at least two overtraining sessions prior to initiation of electrophysiological recordings. As recordings progressed, rats were trained on new object-context association problems that involved novel digging mediums

and contextual cues. Following the initial learning session in which criterion performance was obtained on a new problem, animals were presented with the same problem in a number of additional overtraining sessions, which provided the data for this study.

Surgery.

Anesthesia was induced by inhalation of 5% isoflurane (Webster Veterinary Supply) in oxygen and was maintained at 2-3% throughout surgery. Prior to surgery, animals were injected with the analgesic Buprenex (Buprenorphine hydrochloride, 0.03 mg/kg IM; Reckitt Benckiser healthcare Ltd.), an antiobiotic Cefazolin (330 mg/ml IM; West-Ward Pharmaceutical Corp.), and placed in a stereotaxic frame (Kopf), where an incision was made along the midline to expose the skull. Animals were implanted with microdrives that contained 18-24 independently drivable tetrodes aimed at the junction of perirhinal and lateral entorhinal cortex (centered at anteroposterior AP = -6.92 mm; mediolateral ML = 5.2 mm; 16-20° lateral angle, varied to more directly target LEC at 16° and PRC at 20°) or the dorsocaudal portion of medial entorhinal cortex (anteroposterior AP = -8.0 mm; mediolateral ML = 4.6 mm; 25° angle from anterior to posterior; all coordinates derived from (Paxinos & Watson, 1997)). Each tetrode was composed of four 12 μm RO 800 wires (Sandvik Kanthal HP Reid Precision Fine Tetrode Wire; Sandvik Company, Palm Coast, FL) gold-plated to reduce impedance to between 180 and 220 kΩ at 1 kHz. At the end of surgery, all tetrodes were lowered ~5 mm and ~2 mm into tissue, in PRC-LEC and MEC, respectively. In addition, animals were

injected with post-operative doses of Buprenex and Cefazolin as described above. Animals were allowed to recover for one week before behavioral testing resumed.

Neural Recordings.

Electrophysiological recordings were collected using a 96 channel OmniPlex D Neural Data Acquisition System (Plexon Inc.). Each channel was amplified and band-pass-filtered for both single unit activity (154 Hz-8.8 kHz) and local field potentials (1.5 Hz-400 kHz). Spike channels were referenced to a local electrode in the same region to remove movement related noise. Action potentials were detected by threshold crossing and digitized at 40 kHz. Cineplex Studio (Plexon Inc.) was used for video recording of behavioral training sessions. Single units were isolated using Offline Sorter (Plexon Inc.), and behavioral events were time-stamped using Cineplex Editor (Plexon Inc.). All data analysis was performed using custom scripts for MATLAB (MathWorks). To reduce the likelihood of recording from the same neurons across multiple sessions, tetrodes were lowered prior to each testing session (~0.18 mm or more), and the amount which a tetrode was lowered was based on a visual inspection of the identified units. In order to maximize unit quality, a score of 1 to 10 was generated for each unit based on the separation of each cluster from neighboring clusters and the background noise. Only units with a score of 5 or above were included in the analysis presented here.

Histology.

Upon completion of behavioral testing, rats were anesthetized under 5% isoflurane in oxygen and tetrode placements were confirmed by creating a lesion at the tetrodes tip by passing a 40 μA current until the connection was severed on each wire.

Animals subsequently received an overdose injection of Euthanol (Virbac AH, Inc.) and were perfused intracardially with 0.9% saline followed by 10% formalin phosphate (VWR). Brains were removed and placed in a 20% sucrose solution until processed. Using a cryostat (Leica CM 3050s; Leica Biosystems), brains were cut into 40 μm sections (coronal for PRC-LEC, sagittal for MEC), mounted onto presubbed glass slides, and stained with cresyl violet to determine the location of tetrode tip lesions and tetrode tracks. The stereotaxic atlas of Paxinos & Watson (2007) was used to confirm the localization of tetrode tip lesions within LEC and MEC. This information was used in conjunction with driver turn counts to estimate the neuronal layer for each recording, with each unit categorized as either superficial (layers II and III) or deep (layers IV-VI) for PRC, LEC, and MEC, as well as to distinguish between Areas 35 and 36 in PRC.

Analysis

***Single neuron analysis*.**

Rats could sample the two objects presented on each trial multiple times, and all object sampling events in which the rat dug in the rewarded pot and refrained from digging in the non-rewarded pot were considered in our analysis. To estimate the entorhinal representation of every object sampling event, for each cell the number of spikes fired was counted for up to the first 1.5 s of object sampling and this count was divided by the sampling duration to give the average firing rate for each cell on each object sampling event.

Selectivity Index for individual neurons.

Firing rates during object sampling were calculated as the number of spikes as a function of the time from the onset of object sampling when the animal's snout begins to cover the rim of the pot until the animal began to dig or turn its head away from the pot, using event markers in the video recordings. As previously described (Komorowski, et al., 2009), object, position, and context selectivity for each neuron were measured using a selectivity index (SI) calculated as:

$$SI = \frac{(n - \sum_{i=1}^{n} (\lambda_i / \lambda_{pref}))}{n-1}$$

where *n* is the number of conditions for the dimension under study (e.g., two in the case of objects, four in the case of positions), λ_i is the average firing rate of the neuron for the *i*th possible event type, and λ_{pref} is the average firing rate of the neuron in the condition associated with highest firing rate for the dimension under study. SI = 1 if a cell fired for only one condition. Conversely, SI = 0 if the cell fired equally under all conditions. To test whether the SI values for individual units were larger than that expected by chance, we compared each observed SI value against a distribution of 10,000 SI scores in which the object and/or position identities of all events were randomly shuffled for each session individually. Cells were defined as significantly selective for a dimension if $p < 0.01$ for the observed SI value relative to the shuffling distribution. This analysis was performed for each of four dimensions (Figure 5A and 5B): (1) For context SI, firing rates were compared between the two context conditions; (2) For position SI, firing rates were

compared between the four position conditions; (3) For object SI, firing rates were compared between the two object conditions; (4) For object-position SI, firing rates were compared among the eight object-position combinations (two objects in each of two positions in two contexts).

To further evaluate the observed average SI values for each dimension for each region, we employed a similar bootstrap shuffling procedure. In this case, we shuffled the object and/or position identities for each trial 1,000 times per session. Thus, the observed firing patterns were maintained, albeit with shuffled object and/or position identities. The average values of this shuffling distribution (dotted lines in Figure 5A) reflect a stringent criterion against which we compared the observed average SI values for each dimension for each region to determine significant coding for task dimensions. All post-hocs for SI comparisons utilized a Wilcoxon rank-sum test with a Bonferroni correction for multiple comparisons (significance threshold of $p = 0.05/4$ dimensions = 0.0125) to determine significance.

Characterization of spatial firing patterns of individual neurons.

We additionally examined the spatial firing properties of MEC neurons as animals foraged in an open field, particularly to identify grid cells, border cells, and head direction cells. After each testing session we continued to collect data from the same neurons (see waveforms in Figure 4) as the animals foraged for randomly sprinkled Froot Loop bits in an open field environment over a period of 20 mins. Spatial firing rate maps were estimated using the total number of spikes that occurred when the rat was at a given location (3 x 3 cm bins) divided by the total time spent in that bin. Only bins visited at

least twice for a total time of at least 200 ms were included. Spikes were included if the rat was moving at a velocity > 3 cm/sec. Spatial firing maps were smoothed with a 2D Gaussian filter ($\sigma = 1$ pixel).

Grid scores were calculated using previously established methods (Brandon et al., 2011). Briefly, the six surrounding peaks of the autocorelogram of the smoothed rate map for each cell were identified, and the rate map was corrected for the ellipse of the hexagon. Then, the rotational symmetry of a circular donut of pixels encompassing the six identified peaks was calculated at 30, 60, 90, 120, and 180 degrees. The minimum difference in symmetry of 60 and 120 degrees to that at 30, 90, 120, and 180 degrees was then calculated as the raw grid score. A bootstrap confidence measure of the grid score was adopted (Bonnevie et al., 2013). We calculated the grid score as above for each cell 10,000 times after the spike timestamps were shuffled while preserving the temporal structure of the spike train. A unit was classified as a grid cell if the observed gridness score surpassed the critical threshold of $p = 0.01$ compared to the shuffled distribution.

Similarly, border scores were calculated using methods described previously (Solstad et al., 2008). For each cell, its place fields were defined as contiguous groups of pixels in the smoothed rate map that had a firing rate of at least 30% of the maximum firing rate pixel. Then, the ratio of the place field's coverage of each wall to that place field's average distance from that wall was calculated to represent the border score. Border cells were designated as those with border scores above 0.4 for any of the four walls.

In order to determine the animal's head direction, tracking coordinates for the LED were first smoothed to estimate the animal's location for any missing tracking frames. Then, the angle of displacement was calculated by taking the arc tangent of the difference in coordinates recorded at 40 Hz, providing a heading estimate. As with grid cells, for each cell the spike timestamps were shuffled 10,000 times while preserving the temporal structure of the spike train. The number of spikes at each head direction (in 5 degree bins) was then summed and divided by the total occupancy of that head direction. The length of the resultant vector was then compared to the shuffled distribution. Units with an observed vector length below the critical threshold of $p = 0.01$ were considered head direction cells.

Representational Similarity Analysis (RSA) of neural ensemble activity patterns.

Neural ensemble firing patterns were explored using a representational similarity analysis (RSA) to determine the extent to which multiple task dimensions were encoded by PRC, LEC, and MEC (Kriegeskorte, 2008; McKenzie et al., 2014). To measure the similarity of ensemble representations of different object sampling events, the average z-normalized firing rate for each neuron was calculated for all object sampling. A population vector was then composed for every sampling event based on these normalized rates, and the population vector of each event was then correlated to that for all other events, and then the correlation coefficients of similar comparisons (e.g. all comparisons between events involving different objects of the same value in the same position) were averaged, yielding a pattern of correlation coefficients that reflects the

degree of similarity or separation of population representations between events that differ in multiple task dimensions, and these patterns were similar in each subject (Figure 6). Using the pooled correlations from all sessions for all rats within a brain region (PRC, LEC, or MEC), we calculated the strength of the coding dimension (e.g., object in position) using the ensemble correlations. We first compared the average correlation for events within a given condition (e.g., all sampling events in the same position with Object A) for a task dimension versus events that were between conditions for that dimension (e.g., events in the same position with Object A versus Object B). In this manner, a single d′ was calculated for each dimension as follows:

$$d' = \frac{\mu_w - \mu_b}{\sqrt{\frac{1}{2}(\sigma_w^2 + \sigma_b^2)}}$$

Where, μ_w is the mean correlation coefficient for within condition events for that dimension with variance, σ^2_w, and μ_b is the mean correlation coefficient for between condition events with variance, σ^2_b. The observed d′ was compared to bootstrapped data in which event identities were randomly shuffled 10,000 times and then the correlation analysis and d′ metric for each bootstrap sample were recomputed. When the observed d′ was larger than 95% of the 10,000 shuffled d′ metrics, the dimension captured by the d′ was considered to have been significantly coded by the perirhinal or entorhinal cortices. We used the d′ metric to measure the separation of the distributions of the correlation coefficients for specific task features from zero or against the distribution of coefficients

from an appropriately opposing condition to characterize the population signal of that feature. Conjunctive object-position coding was defined as the d′ distance between correlation coefficients for events that involved that same object in the same position versus events that involved different objects at the same position (Figure 5D Obj*Pos). Object coding was defined as the d′ distance between correlation coefficients for events that involved the same object at different positions versus events that involved different objects at different positions within the same context (Figure 5D Object). Position coding was defined as the d′ distance between correlation coefficients for events at the same position versus events at different positions within the same context (Figure 5D Position). Context coding was defined as the d′ distance between correlation coefficients for comparisons among events in the same context at different positions versus that for all events in the opposing context (Figure 5D Context). All post-hoc d′ comparisons utilized a Bonferroni correction for multiple comparisons (significance threshold of $p = 0.05/4$ dimensions $= 0.0125$) to determine significance.

Cosine Vector Analysis.

To ensure the robustness of the findings in the d′ distance analysis, ensemble representations were also analyzed using the cosine between population vectors to determine the similarity of representations. First, firing rates for each neuron were normalized to the maximum firing rate among all object-sampling events to create a population vector of normalized rates for each event. Then, a cosine score was calculated as 1 - the cosine of the included angle between points made by the pairs of vectors for the comparison of each event to all others of the same type. Strength of a coding dimension

was calculated by comparing the mean cosine score for events within versus between sample conditions for that dimension. As with the RSA analysis, d′ distances were calculated for the cosine scores for the comparisons described in the previous paragraph.

Bayesian Classifier.

As a separate test of event similarity that had a different set of assumptions, a naïve Bayesian classifier was used (MATLAB R2014b function with type set to determine the probability that a pattern of neural activity was recorded for each object and place combination, two objects in four positions; as in McKenzie et al., 2014). Due to uneven sampling, rats often preferred a particular object and position combination and would sample those more often. Therefore, we only considered the last 5 sampling events for each object and place combination. When there were fewer than 5 events, that category of object and position trial was eliminated. Next, the z-scored population vector was calculated for each event, as described above. The dimensionality of the ensemble representation for each event was reduced via principal component analysis (PCA) and only the first four components were used to categorize object/position combinations. Then, the mean, variance, and covariance of each object/position four-dimensional ensemble representation was estimated with one event missing from each object and position combination. Next, a multidimensional normal distribution with the estimated means, variance, and covariance matrices were fit to each cluster of object/position ensemble representations (maximum 8). Finally, the probability of the missing events being any of the possible object/position combinations was calculated based on the

probability of that object/position combination given the ensemble representation as estimated by the normal distributions above.

The degree of dimensional coding was calculated in a similar fashion to that for the correlation coefficients and cosine analysis, though the d′ was calculated based on the probability of classifying within each dimension (e.g., events occurring at the correct position) or across that dimension (e.g., events occurring at a different position). To test significance, we ran a bootstrap analysis in which event identities were shuffled 10,000 times, and if the observed d′ for the difference in probabilities was greater than 95% of the shuffled d′ metrics, we concluded that PRC, LEC, or MEC encoded that dimension.

Temporal Dynamics of Population Firing Patterns.

To assess when coding for different task dimensions emerged during object sampling, the d′ metric was calculated exactly as with the correlation RSA, except that d′ strength was calculated for 200 ms time bins centered ± 3s around object sampling (Figure 8). In order to control for the rats' position in space during the approach to objects, we considered only the first object-sampling event of each trial. Significance testing of the observed d′ values was performed using the d′ bootstrap analysis at each time point with a significance threshold of $p = 0.05$.

Dendrogram Analysis.

To explore the organization of ensemble representations for the 8 types of object sampling events (i.e., conjunctions of 2 objects in 2 positions within 2 contexts), we generated composite ensemble representations for each event type using the firing rates of all principal neurons recorded in PRC, LEC and MEC. The composite

population vector for each type of event was calculated as follows: for each neuron the number of spikes observed was divided by the sampling duration on each event, then these firing rates were standardized into z-scores using the mean and standard deviation of firing rates across events, then the mean z-score firing rates across events were calculated. The relationships between the composite population vectors for the 8 types of events were then assessed using an agglomerative hierarchical clustering algorithm (MATLAB R2014b function 'linkage'). The agglomerative hierarchical clustering algorithm takes the unweighted average distance between pairs of the 8 vectors, where the Pearson's correlation coefficient was used as the distance metric. Of the 8 vectors, the two that were nearest were combined, then calculations of distances between the revised set of vectors was repeated and nearest two vectors were combined. This process was repeated iteratively until only two combinations remained. The height of each line in the dendrogram represents the similarity (mean r value) between the event types being connected.

2.4 Results

2.4.1 Behavioral performance

We recorded activity from neurons in PRC, LEC, and MEC while rats performed a context-guided object-reward association task that required subjects to select one of two objects presented simultaneously within each of two distinctive spatial contexts differing in multiple features (Figure 2). When presented in Context 1, Object A was rewarded in either of two positions, and Object B was not. When presented in Context 2, Object B

was rewarded in either position, and Object A was not. Context, but not position within context, was predictive of object-reward association in this task. Thus, subjects were required to use the current context to guide learning and retrieval of distinct associations for the same objects. Several different problems consisting of different contexts and objects were successively employed (but will all be referred to here as Context 1 and 2 and Objects A and B). In the initial learning session on each problem, rats reached the performance criterion of 70% correct in each context within a 20 trial block on average by trial 38 (range, 30-44 trials) for PRC implanted rats (n = 5), by trial 34 (range, 11-45 trials) for LEC implanted rats (n = 4), and by trial 38 (range, 17-70 trials) for MEC implanted rats (n = 4), respectively. A one-way ANOVA on the average trials to criterion revealed no differences in the rate at which rats learned new problems (F (2, 11) = 0.08, p = 0.91). Subsequently, animals performed in overtraining sessions on each problem where performance was 96.4 ± 1.0% for PRC implanted rats, 97.0 ± 0.8% for LEC implanted rats, and 94.2 ± 1.3% for MEC implanted rats. A one-way ANOVA on performance in overtraining sessions revealed no differences (F (2, 58) = 1.49, p = 0.23). In this study, data analysis focused on these overtraining sessions (14 for PRC, 17 for LEC, 30 for MEC).

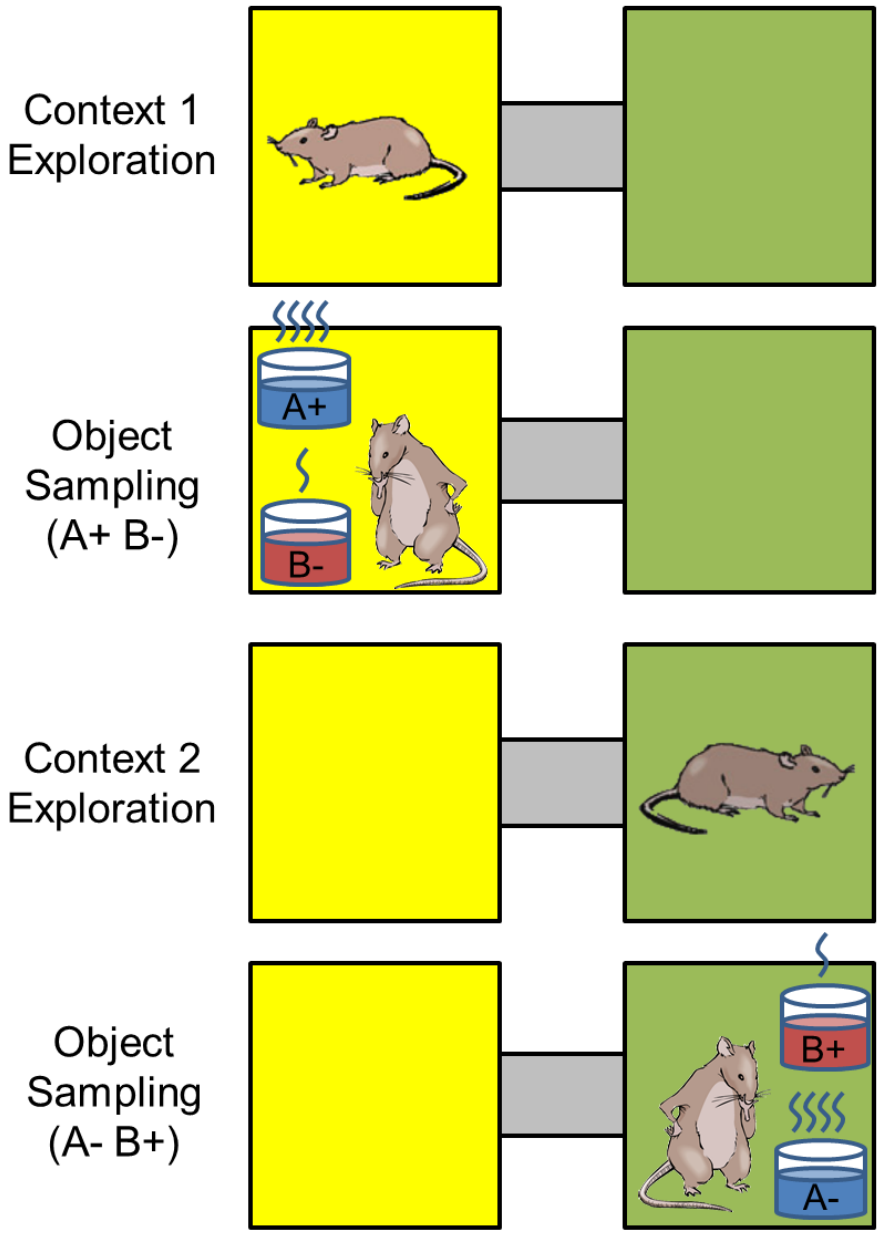

Figure 1: Context dependent object discrimination task.

Rats were trained to perform a context-guided object association task. Each context consisted of unique tactile and visual stimuli. On a typical trial, rats were allowed to explore the context for 10 s (context exploration period). Then, two objects consisting of terracotta pots with unique digging media and odors were presented in either of two positions (object sampling period). Object A, but not B, was always reinforced in either position within Context 1, whereas Object B, but not A, was always reinforced in Context 2.

2.4.2 Single neuron isolation

In five PRC implanted rats, a total of 204 units were isolated. In four LEC implanted rats, a total of 188 units were isolated. In four MEC implanted rats, a total of 323 units were isolated. A 10 Hz firing rate cutoff across the whole session was used to exclude interneurons, yielding 164 PRC neurons, 164 LEC neurons, and 236 MEC neurons for analysis (summarized in Table 1). Neurons were subdivided by whether they were recorded in superficial or deep laminae based on a combination of histological examination, driver turn counts, and maps of tetrode locations within the microdrives. The anatomical distribution of neurons recorded from PRC, LEC, and MEC is presented in Figure 2. Based on these criteria, a total of 92 deep units and 72 superficial units were identified in PRC, a total of 57 deep units and 107 superficial units were identified in LEC, and a total of 133 deep units and 103 superficial units were identified in MEC. In addition, a total of 95 units were identified in Area 35 and 69 units were identified in Area 36 within PRC. Finally, open field exploration sessions following behavioral testing were used to characterize spatial firing properties of MEC units in order to further categorize and analyze spatially heterogeneous populations of grid cells, border cells, and head direction cells. A total of 23 grid cells, 27 border cells, and 125 head direction cells were isolated and analyzed separately from the other MEC units.

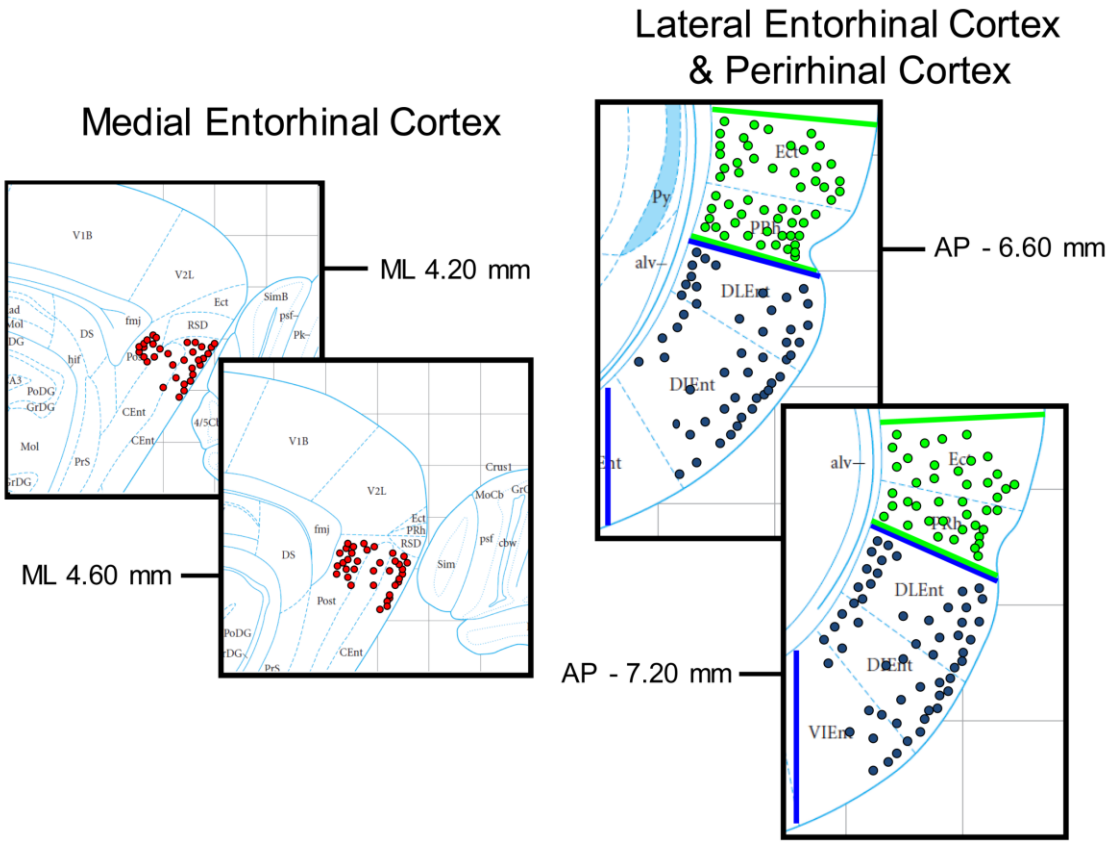

Figure 2: Recording site reconstruction.

In the left set of panels (A), red circles indicate estimated tetrode locations during neuronal recordings in MEC, whereas in the right set of panels blue circles and green circles indicate estimated tetrode locations in LEC and PRC, respectively. Inspection of histology for tetrode tracks and tetrode tip lesions were used in conjunction with driver turn counts and maps of tetrode locations to estimate tetrode locations during neuronal recordings.

2.4.3 PRC, LEC, and MEC neurons encode multiple dimensions of both object and spatial information

During the object sampling period neurons in PRC, LEC, and MEC exhibited remarkable mixed selectivity associated with multiple task dimensions both across the population of cells in each region and within single neurons. Several examples of this pattern are provided in Figure 3 where the firing pattern of each example is illustrated for

each of the eight object-position combinations, four in each context. The beginning of object sampling was defined as the moment when the rat's nose reached the rim of the pot (the 0 time point for the rasters and histograms in Figures 3 and 4) and object sampling ended when the rat either began to dig or turned away, up to a maximum of 1.5 s after onset. Mixed selectivity in each brain region was readily apparent in neurons recorded in both superficial and deep layers, as well as within all the spatially heterogeneous subpopulations within MEC (Summarized in Table 1). For example, PRC Unit 2, LEC Unit 4, and MEC Units 5 and 6 were highly selective for specific object-position conjunctions. LEC Unit 3 fired differentially during sampling of Object A relative to B across multiple positions. MEC grid cell 1 demonstrated particularly striking specificity for Object B in Position 1 of Context 1 (Figure 4). Thus, even neurons typically considered dedicated to spatial representation exhibited object selective firing in animals performing this task, and vice versa.

To quantify selectivity of neurons for features of the task, we calculated a selectivity index (Komorowski et al., 2009) for each of four task dimensions: context, position, object identity, and conjunction of object and position within a context. SI scores ranged from zero, reflecting a lack of selectivity, to 1, reflecting fully selective activation for one condition of a dimension. SI scores were calculated for each dimension in each recording session. We also examined whether the observed average SI value across all single units for each brain region was indicative of significant coding for each task dimension using a similar bootstrap shuffling procedure in which object and/or position identities were shuffled for each trial. The dotted lines in Figure 5A reflect this

bootstrap distribution. We found that each of the four task dimensions was significantly encoded in each area (all p's < 0.001; Figure 5A). Thus, there was significant position as well as object coding in PRC, LEC, and MEC, rather than the selective position coding in MEC and selective object coding in PRC and LEC as one might expect.

We also examined selectivity between brain regions by comparing average SIs in each area for each dimension (Figure 5A) and by comparing the fraction of neurons in each area that individually distinguished conditions of a particular dimension (Figure 5B). MEC neurons exhibited slightly greater average selectivity relative to PRC or LEC neurons (two-way ANOVA, main effect of region, F (2, 2796) = 19.82, $p < 0.00001$; no interaction, F (6, 2796) = 1.76, $p = 0.08$). Post-hoc tests confirmed that MEC exhibited significantly greater selectivity with respect to context (*p's* < 0.002) as well as position ($p < 0.0001$), although the magnitude of these differences is modest (Figure 5A).

In comparing the proportions of cells in different areas that code for specific dimensions, it is important to consider that the proportion of cells significantly coding for dimensions (Figure 5B), but *not* the average SI values (Figure 5A), was sensitive to increases in firing rate. Given a higher average firing rate in MEC (PRC 2.16 ± 0.19 Hz, LEC 2.08 ± 0.17 Hz, MEC 3.07 ± 0.16 Hz; $p < 0.0001$), we randomly down-sampled MEC neurons to an average firing rate equivalent to that of PRC and LEC neurons (Mizuseki & Buzsáki, 2013; Bonnevie et al., 2013). As can be seen in Figure 5B and in greater detail in Table 1, more cells in MEC significantly coded for context, position, and the conjunction of object-position information than in PRC or LEC (*p's* < 0.001), while there were no differences in proportions of cells significantly coding task dimensions

between PRC and LEC (*p's* > 0.3). Thus, although analysis of single unit properties with the selectivity index revealed some quantitative differences in selectivity, the most striking result of this analysis is that all regions exhibit substantial coding for the full spectrum of task dimensions. This observation challenges the commonly held view that PRC and LEC selectively encode object and not spatial information whereas MEC selectively encodes spatial information (Davachi et al., 2006; Eichenbaum et al., 2007).

2.4.4 Selectivity for task dimensions is similar across anatomical subdivisions of PRC, LEC, and MEC

When neurons were separated by laminar location of their recordings, superficial neurons in PRC exhibited greater selectivity overall relative to deep layer neurons (one-way ANOVA, F (1, 810) = 5.22, p = 0.02), but post-hoc tests revealed no differences between subdivisions with respect to specific task dimensions (*p's* > 0.01). In contrast, there was no difference in stimulus selectivity between Area 35 neurons and Area 36 neurons within PRC (one-way ANOVA, F (1, 810) = 0.35, p = 0.55). There was also no difference in stimulus selectivity between superficial vs deep layers within LEC (one-way ANOVA, F (1, 801) = 0.64, p = 0.42). However, within MEC, superficial neurons exhibited greater selectivity than neurons in deep layers (one-way ANOVA, F, (1, 1155) = 30.16, p < 0.0001). Post-hoc tests confirmed that superficial layers of MEC exhibited greater object-context (p = 0.003) and object-position selectivity (p = 0.003). Again, despite some modest differences in coding across laminar subdivisions, these results reflect similar coding of task dimensions across these subdivisions.

Furthermore, contrary to the common emphasis on spatial coding in MEC grid and border cells, we found that grid cells, border cells, and head direction cells exhibited selectivity for all task dimensions, including those involving object selectivity (see bottom half of Table 1; all *p's* < 0.01). Indeed the selectivity of these spatial coding cells was greater than that of the remaining MEC population (two-way ANOVA, F, (3, 1310) = 19.62, $p < 0.0001$). Post-hoc tests confirmed that grid cells and head direction cells exhibited greater selectivity for all task dimensions (p's < 0.01) relative to the remaining MEC population, other than object coding for grid cells ($p = 0.42$) and context coding for head direction cells ($p = 0.015$). Border cells exhibited similar selectivity to the remaining MEC population (*p's* > 0.06), and there were no differences in selectivity between the spatial cell groups (*p's* > 0.01). Given that many grid cells and border cells also exhibit significant head direction modulation, we also compared selectivity between a combined group of grid cells and border cells without head direction modulation against that of cells with significant head direction coding only and found no differences in selectivity between these groups (*p's* > 0.01; see Table 1 for more information). Thus, spatial selectivity properties (identified during open field foraging) may contribute in part to the identification of contexts, positions, and objects during memory performance, although all these dimensions are substantially encoded even by cells that lack the specific spatial firing properties observed during open field.

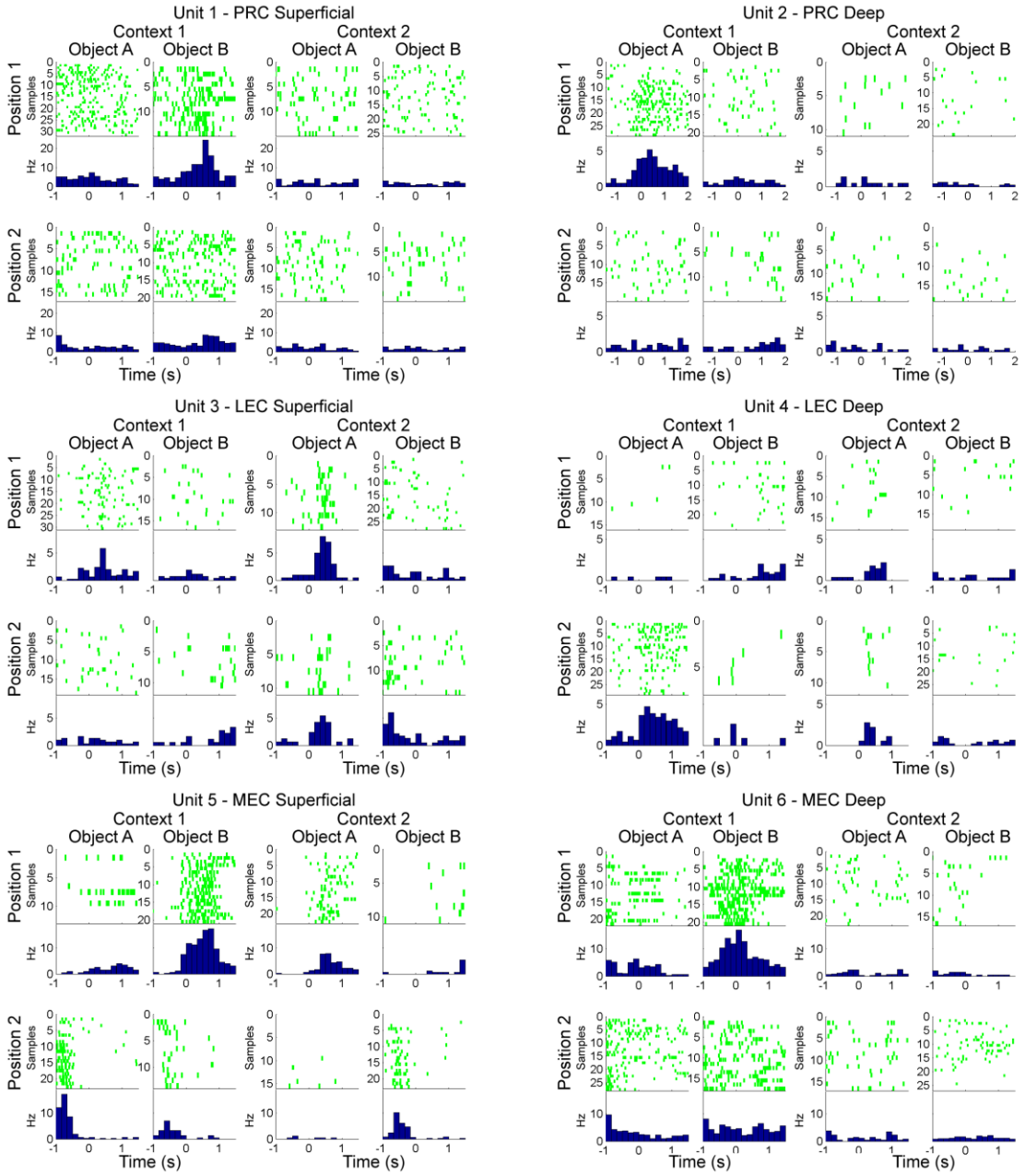

Figure 3: Examples of neuronal firing patterns during object sampling.

Rasters and perievent histograms depict activity patterns during the sampling of each Object (A or B) at each Position (1 or 2) within each Context (1 or 2). Time 0 indicates the onset of object sampling. Histograms represent firing rates in 167 ms time bins. Observed SI (top row for each unit below) and statistical significance as determined by comparing observed SI values against bootstrapped distribution (significance level $p < 0.01$):

Unit 1: C = 0.71; P = 0.66; O = 0.35; O-P = 0.80.

Unit 1: C $p < 0.0001$; P $p < 0.0001$; O $p = 0.04$; O-P $p < 0.0001$.

Unit 2: C = 0.78; P = 0.78; O = 0.74; O-P = 0.83.

Unit 2: C $p < 0.0001$; P $p < 0.0001$; O $p = 0.0001$; O-P $p < 0.0001$.

Unit 3: C = 0.50; P = 0.37; O = 0.62; O-P = 0.73.

Unit 3: C $p = 0.002$; P $p = 0.11$; O $p < 0.0001$; O-P $p < 0.0001$.

Unit 4: C = 0.44; P = 0.79; O = 0.79; O-P = 0.81.

Unit 4: C $p = 0.03$; P $p < 0.0001$; O $p < 0.0001$; O-P $p = 0.0002$.

Unit 5: C = 0.77; P = 0.91; O = 0.82; O-P = 0.92.

Unit 5: C $p = 0.0001$; P $p < 0.0001$; O $p < 0.0001$; O-P $p < 0.0001$.

Unit 6: C = 0.84; P = 0.78; O = 0.57; O-P = 0.82.

Unit 6: C $p < 0.0001$; P $p < 0.0001$; O $p = 0.0004$; O-P $p < 0.0001$.

Abbreviations: C = Context, O-C = Object-Context, O = Object, O-P = Object-Position, P = Position.

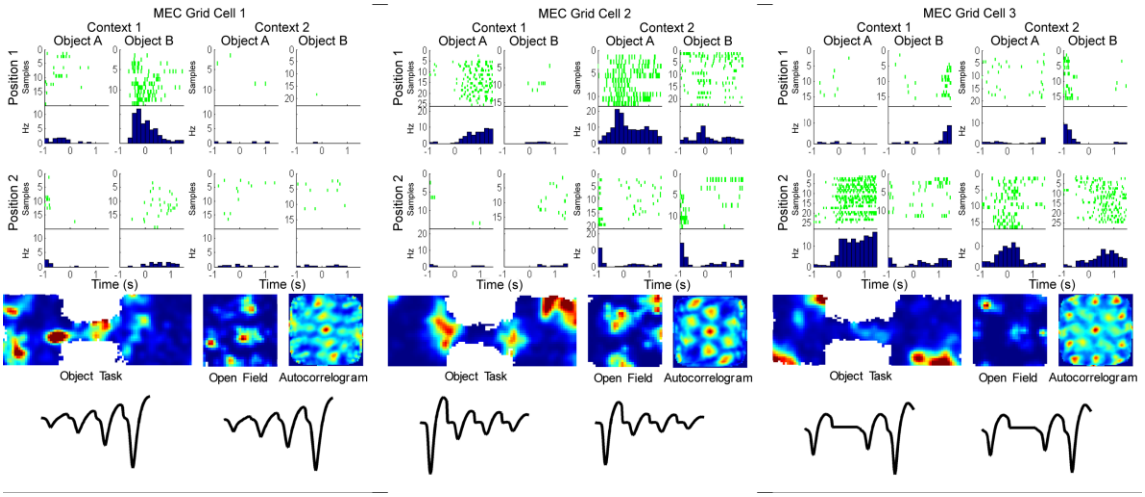

Figure 4 Examples of neuronal firing patterns for grid cells.

Object sampling Rasters and perievent histograms (top half) for grid cells shown as in Figure 3. In the bottom half of each example, from left to right are firing rate maps for the entire session of the behavioral task, the open field session, and an autocorrelogram for the open field session. Below that are the average tetrode waveforms for spikes isolated during the behavioral (left) and open field (right) sessions, respectively.

Observed SI (top row for each unit below) and statistical significance as determined by comparing observed SI values against bootstrapped distribution (significance level p < 0.01):

Grid Cell 1: C = 0.91; P = 0.89; O = 0.94; O-P = 0.96; grid score = 0.15.

Grid Cell 1: C *p* = 0.0004; P *p* = 0.0003; O *p* < 0.0001; O-P *p* < 0.0001.

Grid Cell 2: C = 0.31; P = 0.64; O = 0.23; O-P = 0.83; grid score = 0.42.

Grid Cell 2: C *p* = 0.14; P *p* = 0.0001; O *p* = 0.29; O-P *p* < 0.0001.

Grid Cell 3: C = 0.31; P = 0.76; O = 0.50; O-P = 0.80; grid score = 0.36.

Grid Cell 3: C *p* = 0.14; P *p* < 0.0001; O *p* = 0.007; O-P *p* < 0.0001.

Abbreviations: C = Context, O-C = Object-Context, O = Object, O-P = Object-Position, P = Position.

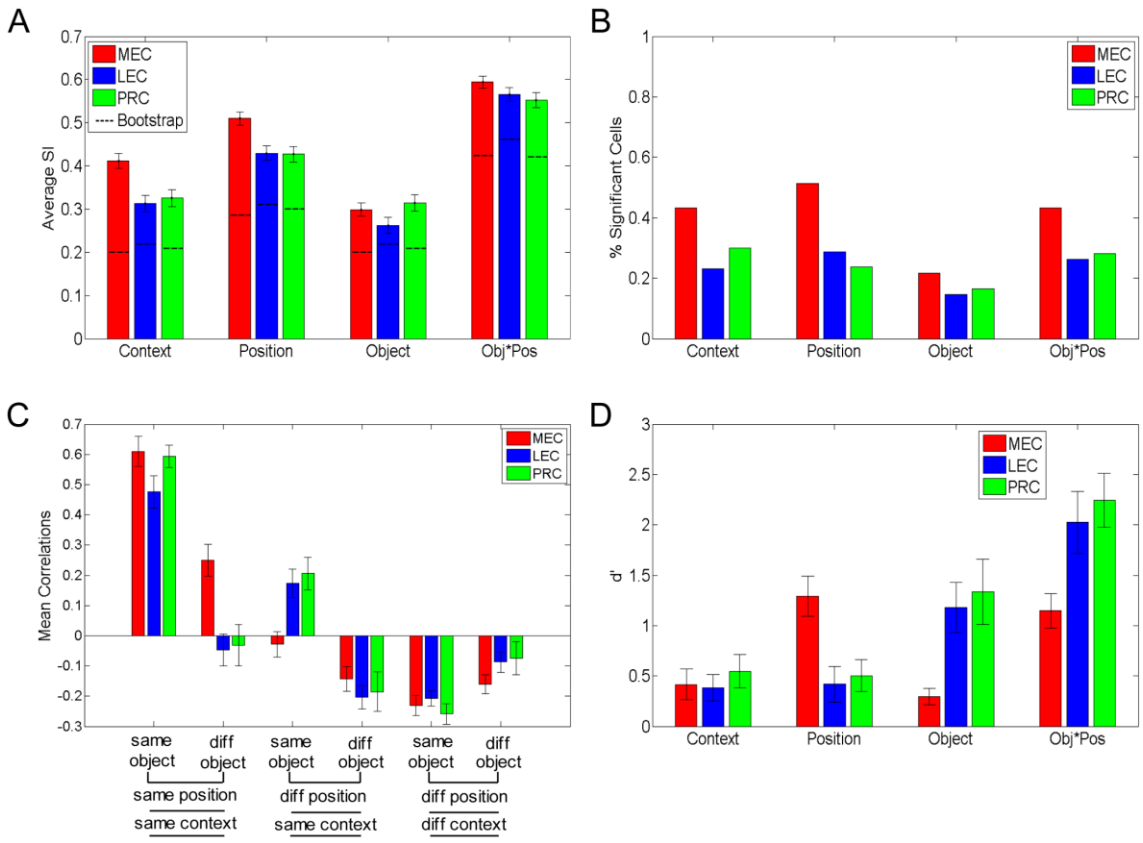

Figure 5: Single unit and population coding for task dimensions.

A) Average Selectivity Index (SI) ± S.E. for task dimensions during object sampling in PRC, LEC, and MEC. Dotted lines indicate the average SI values from a bootstrapped distribution in which the position and/or object identities were shuffled for each trial (preserving firing rates and patterns). Note that even with this stringent criterion to determine coding of task dimensions, we found

significant coding for all dimensions in all three regions. B) Percentage of cells that significantly code for task dimensions after controlling for firing rate differences. C) Mean correlations coefficients ± S.E. for comparisons between object sampling events that are the same or different in distinct dimensions (object, position, context; diff = different). D) Strength of population coding of different task dimensions, measured as d′ distance between distributions of z-scored firing rates for context, position coding, object coding, and objects in specific positions (Obj*Pos).

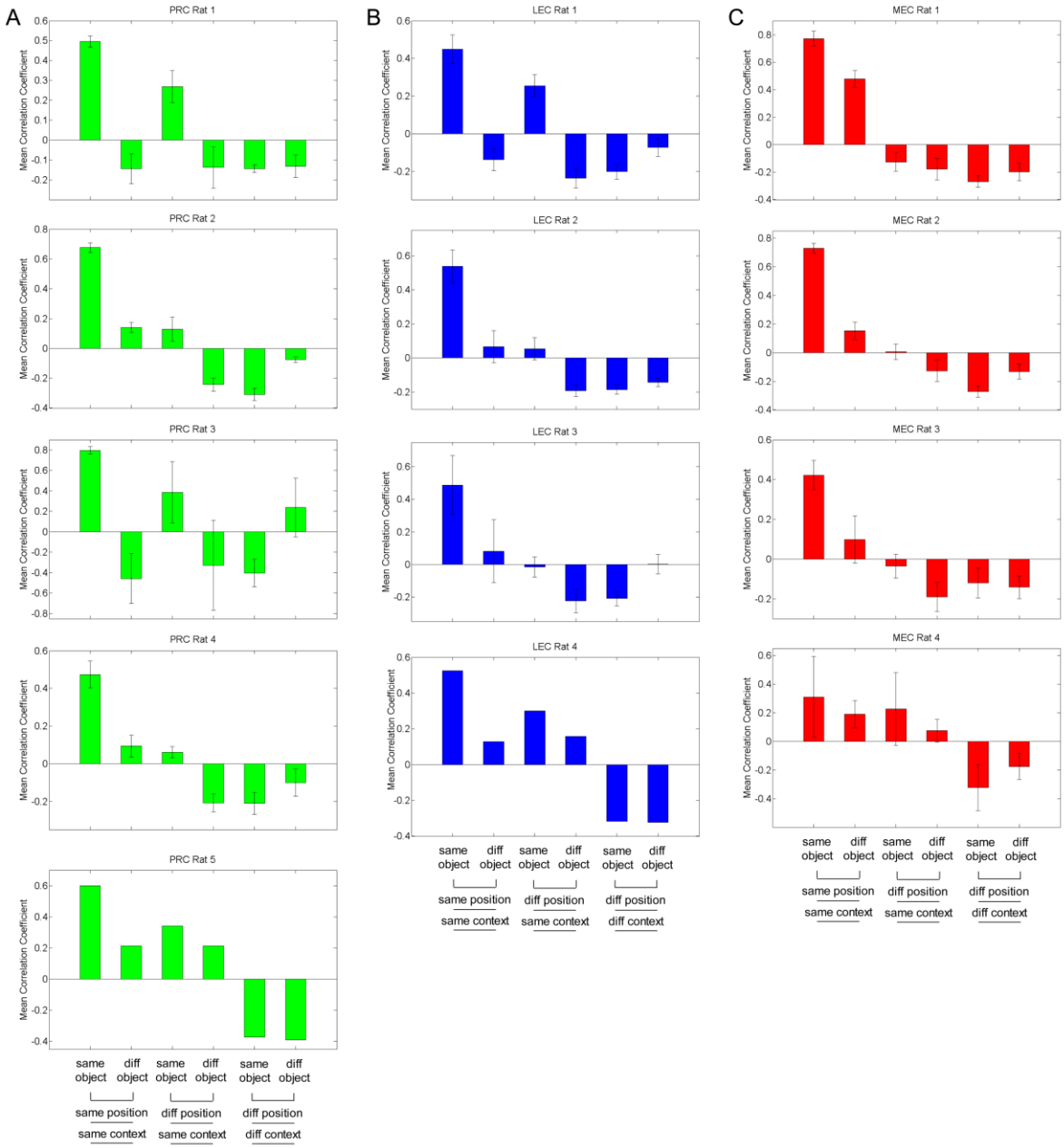

Figure 6: Mean correlation coefficients for individual rats.

Mean correlation coefficients for comparisons between object sampling events that are the same or different in distinct dimensions (object, position, context) for individual subjects in A) PRC, B) LEC, and C) MEC. Diff = different.

2.4.5 Ensemble representations in PRC, MEC, and LEC organize information distinctly

To explore how neural populations represented the task dimensions, we employed a Representational Similarity Analysis (RSA). This analysis yields modest, but highly reliable, correlation coefficients that indicate that ensemble firing patterns are highly consistent between identical individual events (Figure 5C; e.g., sampling events involving the same object in the same position and context).

First, to measure the extent to which identical events were coded similarly, population vectors for odd-numbered events were correlated against those for even-numbered events for each of the two objects within each of the two positions in each of the two contexts. The mean of those eight correlation coefficients was used to measure the ensemble similarity for identical events within each of the recording sessions (14 for PRC, 17 for LEC, 30 for MEC; see Figure 5C, first set of bars). For all other comparisons, population vectors for object-sampling events of each type were correlated with those for a different type of event. To measure the similarity of ensemble representations for different objects sampled at the same position, population vectors for odd-numbered events for one object were correlated against even-numbered events for the other object, and vice versa (even-numbered events for the first object against odd-numbered events for the second object), to compose eight total correlations, and the mean of those correlation coefficients was used to measure the representational similarity for

different objects (holding position and context constant) in each session (see Figure 5C, second set of bars). The same approach was used to measure the representational similarities for the same or different objects at different positions within a context, including the separation of odd- and even-numbered events to ensure that similar amounts of data were used in all analyses. To assess the similarity of ensemble representations for the same object between positions, population vectors for sampling events involving an object in one position were correlated with those for the same object in the other position within the same context (see Figure 5C, third set of bars) or with that for the other object in the other position within the same context (see Figure 5C, fourth set of bars), again comparing odd-numbered against even-numbered events and vice versa. To assess the similarity of ensemble representations of objects between contexts, population vectors for odd-numbered and even-numbered events for the same object (see Figure 5C, fifth set of bars) or different objects (see Figure 5C, sixth set of bars) at positions between contexts were similarly correlated. The mean correlation coefficients for individual rats for all 3 brain regions are presented in Figure 6, showing that the overall pattern of correlations was similar across individual subjects.

Although a statistical comparison of the individual bars in Figure 5C is not easily interpreted, it is clear that PRC and LEC share a highly similar pattern of correlations for events varying across dimensions and on some dimensions these are distinct from that found in MEC. In particular, whereas MEC ensembles are similar for different objects in the same position ($p < 0.0001$), PRC and LEC ensembles have independent representations for different objects in the same position (correlation not significantly

different from zero, *p's* > 0.3). Conversely, whereas PRC and LEC ensembles have similar representations for the same object at different positions (p's = 0.002), MEC ensembles do not ($p > 0.5$). This dissociation reflects stronger position coding in MEC ensembles and stronger coding of object information in PRC and LEC. It is also notable that, in all areas, representations of different objects in different positions and comparisons between contexts were negatively correlated (all p's < 0.005), indicating strong pattern separation of representations across these dimensions.

In order to better quantify these distinct patterns of activity, these correlations were combined in several ways described below to provide a straightforward measure of the similarity of population representations associated with each task dimension. We used a d′ metric (as in McKenzie et al., 2014) to measure the separation of the distributions of the correlation coefficients for specific task features from zero or against the distribution of coefficients from an appropriately opposing condition (see Materials and Methods for each comparison). As seen in Figure 5D, analysis of the ensemble representations revealed both similarities and differences in the representation of task dimensions. A two-way ANOVA on the d′ metric indicated a main effect of task dimension (F, (3, 232) = 23.75, $p < 0.00001$), a main effect of region (F, (2, 232) = 3.57, $p = 0.03$), and a significant interaction (F, (6, 232) = 7.21, $p < 0.00001$). Post-hoc tests indicated that PRC, LEC, and MEC populations equally strongly represented contexts (*p's* > 0.4), while MEC exhibited stronger representation of position information than PRC ($p = 0.001$) and LEC ($p = 0.001$). In contrast, PRC and LEC exhibited stronger representation of object information (*p's* = 0.0001) and object-position conjunction

information than MEC (PRC vs MEC $p = 0.009$, PRC vs MEC $p = 0.001$). Consistent with findings of mixed selectivity from the SI analysis, analysis of ensemble representations in PRC, LEC, and MEC indicated that all regions encode all task dimensions (all *p's* < 0.01), but the observed double dissociation between MEC representation of position and PRC-LEC representation of objects and object-position conjunctions indicates a difference in the underlying organization of representations in PRC-LEC and MEC.

To test the generality of the RSA approach, ensembles of recorded neurons were also analyzed using the cosine separation of population vectors to characterize the similarity of representations. Strength of coding dimensions to different task features were identified by comparing d′ distributions of mean cosine scores similar to the RSA approach. Analysis of these d′ comparisons with a two-way ANOVA revealed a very similar pattern of population coding as with the RSA approach (Figure 7A), indicating a main effect of task dimension (F, (3, 232) = 19.86, $p < 0.00001$), no main effect of region (F, (2, 232) = 0.18, $p = 0.84$), and a significant interaction (F, (6, 232) = 6.42, $p < 0.00001$). Similar to the RSA results, post-hoc tests indicated that PRC, LEC, and MEC populations equally strongly represented contexts (*p's* > 0.3), while also indicating similar representation of object-position conjunctions (*p's* > 0.2). In contrast to those similarities in function, MEC exhibited stronger representation of position information than PRC ($p = 0.006$) and LEC ($p = 0.001$), while PRC and LEC exhibited stronger representation of object information (PRC vs MEC $p = 0.01$, PRC vs MEC $p = 0.0005$). Despite reflecting more similar representations with respect to object-position

conjunctions, these results are nonetheless highly consistent with those found with the RSA approach, and they suggest a distinct, but complementary, organization of object and spatial information at the population level between PRC-LEC and MEC.

We further tested the generality of these findings across analytical approaches by estimating the probability that a pattern of ensemble firing rates was recorded in each of 8 object in position combinations using a Bayesian decoding algorithm. Since there is a probability associated with each object/position combination, we could determine whether there were different hierarchies of coding probabilities among the areas examined. MEC ensembles exhibited nearly equivalent coding probabilities for position and object/position conjunctions, followed by object and context coding probabilities. In contrast, LEC ensembles exhibited object/position and object coding probabilities most strongly, followed by context coding and then position coding probability. In PRC, the hierarchy was less distinct with strong object/position coding, followed by relatively equivalent coding of context, position, and object information. With respect to the decoding probabilities for task dimensions, for all regions ensembles were most likely to have originated from trials with the same object and position combination (mean probability PRC = 0.29; LEC = 0.32; MEC = 0.42), which was greater than the probability of the neural activity originating from trials with different objects or positions (PRC mean probability = 0.15, $d' = 0.66$, $p < 0.01$; LEC mean probability = 0.15, $d' = 0.71$, $p < 0.001$; MEC mean probability = 0.13, $d' = 0.81$, $p < 0.001$). These differences in probabilities reflect strong object-in-position coding. PRC and LEC exhibited the greatest object coding, followed by MEC, indicated by a greater probability of ensembles

originating from sampling events of the same object in different positions (PRC mean probability = 0.18; LEC mean probability = 0.19; MEC = 0.11) than different objects in different positions within a context (PRC mean probability = 0.10, d′ = 0.34, $p < 0.001$; LEC mean probability = 0.07, d′ = 0.42, $p < 0.001$; MEC mean probability = 0.07, d′ = 0.24, $p < 0.001$). In contrast, MEC exhibited the greatest position coding, followed by PRC and LEC, reflected by a greater probability of ensembles originating from sampling events in the same position (PRC mean probability = 0.20; LEC mean probability = 0.22; MEC = 0.28) than sampling events at different positions within a context (PRC mean probability = 0.14, d′ = 0.32, $p < 0.001$; LEC mean probability = 0.13, d′ = 0.53, $p < 0.001$; MEC mean probability = 0.09, d′ = 1.29, $p < 0.001$). Finally, a greater probability of ensembles originated from sampling events within contexts (PRC mean probability = 0.17; LEC mean probability = 0.17; MEC = 0.19) than across contexts (PRC mean probability = 0.08; d′ = 0.59, $p < 0.001$; LEC mean probability = 0.09, d′ = 0.22, $p < 0.001$; MEC mean probability = 0.07, d′ = 0.09, $p = 0.05$, not significant), indicating roughly equivalent context coding in LEC and MEC.

To directly compare the findings among brain regions and relate these findings to the correlation and cosine separation analyses, we compared the decoding probabilities for task dimensions using the d′ metric (Figure 7B). An ANOVA was conducted on the d′ values generated with the Bayesian decoding algorithm. This analysis indicated no main effect of region (F, (2, 168) = 1.04, $p = 0.35$), but did indicate a significant interaction (F, (3, 168) = 5.47, $p < 0.0001$). Post-hoc tests revealed an underlying pattern that was highly similar to those found in the ensemble correlation and cosine separation

analyses. LEC exhibited greater object coding than MEC ($p = 0.005$) and MEC exhibited greater position coding than PRC or LEC (*p's* < 0.001). However, PRC did not exhibit greater object coding than MEC ($p > 0.05$), potentially owing to a higher probability of context decoding in PRC. In contrast, there were no differences between PRC, LEC, and MEC with respect to context or object-position conjunctive coding as determined by the decoding algorithm (*p's* > 0.05). Together, this group of analyses demonstrates reliable patterns of activity in PRC, LEC, and MEC suggesting distinct, but complementary roles in processing object and spatial information.

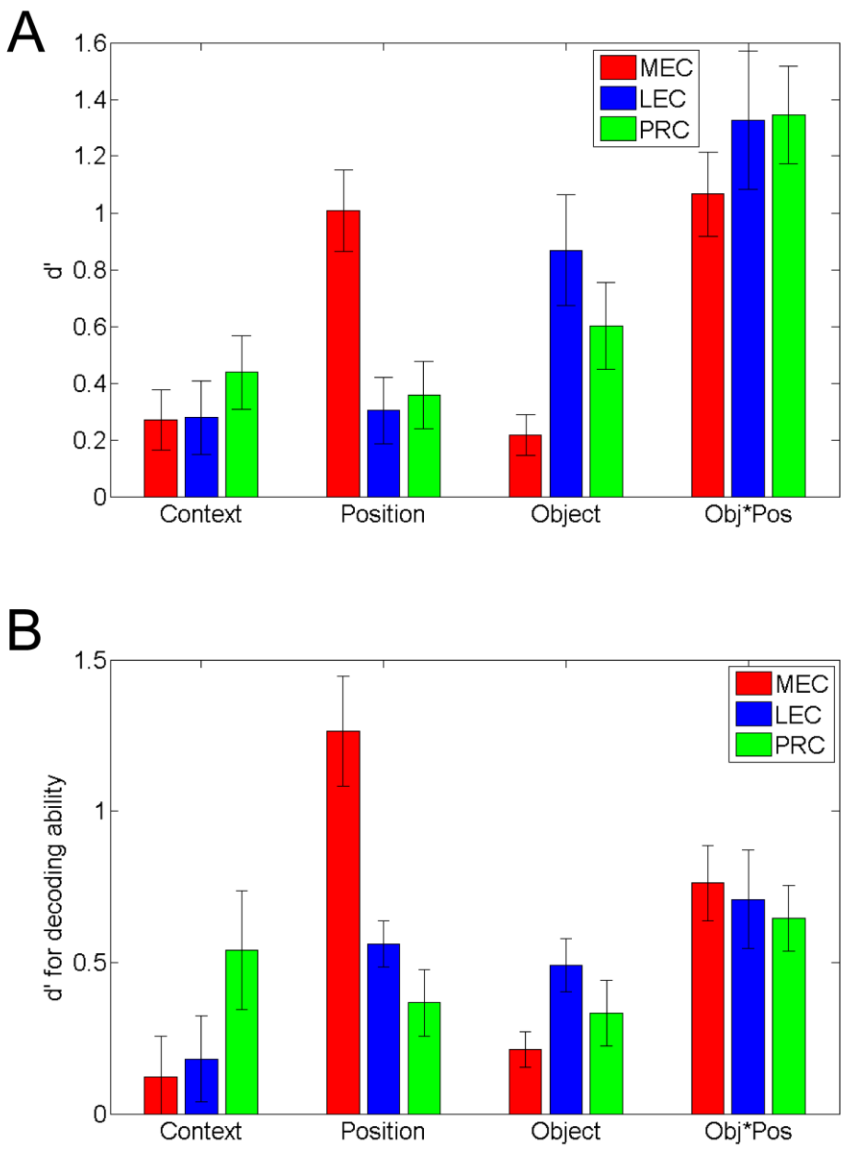

Figure 7: Population coding of task dimensions in MEC and LEC during object sampling.

A) Strength of coding as in Figure 5D, except using d′ distance between distributions of average cosine values for firing rates normalized by the maximum firing rate during object sampling. B) Strength of coding using d′ distance between mean probabilities that patterns of ensemble firing rates were recorded in each of the eight object in position combinations determined by a Bayesian decoding algorithm.

2.4.6 Coding of task dimensions across time during object sampling

We also compared these brain areas with respect to the temporal dynamics of information coding among the different task dimensions based on the correlation RSA (as in Figure 5D). Significant sustained position coding was evident in MEC earliest, followed approximately 1-2 s later by PRC and LEC (Figure 8A). Furthermore, position coding appeared to peak around the onset of object sampling, which was particularly pronounced in MEC (PRC peak = -400 ms, = 0.35, $p < 0.001$; LEC peak = -400 ms, d = 0.30, $p < 0.001$; MEC peak = 0 ms, d′ = 0.82, $p < 0.001$). In contrast, significant object coding was evident in PRC and LEC at the onset of object sampling (Figure 8B) with sustained peak firing beginning at approximately 500 ms after the onset of object sampling (PRC peak = 800 ms, = 0.32, $p < 0.001$; LEC peak = 1200 ms, d = 0.31, $p < 0.001$), whereas MEC did not exhibit significant object coding in this analysis (MEC peak = 600 ms, d′ = 0.07, $p = 0.24$). Despite these differences in position and object coding, there was less difference in the onset of object-in-position coding among PRC, LEC, and MEC (Figure 8C). Sustained, significant coding for this task dimension was evident at or just after the onset of object sampling (0 ms) with peak firing at approximately 1-1.5s after the onset of object sampling (PRC peak = 1200 ms, = 0.82, $p < 0.001$; LEC peak = 1000 ms, d = 0.74, $p < 0.001$; MEC peak = 1400 ms, d′ = 0.71, $p < 0.001$). It should also be noted that the timing pattern is unique for each of these dimensions, reflecting distinct coding of each of these features of events. Collectively, the temporal dynamics of coding of different task dimensions further distinguishes MEC as emphasizing position coding, whereas PRC and LEC population activity reflects

earlier and stronger object coding, consistent with the results of the other population analyses.

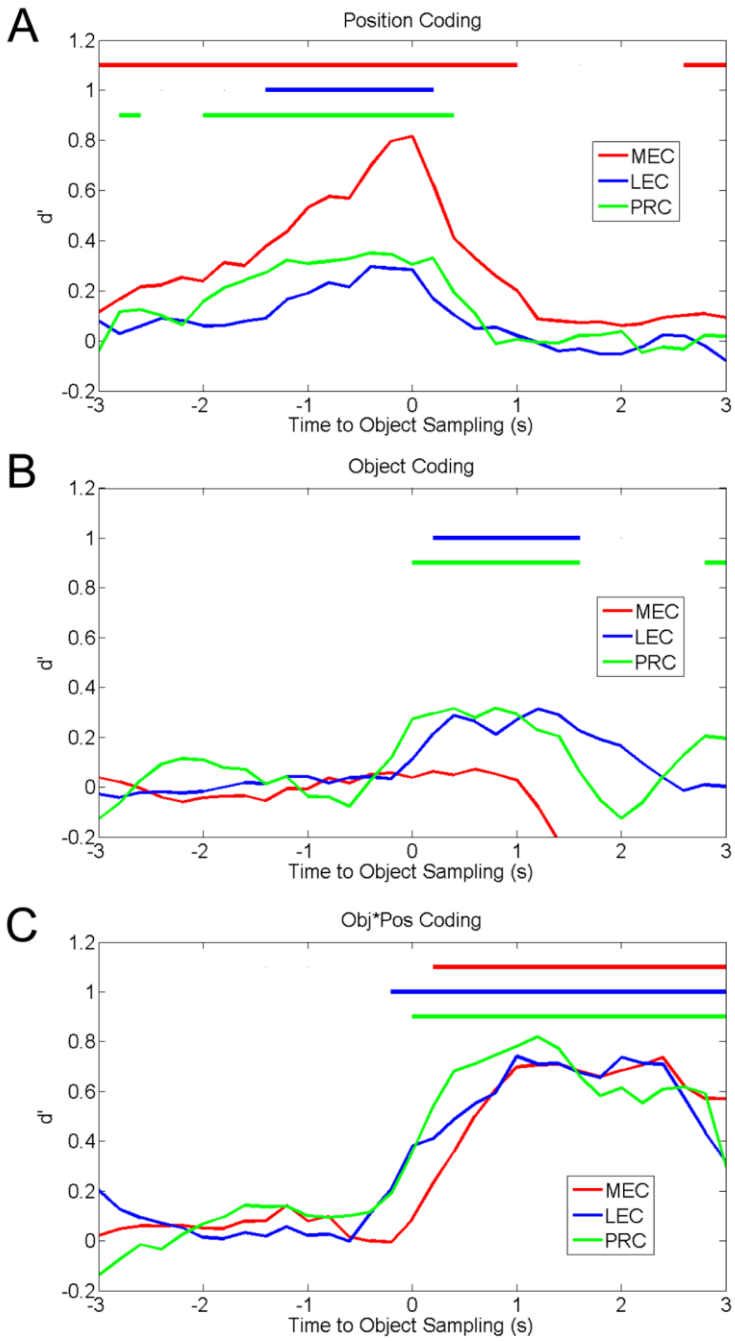

Figure 8: Coding for task dimensions is expressed at different times across regions during object sampling.

The average d′ strength calculated from mean correlations (as in Figure 5D) for each task dimension is depicted over time (using 200 ms bins) before and after the onset of object sampling (0 s). MEC exhibits the earliest and strongest position coding compared to the pattern for PRC or LEC (A), whereas PRC and LEC exhibit early and strong object coding, which is not observed in MEC (B), and all three regions exhibit a similar degree of conjoint object-position coding that peaks later than separate coding of positions and objects (C). Color coded bars at the top of each graph indicate periods in which the dimension was significantly coded.

2.4.7 PRC-LEC and MEC exhibit distinct hierarchical organizations of information

To explore the organization of dimensions represented in PRC, LEC, and MEC populations, we performed an additional analysis in which similarities between population vectors for each sample type were iteratively clustered according to their mean correlation coefficients. The highest correlations result in the tightest clustering of nodes in the organizational structure and successively lower correlations reflect greater separation of representations, resulting in a systematic hierarchical organization of task dimensions (Figure 9). At the top of the hierarchy for all regions, representations were strongly separated (negatively correlated) by events that occurred in different contexts. Within each context-based cluster, in PRC and LEC, events within each context were next separated by the object presented. Then, within each object cluster, the positions where objects occurred were separated. In MEC events within each context were also strongly separated (negatively correlated). Then, in contrast to PRC and LEC, within each context-based cluster, events were separated by the positions in which objects were sampled. Then within each position representation, objects were separated. Finally, in all areas, representations of identical events are most closely associated. Thus, although PRC, LEC, and MEC exhibit great similarity in mixed selectivity at the single neuron

level, RSA revealed an emergent distinction between these areas in complementary organizations of event representations.

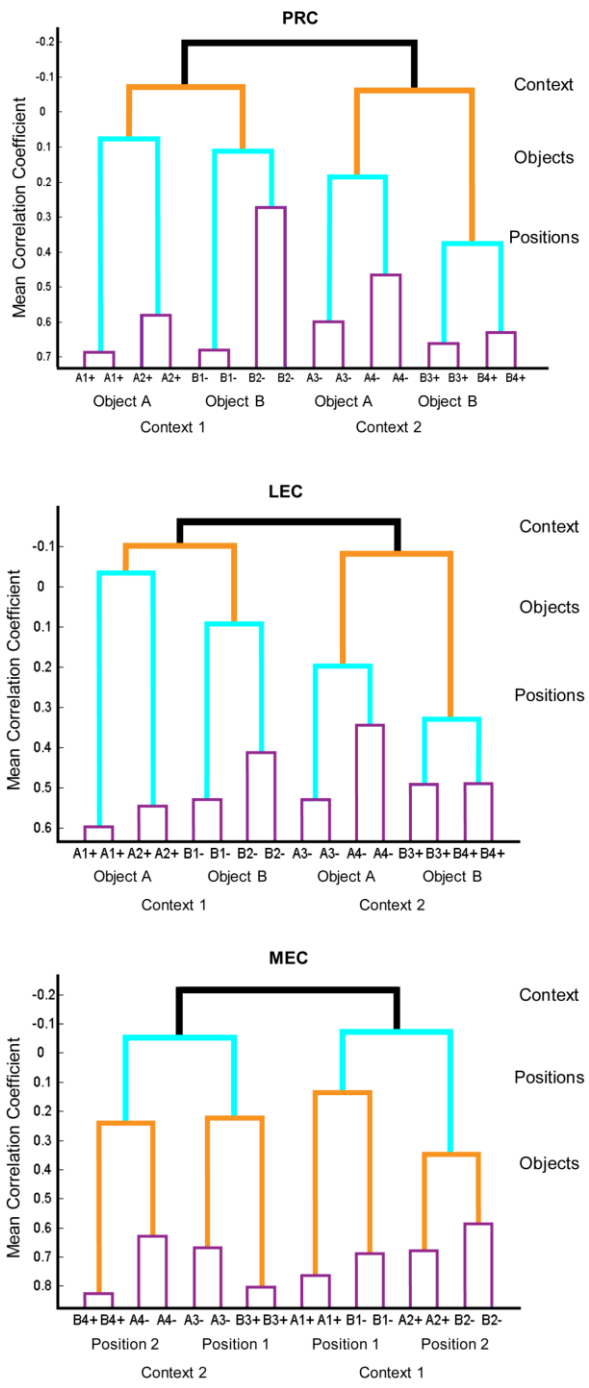

Figure 9: Hierarchical organization of event representations by task dimensions.

Dendrograms illustrating organization of population representations in PRC, LEC, and MEC during object sampling for each specific type of object sampling event (a particular object in a specific position within one context). Letters indicate Objects A or B in Positions 1 or 2 (Context 1) or Positions 3 or 4 (Context 2) with + or – indicating whether the stimulus was reinforced. Repeated events (e.g., A1+ and A1+) indicate comparison of population vectors for even and odd numbered events for that event type (see Online Methods). Black = correlation of population vectors between contexts. Red = correlations between objects. Green = correlations between positions. Blue = correlations between even and odd numbered trials.

2.5 Discussion

The present observations on PRC, LEC and MEC neuronal firing patterns quite dramatically reject the notion that PRC and LEC neurons selectively encode object information whereas MEC neurons selectively encode spatial information. Given the direct and indirect connections between these areas (Suzuki & Amaral, 1994; Witter et al., 1989; Burwell & Amaral, 1998; Kerr et al., 2007), it should be expected that information processed in each of these areas is shared with the other. However, the extent to which individual PRC, LEC and MEC neurons, including even grid cells, border, and head direction cells, process both object and spatial information equally is surprising. At the same time, population analyses strikingly dissociated PRC and LEC from MEC networks as prioritizing object and spatial information, respectively. These observations reinforce conclusions from recent studies that the full content and organization of representations in higher order brain areas is most clearly revealed in population analyses (Rigotti et al., 2013; Shamir, 2014).

Given the previous reports of striking coding of specific spatial dimensions (position, direction, borders) in MEC neurons, it was quite surprising that MEC

neurons of all subtypes (grid, border, head direction, other) strongly encoded object information and did so at least as well as PRC and LEC neurons. Also, given previous observations suggesting a lack of spatial coding by PRC and LEC neurons (Hargreaves et al., 2005; Deshmukh et al., 2012), it was quite surprising that PRC and LEC neurons strongly encoded position and context, although not quite matching that seen in MEC. The most obvious difference in the present study and previous work is that both spatial and object dimensions were salient features of the task demands in this context-guided object-reward association paradigm. However, it is notable that both spatial context, which is important for task performance, and position within contexts, which is not required for task performance, were strongly encoded by PRC, LEC and MEC. Perhaps, once contextual spatial cues are relevant, both global and local spatial information become sufficiently salient to demand representation. This interpretation is consistent with other recent studies that have previously identified spatial coding in a minority of LEC cells (Deshmukh et al., 2011; Tsao et al., 2013). Both studies provided evidence of spatial "memory" fields at prior locations when objects were moved in or removed from the environment, while Deshmukh and colleagues also provided examples of activity similar to place field firing when objects were presented. In addition, studies on earlier stages of information processing prior to LEC and MEC, that is in the PRC and postrhinal cortex, have also reported mixed selectivity of neuronal activity in animals performing memory tasks where objects and spatial choices are relevant (Furtak et al., 2012; Ahn et al., 2015). The present findings suggest that both LEC and MEC also

represent organizations of objects and events within spatial contexts (see also Knierim et al., 2013), and that even PRC exhibits a combination of object and spatial coding.

It was particularly striking that grid cells strongly encoded object information, often differentiating objects sampled at the same location (See Figure 4). In contrast to the common view that grid cells are specialized for position coding, results from the present study strongly suggest that grid cells possess strong object-coding properties that have been largely overlooked to this point. Future investigation of these properties could yield further insights about the organization of information in cortical structures of the hippocampal region and beyond, given the detailed understanding of grid cell function and organization (Moser & Moser, 2013; Moser et al., 2014; Witter et al., 2014).

The Representational Similarity Analysis employed here revealed that, within equivalent coding of specific dimensions by single PRC, LEC and MEC neurons, populations of neurons in all these areas developed distinct systematic organizations of those dimensions. Notably, both areas developed quite separate (anti-correlated) networks consistent with the opposite reward associations of objects in the two contexts. Other recent studies have shown that grid cell firing patterns in MEC are responsive to contextual differences (Marozzi et al., 2015) as well as a merging of spatial contexts (Carpenter et al., 2015). Furthermore, strong pattern separation of contextual representation was also observed in the hippocampus in a previous study that employed the same task (McKenzie et al.,

2014). Thus, contrary to other work suggesting that pattern separation occurs selectively within subregions of the hippocampus (Leutgeb et al., 2004; Lee et al., 2004; Bakker et al., 2008), here the entire hippocampal system responds to a strong demand for reducing interference between the opposite object associations in the two contexts by robust pattern separation.

Within the two context-based networks, PRC, LEC and MEC organize the object and spatial information quite differently. Within each context-based network, the closely interconnected PRC and LEC populations distinguish objects and then only within each object representation distinguish the positions where objects are sampled. Conversely, within each context-based network, MEC populations distinguish the positions where object sampling occurs, and then only within each position representation distinguish the objects at those locations. Notably, the population representation within the MEC is very similar to that observed in the hippocampus (McKenzie et al., 2014), suggesting a prominent role of MEC in driving spatial organization in the hippocampus. Overall, this pattern of findings suggests we move from thinking about modality specific processing areas within the hippocampal system (Eichenbaum et al., 2007) to conceiving the hippocampal system as composed of interconnected areas each of which process all the information but differently organize the dimensions of information processing.

2.6 Accompanying table

Table 1: Unit proportions coding for task dimensions

Number and Percentage of Units Significantly Coding for SI Dimensions and Average SI Value ± SEM based on SI (interneurons excluded) and average SI ± SEM. # Signif. = number of cells with significant coding/total number of cells tested. Obj*Pos = Object X Position.

		SI Dimension							
		Context		Position		Object		Obj*Pos	
Brain Region		# Signif.	%	# Signif.	%	# Signif.	%	# Signif.	%
		Avg SI ± SEM		Avg SI ± SEM		Avg SI ± SEM		Avg SI ± SEM	
PRC	Overall	49/164	29.9%	39/164	23.8%	27/164	16.5%	46/164	28.0%
		0.33 ± 0.02		0.43 ± 0.02		0.31 ± 0.02		0.55 ± 0.02	
	Superficial	28/72	38.9%	24/72	33.3%	16/72	22.2%	26/72	36.1%
		0.36 ± 0.03		0.45 ± 0.03		0.33 ± 0.03		0.58 ± 0.02	
	Deep	21/92	22.8%	15/92	16.3%	11/92	12.0%	20/92	21.7%
		0.30 ± 0.03		0.41 ± 0.03		0.31 ± 0.03		0.54 ± 0.02	
	Area 35	26/95	27.4%	20/95	21.1%	18/95	19.0%	26/95	27.4%
		0.31 ± 0.3		0.42 ± 0.02		0.32 ± 0.03		0.55 ± 0.02	
	Area 36	23/69	33.3%	19/69	27.5%	9/69	13.0%	20/69	29.0%
		0.34 ± 0.03		0.44 ± 0.03		0.30 ± 0.03		0.56 ± 0.03	
LEC	Overall	38/164	23.2%	47/164	28.7%	24/164	14.6%	43/164	26.2%
		0.31 ± 0.02		0.43 ± 0.02		0.26 ± 0.02		0.57 ± 0.02	
	Superficial	29/107	27.1%	35/107	32.7%	19/107	17.8%	28/107	26.2%
		0.31 ± 0.02		0.41 ± 0.02		0.27 ± 0.02		0.54 ± 0.02	
	Deep	9/57	15.8%	12/57	21.1%	5/57	8.8%	15/57	26.3%
		0.31 ± 0.03		0.46 ± 0.03		0.25 ± 0.03		0.61 ± 0.03	
MEC *	Overall	101/236	42.8%	120/236	50.8%	51/236	21.6%	101/236	42.8%
		0.41 ± 0.02		0.51 ± 0.02		0.30 ± 0.1		0.59 ± 0.01	
	Superficial	44/103	42.7%	57/103	55.3%	27/103	26.2%	50/103	48.5%
		0.45 ± 0.03		0.55 ± 0.02		0.33 ± 0.02		0.65 ± 0.02	
	Deep	57/133	42.9%	63/133	47.7%	24/133	18.0%	51/133	38.3%
		0.39 ± 0.02		0.48 ± 0.02		0.28 ± 0.02		0.56 ± 0.02	
MEC Spatial **	All Grids	12/23	52.2%	12/23	52.2%	3/23	13.0%	13/23	56.5%
		0.52 ± 0.06		0.64 ± 0.05		0.32 ± 0.05		0.71 ± 0.04	
	Grid Only	7/12	58.3%	5/12	41.7%	0/12	0.0%	6/12	50.0%
		0.56 ± 0.09		0.66 ± 0.07		0.24 ± 0.06		0.70 ± 0.07	
	Grid x HD	5/11	45.5%	7/11	63.6%	3/11	27.3%	7/11	63.6%
		0.48 ± 0.07		0.62 ± 0.06		0.40 ± 0.08		0.72 ± 0.05	
		62/125	49.6%	81/125	64.8%	37/125	29.6%	73/125	58.4%

	All Head Direction	0.44 ± 0.02		0.55 ± 0.02		0.34 ± 0.02		0.63 ± 0.02	
	HD Only	52/101	51.5%	66/101	65.4%	29/101	28.7%	59/101	58.4%
		0.43 ± 0.03		0.53 ± 0.02		0.32 ± 0.02		0.62 ± 0.02	
	Border x HD	5/13	38.5%	8/13	61.5%	5/13	38.5%	7/13	61.5%
		0.48 ± 0.09		0.60 ± 0.05		0.48 ± 0.06		0.69 ± 0.05	
	All Border	11/27	40.7%	14/27	51.9%	7/27	25.9%	11/27	40.7%
		0.46 ± 0.06		0.53 ± 0.04		0.34 ± 0.05		0.61 ± 0.04	
	Border Only	6/14	42.9%	6/14	42.9%	2/14	14.3%	4/14	28.6%
		0.43 ± 0.07		0.47 ± 0.06		0.22 ± 0.05		0.53 ± 0.06	
	Other	26/85	30.6%	28/85	32.9%	15/85	17.6%	18/85	21.1%
		0.35 ± 0.03		0.45 ± 0.03		0.26 ± 0.02		0.54 ± 0.02	

*** Proportions reflect MEC downsampled data to allow direct comparison to PRC and LEC. Average SI data was not sensitive to firing rate differences and therefore was not adjusted.**

**** Proportions reflect MEC data without downsampling given within region comparisons only. Average SI data was not adjusted.**

Chapter 3. In a Temporally Segmented Experience Hippocampal Neurons Represent Temporally Drifting Context but not Discrete Segments[b]

3.1 Abstract

There is widespread agreement that episodic memory is organized into a timeline of past experiences. Recent work suggests that the hippocampus may parse the flow of experience into discrete episodes separated by event boundaries. A complementary body of work suggests that context changes gradually as experience unfolds. We recorded from hippocampal neurons as male long evans rats performed 6 blocks of an object discrimination task in sets of 15 trials. Each block was separated by removal from the testing chamber for a delay to enable segmentation. The reward contingency reversed from one block to the next to incentivize segmentation. We expected animals to hold two distinct, recurring representations of context to match the two distinct rule contingencies. Instead, we found that overtrained rats began each block neither above nor below chance but by guessing randomly. While many units had clear firing fields selective to the conjunction of objects in places, a significant population also reflected a continuously drifting code both within block and across blocks. Despite clear boundaries between blocks, we saw no neural evidence for event segmentation in this experiment. Rather, the

---

[b] This chapter, in full, is a reprint of a published manuscript hosted on BioRxiv, and was revised and resubmitted at Journal of Neuroscience (Resubmission Date: December 13, 2018) The full BioRxiv Citation is as follows:
Bladon, J., Sheehan, D. J., Freitas, C. S. De, & Howard, M. W. (2018). In a temporally segmented experience hippocampal neurons represent temporally drifting context but not discrete segments . BioRxiv, 1–36. https://doi.org/10.1101/338962
Author Contributions: JHB & Howard Eichenbaum designed the experiment, JHB, DJS & CDF acquired the data, JHB, DJS & MWH analyzed the data, and JHB & MWH wrote the manuscript.

hippocampal ensemble drifted continuously across time. This continuous drift in the neural representation was consistent with the lack of segmentation observed in behavior.

Significance statement:

The neuroscience literature yet to reach consensus as to how hippocampal firing fields support the organizing of events across time in episodic memory. Initial reports of hippocampal activity focused on discrete episodes within which representations were stable, and across which representations remapped. However, it remains unclear whether this segmentation of representations is merely an artifact of cue responsivity. More recently, research has shown that a proportion of the population codes for temporal aspects of context by exhibiting varying degrees of drift in their firing fields. Drift is hypothesized to represent a continually evolving temporal context, however it is unclear whether this drift is continuous or is also a mere artifact of changing experiences. We recorded from the dorsal hippocampus of rats performing an object discrimination task that involved contexts that were segmented in time. Overtrained rats were unable to anticipate the identity of the upcoming context, but may have used context boundaries to their advantage. Event segmentation theory predicts that hippocampal ensembles would alternate between behaviorally-relevant segments. Contrary to these predictions, animals showed weak evidence of context segmentation, even across blocks with different reward contingencies. Hippocampal ensembles showed neither evidence of alternating between stable contexts nor sensitivity to context boundaries, but did show robust temporal drift.

3.2 Introduction

Episodic memory refers to the vivid recollection of a specific event situated in a unique place and time (Tulving & Madigan, 1970). In his description of episodic memory, Endel Tulving emphasized that a crucial distinction between episodic and semantic memory is that episodic memories are temporally dated, or are remembered in relation to other events across time. The hippocampus is essential for episodic memory and is thought to mediate this function by binding events to a representation of spatial and temporal context (Eichenbaum et al., 2007; Tulving, 1972). Indeed the hippocampus is specifically involved in both remembering the temporal order of past events and making associations across a temporal gap in both humans and animals (Caparelli et al., 2012; Dede, Frascino, Wixted, & Squire, 2016; Fortin, Agster, & Eichenbaum, 2002; Kesner, Hunsaker, & Gilbert, 2005). Hippocampal ensembles are theorized to represent a 'cognitive map' (O'Keefe & Nadel, 1978) that acts as a contextual or relational scaffold onto which events may be bound together for later retrieval (Davachi, 2006).

There are two complementary models for how spatiotemporal context is structured in the hippocampus. Event segmentation theory suggests experience is segmented across time into discrete situational contexts (Figure 1 "Event Segmentation") (Baldassano et al., 2017; DuBrow, Rouhani, Niv, & Norman, 2017; Muller & Kubie, 1987; Zacks, Tversky, & Iyer, 2001). Temporal context theory suggests that the hippocampal representation of context evolves continually (Figure 10, "Temporal

Context”) (Howard & Eichenbaum, 2013; Howard et al., 2005). There is behavioral, neuroimaging and animal neurophysiological evidence consistent with both theories.

Consistent with event segmentation theory, behavioral and neuroimaging evidence suggests that experiences are segmented in time. Studies on human recall have found that memories are organized by discrete situational contexts (Baldassano et al., 2017; DuBrow et al., 2017; Muller & Kubie, 1987; Zacks et al., 2001). Abrupt changes in environmental or contextual cues across time can cause a behavioral separation in memory traces (Ezzyat & Davachi, 2011; Sols, Dubrow, Davachi, & Fuentemilla, 2017; Zacks et al., 2001). Hippocampal BOLD activity in humans, and ensemble activity in rodents increases when a border between contexts is perceived, as if the hippocampus parcellates experience into contextual chunks (Baldassano et al., 2017; Bulkin, Sinclair, Law, & Smith, 2018; DuBrow et al., 2017; Mack, Love, & Preston, 2016; Place, Farovik, Brockmann, & Eichenbaum, 2016).

Although event segmentation has yet to be explicitly studied in rodents, electrophysiological evidence consistent with event segmentation can be found in the hippocampal representation of space (but see Bulkin et al. 2018 for a recent exception). In agreement with event segmentation theory, hippocampal ensembles generate separate maps across different spatial environments (Brandon, Koenig, Leutgeb, & Leutgeb, 2014; Komorowski et al., 2009; Stefan Leutgeb et al., 2005; Wills, 2005). In addition, hippocampal ensembles generate separate maps across a variety of explicit contextual designations that occur in the same physical space (Kobayashi, Nishijo, Fukuda, Bures, & Ono, 1997; Markus, Barnes, McNaughton, Gladden, & Skaggs, 1994; Smith & Bulkin,

2014; Wills, 2005). In a particularly clear example, neural segmentation across two physical contexts was found to develop as rats learned to discriminate between the two contexts (Komorowski et al., 2013, 2009). These studies suggest that hippocampal ensembles segment continuous experience to support discrimination between different spatial and behavioral contexts.

Consistent with temporal context theory, behavioral and neuroimaging experiments suggest a continuous temporal signal that supports the organization of memories in time. The temporal contiguity effect describes the tendency for subjects to bind together unrelated events that occurred together in time, and has been shown across timescales in both neural and behavioral datasets (Folkerts, Rutishauser, & Howard, 2018; Howard, Youker, & Venkatadass, 2008; Kahana, 1996; Manning, Polyn, Baltuch, Litt, & Kahana, 2011; Zaromb et al., 2006). Conversely, a continually evolving hippocampal signal also allows for segregation of related events that occur far apart in time (Cai et al., 2016; Manns et al., 2007). Human fMRI data show the representational similarity of hippocampal BOLD signals during recall of events reflects a broad continuum of relatedness that maps onto the temporal and spatial proximity of those events (Deuker, Bellmund, Navarro Schröder, & Doeller, 2016; Hsieh, Gruber, Jenkins, & Ranganath, 2014; Jenkins & Ranganath, 2016; Nielson et al., 2015; Schapiro, Kustner, & Turk-Browne, 2012; Schapiro, Turk-Browne, Norman, & Botvinick, 2016).

There is a large body of neurophysiological evidence both in rodents and in humans that supports the temporal context theory. The classic view of hippocampal place fields suggests the hippocampal map represents the same spatial context across long

periods of time, extending for weeks to months (Thompson & Best, 1990). However these initial studies focused on only a small population of cells specifically sought out for their stability. Numerous studies have reported slow changes in the representation of place across extended time (Folkerts et al., 2018; Mankin et al., 2012, 2015; Manns et al., 2007; Mau et al., 2018; Paz et al., 2010; Rubin, Geva, Sheintuch, & Ziv, 2015; Ziv et al., 2013). Crucially, these reports consistently show that there are both stable and drifting units in the active ensemble, suggesting hippocampal ensembles are tracking both the similarities and differences in experiences across time. Indeed, multiple reports have found that while a minority of units are active across many days, there remains a stable population from which one could decode the animal's spatial context and location within that context across large temporal lags (Mau et al., 2018; Rubin et al., 2015; Ziv et al., 2013). These reports span temporal scales and show both stability and drift on the order of seconds, minutes, hours, and days. Moreover, these phenomena have been observed across a wide variety of recording methodologies suggesting this is a feature of the system, rather than a measurement artifact (Cai et al., 2016; Mankin et al., 2012; Manns et al., 2007; Mau et al., 2018).

There is behavioral, neuroimaging and animal neurophysiology evidence consistent with both temporal drift and event segmentation, and the two hypotheses are not mutually exclusive (Figure 10 "Segmented Temporal Context'). However, these two bodies of work have never been directly compared in the same preparation. The goal of this experiment was to examine whether or how these two forms of context representation are observed in a task that leverages a temporally defined context. This

task paradigm involves two distinct behavioral contexts that are separated by a behavioral boundary. The hippocampus is hypothesized to map these contexts into discrete event representations as proposed by event segmentation theory, and to also contain a slowly drifting signal as proposed by temporal context theory.

3.3 Experimental Methods

In order to determine how the hippocampal map segments similar experiences that occur across minutes, rats performed a task in which distinct behaviors were reinforced in different temporal blocks of trials in the same spatial environment. The boundary between blocks was cued by shuttling the animal to a separate chamber for 1 minute, but there were no overt cues to signal the behavioral context at the time of the choice behavior. A representation of temporal context that changes continuously across blocks would be behaviorally suboptimal in this experiment (Figure 10 "Drifting Temporal Context"). Rather, the strategy to maximize reward would be to segment the experiment into behaviorally meaningful contexts by using the boundary cue (Figure 1 "Event Segmentation").

During performance of this task, we recorded extracellularly from dorsal CA1 ensembles. As in earlier work that showed evidence for spatial event segmentation (Komorowski et al., 2013, 2009), rats were presented with pairs of pots containing unique odors and digging media and the rat was rewarded for choosing the correct pot from the pair. The identity of the rewarded pot was consistent for each block of 15 trials after which the 1-minute boundary cue was imposed; for the next 15 trials the other pot was

rewarded. The event segmentation hypothesis predicts two stable mappings of objects and places, one for each rule condition (Figure 10 “Event Segmentation” panel). In contrast, the temporal context hypothesis predicts a continuous decorrelation of neural representations that was unaffected by the blocked structure of the experience (Figure 10 “Drifting Temporal Context” panel). A representation validating both theories might involve a new but stable context instated at the start of each block of trials (Figure 10 “Segmented Temporal Context” panel).

***Subjects*.** Subjects were 5 male Long-Evans rats (Charles River) weighing between 350 and 450 grams and between the ages of 6 months to 1 year for the duration of the experiment. All animals were single housed and maintained on a 12 h light/dark cycle (lights on 8:00 A.M. to P.M.). Behavioral training and testing were conducted exclusively during the light phase. Animals were maintained at a minimum (85%) of their *ad libitum* feeding body weight during all behavioral training and testing periods. Procedures were conducted in accordance with the requirements set by the National Institutes of Health and Boston University Institutional Animal Care and Use Committee (IACUC).

***Behavioral Apparatus*:** The behavioral training and testing environment was a custom-built wood apparatus (40 l x 60 w x 40 h cm) consisting of a 40 cm x 40 cm box, and a 20 cm x 20 cm side alleyway. The objects consisted of identical circular terra cotta pots (10 cm high with an internal diameter of 9 cm), each with their own unique digging media and odors (e.g., purple beads with grapefruit scent). The pots were distinguishable

only by their scent and digging media, requiring the animal to overtly sample before choosing to dig. In order to prevent the animals from being guided by odor of the Froot Loop (Kellogg's) cereal reward, finely crushed Froot Loops were sprinkled into all digging media.

Surgery. Anesthesia was induced by inhalation of 5% isoflurane (Webster Veterinary Supply) in oxygen and then a stable plane was maintained at 1.5%-3% throughout the entirety of surgery. Before surgery animals were injected with the analgesic Buprenex (buprenorphine hydrochloride, 0.03 mg/kg i.m.; Reckitt Benckiser Healthcare), and the antibiotic cefazolin (330 mg/ml i.m.; West-Ward Pharmaceutical). The skin of the animal's head covering the skull was shaved and cleaned with alcohol swabs before then being placed in a stereotaxic frame (Kopf). A longitudinal incision was made to expose the skull and the bone, and underlying fascia was cleared in order to gain access to stereotaxic coordinates and locations for anchoring screws. Animals were implanted with microdrives containing 18-24 independently drivable tetrodes targeting the dorsal pole of the CA1 cell layer of the hippocampus (centered at 3.6 mm posterior and 2.6 mm lateral from bregma). Finally a screw was placed above the cerebellum to serve as a ground signal. Each tetrode was composed of four 12 um RO 800 wires (Sandvik Kanthal HP Reid Precision Fine Tetrode Wire; Sandvik). Tetrodes were plated with non-cyanide gold solution, via electrolysis in order to reduce impedance to between 180 and 220 k**Ω**. At the conclusion of the surgery, all tetrodes were gradually lowered ~0.5 - ~1.5 mm into tissue. Upon recovery from anesthesia, animals underwent post-

operative care for 3 days and received doses of Buprenex and cefazolin, as described above, two times a day (12 hour intervals). Animals were allowed to recover 1 week before behavioral testing commenced.

***Neural Recordings*.** Electrophysiological recordings for this project were collected on a 96 channel OmniPlex D Neural Acquisition System (Plexon). Each channel was amplified on head-mounted preamps and then amplified again for total of 1000x to 10,000x before being digitized at 40 kHz. Spike data were band-pass filtered from 200 Hz to 8.8 kHz and local field potentials from 1.5 Hz to 400 Hz. Spike channels were referenced to a local electrode in the same region in order to remove both movement-related and ambient electrical noise. That local reference electrode was then referenced to ground and provided the LFP signal in the region. Action potentials of neurons were detected via threshold crossing and then sorted later using Offline Sorter (Plexon). Cineplex Studio (Plexon) was used for capturing behavioral tracking data, and Cineplex Editor (Plexon) was employed to enter event markers and to verify animal tracking data. Between recorded training sessions tetrodes were advanced at a minimum of 40 µm and positioned based on visual inspection of spike clusters in order to maximize neural unit yield. Tetrodes were allowed to settle after turning over a period of days to prevent contamination of neural signals with tetrode drift.

***Histology*.** Upon completion of behavioral testing, rats were anesthetized with <5% isoflurane in oxygen. Anatomical recording sites were confirmed by creating a

small lesion in the brain tissue by passing a 40 µA current until the connection was severed (generally 2-8 seconds). Immediately after completion of electrolytic lesions, animals received an overdose injection (interperitoneal) of Euthasol (Virbac AH) and upon cessation of breathing were immediately transcardially perfused with ice cold 0.5% potassium phosphate buffered saline followed by 5% phosphate buffered formalin (VWR). Brains were then removed and placed in additional 5% formalin phosphate for at least 36 hours. Brains were then submerged in 30% sucrose for cryoprotection until sectioning into 40 µM thick sections via cryostat (CM 3050s; Leica Biosystems). Brain sections were processed using standard Nissl staining protocol in order to visually confirm tetrode-recording sites (Figure 1c).

Animal Training and Task. Once each animal recovered from surgery they were initially trained to dig for Froot Loop (Kellogg) bits in an aloe-scented pot over a cloves scented pot (both in sand). Once they reliably dug in the aloe pot and refrained from digging in the cloves pot, training began in the blocked-reversal task. Each training and recording session consisted of 6 blocks of 15 trials for a total of 90 trials. Once the rat reached a criterion of 70% correct across a given session, recording commenced. Some sessions were terminated early (the shortest session was 85 trials) due to lack of motivation by the subject. Within each 15 trial block the reward contingency was set so that one pot always had food and the other pot did not. Each trial started with the insertion of a divider so that the experimenter could place the pots in a pseudorandom position. Once pots were placed, the divider was removed and the animal was allowed to

sample each pot, but only allowed to dig in one. Upon digging, the unchosen pot was immediately removed and the animal was allowed to dig until he found reward or gave up because he chose incorrectly. After either completion of reward consumption or a 3 second delay following pot removal, the rat was shuttled to the far half of the chamber and the divider replaced. The next trial commenced immediately until trial 15 was reached. After the last trial of each block, the rat was shuttled into the side alley to wait for 60 seconds. After the break, the reward contingency was reversed and the next block of 15 trials was performed.

Quantitative & Statistical Analyses: All analysis of the collected data were performed using custom scripts from MATLAB (MathWorks). ANOVAs were performed using the 'anovan' function in MATLAB under a standard type 2 sum of squares. For individual unit analyses, peri-event histograms were generated from 120 to 160 millisecond bins and smoothed using a moving average of a three bin span. All trials were included in peri-event rasters including those in which the rat responded incorrectly, but only the first sample in each trial is shown. Right and left samples correspond to each of the two pseudorandomized locations of the reward pots. Error bars on firing rates were calculated using the standard error of the mean. Spatial firing rate plots were generated using a 3 cm pixel size, and then convolved with a Gaussian smoothing kernel with a standard deviation of one pixel. Selectivity was evaluated by calculating a selectivity score below, where n represents the set of trial-types(two in the case of object and position, four in the case of object by position), and λ represents the mean firing rate for that event type. $\lambda pref$ represents the trail type with the largest firing rate.

$$Selectivity\ Index = \frac{(n - \sum_{i=1}^{n}\left(\frac{\lambda_i}{\lambda_{pref}}\right))}{n-1}$$

Significance was determined by generating a null distribution of selectivity scores after randomizing the trial identity of each sample. Only units that passed a 99% significance threshold from 10,000 boots were considered to code a particular dimension (Keene et al., 2016).

For waveform and spike rate drift metrics, average waveform amplitude and spike rate was estimated for each 10 second bin spanning the whole recording session. We then measured the average absolute Euclidean distance and absolute difference in firing rate between each bin to all other bins. From that matrix, we regressed the values as a function of distance from the diagonal but excluding the diagonal to obtain an average waveform or spike rate distance as a function of temporal lag between bins for each cell. Units with an average firing rate of >10 Hz across the whole recording session were assumed to be interneurons and were removed from all population analyses.

For population analyses, trial rate vectors were constructed for each cell by averaging the firing rate across the two seconds surrounding the first sampling event on each trial, and then z-normalizing the rate across trials for each individual neuron. All trials were included in these analyses, so as to reveal any performance effects as well as for statistical reasons. A z-transform was employed to prevent overreliance on highly active units or under reliance on sparsely active units. A population vector correlation matrix was generated for each rat by calculating the Spearman correlation of the population vector for each trial to each other (Figure 16B). That correlation matrix was

then averaged across all sessions to generate the 'super rat' matrix observed in Figure 6A. All measures of drift were constructed by first generating a mean value for each session onto which statistics were performed, and the mean +/- SEM across sessions was plotted. Bootstrap permutation tests were performed as described with a standard 10,000 randomized samples in which the group index was randomized without replacement. Bayes factors were obtained by inputting summary statistics into an online engine accessible at http://pcl.missouri.edu/ (Liang, Paulo, Molina, Clyde, & Berger, 2008).

3.4 Results and Figures

3.4.1 Rats performed a temporally blocked object discrimination task

We recorded from 768 cells across 25 sessions from 5 rats each implanted with a 24-tetrode hyperdrive aimed at dorsal CA1 (Figure 10C). After removing putative interneurons and keeping only units with an average firing rate of below 10 Hz and with at least one spike for at least 5 sampling events we obtained 642 putative pyramidal cells. Rats were trained to perform a blocked object discrimination task designed to segment memory into six 15 trial blocks (Figure 10A). Within each block of 15 trials, one of the two distinguishable pots contained hidden reward. After each 15 trial block, a temporal delay signaled the end of a block; the reward contingency was reversed to the other pot for the subsequent block of trials (See Figure 10 "Event Segmentation"). Between blocks the rat was shuttled into a side chamber for 60 seconds so that the end of a block was signaled not only by an increased trial duration *per se* but also by an intervening experience. Individual trials took on average a little under 30 seconds to perform (26.0

+/- 0.40 sec), each block of trials took about 6 minutes (6.04 +/- 0.56 min), and a session lasted roughly 45 minutes (45.44 +/- 1.1 min). Each session contained an unequal but roughly similar number of sampling events at each item and position, however some animals showed a slight bias towards sampling the item on one side of the maze more often. Furthermore, we restricted our analyses to the first sampling event on each trial, as the identity of the object on the first sample remained pseudorandomized per task design. Only after the sample had terminated and a response was offered did the behavior systematically change towards rejecting the incorrect object and digging in the correct pot.

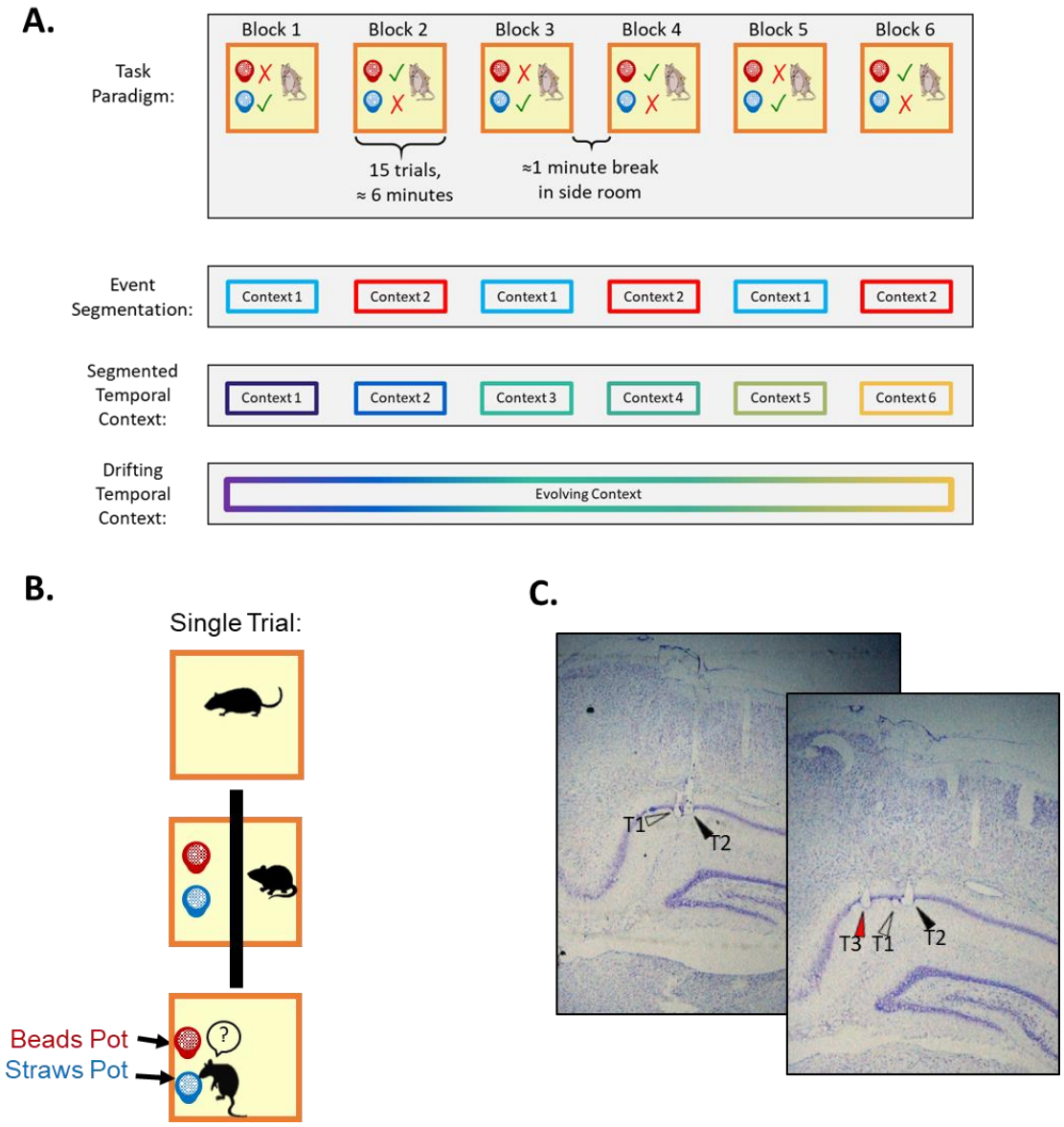

Figure 10: Task design and tetrode locations.

A. Rats performed a blocked object discrimination task in which the reward contingency was held constant for 15 trials in a row and then reversed for the next 15. Each block took roughly 6 minutes, and each delay between blocks was fixed at 1 minute. B. Each trial consisted of three phases, a short inter trial interval, the pot setup phase, and the sample/choice phase. C. Recording locations of three individual tetrodes. Arrowheads indicate final tetrode locations in the pyramidal layer of dorsal CA1.

3.4.2 Rats performed as though each block of trials was a new episode.

Following pre-training on simple pot discrimination, rats took roughly a week to reach a criterion of 70% correct within a given session. Recording began after criterion was reached. Once trained, all rats performed similarly to each other (Mean across rats=80% +/- 1.97%, ANOVA, F(4,20)=0.1), and all rats performed similarly across days (Mean across days=79% +/- 0.52% ANOVA, F(7,17)=1.61) and blocks within each day (Mean across blocks=79%+/-1.13% ANOVA, F(5,144)=1.73). Typically, errors were concentrated around the beginning of each block, but were not restricted to the beginning of the recording session (Figure 11). We generated two alternative hypotheses regarding behavior. We hypothesized that the rats would recognize the block transitions as a cue to change their response strategy, and would begin each block by switching their response towards digging in the now-correct pot. Alternatively, rats could have ignored the boundary cue. In this case the animals would begin each block by erroneously perseverating with the (now-incorrect) response from the previous block. We evaluated these hypotheses at the group level, but also at the individual animal level (if some rats respected the contextual cues while others did not, the group could perform at chance on average despite none of the individual rats performing at chance). To investigate both hypotheses, we compared each rat's performance for each trial across blocks to chance by performing a binomial test on each animal. A two-sided binomial test asks whether the probability of correct responses was *either* above *or* below chance. Contrary to both hypotheses, only one rat performed different from chance for either of the first two trials in each block before a Bonferonni correction (Figure 11, Two Sided Binomial Test, Rat 1

Trial 1: 30% uncorrected binom p=0.03, trial 2: 38%, binom p=0.24: Other rats Trial 1: 45.6%+/- 5.7%, minimum p=0.09, trial 2: 50.4%+/- 6.21%, minimum p= 0.31). By trial 5 all rats were performing significantly above chance (Figure 2, trial 5: 81.5%+/- 4.38%, All binom. P<0.05, trials 6 to 15: 90.7% +/- 1.2%, All Binom. p< 0.005). Rats appeared to begin each block by impulsively digging in the first pot they encountered, as the probability of rejecting the first encountered pot on the first trial of each block was lower than for the last 8 trials of each block (Trial 1 reject rate mean=0.32 +/- 0.038% , trials 11:15 reject rate mean=0.42 +/- 0.014%, ranksum p<0.05). Thus, rats appeared to begin each block of trials by guessing, and then rapidly learning the new rule contingency. The performance of each rat on each block could be described as either a recency-weighted averaging over recent experiences. Alternatively, they may have perceived the block delay as a new context but the behavioral contingency of that context was unknown to the rat. Both hypotheses account for the chance performance following the inter-block delay and also the learning of the new reward contingency within block (Figure 11 Right). However, an interpretation consistent with recency weighted averaging predicts a neural representation consistent with drifting temporal context (Figure 10), whereas recognition of the boundary but not anticipation of the rule predicts a neural representation consistent with either a segmented temporal context, or event segmentation (Figure 10).

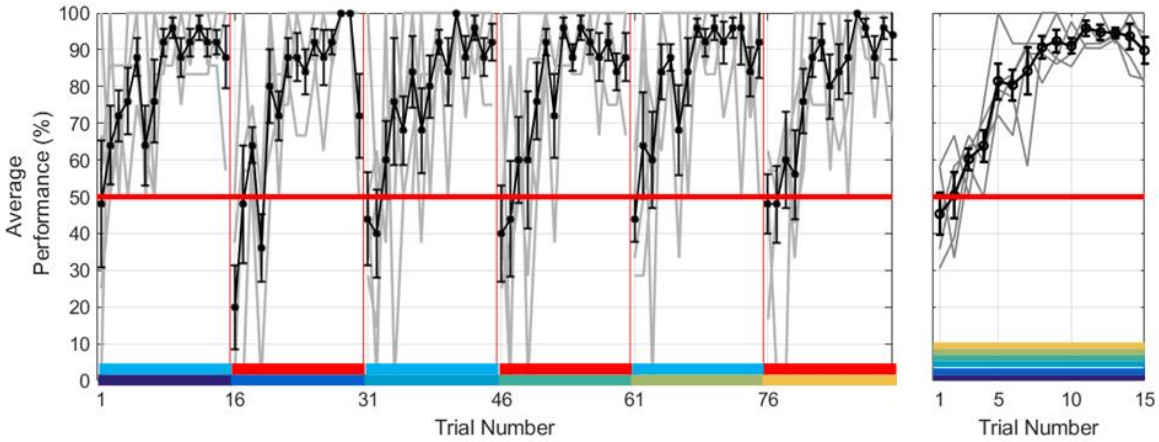

Figure 11: Rats did not anticipate the reversal in reward contingency across blocks.

Left: Mean +/- SEM performance throughout each recording session. Gray lines represent individual rats. Rats began each block in a session at chance regardless of the position of that block in the session. (Colored Bars represent changing context per Figure 1) Right: When all blocks were concatenated (colored blocks stacked), no rat performed better or worse than chance at the beginning of each block. Gray lines represent individual rats while black represents mean across all rats. Red line is chance performance. All rats behaved as though each block represented a novel context in which to learn the rule contingency (colored bars represent evidence towards 'temporal context' as denoted in Figure 1).

3.4.3 Single units replicated prior findings of object and position selective fields, but were impacted by context

Single unit activity was observed by generating spatial heat plots (Figure 12), and peri-event rastergrams, and histograms centered on pot-sampling events (Figure 13). Consistent with previous reports, a large proportion of hippocampal cells had firing fields where the objects were presented (Figure 12, cells 1, 3, 5, and 6). When event-locked firing was examined, there was a large overlapping population of units whose firing fields discriminated between sampling events. Some units had firing fields consistently discriminated item regardless of position (Figure 13 top row, 43 cells (8% of putative pyramidal cells), showed an object selectivity score greater than 99% of 10,000 bootstrap

permutations). There were also units whose fields were specific to one position (Figure 12, 106 cells (17% of putative pyramidal cells) showed a position selectivity score greater than 99% of 10,000 bootstrap permutations) as well as those specific to one item in one place (Figure 13 bottom row, 80 cells (12% of all putative pyramidal cells) showed object by position selectivity greater than 99% of 10,000 bootstrap permutations). Upon further investigation firing fields showed clear dependence on the shifting context (McKenzie et al., 2014) (Figure 14).

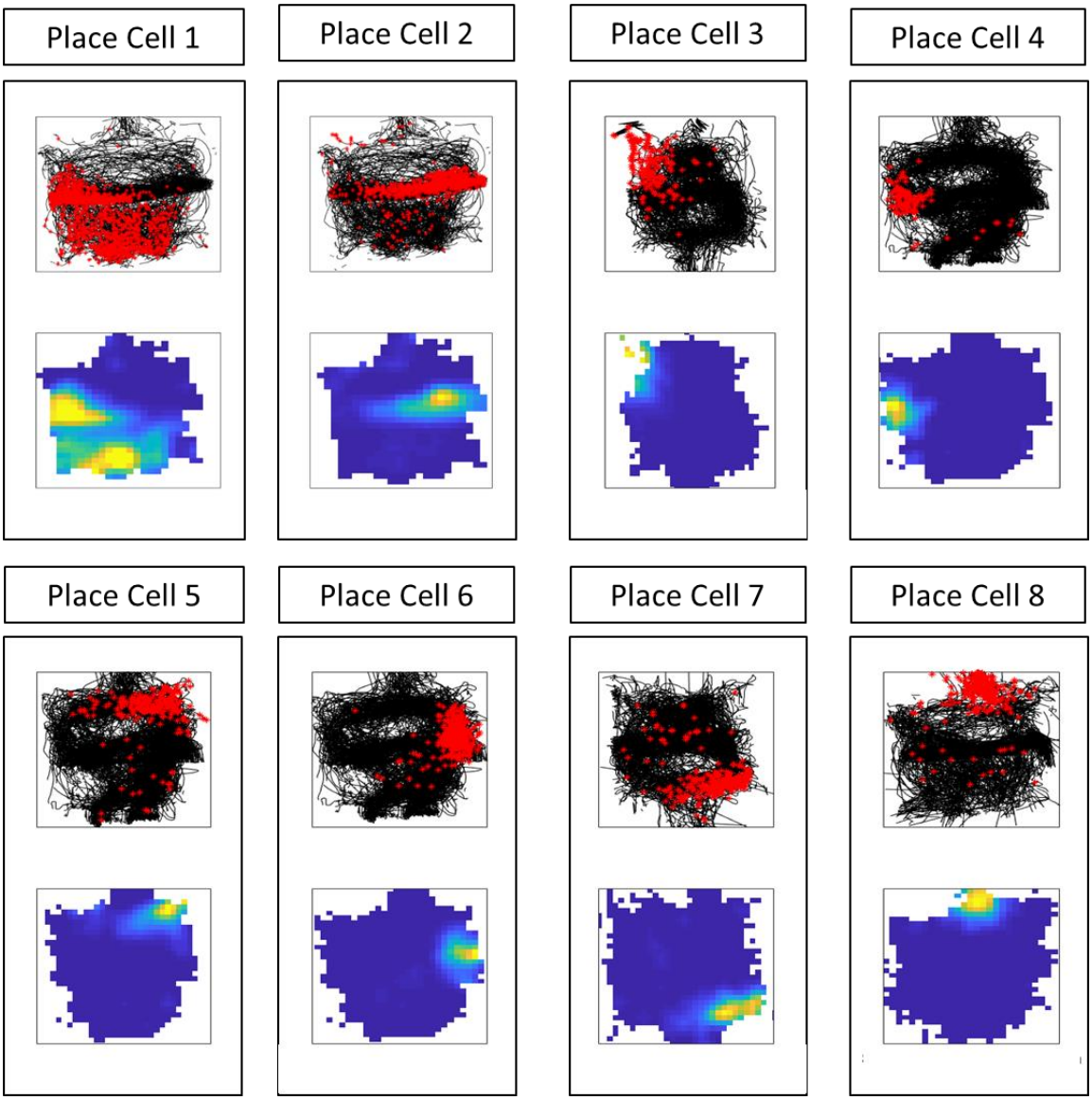

Figure 12: Many units showed spatially localized firing fields.

Top plots: Black lines denote the running trajectories of the rat, while red dots denote the locations of spikes recorded from one unit. Bottom plots: Spatial heat maps of binned-firing rates for each unit. Yellow denotes maximal firing, blue denotes minimal firing.

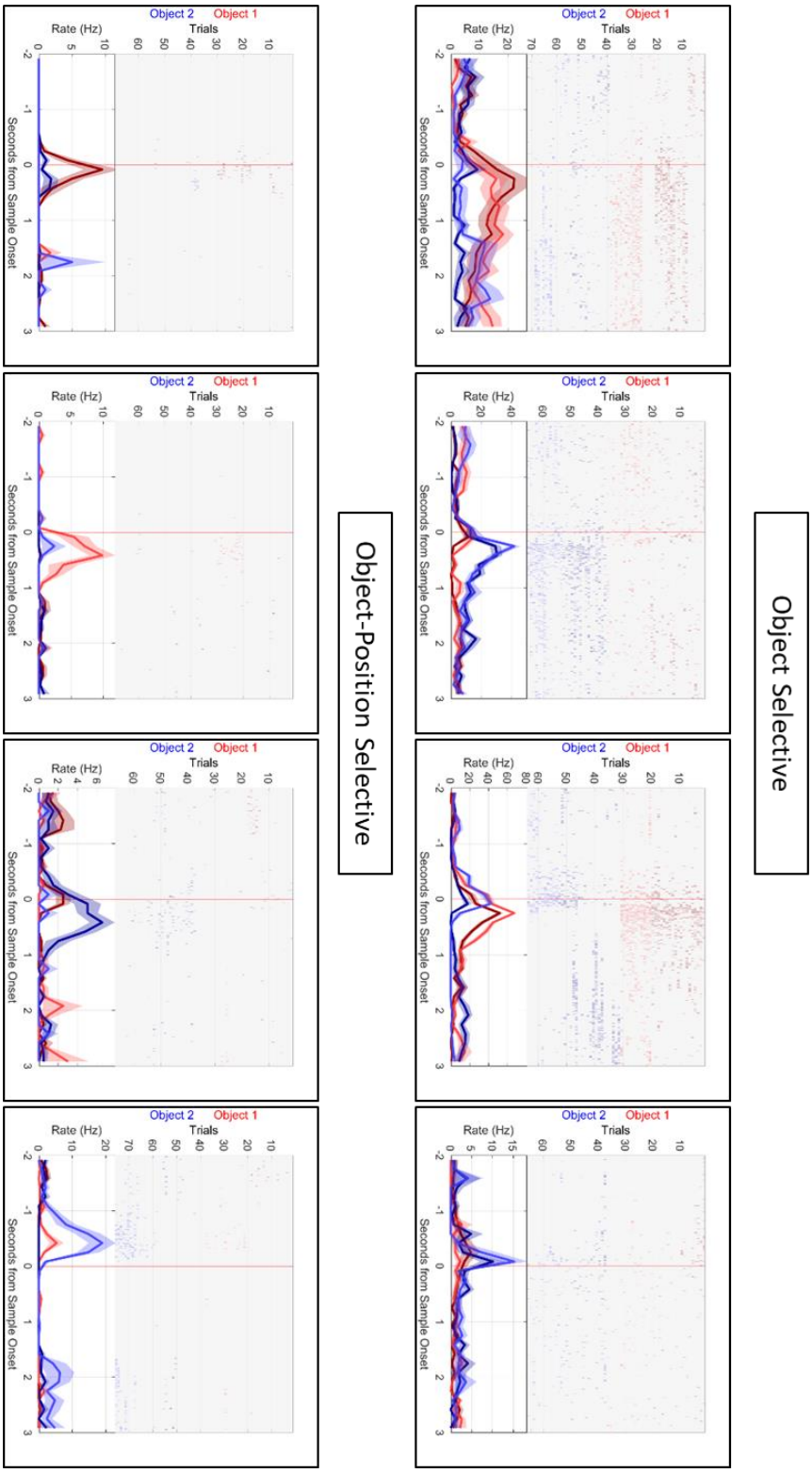
Object Selective
Object-Position Selective
Object 2
Object 1
Trials
Rate (Hz)
Seconds from Sample Onset

Figure 13: Many units showed object-specific firing, (top four) and conjunctive object -position firing (bottom four).

Peri-event rasters and histogram plots centered on object sampling. Time refers to seconds from sample onset, and rate refers to firing rate in Hz. We found some units to be object selective (red vs. blue) regardless of the position of the object (light shades v dark shades), as well as some objects to be selective to one object-position combination.

3.4.4 A drifting contextual representation replicates previous findings and is uncorrelated to waveform drift

Many units showed firing fields that were modulated by the changing context. The temporal context model and the event segmentation model each make a strong prediction for how context may modulate hippocampal firing fields (Figure 14). While putative pyramidal cells maintained the same spatial and object selectivity across blocks of trials, their rates showed obvious changes across contexts that seemed to resemble predictions from the temporal context model (Figure 14, bottom). Figure 14contains plots that include all trials including error trials, and each trial was color coded based on block (Figure 5, Color Scheme: Figure 1 “Segmented Temporal Context”). Briefly, event segmentation theory predicts that in this experiment firing fields should alternate across blocks so that units' response should be similar in the same the behavioral context. Conversely, temporal context theory predicts that in this experiment firing fields should change continuously without regard to the alternating behavioral contexts. For example, the first example cell (Figure 14) had a firing field that was selective to leftward samples of object 1, and was most robust for the first two blocks of trials. That is, this unit fired across two blocks of trials with different behavioral contexts and then ceased firing despite the repetition of those behavioral contexts.

3.4.5 Gradual changes in firing rate were uncorrelated with electrode stability

To exclude the possibility that cells were drifting due to acquisition error, spike clusters from each tetrode were carefully examined as a function of time. First, tetrodes that included waveform clusters that obviously appeared not stationary with regard to time we excluded (Manns et al., 2007). Then, drift in spike amplitude was correlated to drift in spike rate in the remaining population of cells. For each cell, the Euclidean (4 dimensional) distance was measured between the average spike amplitudes of each 10 second bin in the session and then the distances were regressed against their bin lag to obtain a measure of waveform drift. The same was performed for absolute difference in average firing rate at the same 10-second bins to obtain a measure of firing rate drift. While there was a distribution of spike amplitude drift rates and activity drift rates, there was no relationship between the two measures (Figure 6, Spearman's Rho, r^2 (642) = 0.0606, $p>.05$).

These data revealed a wide spectrum of firing rate drift rates, as well as a wide spectrum of spike amplitude drift rates. However, as there was no relationship between these two distributions, the single unit data suggested that individual units exhibit a continuous spectrum of drift rates across time that is not due to recording artifact.

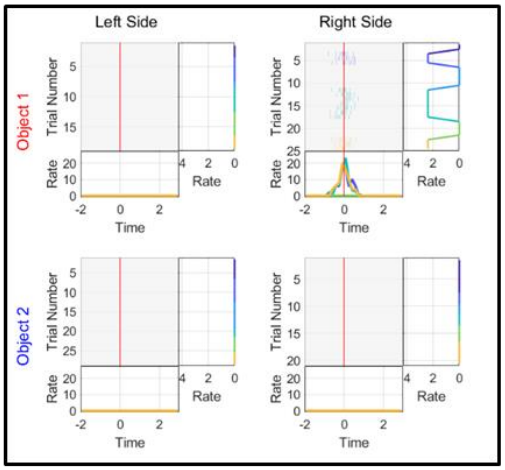

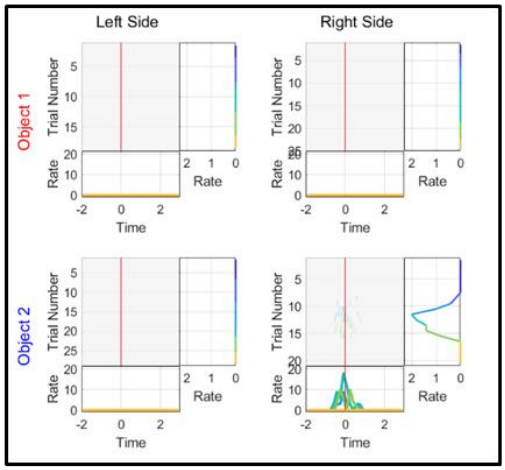

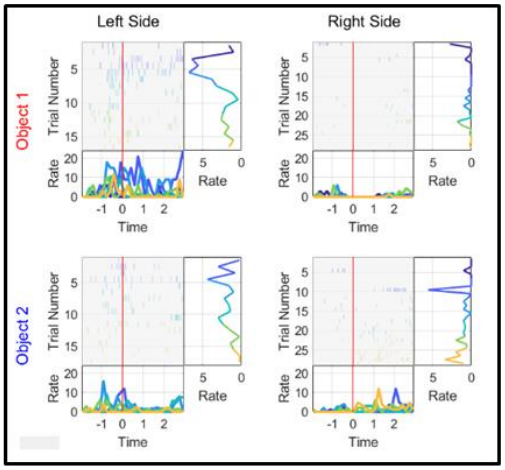

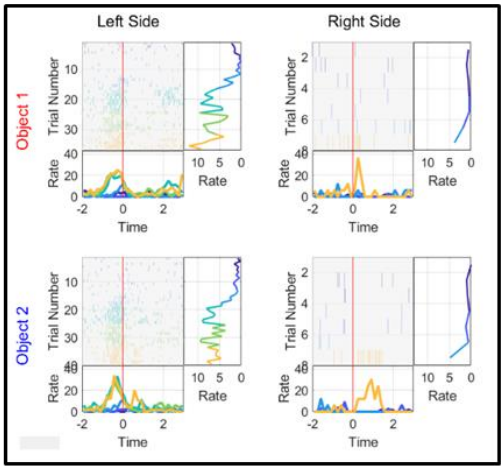

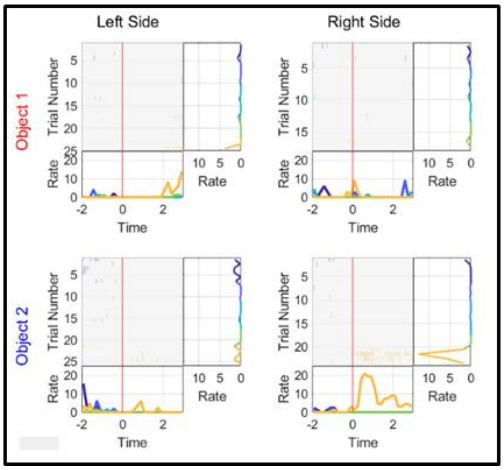

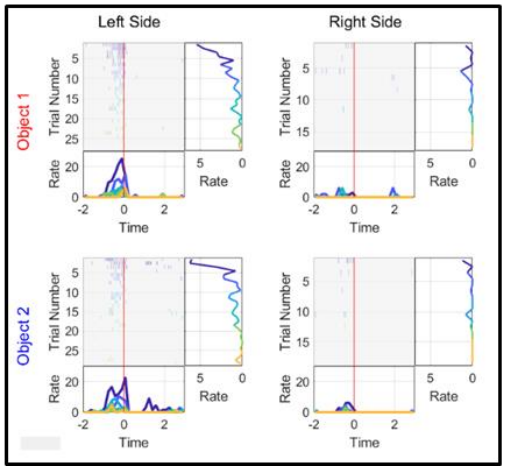

Idealized Rule Coding Cell

Idealized Time Coding Cell

Empirical Context Coding Cell

Figure 14: Many cells had context dependent firing fields.

Top: Idealized firing fields of dCA1 units in the temporally blocked object discrimination task. Each color in rasters and line plots represent samples in one block of trials (See Figure 1A and Figure 2). Top Left: Ideal cell that responds selectively during one object-position combination, and does so only during blocks 2, 4, and 6 when object 2 is rewarded. Top Right: Idealized object-position conjunctive cell that responds maximally during block 4. Each idealized cell provides information about the object, position, and temporal structure of the task. Bottom: Empirical cells showed firing fields that seemed to be centered on a small contiguous block of trials, suggesting temporal drift. No empirical cells showed firing fields that alternated with blocks, showing a lack of evidence for event segmentation.

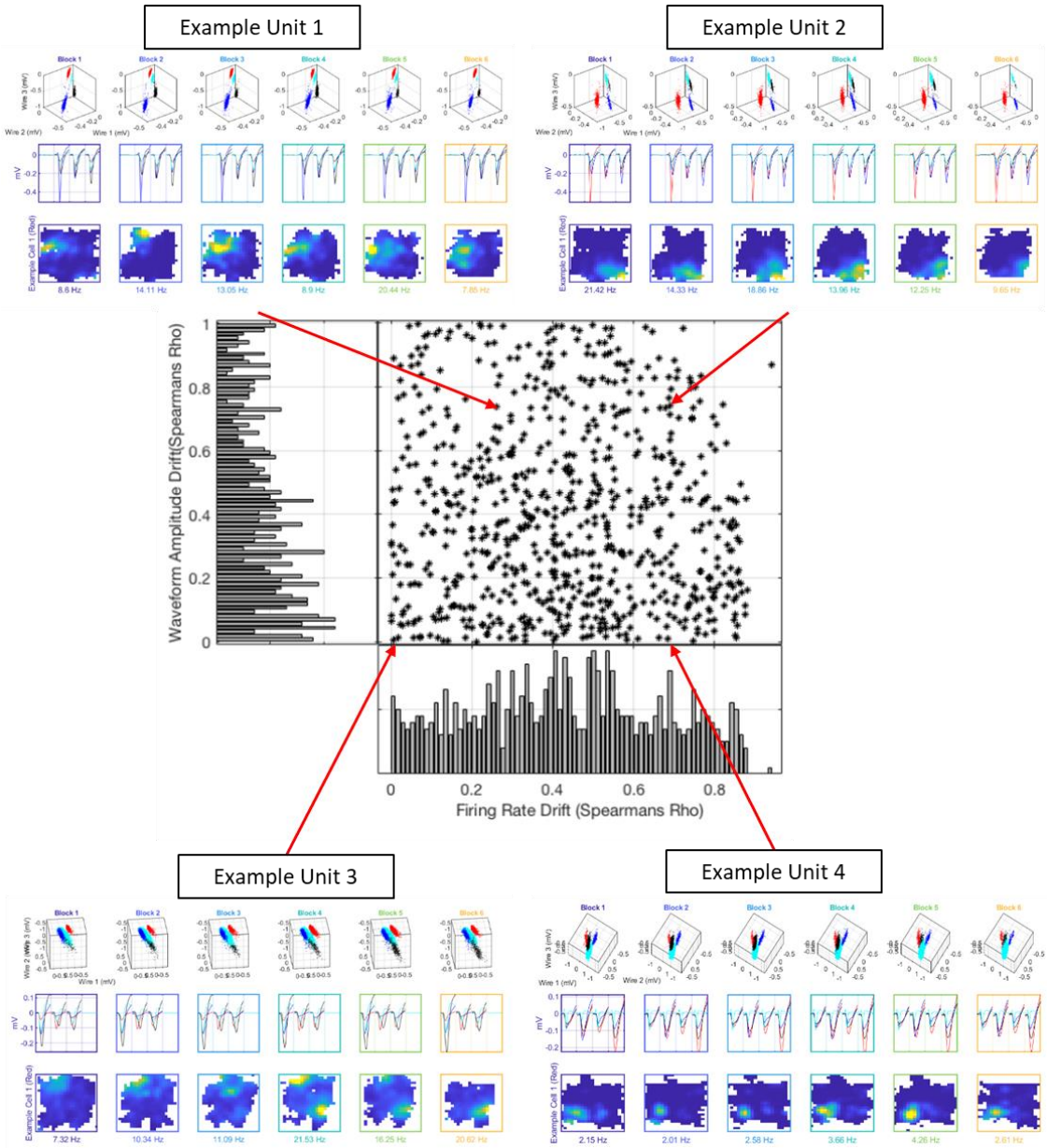

Figure 15: Waveform drift is unrelated to spike rate drift.

For each cell we measured the average spike rate and waveform shape for each 10 second bin across the recording session, and then measured the similarity within each metric at bins of increasing lag (see methods). Cells showed a wide distribution of spike-rate drifts (vertical line plot at bottom), and a wide distribution of spike shape drift rates (horizontal bars at left). However, the spike-rate drift was unrelated to spike shape drift. Each example represents one cell at each corner of the scatter plot. Each unit cluster and waveforms are represented in red, and other units on that tetrode are included. Peak firing rates are listed below place plots for each unit during each block. Firing rate and waveform drift rates for each example unit, respectively: Unit 1: 0.26, 0.73; Unit 2: 0.69, 0.73; Unit 3: 0. 07, 0.01; Unit 4: 0.70, 0.08.

3.4.6 Ensemble activity suggests hippocampal patterns slowly drift

To supplement the analysis on individual units, population analyses were used to determine whether hippocampal ensembles showed evidence for event segmentation, a drifting temporal context, or both. Event segmentation predicts that the hippocampus generates two stable representations, one for each rule condition (Figure 16A top left). This would manifest in alternating high correlations between blocks of the same rule condition, and low correlations between blocks of opposing rule condition. A drifting temporal context predicts that ensembles slowly change, and new representations would be continually generated (Figure 16A top right). This would manifest as a slow fall in the correlation between blocks at increasing temporal lag. We calculated the Spearman correlation of the population vector from each trial to all others to generate a correlation matrix for each rat (Figure 16B, Methods). We then averaged that matrix across all rats and sessions to generate a grand mean correlation matrix (Figure 16A Bottom). The empirical pattern of ensemble activity showed strong support for drift, characteristic of temporal context (Figure 16A right) but no apparent evidence that representations from past blocks with the same reward contingency were repeated (Figure 16A left). Correlation values were greater at the beginning and the end of the session, but this may have been due to the lack of an acclimatization period at the start, and the fact that some sessions were shorter than others (Monaco et al., 2014). Importantly, the correlation values did not fall smoothly at increasing distances from the diagonal of the matrix. This was likely due

to behavioral variables, such as where the rat was during the sampling event, and which pot the rat was sampling. Correlation matrices were reorganized to control for these variables. First trials were sorted by position such that the first and fourth quadrants contained trial pairs in the same position. This revealed a strong ensemble code for space, as exemplified in rats 2 and 4 (Figure 16B) where higher correlations were clustered at same position comparisons. The events were then sorted by object and lastly by time, to reveal correlations that fell more smoothly with increased distance from the diagonal (Figure 16B right). Furthermore, temporal proximity was evident across object and place representations in some rats as evidenced by yellow streaks parallel to the diagonal of the matrix, but away from the diagonal of the matrix (Figure 16B right, rats 1 and 4). These stripes signify that temporally proximal trials that differed in object or place were represented more similarly than those that were farther apart in time. Thus, there was also a portion of the ensemble that tracked trial lag, but not object or position.

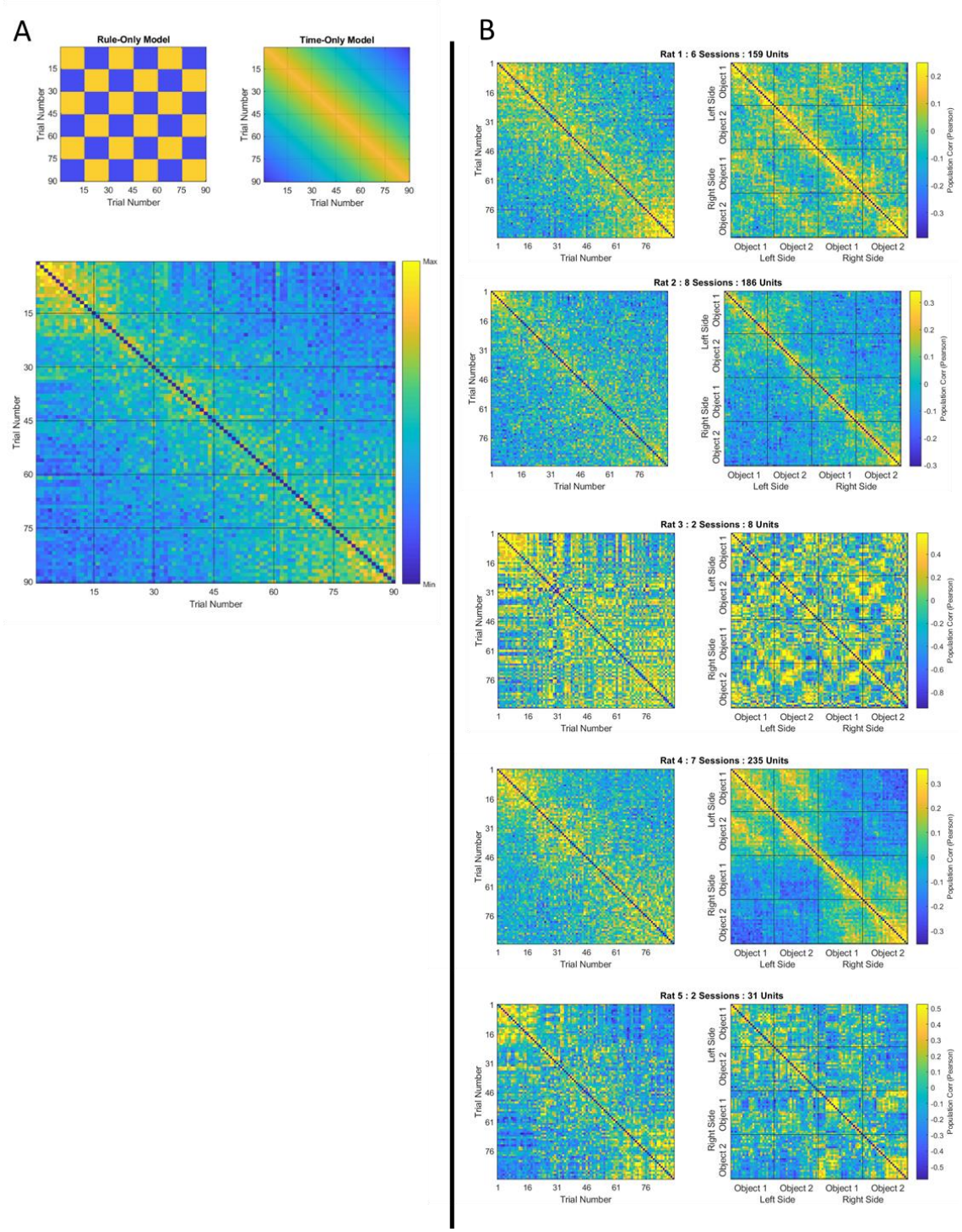

Figure 16: Drift, and not a representation of the repeating rule conditions was apparent in correlation matrices.

A. Observed correlation matrix suggests continuous temporal drift. Top left: Predicted correlation matrix if ensembles represent a context code consistent with event segmentation. Top right: Predicted correlation matrix if ensemble code is consistent with drifting temporal context. Bottom: Empirical correlation matrix averaged across animals more closely resembles predicted matrix under the temporal context hypothesis. B. Trial-by-Trial correlation matrices for each rat also show temporal drift. Left: Matrices were sorted by trial number as was done in A. Right: Matrices sorted by position, then by object, then by trial number. Position coding can be seen as higher correlations in the top left and bottom right quadrants of each matrix. Object coding can be seen as nested quadrants within each position quadrant. Note that once trials were sorted by object and place that high correlations still clustered adjacent to the eye of the matrix, indicating that ensembles were more similar between trials at closer temporal proximity. Similarity was calculated by generating z-normalized firing rate vectors for each cell across sampling events, and then calculating the spearman's rho between the population vectors on each trial. The color scale is equivalent across the two matrices for each rat, but a different scale was used for each rat.

3.4.7 Hippocampal populations showed drift across blocks

The effects observed in the correlation matrices were then quantified. If hippocampal ensembles reflected the two rule states, hippocampal activity would be more similar between blocks that shared a rule condition (at lag 2, and 4), versus those that involved opposing rule conditions (at lag 1, 3, and 5) (Figure 17 top left). Conversely, if hippocampal ensembles tracked time, then hippocampal activity would become progressively less similar between blocks at increasing lag (Figure 17 bottom left). The overall population correlation between blocks consistently fell as the block lag grew (Figure 17 Right, purple line) (across all trials slope=-0.025, Observed slope exceeded all 10000 perms, permutation mean $-2.38\text{x}10^{-7}$, σ=0.0034). The representation for the same behavior (e.g. same object, position, and response) also progressively decorrelated with block (Figure 17, Right, yellow line) (Permutation test: slope=-0.048, the observed slope exceeded all 10,000 bootstrapped permutations, permutation x=$-1.5\text{x}10^{-5}$, σ=0.0073). Correlations for the same item, position, and response remained higher than those across all sample types at each block lag (Bonferonni corrected Ranksum test: Lag 1: Within object, position, response mean correlation = 0.16, across mean correlation =0.03,

$p<1x10^{-4}$, Lag 2 within mean =0.08, across mean =-0.02, $p<0.001$, Lag 3 within mean =0.03, across mean =-0.06, $p<0.001$, Lag 4 within mean =0.01, across mean =-0.07, $p<0.001$, Lag 5 within mean =-0.05, across mean =-0.08, $p<0.05$) suggesting a robust code for objects and places even though both populations drifted. Finally, when these results were reevaluated after only using units with the most stable waveform clusters (most stable quartile, see Figure 15) the population still significantly decorrelated with increasing temporal lag, and at a similar rate (Slope=-0.038, Observed slope exceeded all 10,000 perms, permutation mean $1.12x10^{-4}$, σ=0.0087). Finally, the representation of each delay in between blocks also progressively decorrelated with increasing lag (Figure 17 Black line, Slope of correlation vs. lag=-0.076, observed slope exceeded all 10,000 perms, perm mean=-3.6×10^{-3}, σ=0.017). Therefore, all empirical curves replicate previous findings of a temporal context coded in conjunction with a stable code for items, places, and behavior. Note that deviations from the smoothly decreasing curves are small- any contribution from discrete event coding would have to be much smaller than the contribution due to gradually-changing temporal context. Moreover, event segmentation would predict that the deviations from a smooth curve should be consistent from one type of comparison to the other, resulting in parallel curves (Figure 17, top left). However, to the extent there were deviations in the different empirical curves, they were not systematic across the type of comparison. Thus, consistent with behavior, there was no evidence that hippocampal populations represented blocks in discrete segments based on the two rule conditions.

Overall hippocampal ensembles showed strong temporal drift with no evidence that past blocks of the same rule condition used the same code. This was true for the overall population, but was also found in conjunction with a code for places, objects, and object-place conjunctions. Furthermore the code for objects and positions remained across all blocks. Thus even though hippocampal populations drifted from block to block, there remained a code for objects and positions that persisted throughout the recording. Temporal drift also persisted during the inter-block-delays, where there was also no evidence for an alternating neural structure.

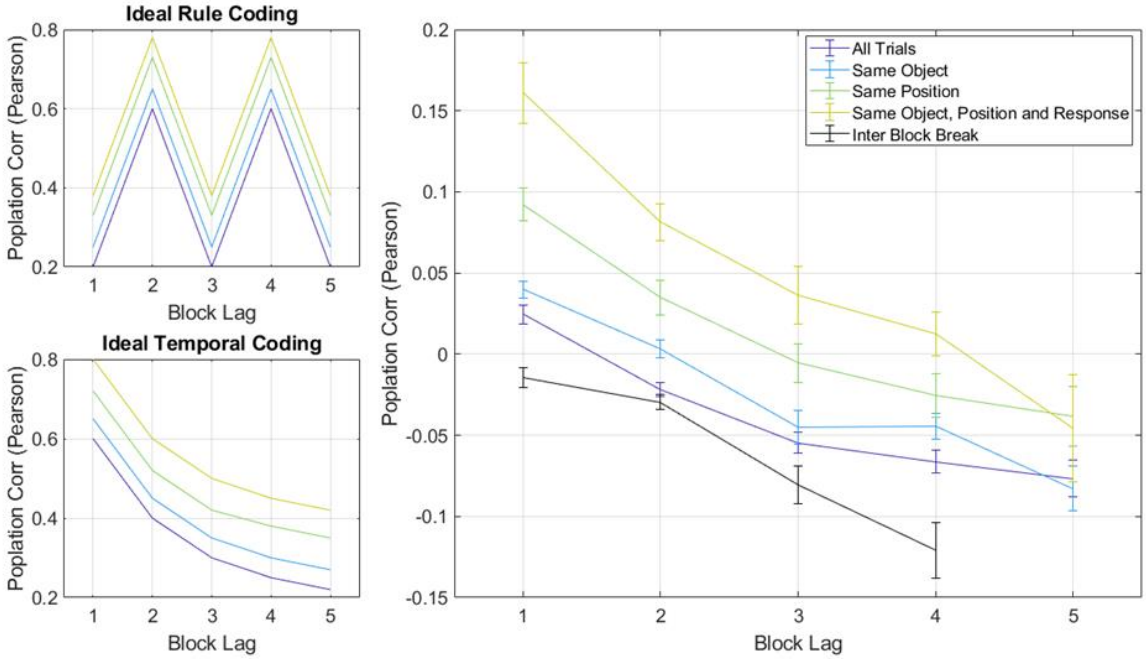

Figure 17: Ensembles reflected a context code that continually changed across blocks and did not recur.

Top left: Ideal curves under event segmentation hypothesis. Event segmentation predicts high correlations between blocks of the same rule condition at lags 2 and 4. Bottom left: Ideal curves under the contextual drift hypothesis. Contextual drift predicts a monotonic decrease in each curve. Right. Observed curves for ensemble correlations fell as the block lag between the trials grew. This was true for the overall population (purple line) as well as in the ensemble coding the same object (blue) or position (green) or same object, position and behavioral response (yellow), and finally the intervals between the blocks (black line). All curves show a systematic decrease from small to large lags with no obvious alternation. To the extent that there are fluctuations in the curves, these fluctuations were small and not consistent across different trial comparisons.

3.4.8 Hippocampal populations showed drift within block

The foregoing analyses demonstrate that the hippocampal ensemble changed gradually across blocks on the scale of tens of minutes. This subsection examines changes in hippocampal representation within a block on the scale of about a minute. To replicate previous findings, population correlations were compared between individual

trials (Figure 18) (Manns et al., 2007). There was significant temporal drift in the overall representations across trials (Figure 18 purple line, observed slope=-6.8x10^{-3}, observed data exceeded all 10,000 perms, perm. x =-8.16 x10^{-6}, σ=8.4x10^{-4}). Temporal drift within a block was apparent after controlling for object, (Figure 9 blue line, Observed slope= -8.5x10^{-3}, observed data exceeded all 10,000 perms, perm. x=6.98 x10^{-6}, σ=1.1x10^{-3}), position (Figure 18 green line, Observed slope= -7.1x10^{-3}, observed data exceeded all 10,000 perms, perm. x =-1.58 x10^{-5}, σ=9.0x10^{-4}), and object, position, and response (Figure 9 yellow line, Observed slope= -0.013, observed data exceeded all 10,000 perms, perm. x =-4.65 x10^{-7}, σ=1.3x10^{-3}). Drift was also apparent across exclusively correct trials (Not shown, Observed slope= -0.0095, observed data exceeded all 10,000 perms, perm. =-1.32 x10^{-5}, σ=1.7x10^{-3}) suggesting that this is not an artifact of the learning curve observed in Figure 11. This drift occurred individually in the overall population of each rat tested except for Rat 3 (Figure 17B, Rat 3 included 2 sessions with 12 units total, observed slope=-0.011, observed data exceeded 716/1000 perms, perm x=-1.24 x10^{-4}, σ=0.0076). This failure to observe robust drift in Rat 3 is perhaps because Rat 3 only contributed a total of 12 units over 2 sessions.

These data replicate previous findings that show drift is observable across individual trials. Drift on the order of seconds was observed in the overall code, as well as the code for objects, positions, and object-position conjunctions. Thus, reliable population drift was observed even across iterations of the same behavior and context, and over a scale of seconds.

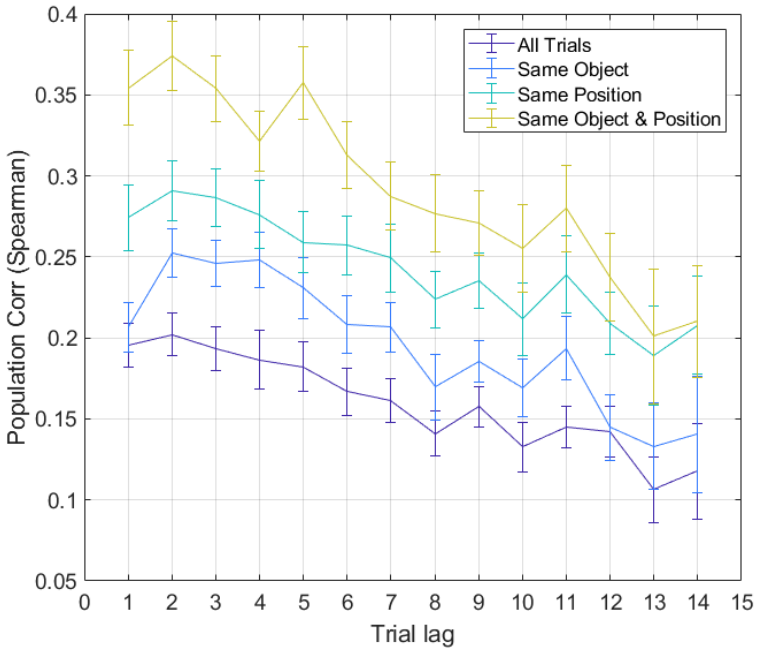

Figure 18: Ensemble correlations within a block reliably fell as trial lag increased.

This effect was evident both in the overall population activity (purple line), as well as when we controlled for object (blue), position (green), or object, position, and response (yellow). The overall correlations across lags were higher after controlling for object, position, and object-position conjunctions, revealing a population code for objects and positions.

3.4.9 Hippocampal shifts between blocks can be accounted for by time

We observed robust drift in the hippocampal population occurring both across blocks of trials as well as on a trial to trial basis. However, it is possible that in conjunction with drift within each block, there exist shifts in population state at the transitions between blocks (see Figure 10, Segmented Temporal Context vs. Drifting

Temporal Context). This would manifest as an increase in the population drift rate across blocks over what was observed within a block. To isolate this possible effect, trial pairs within a block (Figure 19 left, blue line) were examined separately from those that spanned a block transition (Figure 19 left, red line) after controlling for object and position effects. We observed significant drift both within each block as well as across blocks (Within block observed slope=-.395, observed data exceeded all 10,000 perms, perm mean=-7.66×10^{-4}, σ=0.055. Across block observed slope=-0.279, observed data exceeded all 10,000 perms, perm =-5.276×10^{-4}, σ=0.0543). After controlling for trial lag the block transitions induced a separation in representations of contexts as other studies have suggested (Baldassano et al., 2017). Because quantification of segmentation is inversely related to that of drift in this instance, choosing segmentation as the alternative hypothesis leaves drift as the null. Standard statistical testing was therefore problematic, as it provides only positive evidence for one alternative hypotheses over the null. Therefore, we used a Bayes Factor to directly compare the likelihoods of segmentation and drift and find positive evidence for the more likely hypothesis, equally assessing the alternative and null. The correlation between trials in the same block was significantly greater than that in adjacent blocks after controlling for trial lag (JZS Bayes T-Test yielded a Bayes Factor strongly in favor of a difference in means, odds ratio 400:1). This suggests that the transition between blocks induced a separation between representations of trials that happened in different blocks consistent with event segmentation.

This could either be because the boundary cue induced a separation in hippocampal representations, or that the separation in representations was merely a

consequence of the extended time between the two trials spanning the delay. To address whether the extended temporal lag fully accounted for the apparent boundary effect on the hippocampus, we plotted the correlation between trials by their *temporal* lag and then organized pairs by whether there was a block transition between them (Figure 19 right). When we compared trial pairs in the same block with those in adjacent blocks in this way, we found that the block break caused no more reduction in the population vector correlation than would be expected by elapsed time (JZS Bayes T-Test yielded a Bayes factor strongly in favor of a single mean, odds ratio 31:1). Thus the separation of trials spanning a block transition observed in the left figure was completely eliminated by accounting for elapsed time. This was also true after removing trials at the beginning of the block when performance was poor (Trials 4:15 of each block only, JZS Bayes T-Test yielded a Bayes Factor strongly in favor of a single mean, odds ratio 15.9:1) removing the possibility that the representation of context only shifted after the animal had switched behavioral strategy. Thus, even though every animal reliably alternated their choices between blocks and no rat perseverated into the next block, there was no evidence that hippocampal code segmented experience any more than what would be expected from elapsed time.

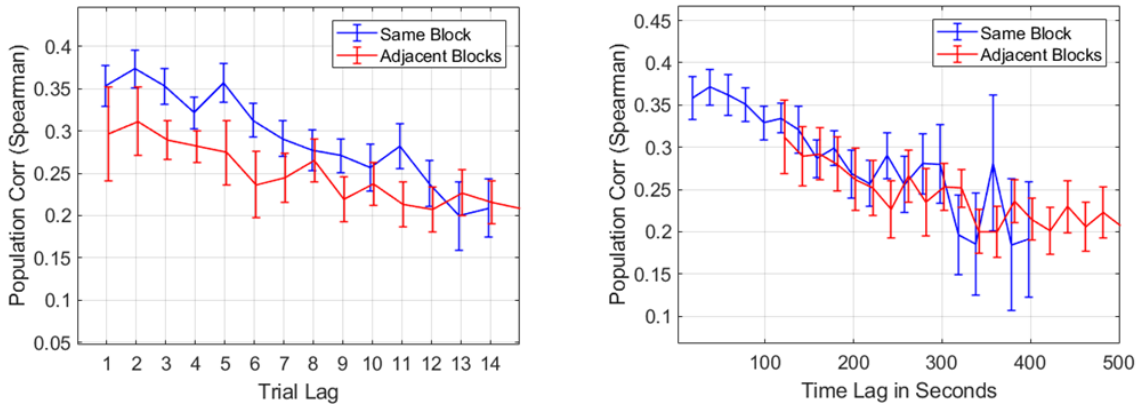

Figure 19: Time fully accounts for shifts in population state across blocks.

Left. Population vectors within a block (blue) were more similar than those in adjacent blocks (red) when trial lag was considered. Alone, this might have been evidence for event segmentation. Right. Population vectors within block (blue) were *not* more similar than those in adjacent blocks (red) when time was considered. Population vector correlations were lower in adjacent blocks, but time was sufficient to account for this decrease. Thus, there was no evidence for event segmentation between blocks above and beyond the change attributable to the temporal delay between blocks. Population vectors were constructed in the same manner as Figure 10.

3.5 Discussion

In this experiment we sought to determine how the hippocampus codes for behaviorally-relevant context in a task in which animals were required to segment experience in time to distinguish between two rule contingencies. Event segmentation predicts that animals would have parcellated experience into discrete episodes based on contextual boundaries; temporal context predicts that the hippocampal representation should provide a continuous relational metric that progressed consistently across time. We provided rats with a temporally blocked task such that an event boundary (removal

from the testing chamber) cued a reversal in the reward contingency. Importantly, the context boundary was a transient cue that signaled a change in which object was rewarded, but was not an explicit cue that would be available to the animals as they made the choice.

Interestingly, well-trained animals neither perseverated across cued block transitions, nor did they anticipate the rule reversal. Instead, every rat tested began every block at chance, frequently digging in the first pot he encountered. Thus, while no rat learned that there were two alternating rule conditions, they all benefitted from the boundary cue by changing their behavior across the block boundaries. Hippocampal units showed selectivity for the position, object, and object-position conjunction of sampling events while also showing sensitivity to the changing context. Indeed, the ensemble code showed strong evidence for temporal drift both across blocks and within each block. Conversely, there was no evidence that the ensemble code was more similar for blocks that shared a rule contingency. Furthermore, there was no greater separation in the hippocampal representation than was expected by the passage of time across the event boundaries that marked block transitions.

3.5.1 The methodological design could have prevented a segmented neural representation

The behavioral results suggest that while no rat learned to anticipate the reversal of the reward contingency between blocks that nonetheless they all were sensitive to the boundaries between blocks. There are multiple interpretations of these curious results.

One clue was that the probability of rejecting the first pot encountered was significantly lower at the start of each block, suggesting the rats began a block with no a-priori preference. Perhaps rats forgot the past rule condition during the block transition and entered the box naïve, only remembering that one of the pots contained reward, but not which pot. Alternatively, they may have merely grown impatient during the delay, and therefore were unwilling to reject either pot. Previous data suggest this behavior may reflect a hippocampal dependent cognitive flexibility, rather than mere impatience. Numerous studies on blocked alternative choice behaviors revealed that hippocampal lesions caused rats to perseverate more after switches in rule contingency or reward location (Hsiao & Isaacson, 1971; Kimble & Kimble, 1965). Importantly, each of these studies involved behavior that was fixed for a large block of trials followed by an abrupt change in reward contingency. Considering our animals showed no consistent perseveration across blocks, these results suggest that the dorsal hippocampus might have been involved in the small savings the rats exhibited at the beginning of each block. Indeed, the drift we observed in the hippocampal representation aligns well with the observed behavior as if the dorsal hippocampus played a role in supporting the flexible changes in responses across time.

Further support for this interpretation may be found in studies on the recency effect observed in human and animals that also show a moderately hippocampal dependent strengthening of memory for recent list items (Kesner et al., 1988). Under this interpretation, the long delay caused a weakening of memory that contributed to the rats' uncertainty at the beginning of each block. This uncertainty might have manifested as a

reduced rejection rate. These two accounts suggest that even though animals were unable to track the two recurring rule conditions, their behavior in this task may have been supported by hippocampal processing.

3.5.2 This experiment differed from other context dependent experiments

Consistent with behavior, we found no support in the activity of hippocampal ensembles for a rule-specific code. These data are in stark contrast to previous experiments that presented animals with distinct behavioral contexts (e.g. Markus et al., 1995; McKenzie et al., 2014). However, it is important to note the difference between the contextual cues in this experiment and those in previous experiments. Those experiments that did observe segmentation used spatially distinguishable contexts (Komorowski et al., 2013, 2009; McKenzie et al., 2014) or overt external cues to discriminate the context, such as an ambient sound, odor, or object (McNaughton et al., 1996; Zaremba et al., 2017). The task in the present experiment was specifically designed to be devoid of such ambient cues, as a neural response to that cue could be mistaken for a new context signal, providing false evidence for event segmentation. Other tasks generated contexts consisting of separate behavioral tasks or event sequences in the same physical space (M. R. Bower, 2005; Ferbinteanu & Shapiro, 2003; Markus et al., 1995). But in those paradigms context was designated by overt changes in the physical behavioral sequences, and reward locations differed between contexts (Kobayashi et al., 1997; Markus et al., 1995). Thus, trajectory dependent firing ‘splitting,’ or cue responsivity may have been responsible for the context signal in these experiments (Ferbinteanu & Shapiro, 2003;

Grieves, Wood, & Dudchenko, 2016). As the spatial layout of this task was held constant across the two rule conditions, there were no systematic changes in the animal's trajectory, which could explain the absence of an alternating neural code.

A previous study found that in rats successfully performing alternation behaviors, alternation in the hippocampal code was not always apparent, and was sensitive the location of the reward itself (M. R. Bower, 2005). This study suggests that the shaping procedure in rodent experiments has a profound effect on context disambiguation in the hippocampus (M. R. Bower, 2005). Therefore, we hypothesize that rats may benefit from the opportunity to first explicitly learn two alternating rule conditions through training with an explicit contextual cue, such as wall color, or ambient sound. Rats might then continue to track the alternating context even after the ambient contextual cues are removed. This might also reveal a hippocampal representation of the two contexts and provide evidence for event segmentation when only boundary cues segment context. On the other hand, the hippocampus may code temporal context in a unique manner, and that other regions such as the Lateral Entorhinal Cortex may have shown segmentation in this task (Tsao et al., 2018).

3.5.3 These data add to a growing literature that describes temporal drift

Hippocampal populations showed robust drift through time both across seconds as well as minutes. These data add to a growing body of literature that suggests that hippocampal representations change across, and are sensitive to time. Importantly, this type of temporal drift has been observed in experiments employing a variety of recording methodologies (Cai et al., 2016; Mankin et al., 2015; Manns et al., 2007; Mau et al.,

2018; Rubin, Geva, Sheintuch, & Ziv, 2015; Ziv et al., 2013). Hippocampal drift has also been observed in both hippocampal dependent tasks as well as tasks with no mnemonic demand (E. A. Mankin et al., 2012; Manns et al., 2007; see also: Tsao et al., 2018b). This experiment is to our knowledge the first direct evidence that population drift is uncorrelated with waveform drift in chronic tetrode recording preparations. Further suggesting that these time signals are unlikely to be a recording artifact, many units observed in the Lateral Entorhinal Cortex by Tsao et al. showed slow changes in spike rate that repeated multiple times and were triggered by entry into a new environment (Tsao et al., 2018). Because drift is observed with recording techniques ranging from tetrode recording to calcium imaging to immediate early gene expression, this reduces the possibility that it is simply a measurement artifact - all of the recording methodologies would have to have independent artifacts that happen to produce the same results. This raises the possibility that population drift reflects a functional correlate of hippocampal processing that occurs continually even under no mnemonic demand, or when behavior is clamped.

A drifting representation of context supports the behavioral results in this experiment, and suggest that hippocampal processing contributed to the flexible behavior that was observed. This representation was supported on the individual unit level through firing fields centered on sampling events that were specific to position and object, but that peaked around a window of trials over the experimental session. Thus, drift occurred both in neurons coding for places and objects as well as in units without obvious place or object selectivity. Crucially, while some of these firing fields remained stable, across the

population there was a spectrum of drift rates (Figure 15). The drifting representation of context is useful, as it provides a continuous dimension for relating experiences and is a likely mechanism for tracking the temporal relationships of events across many scales of time (Cai et al., 2016; Eichenbaum, 2017). This may have enabled rats to forget past rule conditions and learn new ones by providing a mechanism for separating old experiences from more recent experiences. Specifically, this drift would enable rats to both associate very recent trials occurring in the same block and disassociate distant trials occurring in the previous block. Drift in the hippocampus may therefore enable the rapid learning that occurred around the beginning of each block.

3.5.4 Was the hippocampus really insensitive to the event segmenting cues?

If the animals were generating new contextual representations at the onset of each block of trials, one might hypothesize that the boundary cue may have impacted the hippocampal code. Recent modeling suggests that event segmentation may occur when the actor detects shifts in the latent causes governing the set of rules in a given context, and that the hippocampus is necessary to properly assign a new context (Gershman, Monfils, Norman, & Niv, 2017; Gershman & Niv, 2010). Indeed the boundary cue, in this case the prolonged delay and removal from the task environment, did impact the rats' expectations, as no rat showed response perseveration on the first trial of a block. fMRI studies in humans suggest this effect is caused by increased hippocampal activation coinciding with recognition of an event boundary (Baldassano et al., 2017; Swallow et al., 2011). This boundary effect has been recently replicated in the rodent hippocampus during two paradigms where space served to contextualize experience (Bulkin et al.,

2018; Place et al., 2016). In this experiment, there was an increase in drift between trials separated by a block boundary, but the increased separation in representations was completely accounted for by the passage of time between blocks. This result suggests that removal from the environment had no impact on the hippocampal representation. However an alternative explanation is that time was sufficient to separate the hippocampal representation of context and promote a change in the rats' expectations. Perhaps the temporal delay between blocks somehow inhibited the identification of a discrete change in the latent cause governing the reward contingency. Under this interpretation other cues may separate contexts as well if they were only given the right opportunity. Future experiments could dissociate the impact of each of these cues by imposing either the prolonged delay or the removal from the environment alone, or both in combination to observe different levels of separation in the hippocampal representation across time.

3.5.5 A combined model of event segmentation and drift

In this study we examined the hippocampus for a neurophysiological signature of event segmentation in a behavioral task with a clear event boundary (removal from the testing environment). The assumption in designing the experiment was that it would be advantageous to map behaviorally-similar blocks of trials onto distinct cognitive maps and that the neural code would alternate across blocks of trials. As discussed above, there might be some methodological change to the experiment that would have enabled a successful event segmentation strategy. But another reason we failed to observe neural evidence for event segmentation is that our a priori expectations about how event

segmentation would manifest at the resolution of individual neurons in the hippocampus may have been incorrect.

In humans, there is an active literature on how people segment continuous experiences, such as movies of real world scenes or radio plays (Zacks, Kurby, Eisenberg, & Haroutunian, 2011; Lositsky et al., 2016; Baldassano et al., 2017). Participants place event boundaries where they note meaningful changes in the ongoing structure of the world. One of the key findings from this literature is that people can segment boundaries at a range of time scales (Kurby & Zacks, 2008, 2011). For instance, suppose participants identify a segment several minutes long in a scene where a person makes a salad. At the same time people can also identify shorter segments within the larger segment corresponding to steps such as retrieving ingredients from the refrigerator, washing the vegetables, or chopping the vegetables. Indeed different environmental inputs in the real world change at many different rates, reflecting the complex multiscale structure of our world (Sreekumar, Dennis, Doxas, Zhuang, & Belkin, 2014; Voss & Clarke, 1975). Furthermore, fMRI evidence suggests different cortical regions may segment continuous experience into event segments at varying timescales (Baldassano et al., 2017). How might the hippocampus support the formation of event segments and the organization of segments across time?

One possibility is that hippocampal time cells possess all the properties necessary to support behavioral event segmentation. Critically, time cells respond at a wide range of delays tiling intervals that have been studied thus far up to at least tens of seconds (Salz et al., 2016). Furthermore, time cell sequences may be specific to certain past events,

such as presentation of a specific odor (Macdonald et al., 2013; Terada et al., 2017). Time cells may also track time at multiple time scales from minutes, to hours, to even days (Mau et al., 2018). These properties together suggest time cells may support our ability to bridge the gap between events at multiple scales to relate those experiences. A time cell sequence could provide a common temporal context that spans any boundary that occurred between experiences, thus providing a mechanism to relate those two experiences. Conversely, activity of overlapping time cells would also provide specific details about before and after a boundary has occurred, providing a mechanism to contrast those experiences.

As has been previously proposed, the hippocampus may provide pointers that index past events, rather than storing the content of those events per se (Teyler & DiScenna, 1986). At the ensemble level, pointers that drift across time enable the pointer system to reflect the temporal organization of events across time. In this way, temporally modulated drift coupled with the hippocampal place code enables a spatiotemporal scaffold onto which memory for events are stored.

Chapter 4. The LEC and vHPC Encode Time Differently than the dHPC[c]

4.1 Summary

Recent literature has focused on the mechanism by which the hippocampus and cortex organize experience across time to support episodic memory. Recently discovered time cells in the dorsal hippocampus and medial entorhinal cortex present a potential mechanism underlying this function. Time cells organize into a sequence of temporally circumscribed elevated activity that tile a mnemonic delay and provide an estimate of how long ago an event occurred. Time cells may exist in a broad range of cortical and hippocampal regions. Recent work has shown units in the LEC track time over the course of a day, suggesting a potential role in organizing events across time. We recorded from dHPC, vHPC and LEC as rats performed a delayed matching task across an 8 second delay. While activity in all three regions was time modulated during the delay, single units expressed markedly different activity patterns. Dorsal hippocampal units exhibited typical 'time cell' firing fields. Although time could be accurately decoded from ventral hippocampus and LEC, units did not show clear time fields, and instead exhibited slow time modulation during the delay.

[c] This chapter was in preparation for submission to an academic journal at the time this dissertation was submitted. Contributing authors include; John H. Bladon, Frascesca Marino, Cindy Liu, Joseph O'Keefe, and Marc Howard. JHB, FM, CL, & JO acquired and processed data, JHB & MWH analyzed data and wrote the manuscript, and JHB & Howard Eichenbaum designed the experiment.

4.2 Introduction

Episodic memories are characterized by their placement in the unique time and place at which they occurred (Tulving, 1972). The hippocampus is necessary for the spatial and temporal organization of memory, and accordingly shows spatially and temporally structured unit activity (Caparelli et al., 2012; Gill et al., 2011; O'Keefe & Burgess, 1996; Pastalkova et al., 2008; Vargha-Khadem et al., 1997). Place cells fire in specific locations in an environment (O'Keefe, 1976), and time cells fire at a specific moment during a delay (Macdonald et al., 2011; Pastalkova et al., 2008). Time cells contain information about how long ago an event took place, but also contain information about the nature of that past event (Macdonald et al., 2013; Otto & Eichenbaum, 1992). In this way, time cells are thought to bridge gaps in time, acting as a continuous record tracking when past events occurred. Time cells arise even without a mnemonic demand, and time cell integrity correlates with memory across a delay (Pastalkova et al., 2008; Robinson et al., 2017; Salz et al., 2016). Time cells have been described in multiple memory related brain regions, including dorsal CA1, dorsal CA3, and the medial entorhinal cortex. The extent of the time cell network remains unclear, and may include other cortical and hippocampal regions such as the ventral hippocampus and LEC. Furthermore, the mechanism generating time fields is unclear, and competing hypotheses suggest they may either be organized by internal hippocampal processes such as recurrently connected attractor dynamics, or that they may integrate slowly changing cortical inputs (Eichenbaum, 2014).

The dorsal hippocampus and MEC have been closely examined for their spatial firing characteristics. However, each of these regions is organized in parallel with two less well-studied regions, the ventral hippocampus and lateral entorhinal cortex. The LEC and MEC provide parallel but segregated inputs to the hippocampus such that the LEC projects to more distal dendrites in the dentate and CA3, selectively innervates CA1 units residing in more superficial layers, and projects more heavily to the distal region of CA1 (Amaral, 1993; Danielson et al., 2016). While the MEC and LEC may appear segregated in their anatomical connections, there is considerable overlap in firing characteristics when animals perform tasks that require episodic-like associations (Keene et al., 2016). The lateral entorhinal cortex has also been found to be necessary for memory across a delay, and contains firing fields that are selective for individual objects and odors (Tanninen, Morrissey, & Takehara-Nishiuchi, 2013; Xu & Wilson, 2012; Young et al., 1997). Interestingly, there are also units who respond selectivity to the location of past objects, and following past odors, suggesting a mnemonic role for the LEC (Tsao et al., 2013; Young et al., 1997). A recent report examining the LEC found temporally-modulated activity across lags of minutes and hours (Tsao et al., 2018). Units in the LEC tracked time at this minute-to-minute resolution more reliably than hippocampal regions and the MEC. However, the LEC activity in that study did not resemble the time fields that had previously been observed over shorter timespans. Instead, activity levels either slowly fell, or slowly rose as time wore on. Together, these studies suggest that the LEC is crucial for memory across time, and that it contains a reliable time signal across minutes to hours. It remains unclear, however, whether this code also exists across

seconds, at the resolution at which time cells are observed. Moreover, it remains unclear whether the time code in the LEC is similar to time cells observed in the dorsal hippocampus.

Along with the LEC, the vHPC has received little attention in comparison to the dorsal hippocampus and MEC. Lesions to the ventral hippocampus, like those to the LEC cause impairments in associating objects and odors across time (Hunsaker & Kesner, 2008; Rogers, Hunsaker, & Kesner, 2006). Both recording and lesion studies suggest the hippocampus is stratified along its dorsoventral axis such that spatial memory relies more heavily on dorsal regions, whereas stress and emotional memory rely more heavily on ventral regions. Accordingly, the dorsal hippocampus contains place fields that cover a smaller proportion of the arena, and thus represents space on a finer scale (Kjelstrup et al., 2008; Royer, Sirota, Patel, & Buzsáki, 2010). The ventral hippocampus contains a greater proportion of units whose activity is modulated by the emotional valence of a situation (Jimenez et al., 2018). However, this may be an artifact of larger place fields in the ventral hippocampus, or a denser representation of space (Jung, Wiener, & McNaughton, 1994). These observations together suggest the ventral hippocampus may represent experience more densely, or over a broader scale. Accordingly we hypothesize that the ventral hippocampus may contain either a denser representation of time, or may represent time across a broader scale. However, the ventral regions of the hippocampus are less well studied than dorsal regions, and temporal selectivity of the ventral hippocampus has yet to be examined. We explored whether vHPC and LEC contain a time code across seconds embodied by ‘time fields’ similar to those observed in the

dorsal hippocampus. To do so we recorded simultaneously from the LEC, vHPC, and dHPC of rats as they performed a delayed matching task and examined delay period firing in each region.

4.3 Methods

Subjects. Subjects were 5 male Long-Evans rats (Charles River) weighing between 350 and 450 grams and between the ages of 6 months to 1.5 years for the duration of the experiment. Animals were single housed and maintained on a 12 hour light-dark cycle (lights on at 8:00 am) for the duration of the experiment. All behavioral training and experimentation was performed during the light phase. Animals were given ad-libitum water and maintained at a minimum of 85% of their ad libitum feeding body weight during all behavioral training and testing. All procedures were conducted in accordance with the requirements set by the National Institutes of Health, and were approved by the Boston University Institutional Animal Care and Use Committee (BU IACUC).

Behavioral Apparatus: The behavioral apparatus consisted a custom-built 355-cm long by 7.5 cm wide circular track with an integrated treadmill using commercially available parts (Columbus Instruments). The treadmill had walls funneling into a small exit to ensure the animals head position was fixed for the duration of the treadmill run. At the end of the treadmill was a 20x20 cm square platform onto which the test objects were placed. The track was elevated 95 cm above the floor, positioned at least 20 cm away from all walls but in a position in which various distal visual cues were available to the

rat. The maze contained two automatic doors, one at the front of the treadmill and one on the return arm that were controlled by infrared beam breaks (Adafruit industries).

Training procedure: Rats were trained in a similar manner to previous experiments (Robinson et al., 2017). Briefly, rats were initially trained to run in one direction around the maze for froot-loop (Kelloggs, Battle Creek, MI) reward. Once rats reliably looped, they were shaped to retrieve the reward hidden in a flower pot after each lap (roughly 4 days). Then, rats were trained to perform an object-pot matching task that involved two object-pot pairs. To do this, rats sampled one of two study objects before running through the treadmill platform and then choosing correctly between two terra cotta pots discriminable by scent and digging media (Keene et al., 2016). The terra-cotta pots were always placed side-by-side on the platform in a pseudorandomized position. A choice was determined to be made once the animal disturbed the surface of the media at which point the opposite pot was immediately removed at this and all subsequent stages of behavior. One crushed froot loop was added to each pot at the beginning of each day, and every 7-9 trials neither pot contained a food reward, and reward was given after 1 second of digging to prevent the possibility of reward scent guiding behavior. This shaping was performed by initially running each object-pot pair in large blocks of trials (>10 consecutive trials) and progressively weaning down to random presentation over the course of 2 weeks. Once animals were performing at >80% discrimination, two new objects were added one at a time to the study set using the same progressively shrinking block design. Once animals were able to discriminate between the 4 objects to retrieve reward from the correct terra-cotta pot of the two with >90% accuracy, a running delay

was imposed. Initially, animals were trained to wait for a fraction of a second while the treadmill was nudged forward between the study and test phases. Once rats were able to perform at ~80% accuracy for at a two second delay, they underwent stereotaxic surgery. Following surgery and recovery, an abbreviated training regime was used to return the animal to good performance at 2 seconds. The treadmill delay was progressively increased until performance fell to between 70 and 80%, or until an 8 second delay was reached. Typically, this training schedule took roughly 1.5 months to train animals on the first pair of study objects, and then another 1.5 months for rats to perform with 4 study objects and with a sufficiently long treadmill delay. Following surgery, tetrodes were lowered over a 2-3 week period while the rat relearned the task and reached performance criterion at a long delay.

Surgery: All surgeries were performed using standard aseptic techniques. Anesthesia was induced by inhalation of 5% isofluorane (Webster Veterinary Supply) in oxygen, and then a stable plane of anesthesia was maintained at 1.5-3% throughout the entire surgery. Immediately following induction, animals were injected with the analgesic Buprenex (Buprenorphine hydrochloride, 0.03 mg/kg i.m.; Reckitt Benckiser Healthcare), antibiotic cefazolin (330 mg/ml i.m.; West-Ward Pharmaceuticals), and the NSAID carprofen (Rimadyl,). The rat was then fixed to a stereotaxic frame (kopf). Craniotomies then were made above the rostral lateral entorhinal cortex (LEC)/ventral hippocampus (vHPC) (AP-6.8, ML 4.5), and in some animals the dorsal hippocampus (dHPC) (AP-4.1, ML 3.0mm). Six to eight sterile stainless steel screws were then fixed to the skull, and the remaining skull surface was covered with metabond. A hyperdrive

consisting of 24 independently moveable tetrodes in a single bundle, or split into two preconfigured bundles (bundle tips at the above conformation with the LEC bundle angled 16° in the lateral direction) was then lowered into the two craniotomies, and fixed to the skull using dental cement. Two ground screws were inserted above the cerebellum, and soldered to a ground lead fixed to the electrode interface board prior to surgery. Each tetrode was composed of four 12 uM RO 800 wires (Sandvik Kanthal HP Reid Precision Fine Tetrode Wire; Sandvik). Tetrodes were plated with non-cyanide gold solutions via electrolysis in order to reduce impedance to between 180 and 220 kOhms. At the conclusion of surgery, dHPC tetrodes were lowered ~1 mm into dorsal cortex, and LEC/vHPC wires were lowered at a minimum of 5 mm into brain tissue. Animals were given Buprenex and Cefazolin twice a day as needed for up to three days post-surgery.

Histology: At the completion of recordings, rats were anesthetized with <5% isoflurane in oxygen. The recording site of each tetrode was confirmed by passing 40uA of current through the tetrode tip until the connection was severed (generally 2-4 seconds). Immediately following electrolytic lesions, animals received an interperitoneal overdose injection of Euthasol (Virbac AH). Immediately following cessation of breathing animals were transcardially perfused with ice cold 0.5% potassium phosphate buffered saline followed by 5% formalin in phosphate buffer (VWR). Brains were then extracted and submerged in 5% formalin as above for a minimum of 36 hours. Brains were then submerged in 30% sucrose in phosphate buffer for 36 hours until rapid freezing and sectioning into 30-50 um thick sections in a cryostat (CM 3050s: Leica Biosystems).

Sections were mounted on gelatin subbed slides and then processed using standard Nissl staining protocol to visually confirm tetrode recording sites (Figure 22).

Data acquisition: All electrophysiological recordings were performed using a 96 channel multichannel Acquisition Processor (MAP) recording system (Plexon). Each spike channel was amplified 1000x, then between 3-10x depending on the region. Spike channels were manually referenced to a local tetrode with no apparent unit firing, bandpass filtered between 200 and 10 kHz, and digitized at 40 kHz. LFP signals were uniformly referenced to ground, amplified 2000x, and bandpass filtered between 0.5Hz and 300 Hz. The animals' position and behavior were tracked via two LEDs fixed to his hyperdrive on one overhead camera, and on one camera positioned behind the two terra-cotta pots each recording at 30 fps. Tetrodes were moved a minimum of 60uM after each recording session to prevent resampling the same units. Tetrodes were lowered a minimum of 12 hours before all recording sessions to ensure tetrode stability. IR beam crossings and door movements were automatically logged, and behavioral events were scored manually using video feeds from the two cameras (CinePlex software, Plexon).

Spike Sorting and Data preprocessing: Spikes were assigned to individual units by offline manual clustering of waveform characteristics (valley amplitude, peak-valley, energy, principal components, and waveform width at half max). Tetrode localization was performed using histology, and further guided by the LFP theta amplitude and phase, and sharp-wave ripple amplitude. Briefly, ventral hippocampal units were acquired from tetrodes just exiting the superficial layers of the hippocampus, where a characteristic theta-phase reversal, and ripple amplitude change could be found (Buzsáki, 2002). LEC

units were only acquired when theta amplitude was low, at depths greater than 6.8 mm (24 turns) ventral to the brain surface, or at depths greater than 1.13 mm (4 turns) ventral to the identified vHPC cell layer (Deshmukh, Yoganarasimha, Voicu, & Knierim, 2010).

Standard L-ratios and isolation ratings were calculated from a 17 dimensional space that included the valley, peak-valley, full width-half max, and energy from each tetrode for each clustered spike, and the first principal component of variance across tetrodes for each spike(Schmitzer-Torbert, Jackson, Henze, Harris, & Redish, 2005). These parameters were chosen because they were the dimensions that were used to initially sort spike clusters.

Behavior was monitored from an overhead camera and a second camera with a close-up view of the test pots (Supplemental Video). The rats' position was tracked via two LEDs attached to the implant (one red and one green) and customized MATLAB code. Briefly, after removing the average picture, a luminance and color (one red and one green) threshold were applied to find groups of contiguous pixels that could correspond to LED locations. Then regions were filtered for size and proximity to the previous rat location to yield the most likely LED positions at all frames. Door movements, and treadmill onset and offset were automatically strobed into the recording amplifier. Test object sampling events were hand coded using CinePlex editor (Plexon) using video taken at 30 Hz (See Supplemental Video). All analyses of behavior were performed as described in results.

Spike-Field coherence and Burst Indices: All Spike-local field potential relationships were performed using the LFP from the same wire the unit was recorded

from. Briefly, 1000 Hz LFP signal was z-scored and filtered in the theta frequency (5:12 Hz) using a Butterworth filter, and then the instantaneous phase and amplitude were extracted using the Hilbert transform. Then the phase of each spike was interpolated using a nearest neighbor method. Statistics were performed on the histogram of spike phases binned in 12 degree increments (30 bins). The mean vector length and Rayleigh test were calculated as previously described (Jones & Wilson, 2005). The burst index was calculated from the autocorrellogram generated by binning each spike into 1 ms bins, and calculating the correlation at maximum lag of 50 ms. The burst index was calculated as the maximum in the autocorrelogram between lags 0 and 10 ms divided by the average in the autocorellogram between lags of 10 ms to 50 ms. The burst probability of each unit was calculated as the proportion of spikes with a neighboring spike occurring less than 9 ms away. The theta index in the autocorrelogram was calculated using two methods. The first method was calculated form an autocorrelogram sampled at 1000 Hz and at a maximum lag of 500 ms. Briefly, the Welch's power spectral density was estimated using ten 50 ms bins at frequencies from 2 to 50 Hz. The power estimate was frequency normalized and then the maximum power between 7 to 12 Hz was divided by the average power below and above that frequency.

The second method was adapted from a previous study comparing the dorsal and ventral hippocampus (Royer et al., 2010). For each cell an autocorrelogram was generated by binning each spike into 10 ms bins and taking the correlation at a maximum lag of 700 ms. Only units with at least 100 counts were analyzed, the zero lag was

removed and then the autocorrelogram was normalized to the maximum value. A curve was then fit to this autocorrelogram with the following form:

$$\boldsymbol{y(t) = (a * (sin(ft) + 1) + b) * e^{-\frac{|t|}{tau1}} + c * e^{-\frac{t^2}{tau2}}}$$

Where a, b, c, f, tau1, and tau2, were all fitted constants with the bounds listed (0<**a**<10, 0<**b**<10, -10<**c**<10, .02<f<.07, 300<tau1<inf, 0<tau2<150). The variable *a* was bounded to prevent negative weight to the theta argument, *f* was bounded such that the period of the sine wave was between 7 and 12 Hz, *tau2* was bounded such that the decay was necessarily slower than the bursting argument, *tau1*. The fit was performed twelve times wherein each parameter started randomly but within its bounds, and each fit was halted after 1,000,000 iterations or after a delta fit value was below $1x10^{-10}$. The best of the twelve fits was chosen as the final fit for each unit, and the theta index was calculated as the ratio of a/b.

Single Unit Information Scores and Temporal Modulation: Information scores were calculated as previously reported using 0.2 second bins for the entire delay. The standard deviation of the spike rates across time during the delay was performed on the same 0.2 second time bins. Significance was determined for each method through a bootstrap randomization where spike timestamps during the delay were circularly shifted by between 1 and 7 seconds for each trial. This randomization was performed 1000 times to generate 1000 random curves on which the above statistics were performed. We adopted a threshold for significance of a higher information score or standard deviation than 99% of the shuffles.

Population Vector Analyses: For all population vector analyses population firing rate vectors were generated by gathering the firing rate for each cell during each 0.2 second bin during each trial at 0.2 second steps relative to delay onset. The resulting x cell by y trial by z timestep population matrices were then trial averaged, and then z-scored across trial time. The Pearson correlation was then calculated between population vectors of all time bins to vectors for all other time bins to generate a matrix for each session. Each units' firing rate vector was z-scored across time or across trials to ensure each unit contributed equally to the correlation matrix. Mean and SEM estimates were calculated across session matrices.

Linear Discriminant analysis: Linear discriminant analysis was performed in a leave-one-trial out fashion on all sessions in which 4 or more units in a given region were recorded. For time decoding, 0.2 second timebins were used at 0.2 second increments from the start to the end of the delay. The decoder was trained on all trials except the left out trial, and then used to predict all time bins for that left out trial. No normalization was performed, as LDA does not benefit from nonlinear data transforms. The posterior probability matrices for each time bin were averaged across trials for each session and the resulting peaks was calculated as the series of decoded times for that session. The accuracy of the decoder for each session was measured as the absolute difference in the decoded time and the actual time and plotted +/- SEM. The shuffling procedure involved shuffling the training matrix across classes (time bins) but not across cells. This null decoder was then used to predict the unshuffled left out trial data.

4.4 Results

4.4.1 Rats learned object-trace-object associations across the 8 second delay

Rats were able to associate objects across the 8 second treadmill running delay (Figure 20A). In each session, the rat performed significantly higher than chance (One sided Binomial Test against chance, all p<=.01). However, some rats performed better overall than others (Mean across rats=78%+/-1%, 1 way ANOVA F(5)=2.98, p<.003). In a post-hoc multiple comparisons test, one rat performed significantly worse than one other (Students Post-hoc test of multiple comparisons lower rat performance 74%, higher rat 83%, Estimated difference in performance=8.6%, p=0.0425). Overall, rats were given 12.2 +/- 1.2 seconds to study, the overall delay took 8.6+/-0.4 seconds, and the rats sampled for 1.48+/-0.3 seconds before making a choice. While there was significant variance in the amount of time each rat took to study (1 way ANOVA on study length F(5)=33.84, $p<10^{-10}$), the time of each delay (1 way ANOVA on overall delay length F(5)=8.16, $p<10^{-4}$), and the time each rat sampled the pot before choosing whether to dig (Figure 20C 1 way ANOVA on sample length F(5)=46.43, $p<10^{-10}$), none of these parameters interacted with performance across rats (1 way ANOVA on study length, F(1)=1.61, 1 way ANOVA on study length, F(1)=0.0007, 1 way ANOVA on study length, F(1)=1.74). Within any session, the length of study never impacted performance (one way ANOVA, max F(1)=1.65, Bonferonni corrected min(p)=0.2) and neither did the delay length (one way ANOVA, max F(1)=4.67, Bonferonni corrected min(p)=0.186). However, two rats sampled the test objects for a shorter period of time before making

errors (One way ANOA, $F(1)=0.27, 0.01, 1.0, 8.1, 13.6, 6.3, 1.8$, $p=1, 1, 1, 0.028, 0.002, 0.72, 0.18$). This suggests that these rats may have behaved impulsively during error trials, acting before testing for a match, and therefore may still have remembered across the delay. All rats also tended to make errors in clusters such that the probability of a correct response following an error trial was slightly lower (75%), than following a correct trial (80%) (Paired T-test, $T(47)=2.26$, $p<0.03$). This suggests a potential slow waxing and waning of effort or attention on the animals part.

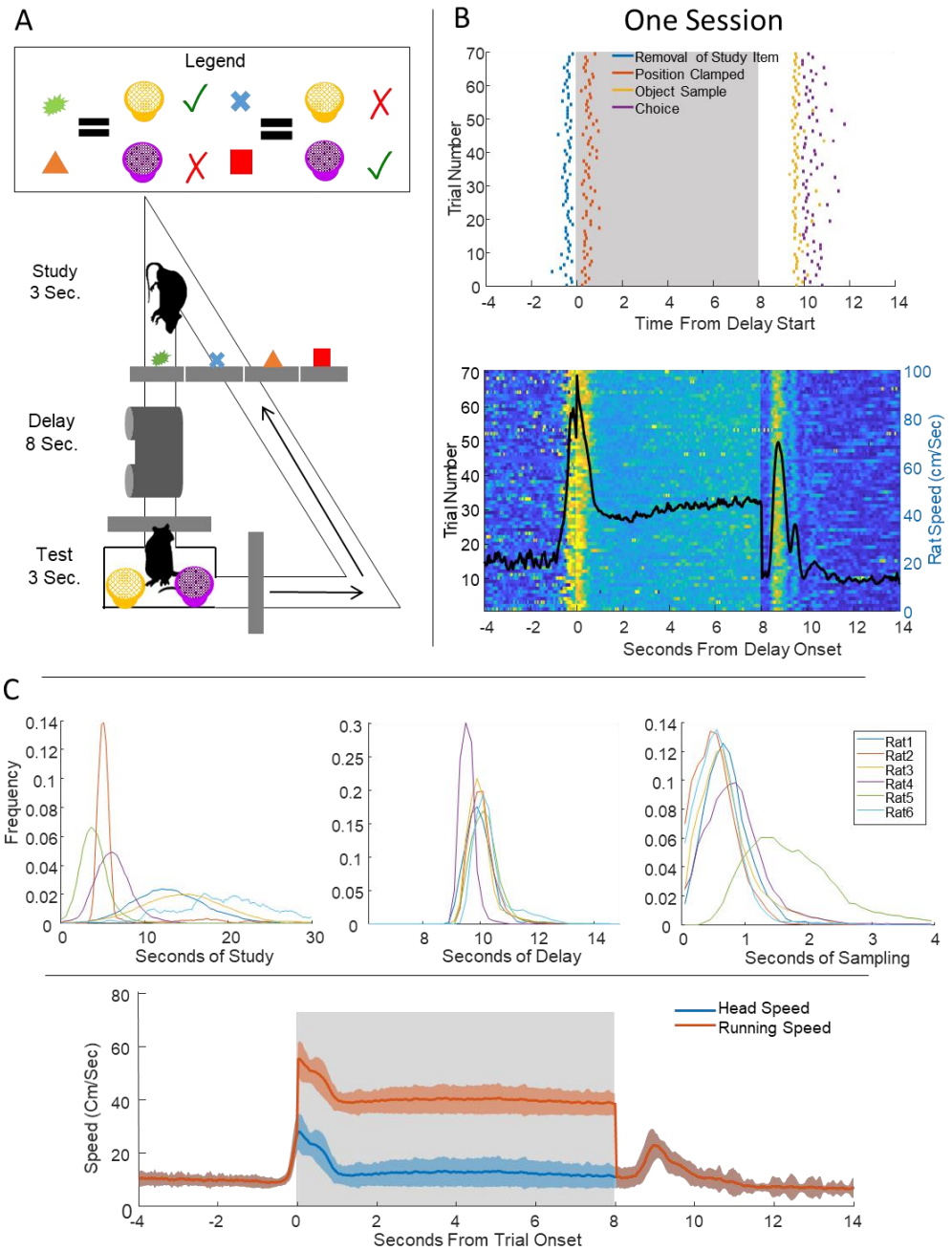

Figure 20. Rats Performed a Delayed Matching Task.

A. Task involved four study items mapped to two response items. B. Example of rats' behavior during a single session. C. The duration of each task phase varied across rats, but differences in study length and test length did not impact performance. Bottom: the treadmill often began before the rats' position was clamped at the end of the treadmill. Thus rats briefly sprinted at the onset of treadmill movement. Note: Head speed was rarely zero due to head-bobbling movement both during running and rest.

4.4.2 Each region exhibited unique intrinsic spiking properties and network interactions

Simultaneous recordings were performed in dHPC, vHPC, and LEC as rats performed the delayed matching task (Figure 22A). Overall, 552 clusters were isolated from LEC tetrodes, 717 clusters from dHPC, and 313 from vHPC. We verified the quality of each cluster by calculating the L-distance and isolation rating against all other isolated waveforms. There were no differences in mean isolation ratings (one way ANOVA, $F(2)=2.1$), or L-ratio (one way ANOVA, $F(2)=2.74$, $p=0.065$), between any region (Figure 21). However, to be conservative, we adopted the same threshold as previous reports and removed all clusters with an isolation rating below 25 (Schmitzer-Torbert et al., 2005). These cluster quality metrics were similar despite other differences between regions. The average firing rates differed between regions, with the vHPC exhibiting significantly higher overall rates than either the dHPC or LEC (vHPC mean=3.34 +/-0.40, dHPC mean=1.94+/- 0.25 LEC mean=2.19 +/- 0.16 Hz, ANOVA $F(3)=4.16$, $p<0.02$). Similarly, tetrodes in dHPC on average had about twice the units per tetrode (5.56 +/- .4) than LEC, (2.59 +/- .12) and vHPC (2.79+/-.2, ANOVA, $F(2)=45$, $p<10^{-10}$).

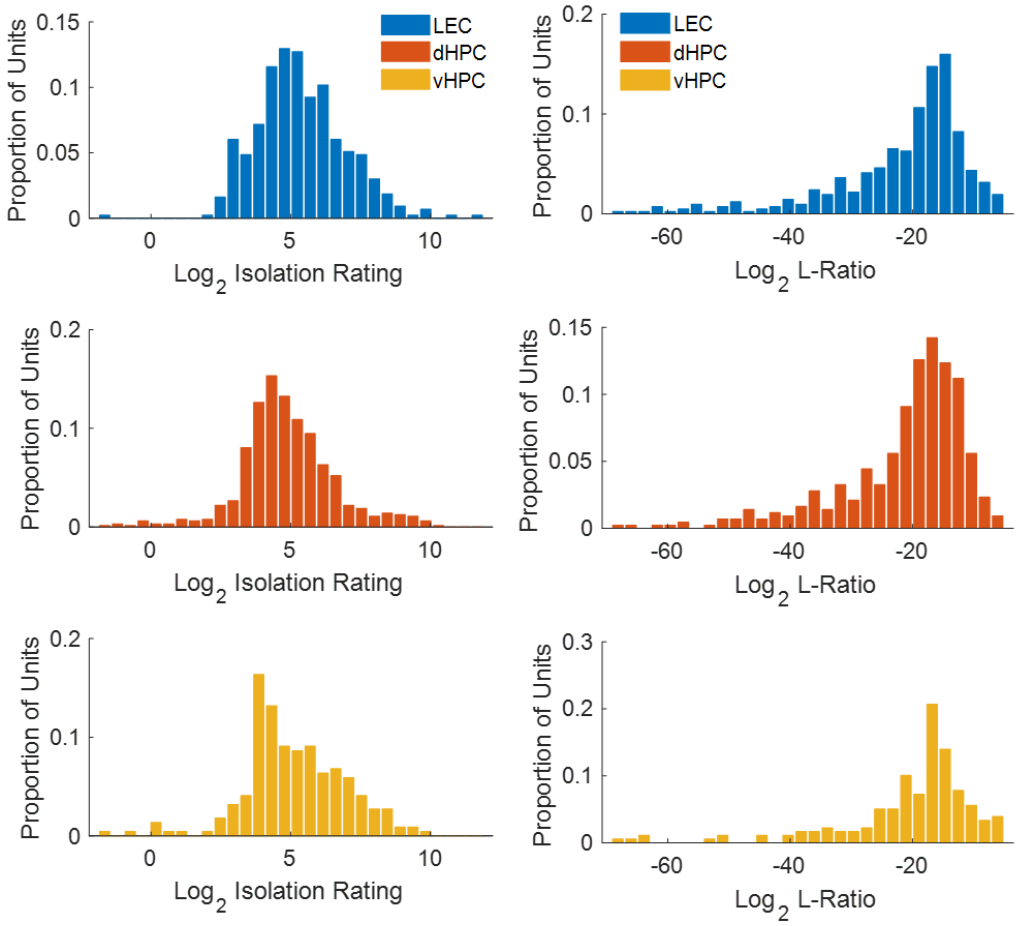

Figure 21: Supplement: Cluster quality was equivalent across regions.

Left: Histograms show a similar distribution of isolation ratings across regions. Mean isolation rating did not differ across regions. Right: The distribution of L-ratios for units in each region had a similar mean.

The dorsal hippocampus contains complex-burst cells that fire rapid bursts of action potentials that tend to occur at specific phases of the local theta rhythm. These bursts can be observed in cells' autocorrelograms as well as in the distribution of inter-spike-intervals. One report observed less intrinsic theta rhythmicity and burst activity in

the vHPC than the dHPC (Royer et al., 2010). Previous reports examining LEC units suggest they do not interact with the theta rhythm, seldom have subthreshold membrane oscillations and rarely exhibit bursting activity (Canto & Witter, 2012; Deshmukh et al., 2010; Hamam, Amaral, & Alonso, 2002). To validate our recording locations and in turn replicate these previous findings, we examined the different firing properties and network interactions of units in each region by constructing autocorrelograms and spike-phase histograms for units in all regions (Figure 22B). Consistent with previous reports, there was a wide variability in the autocorrelogram shape that appeared related to the region in which the unit was recorded. Specifically, hippocampal units appeared to show high peaks in the autocorrelogram within a 10 ms lag, whereas LEC units showed a valley (Figure 22 B, leftmost unit is from LEC, rightmost unit is from dHPC). Similarly, rhythmic peaks in the autocorrelogram were evident in dHPC and vHPC at lags roughly correlating to the theta frequency (Figure 22b, right two units are from vHPC and dHPC, respectively).

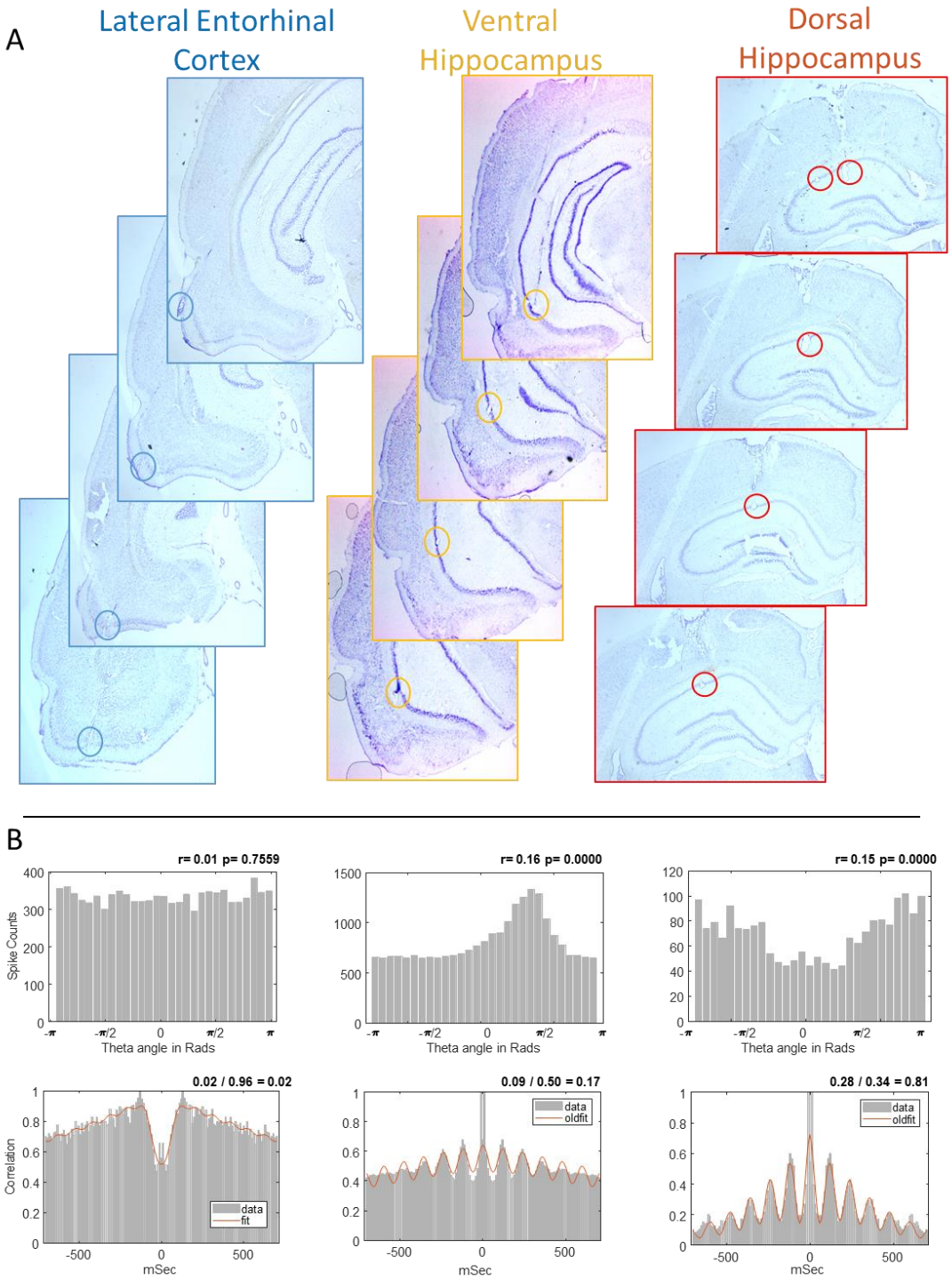

Figure 22: Tetrode locations of LEC, dHPC and vHPC units, and characterization of intrinsic spiking properties in three example neurons.

A. LEC tetrode locations are circled in blue, vHPC tetrode locations are circled in yellow, and dHPC tetrode locations are circled in red. The rostral LEC was targeted to prevent contamination of MEC units. Distal CA1 was targeted both in the dHPC and vHPC to prevent contamination of CA3 units. B. Top: Theta phase distribution of spikes arising from three recorded units. Theta modulation strength and p value shown above each plot. Bottom: Intrinsic theta rhythmicity and burst indices were measured for the same three neurons via the autocorrelogram. Intrinsic theta modulation is quantified above each plot (methods). The unit to the left showed a low burst index, low theta in the autocorrelogram, and low coherence to the theta rhythm. The center unit showed a moderate burst index and intrinsic theta rhythmicity, and a high coherence to theta. The unit on the right showed a high burst index, high intrinsic theta rhythmicity, and high coherence to the theta rhythm.

We quantified these observations by first calculating the burst probability of units in each region (Figure 23, left) (Mizuseki, Sirota, Pastalkova, & Buzsáki, 2009). Consistent with these previous findings, LEC units showed exceedingly low burst probability (mean: 0.085 +/- 0.0048) whereas units in the ventral hippocampus showed a range of burst probabilities (mean 0.16 +/- 0.008) and dorsal hippocampus units showed high burst probabilities (mean: 0.28 +/- 0.0059). This statistic easily distinguished the regions (ANOVA, $F(2)=309.5$, $p<10^{-10}$) and a post-hoc comparison revealed each region was dissociable from the other two (Tukey's HSD correction, dHPC-vHPC $p<10^{-10}$, dHPC-LEC $p<10^{-10}$, & vHPC-LEC $p<10^{-10}$). We then examined the intrinsic theta rhythmicity of units in each region as it manifested in the autocorrellogram. First, the theta power was extracted using Welch's psd and then its amplitude was normalized to the average power from 1:50 Hz. Units in the dorsal hippocampus showed the strongest theta power in their autocorrelogram (dHPC mean index: 4.33+/-0.11) followed by vHPC (mean index=2.75+/-0.15) and finally the LEC showed uniformly low theta modulation (LEC mean index: 0.89+/-0.03). This metric easily discriminated regions (Tukey's hsd correction for multiple comparisons, dHPC-LEC $p<10^{-8}$ vHPC-LEC $p<10^{-8}$, dHPC-vHPC

$p<10^{-8}$). We confirmed these results by using a previously published curve fitting method (Royer et al., 2010) (Tukeys HSD correction for multiple comparisons, all $p<10^{-8}$). Finally, we examined the magnitude of coherence of units in each region to the local theta rhythm. Units in the dorsal hippocampus showed slightly stronger theta coherence than units in vHPC, (mean Rayleigh vector length, dHPC= 0.17+/-0.004 vHPC mean=0.15+/- 0.007, $p<0.02$) but hippocampal units were much more strongly modulated than units in the LEC (mean Rayleigh vector length=0.05+/- 0.002, LEC-dHPC $p<10^{-10}$, LEC-vHPC $p<10^{-10}$). As theta power is significantly different between dHPC, vHPC, and LEC, these effects may have been driven by differences in the LFP itself, rather than in its interaction with units. Therefore, we confirmed these analyses by referencing spikes to the theta rhythm in the dorsal hippocampus and found similar results. The dorsal and ventral hippocampus showed equally strong coherence to local theta, (mean Rayleigh vector length, dorsal HPC= 0.19+/-0.004 vHPC mean=0.18+/- 0.009, $p=0.67$) and both were more strongly modulated than units in the LEC (mean Rayleigh vector length=0.05+/- 0.002, LEC-dHPC $p<10^{-10}$, LEC-vHPC $p<10^{-10}$). Consistent with previous reports, these data show drastically differing intrinsic firing properties of units in dHPC, vHPC, and LEC and confirm the recording locations in our experiment. These results suggest that units each region exhibits a unique landscape of intracellular and network properties that likely shapes the manner in which they convey information.

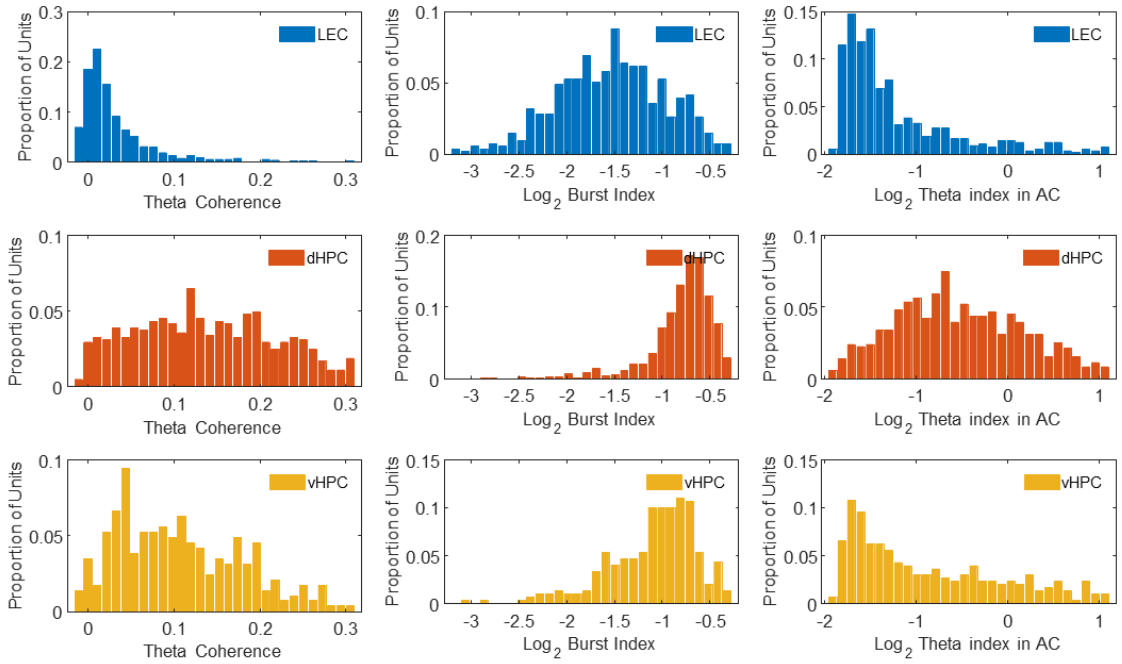

Figure 23: Each region exhibited a unique distribution of intrinsic firing characteristics that was consistent with prior work.

The LEC exhibited low theta coherence, low burst indices, and low intrinsic theta rhythmicity. The dHPC exhibited high theta coherence, burst indices and intrinsic theta rhythmicity. The vHPC exhibited high theta coherence, high burst indices, but low intrinsic theta rhythmicity.

4.4.4 Delay activity differed between regions

We then examined time-locked delay activity from units in each region during the running delay. To do this, we examined peri-event rasters, and trial averaged histograms of each cells' activity during the delay. We then ordered example units in each region by their center of mass, and examined their standard deviation, and temporal information content (Skaggs & McNaughton, 1998). Upon close examination of the activity patterns of temporally modulated cells, stereotypical time cells were evident in dHPC whose peaks tiled the delay (Figure 25, A through E). These cells often showed sparse activity

patterns that included narrowly circumscribed increases in activity that were centered on a moment during the delay (Figure 25). Many units showed a narrow peak early in the delay but were otherwise silent (Figure 25, unit A-E). Similarly, some cells peaked towards the end of the delay, but the peak was less narrow (Figure 25, units I, J, K, L). Overall units in dHPC appeared to generate firing fields that tiled the delay, and became progressively wider as the delay progressed. These observations are consistent with previous reports describing time cells (Kraus, Robinson, White, Eichenbaum, & Hasselmo, 2013; Macdonald et al., 2011).

Units in the vHPC showed what appeared to be time cell responses through the delay as well, however these patterns were less punctate (Figure 26). Much like the dHPC, there were many units with peaks early in the delay, however these peaks appeared broader than those in dHPC (Figure 26, units B, C, D, & E). While a few units exhibited peaks towards the middle or end of the delay, more often cells exhibited decaying rates that fell from the onset of the delay (Figure 26, C, D, E, I). Many units with activity peaks early in the delay also exhibited broader peaks later in the delay (Figure 26, units F, & H). We also observed many vHPC units whose firing rate slowly ramped from delay onset, (Figure 26, units J, K, & L). While some units appeared to have time cell properties, many of those units were locked to delay onset, or had multi—peaked activity patterns. Instead, many vHPC units exhibited slowly decaying or ramping firing rates that changed slowly across the delay.

LEC units showed temporally modulated responses during the delay that appeared to be different than those in the hippocampus and did not appear to center on specific

moments in the delay (Figure 24, units A, B, & D). Very few units in the LEC exhibited a peak firing rate at moments into the delay with a rapid decay in rate from that peak. Those that did appear to have narrowly circumscribed elevations in activity did so early in the delay, potentially coincided with the beginning of the delay (Figure 24, units A-E). These cells with peaks within the first second of the delay exhibited a wide spectrum of activity decay rates moving forward into the delay (units A, B, & D exhibited more rapid decay than units E, G, H & I, even though their peaks were at similar times, Figure 24). Conversely, many units showed a dip in firing rate at delay onset, and slowly ramped up (increased) their firing rate as the delay progressed (Figure 24, units J & K). Overall, LEC units changed their rates much more slowly across the delay than those in dHPC, but exhibited similar activity to units in vHPC.

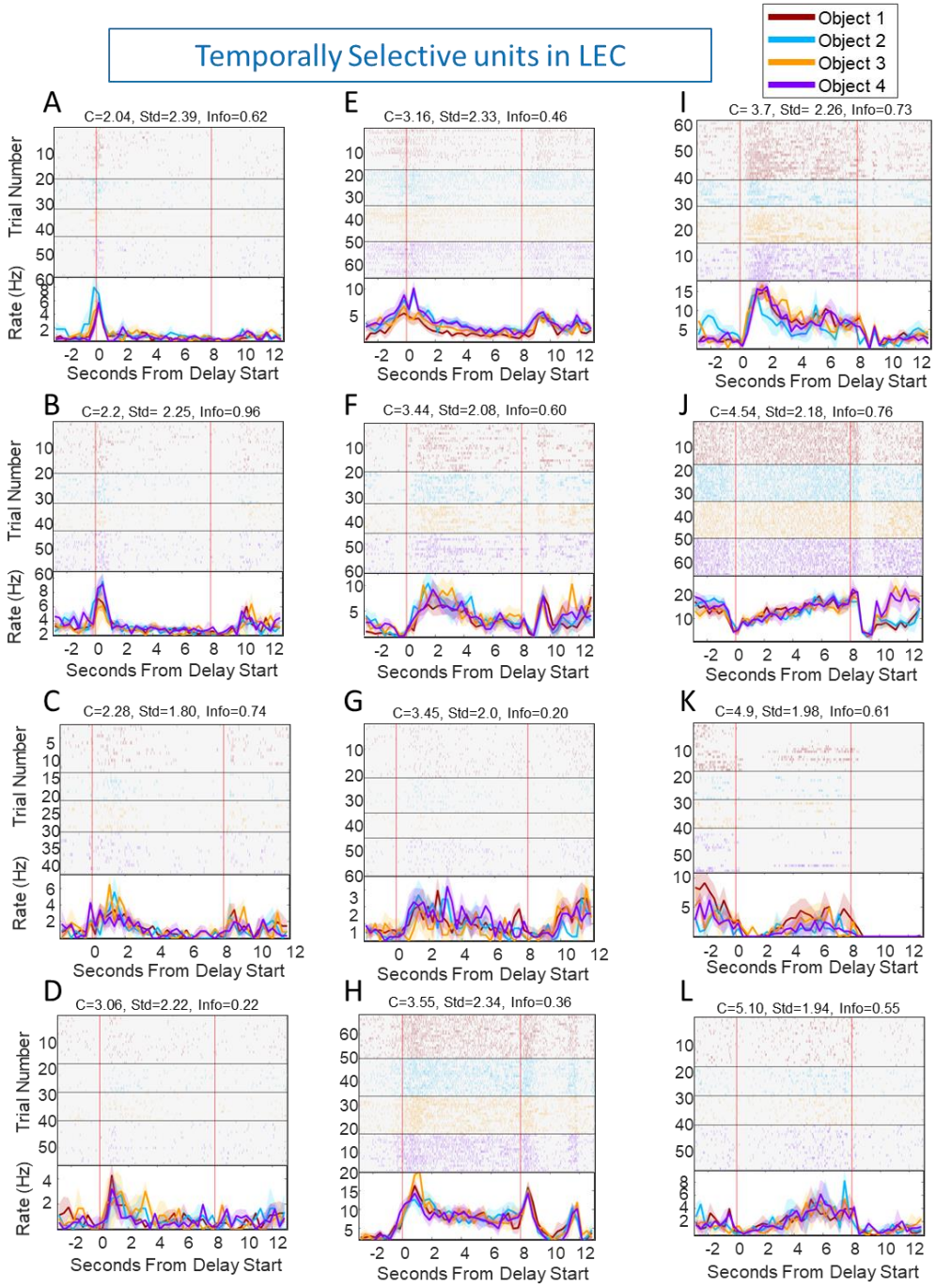

Figure 24: Temporally Selective units in the LEC.

Twelve temporally selective units recorded from the LEC. Units are ordered by center of mass. Top: rastergram of spikes during each trial ordered by the identity of the study object. Bottom: Histogram of average firing rate for each trial type (mean +/- SEM). Many units exhibited a peak early in the delay with a spectrum of decay rates (left two columns). Some units exhibited slow ramping activity

towards the end of the delay (right column). C=center of mass in seconds, Std=Standard Deviation in seconds, Info=Temporal information in bits per spike).

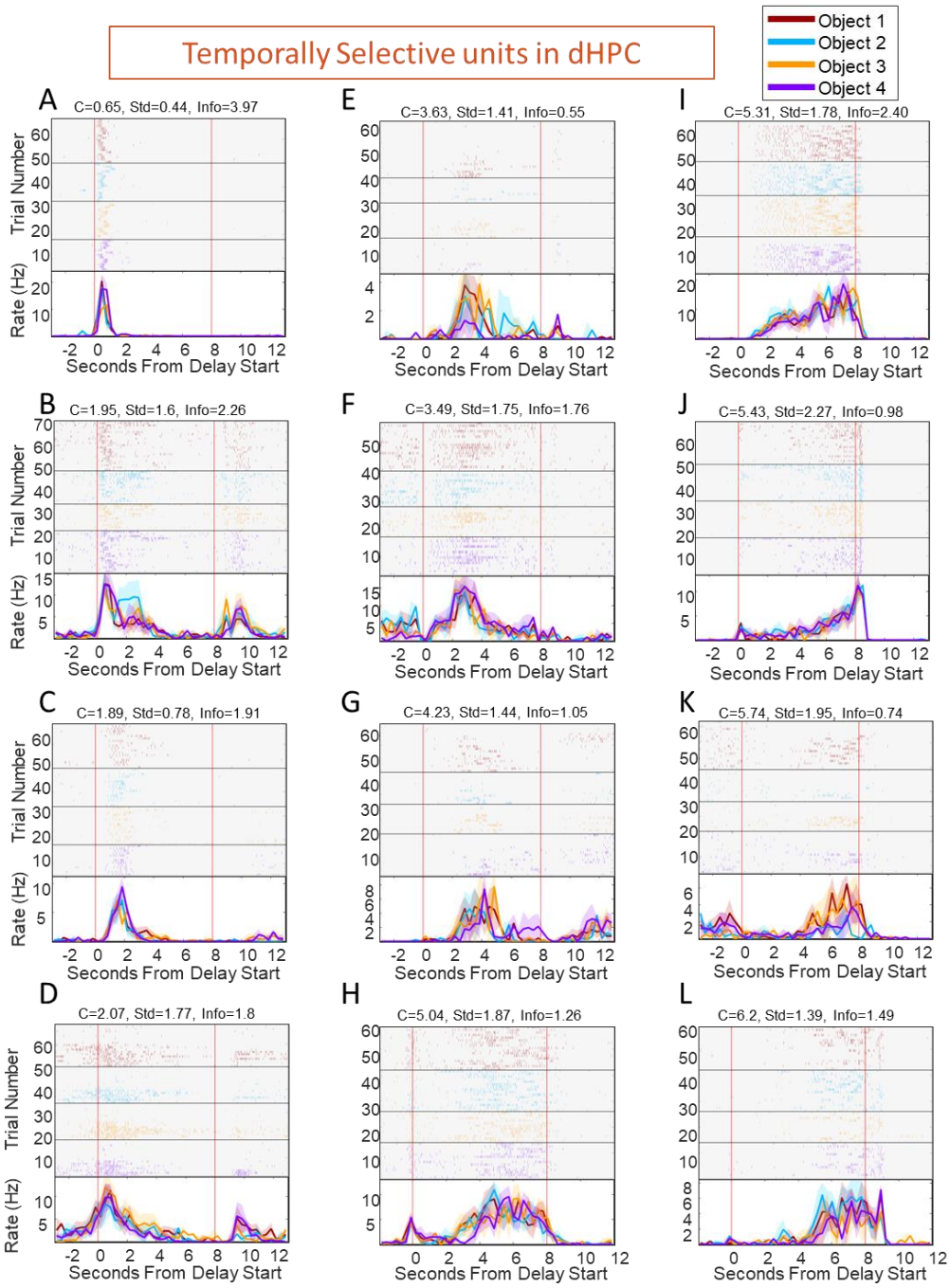

Figure 25: Temporally Selective Units in the dHPC

Twelve temporally selective units recorded from the LEC. Units are ordered by center of mass to show tiling across the delay. Top: rastergram of spikes during each trial ordered by the identity of

the study object. Bottom: Histogram of average firing rate for each trial type (mean +/- SEM). dHPC units exhibited typical time cell activity, with narrowly circumscribed activity centered on a specific moment during the delay. Similar to previous reports, many units exhibited peak rates early in the delay, and fewer units peaked later in the delay. C=center of mass in seconds, Std=Standard Deviation in seconds, Info=Temporal information in bits per spike).

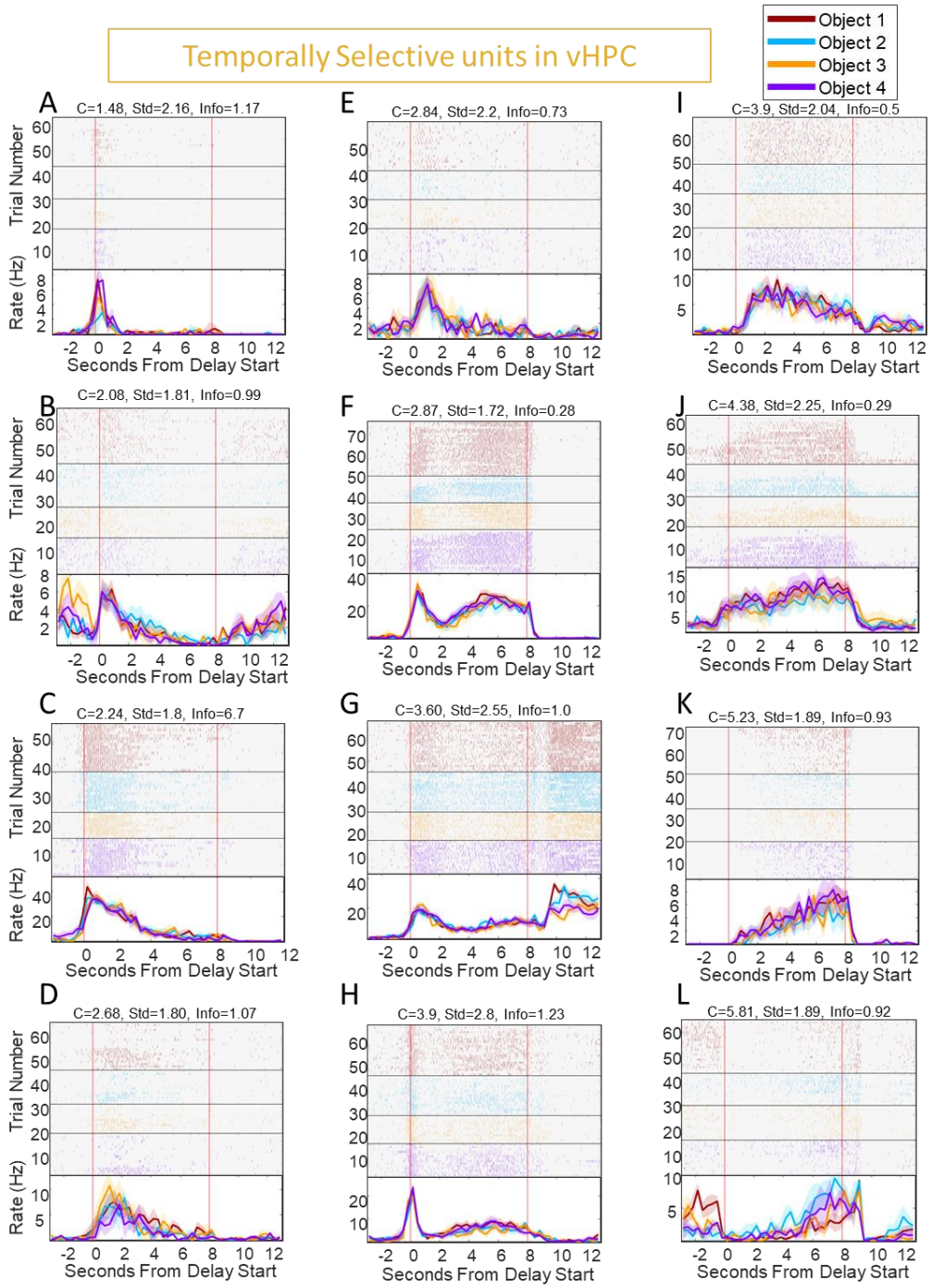

Figure 26: Temporally Selective units in the vHPC.

Twelve temporally selective units recorded from the LEC. Units are ordered by center of mass. Top: rastergram of spikes during each trial ordered by the identity of the study object. Bottom: Histogram of average firing rate for each trial type (mean +/- SEM). Some units exhibited peaks early in the delay with varying decay rates. Others had multi-peaked activity, with a narrow peak early and a wide peak later in the delay. Finally, some units slowly ramped in firing rate towards the end of the delay (right column bottom two). C=center of mass in seconds, Std=Standard Deviation in seconds, Info=Temporal information in bits per spike).

A number of descriptive statistics were used to quantify the differences in how individual unit activity was modulated by time in each region. The center of mass has been used previously to characterize place field activity, and can discriminate between place fields in different brain regions (Roth, Yu, Rao, & Knierim, 2012). When the center of mass of the trial averaged tuning curve for temporally modulated cells was measured in each region, cells in the dHPC showed earlier centers than those in vHPC or LEC (Figure 27 B: LEC: 3.8+/- 0.46 sec, dHPC: 2.97+/-0.99, vHPC:3.6 +/-0.81 ANOVA $F(2)=46.48$, $p<10^{-13}$, students-t post-hoc: LEC:dHPC $p<10^{-9}$, dHPC:vHPC $p<10^{-6}$, LEC-vHPC $p=0.27$). The standard deviation of the spike indices quantifies how tightly locked a units' activity is to one moment in the delay across trials. When the standard deviation was measured for each temporally modulated unit, dHPC activity patterns showed a much smaller standard deviation than those in vHPC or LEC (Figure 27 B: LEC mean: 2.239+/-0.013, dHPC mean: 1.776+/-0.37, vHPC: 2.17+/-.022, ANOVA $F(2)=81$, $p<10^{-30}$). Finally, sparsity has been used as measure of the proportion of a sampling area in which a cell fires, and has previously discriminated unit activity in the dorsal from the ventral hippocampus. We observed a large difference in sparsity between regions overall (Figure 27 B, ANOVA, $F(2)=147$, $p<10^{-50}$). Each region exhibited a different mean sparsity than each of the others (LEC: mean=0.843 +/-0.01, dHPC: mean=0.51 +/-0.02,

vHPC: mean=0.78 +/-0.02, Students multiple comparisons, LEC v dHPC $p=10^{-10}$, LEC v vHPC p=0.02, vHPC v dHPC=10^{-10}). Overall these data show significant differences in the way that units in the dHPC, vHPC and LEC code for time. dHPC activity was sparse, exhibiting narrow firing fields whose centers tended to occur earlier, but that tiled the delay. Conversely, activity patterns in vHPC and LEC were less sparse, covering a larger proportion of the delay without a single clear peak.

Previous studies examining time cells in dHPC and MEC show that fields that occurring earlier in a delay are often more narrow than those occurring later (Kraus et al., 2015, 2013). Consistent with these results, the standard deviation of the spike times was highly correlated to the mean spike time in dHPC. Importantly, this effect was absent in both vHPC or LEC, and the slope of the relationship was significantly steeper in dHPC than either vHPC or LEC (Linear Regression, dHPC $r^2=0.55$, $p<10^{-15}$, vHPC $r^2=0.22$, $p<10^{-8}$, LEC $r^2=0.02$ $p>0.05$, Comparison of slopes: dHPC vs. LEC $p=10^{-5}$, dHPC vs. vHPC $p<10^{-9}$, LEC vs vHPC p=0.21). Thus, typical time cell properties of dHPC replicated in this experiment did not extend to firing fields in vHPC or LEC. These data therefore suggest that the individual units in vHPC and LEC that track time during the delay do so through a different mechanism than canonical time fields.

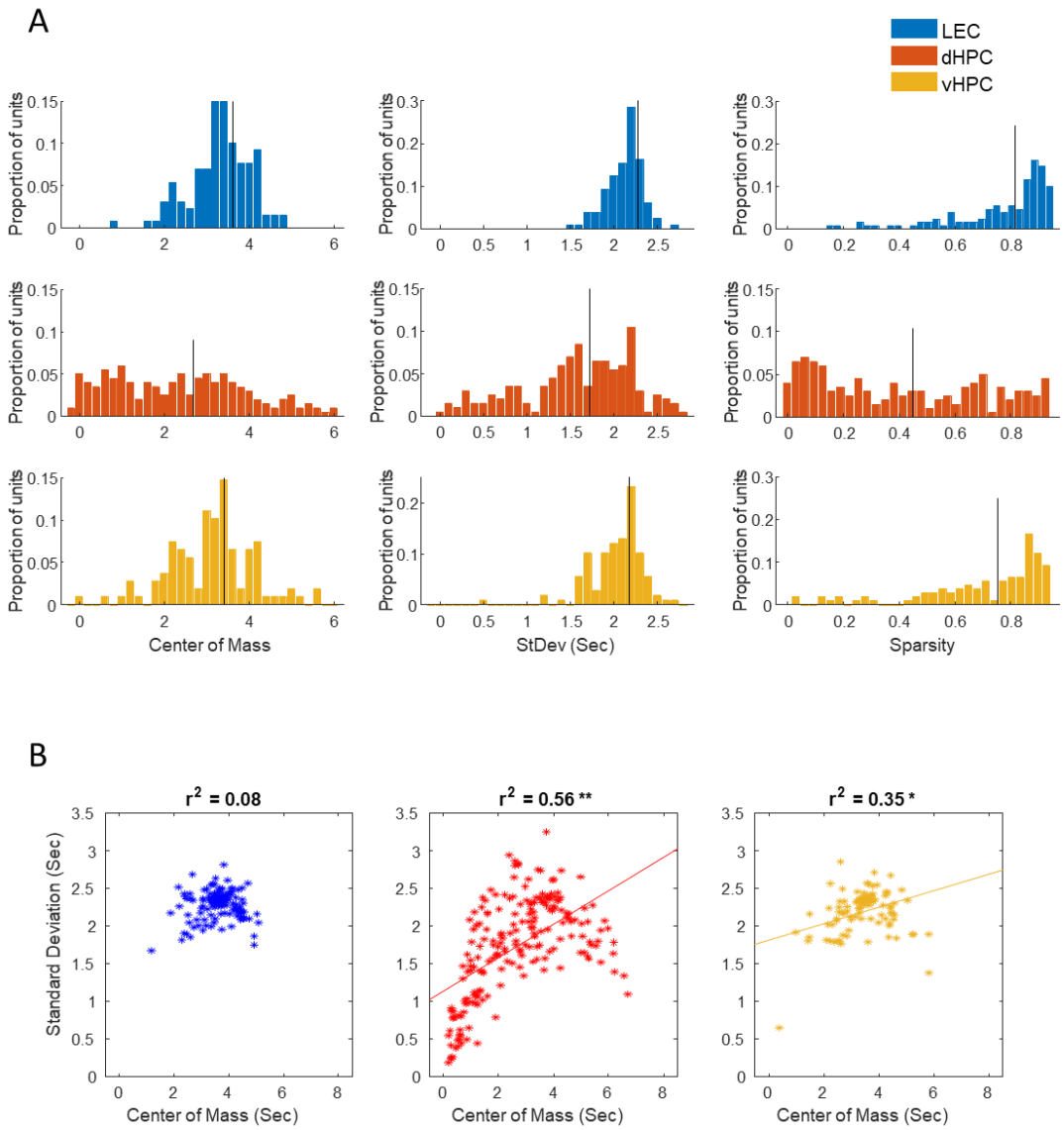

Figure 27: Temporally selective units in dHPC exhibited sparse, narrow peaks that became progressively wider across the delay, whereas those in vHPC and LEC did not.

A: dHPC exhibited a distribution of field center of mass and field standard deviation with a greater skew towards narrower fields earlier in the delay that were characteristic of time fields. dHPC units also showed sparser activity patterns then either vHPC or LEC. LEC and vHPC units showed a narrow distribution of center of mass and large standard deviation of activty across time even though their firing fields varied widely across the delay. B: Consistent with previous descriptions of time cells, dHPC units showed a tight relationship between the center of mass and field width. This effect was weaker in vHPC, and absent in LEC. LEC average center of mass: 3.62 +/- 0.7, dHPC: 2.68 +/- 1.62, vHPC: 3.41 +/- 0.98. LEC average Standard Deviation: 2.28 +/- 0.19, dHPC:1.73+/- 0.65, vHPC: 2.18+/- 0.31. LEC average sparsity: 0.82+/- 0.18, dHPC: 0.45+/- 0.3, vHPC: 0.75+/- 0.18

4.4.3 Units in all three regions contained information about time

Units with temporally modulated activity during the delay were immediately apparent in all three regions (Figure 24, Figure 25, and Figure 26). Many units in all regions contained high levels of temporal information during the delay (Figure 24, Figure 25, and Figure 26 Information indicated above plots, all are significantly above chance). To determine cells with significant temporal information, a shuffling procedure was used wherein the spike train of individual trials was circularly shifted around a random point. After filtering for significance, units in dHPC exhibited more temporal information than inuts in vHPC or LEC (Bootstrap shuffle on Skaggs information score, methods, LEC: 213/505, 42%, mean bits/spike=0.27 +/- 0.03, dHPC: 255/425, 60%, mean bits/spike=0.91 +/- 0.06, vHPC: 151/282, 53% mean bits/spike=0.46 +/- 0.05, ANOVA on information scores, $F(1)=49.96$, $p<10^{-10}$). To complement these analyses, we measured the standard deviation of the trial averaged tuning curve across time against a bootstrap shuffle. This method revealed a highly overlapping population of units whose firing rate varied across the delay (Methods, LEC: 163/505, 32%, dHPC: 256/425, 60%, vHPC: 122/282, 43%). The proportion of units that passed both thresholds was only slightly lower than each threshold individually, so we used both criterion for subsequent analyses (LEC cells passing both thresholds: 132/505, 26%, dHPC: 208/425, 49%, vHPC 110/282, 39%). This method revealed a significant proportion of time-modulated units in all three regions, however it revealed a higher proportion of temporally modulated units in dHPC than in vHPC and LEC (Chi square test, $\chi^2(2)=23.94$, $p<10^{-6}$). Finally, vHPC

units exhibited a marginally higher mean firing rate during the delay than both dHPC and LEC, but there were no differences between dHPC and LEC (LEC: 3.365 +/-0.28, dHPC: 2.51 +/-0.36, vHPC: 4.9+/- 0.62, ANOVA F(2)=4.6, p=0.01, Students Post-Hoc: LEC:dHPC p=0.83, LEC:vHPC p=0.05, dHPC v vHPC: p<0.01).

4.4.5 Ensemble activity was similarly sensitive to the evolution of time across regions

We observed a higher proportion of temporally selective units in the dHPC than in the vHPC and LEC. Notwithstanding, there was a significant proportion of units coding time in all three regions. This suggests that the dHPC ensembles may contain temporal information than those in vHPC or LEC. Population vector analyses were used to compare the overall temporal specificity of ensembles in each region. To do this, ensemble firing rate vectors were generated from each units' trial averaged tuning curve relative to delay start for all consecutive 200 millisecond bins during the delay. Then, the average Spearman correlation of the population vector between each time bin during the trial was calculated for each region and each session (Figure 28). The resulting cross-temporal correlation matrix for each region revealed how ensembles in each region changed as the delay progressed. When these matrices were examined, it was clear that the populations in each region evolved across time (Figure 28). High correlation values clustered towards the diagonal of the matrix for each region, indicating that populations in all three regions evolved across the delay. Indeed, when correlation values were aggregated based on their temporal lag, population vector correlations reliably fell in all regions and sessions as the temporal lag between sample times grew (Figure 28 center

column). However, there was no considerable differences in the rate of drift between each region, such that differences between slope of the correlation values against temporal lag between regions was not significantly different (Figure 28 E) (LEC slope -0.088 +/- 0.013, dHPC slope -0.073 +/-0.012, vHPC slope -0.056 +/- 0.013, one way ANOVA, $F(3)=1.6$, $p=0.205$). As there was considerable variability in the drift rate across sessions within each region, this effect could have been masked (Figure 28 C). While it reduced the size of the dataset, we were able to test this hypothesis within sessions with simultaneously recorded units in multiple regions. When session variability was controlled, there was still no significant difference in slopes (Bonferonni corrected Signrank test, $z=1.64$). These results suggest that despite major differences in individual unit characteristics, the overall ensemble activity in each of these regions are similarly sensitive to the evolution of time during the delay.

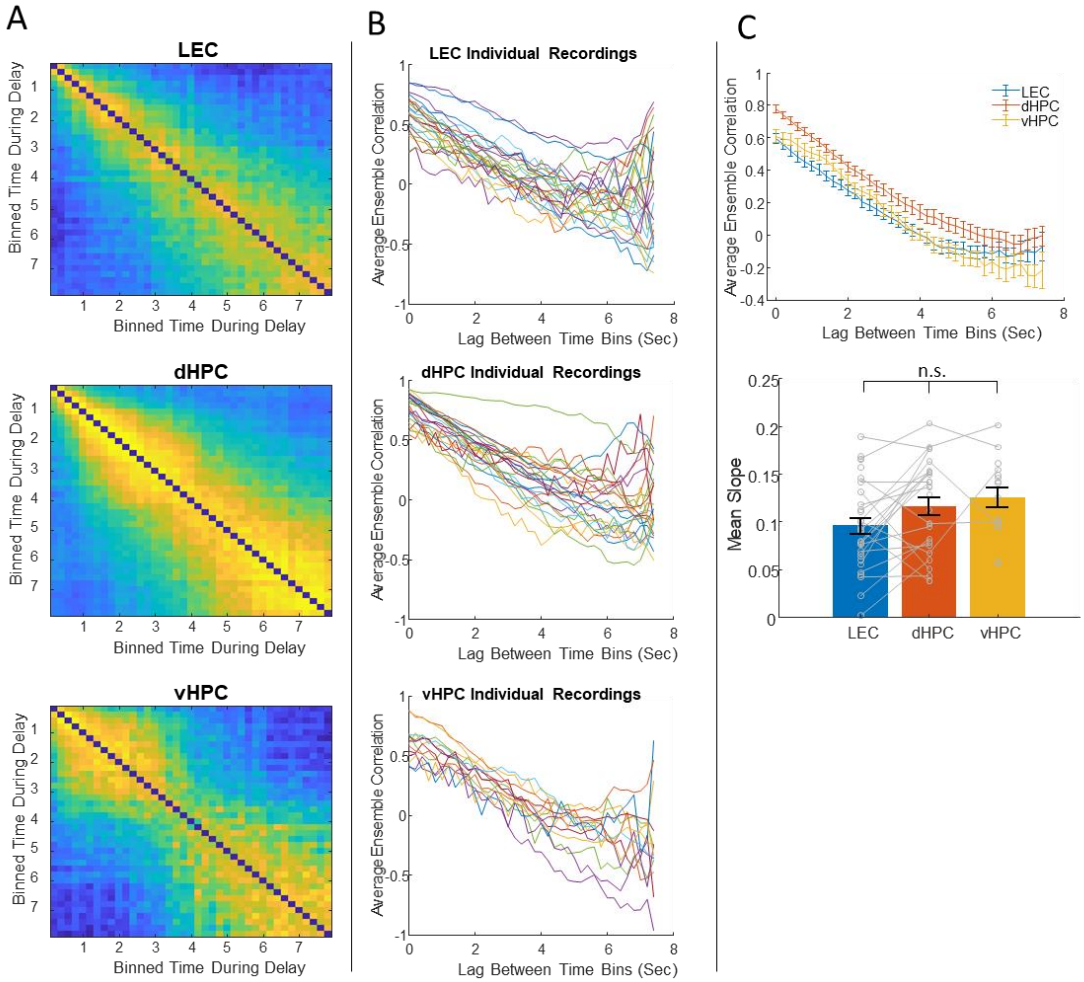

Figure 28: Correlation Matrices of LEC, dHPC and vHPC ensembles suggest comparable temporal specificity.

A. **Cross temporal correlation matrices in LEC, dHPC and vHPC for the delay period. B. Correlation values fell between time-bins as their temporal lag grew in all regions, however there was considerable heterogeneity in the slopes within each region. C: Top: the mean slope from each region in B. Middle: the slopes from the above plot were greater than zero for all regions, however the slopes were not significantly different between regions.**

To test the trial-to-trial reliability of the time code in each region, we used linear discriminant analysis to decoded time using out-of-sample data. This analysis allows for the prediction of time using individual trial activity, and therefore is good measure of

reliability on a trial-to-trial basis. Indeed time could be accurately decoded better than chance in all three regions for the majority of the delay (Figure 29, colored bars below figure in C signify significant accuracy). Interestingly, decoders trained on LEC and vHPC failed to accurately predict times towards the center of the delay. Indeed we rarely found individual units in either region that exhibited elevated firing towards the middle of the delay and not at the beginning or end. Conversely, numerous units in the dHPC fired selectively during moments towards the middle of the delay, and may have contributed to the accuracy of the decoder at these time points.

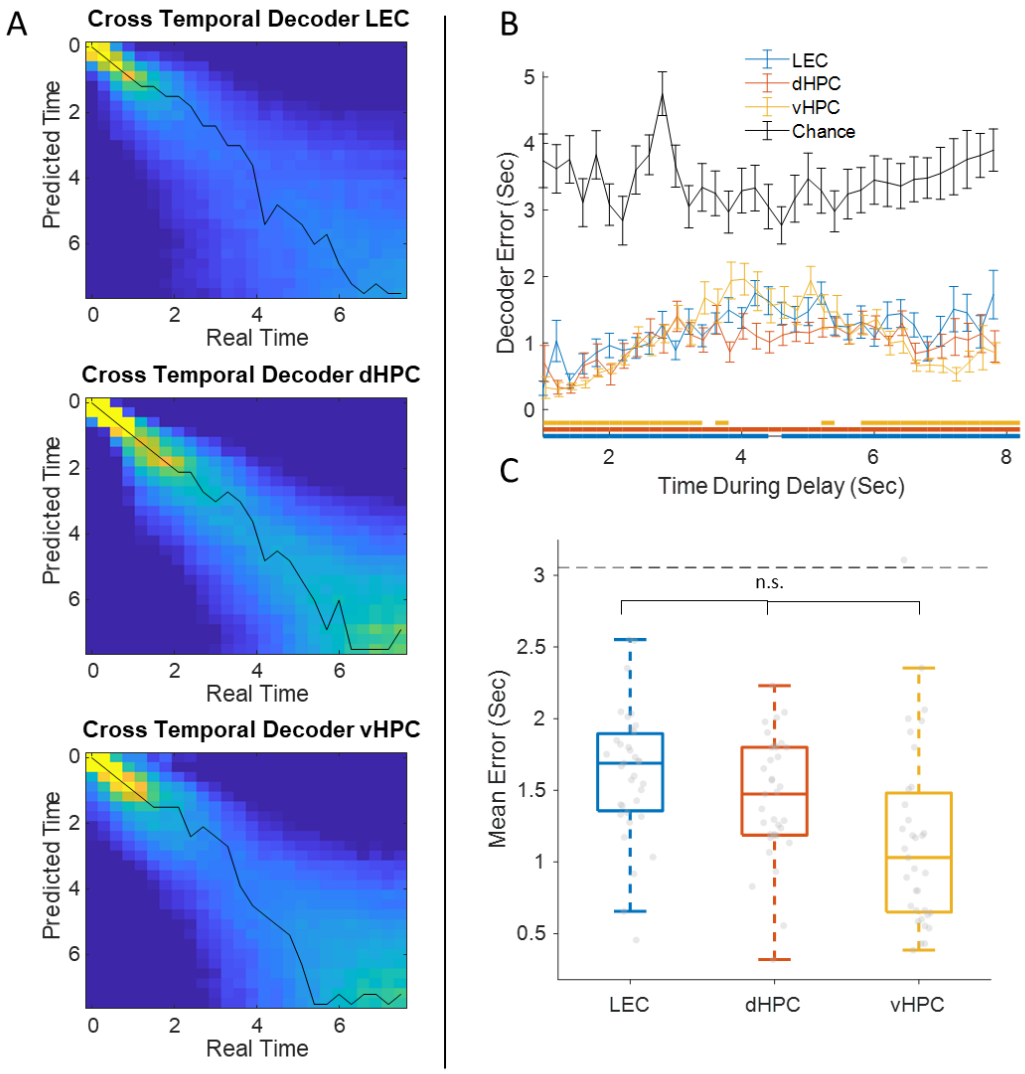

Figure 29: Linear Discriminant decoding of time is similarly accurate for dHPC, vHPC and LEC ensembles.

A: Cross temporal decoder performance for LEC, dHPC and vHPC ensembles. Decoders trained on each region could accurately predict time during the delay. B: Decoders from all three regions were more accurate at the onset of the delay and became less accurate as the delay wore on. Colored lines below errorbars indicate significance from chance for each region. C: Decoders from all regions were more accurate than chance, and we failed to observe differences in decoder accuracy between regions. Dotted line at top represents lower margin for chance levels.

4.5 Discussion

4.5.1 The LEC, dHPC and vHPC exhibit different intrinsic activity patterns

In this study, we performed simultaneous recordings in dorsal hippocampus, ventral hippocampus and LEC to directly compare the coding properties of these regions during a mnemonic delay. Before examining behaviorally dependent firing, we observed differences in the intrinsic temporal organization of spiking in units across the three regions. Confirming previous results, we found that both the dHPC and vHPCs contain units that fire in rapid bursts that are nested in the theta frequency (7-12 Hz) (Kjelstrup et al., 2008; Patel, Fujisawa, Berényi, Royer, & Buzsáki, 2012; Royer et al., 2010). However, the intrinsic theta rhythmicity was stronger in the dorsal hippocampus than in either the ventral hippocampus or LEC (Royer et al., 2010). While previous reports have shown the LEC to contain units with much lower theta rhythmicity than MEC, none have directly compared the LEC to the hippocampus in the same preparation (Deshmukh et al., 2010). Here we observed much lower levels of bursting activity and intrinsic theta rhythmicity in LEC than in either region of the hippocampus. Furthermore, while vHPC units show reduced theta coherence when compared to dHPC, they still exhibit higher coherence than units in LEC. This may suggests that the theta nested computations occurring in MEC and the dHPC could be less prevalent in the vHPC and may even exclude the LEC. It is likely that units in the LEC engage in oscillatory coupling at other frequencies, as others have observed strong oscillations in the beta (~15-35 Hz), and gamma (~40-80 Hz) bands in the LEC (Xu & Wilson, 2012).

4.5.2 Time was coded differently in LEC and vHPC than in dHPC

Units in each region exhibited temporally selective firing during the delay that differed in a number of properties. Primarily, dHPC units showed properties of canonical time cells including sparse delay activity, with transient activation increases that showed a small standard deviation. Furthermore, time cell activity in dHPC showed a reliable relationship between center of mass and standard deviation. These activity patterns were consistent with previous reports using a range of preparations that describe 'time fields.' (Gill et al., 2011; Howard et al., 2014; Kraus et al., 2015; Y. Liu, Tiganj, Hasselmo, & Howard, 2019; Macdonald et al., 2013; Villette et al., 2015). In contrast, vHPC and LEC units exhibited significantly less sparse delay activity, and activity increases were significantly broader with a large standard deviation (Jung et al., 1994). Thus, in this preparation we found weak evidence for time cells in either vHPC or LEC. These data are consistent with previous reports showing sparser activity across space in the dHPC when compared to the vHPC (Jung et al., 1994). While it is broadly accepted that units in the dorsal hippocampus organize into firing fields that center on points along a continuous delay, this study makes clear that units in the ventral hippocampus and LEC organize their firing across time in a different manner.

4.5.3 All three regions coded for time

Despite differences in the way individual units represented time between regions, we found significant temporal modulation in all three regions both in single unit activity as well as in populations. Indeed population vector analysis showed significant change in

ensemble activity across time in each region, and the rate of change across the delay was similar across regions. Considering the interconnectedness of these three regions, temporal information may be transferred from one of these regions to the others. Alternatively, the temporal specificity we observed may arise in the interactions between these regions, rather than in the activity of units from one region alone. Interestingly, one previous report employed similar population vector analyses to reveal significant differences in ensemble drift rates between the dHPC and LEC. However, this experiment observed time modulated activity across hours to days (Tsao et al., 2018). Moreover, in Tsao et al, behavior was loosely clamped, and animals were continually experiencing different environmental enclosures. In the current experiment, time was isolated from changing sensorimotor experiences as the animal was fixed spatially and ran at a constant speed as time wore on. Here, we failed to observe gross differences in the ensemble code of time across dHPC, vHPC and LEC.

The delay activity we observed in individual units in both the vHPC and LEC often showed peaks at the onset or offset of the delay that gradually decayed as time progressed. These characteristics are similar to those observed in Tsao et al. who observed units slowly decay or rise across time (Tsao et al., 2018). Our observations add to those from this previous work and indicate that the LEC and vHPC may code for time in a similar manner across different time scales from seconds to hours via slowly decaying and rising firing rates.

4.5.4 The differences in temporal processing between dHPC and LEC and vHPC might be consistent with a more general framework.

These two cellular properties may coincide with differences in the cognitive processes that the LEC and each segment of the hippocampus support. A prominent theory suggests that the hippocampus can be divided into separate structures, with a dorsal region supporting spatial and relational memory and cognition, and a ventral zone supporting emotional and abstract memory and cognition (Aggleton, 2012; Fanselow & Dong, 2010; Kheirbek et al., 2013). A number of studies have confirmed this duality, showing a shift in gene expression, and biochemical and electrophysiological properties along the dorsal-ventral axis of the hippocampus (for a review see: Fanselow & Dong, 2010). Indeed the spatial scale of place fields increases from dorsal to ventral hippocampus, coinciding with an increase in sensitivity to anxiety state (Jimenez et al., 2018; Kjelstrup et al., 2008; Royer et al., 2010). The high spatial acuity of the dHPC observed in other studies is consistent with the high temporal acuity observed in this experiment. During running, animals change location rapidly across time and this may require a region to maintain high temporal acuity to accurately discriminate changing location. Conversely, the ventral hippocampus and LEC are both thought to process non-spatial and potentially emotionally relevant information, which may coincide with a greater role in integration rather than discrimination across time. The defining features of objects and companions may change over a slower or less predictable rate, and interact with each other in a less temporally rigid manner. As such, this may require a brain region to smooth the representation of these features across time and across modalities to

capture their relationships. The gradual changes in firing rate we observed across the delay in both the LEC and vHPC might suggest that these regions generate representations that may fade slowly as time progresses.

Chapter 5. General Discussion

Observations from the first experiment of this dissertation challenge the notion of segregated information streams entering the hippocampus, by showing associative item-place information coded in the both the medial and lateral entorhinal cortex as well as the perirhinal cortex. These data implicate the entorhinal cortex and perirhinal cortex in the processing of item-place conjunctions that were initially thought to form only in the hippocampus. The third chapter of this dissertation explored how the hippocampal representation of item-place conjunctions changes across time in a task where the time frame was behaviorally relevant. These conjunctive units coded for time by exhibiting a spectrum of temporal drift rates, some changing rapidly across trials, and some changing more slowly. These results suggest that event and place information are organized onto a timeline in the hippocampus by units that code time at a variety of resolutions. The fourth chapter of this dissertation examined whether temporal selectivity exhibited in the dorsal hippocampus is found more broadly in the medial temporal lobe. While time could be decoded from ensembles in dHPC, vHPC and LEC, a qualitatively different time code was observed in the LEC and ventral hippocampus at the unit level. Together these observations suggest a model wherein item, place, and time information are shared throughout medial temporal lobe structures to support declarative memory.

5.1 A reorganization of the dual stream hypothesis

A large number of recording studies support the dual stream hypothesis, showing spatially modulated firing in the medial entorhinal cortex, and weak spatial modulation in the lateral entorhinal cortex (Hafting et al., 2005; Hargreaves et al., 2005). Lateral entorhinal cells respond to non-spatial features such as odors and locally placed objects (Deshmukh & Knierim, 2011; Young et al., 1997). In chapter 2 we observed a striking contrast to this model, finding object-selectivity in the medial entorhinal cortex, and position selectivity in the lateral entorhinal and perirhinal cortices. When animals were required to make object-place associations, we observed engagement of units in both regions that were selective to objects and positions together.

These observations appear to conflict with the dominant model, but they do not directly conflict with other experimental observations. Primarily, no other studies have directly examined object-selectivity in the MEC. However, a number of studies have shown an extended role of the MEC beyond purely space, by observing route and time selective firing (Heys & Dombeck, 2018; Kraus et al., 2015; Lipton, White, & Eichenbaum, 2007). Kraus et al. (2015) found that MEC neurons generated firing fields during running in place, and that these fields were not purely coding for distance. Similarly, Lipton et al. (2007) observed cells whose firing fields selected for upcoming right or left turns. Finally Heys and Dombeck (2018) reported sequences of cells in the MEC that tiled time as mice stopped running to wait for reward. Interestingly, the unit firing related to the animals' estimation of elapsed

time. Together, these studies corroborate our findings and suggest MEC units may generate firing fields that organize across non-spatial dimensions such as time.

Similarly, experiments observing a stark contrast in spatial selectivity between the MEC and LEC have done so under exclusively passive behaviors; mainly random foraging in open fields containing scarce local landmarks. When objects were placed in the arena, one group observed lateral entorhinal cells that appeared spatially selective for objects, but also after those objects had been removed (Deshmukh & Knierim, 2011; Knierim et al., 2013; Tsao et al., 2013). The results in Chapter 2 are consistent with these findings and suggest that the LEC may express spatially selective firing, but only in locations where there is relevant non-spatial information.

While our observations are consistent with previous studies, they suggest a revision to the dual stream model. Specifically, they invalidate a version of memory processing wherein associative memory is contained exclusively within the hippocampus. Instead, these data support a role for the entorhinal and perirhinal cortices in holding schematic representations that transcend the spatial/non-spatial boundary. Specifically, item and spatial information may dominate in LEC/PRC and MEC respectively, but when specific item-place conjunctions are relevant task dimensions, all three regions incorporate item-place conjunctive information.

Previous studies have examined the development of conjunctive item-place representations in the dorsal hippocampus, and context dependent representations

in the ventral hippocampus as rats learn these associations (Komorowski et al., 2013, 2009). One model of hippocampal-entorhinal interactions describes a 'semantic' memory store residing in cortical regions that is modified by hippocampal processing of episodic experiences. Applying this model to the present experience, information enters the hippocampus as a lexicon of already-learned semantic representations (items, places separately) and the hippocampus updates these representations to incorporate common or meaningful item-place conjunctions (Schacter et al., 1978). This theory suggests that conjunctive coding in the MEC, LEC and PRC may develop with learning, and may require the hippocampus to organize. Future experiments examining the development of conjunctive selectivity in the rhinal cortices might could test whether this process is facilitated through hippocampal interactions.

5.2 Gradual temporal drift accommodates events and boundaries

In Chapter 3 we observed that the hippocampal representation of items in a particular place evolve continuously through time. Others have observed a similar phenomenon during a variety of behaviors, including free foraging and during a temporal ordering task (Deuker et al., 2016; Mankin et al., 2012; Manns et al., 2007). Other experimental configurations have argued that contextual boundaries induce discrete remapping events in the hippocampal code (Bulkin et al., 2018; Kobayashi et al., 1997; Swallow et al., 2011). From these studies it was unclear whether the addition or removal of novel stimuli was responsible for the apparent 'time' code. The experiment in chapter 3 was conceived with the goal of clamping behavior and

stimuli across time in order to resolve this question. We hypothesized that hippocampal representations would change at the transitions between blocks, but activity would remain stable within a block of time.

Contrary to our hypothesis, the hippocampal code did not alternate with the task demands, and instead drifted across time continuously. Even though temporally defined contexts repeated, this code reflected time in a continuous manner. Admittedly, rats may not have realized there was an alternating block structure to the task, even though each block transition was signaled by removal from the testing environment for 1 minute. All rats showed sensitivity to the boundary event by not perseverating at the onset of each segment. The hippocampal code, however was not modulated by boundaries and did not separate experiences across these boundaries any more than chance. Instead, individual units exhibited a spectrum of temporal drift rates, such that cells activity changed at varying rates across time.

The individual unit activity we observed across time potentially incorporated abrupt changes in experience into an ensemble code. The spectrum of activity drift rates across units that we observed could provide a substrate to encode both the changes between and similarities across boundary conditions. Non-overlapping ensembles of rapidly changing units represented events in the earlier context before and those in the later context after the boundary independently via their separation in time. Conversely, slowly changing units that were active before *and* after the delay captured the similarities in events across the boundary as a unified context.

Indeed the hippocampus is necessary to accurately capture hidden similarities between experiences, but to also discriminate between similar experiences across time (DeVito et al., 2009; Fortin et al., 2002; Schapiro et al., 2016). This property, wherein some hippocampal units exhibit a spectrum of change rates from fast to slow across time may be the mechanism by which the hippocampus supports behavioral and cognitive flexibility (Kimble & Kimble, 1965; Kosaki & Watanabe, 2012; Preston et al., 2004).

An alternative coding scheme has been proposed that incorporates multiple timescales of experience. Mau et al. (2018) observed temporally ordered hippocampal sequences that nested within multiple time scales. In this experiment, they observed cell sequences appearing within a given trial that also exhibited drift across trials. Importantly, the within trial sequences were observed during a treadmill delay, when no changes in behavior or stimuli were occurring. Chapter 3 involved six similarly nested blocks into a single recording session. However, we did not observe sequences playing out in each block that repeated during subsequent blocks. Instead we observed a continuous representation of time that was supported by some rapidly changing units and other more slowly changing units. These two observations appear in conflict; do individual hippocampal neurons code time at one timescale, or do they code time at multiple scales via nested sequences? One possibility is that the short sequences observed in Mau et al. are qualitatively different than those we observed, and only exist at very short time scales (Mau et al., 2018). Future studies could either extend the duration of a single trial, or

alternatively incorporate a time delay into a blocked experiment similar to that in chapter 3. These studies might reveal a maximum trial duration for which sequences can persist. On the other hand, given a more explicit cue to chunk experience, hippocampal units may shift to representing multiple timescales in a nested fashion.

The data from chapter 3 contribute to a growing literature that show hippocampal firing fields organize along a timeline. Complementary studies have observed time coding across seconds, hours and days (Mankin et al., 2012; Manns et al., 2007; Mau et al., 2018). Interestingly, while Mankin observed this drift under the backdrop of spatial coding, Manns observed this under the backdrop of object coding, and we observed drift in cells coding objects and place together. Together, these studies show that hippocampal ensembles can represent item-time information, place-time information, and finally item-place-time information which together underlie episodic memory.

5.3 Temporal selectivity was observed throughout the medial temporal lobe

In Chapter 4 we examined whether timing signals like the one observed above can be found in the LEC and vHPC during a mnemonic delay. While a variety of studies have reported slow changes in population activity, it remains unclear how this phenomenon may occur on an individual cell basis (Mankin et al., 2012; Tsao et al., 2018). Tsao et al. observed a time signal in the lateral entorhinal cortex that changed across hours, that contained greater temporal information than the dorsal hippocampus (2018). In that experiment, they reported slowly rising or slowly

decaying firing rates across minutes spent in a chamber, or across hours exploring multiple chambers. This result was surprising, as this code appeared different than time cells in the dorsal hippocampus and MEC that have been observed in a variety of preparations. Time cells provide a precise estimate of elapsed time via punctate temporal firing fields rather than continuous ramping or delay (Heys & Dombeck, 2018; Kraus et al., 2015; Mau et al., 2018; Pastalkova et al., 2008). Before chapter 4 it was unclear whether the LEC coded time during mnemonic delays, and how this activity compared to canonical time cell signals in the hippocampus and MEC. In order to address this question, we recorded from LEC and vHPC units simultaneously with those in dHPC across a mnemonic delay and observed their temporal modulation. Simultaneous recordings enabled the direct comparison of the timing properties between these regions in the same animals.

When we examined time-modulated activity in the dHPC, vHPC and LEC during a mnemonic delay, time cells were evident in dHPC, but they were conspicuously absent in vHPC and in LEC. Despite these differences, many units in all three regions coded for time, and time was predicted from ensemble activity in each region with similar precision. Studies that have examined timing signals across mnemonic delays describe time fields and liken their characteristics to place fields (Macdonald et al., 2011; Pastalkova et al., 2008). Both time and space are coded in the dorsal hippocampus by the organization of cell sequences that span these dimensions. This analogy is similarly useful when examining spatial and temporal coding in the MEC. One prominent feature of these MEC units was their multi-

peaked firing patterns that previously distinguished the MEC from other regions such as the hippocampus (e.g. grid cells: Hafting et al., 2005). These studies suggest that the dorsal hippocampus and MEC code for time in a similar manner to how they code space.

Extrapolating these space-time similarities to the LEC, units may express time but only with regard to specific objects or events, in an analogous manner to object-cells and object trace cells (Tsao et al., 2013). Over longer delays, a separate study by Tsao et al. (2018) observed LEC units who peaked at either the beginning or end of an experience. Indeed we observed units whose firing rate could be interpreted as peaking during specific events (initiation of the delay) and whose firing rate slowly diminished thereafter. Conversely, we observed other LEC units whose firing rate slowly ramped in anticipation of a separate event; the termination of the delay. This activity may be more similar to spatially modulated border cells also found in the MEC (Solstad et al., 2008). One interesting feature of cells in the LEC was that they appeared to exhibit a spectrum of decay rates following the onset of the delay. This characteristic is computationally relevant, as it provides a mechanism for the generation of time field like units in downstream structures (Howard et al., 2014).

Interestingly, the ventral hippocampus did not appear to have time cells in this experiment. This study was the first to examine ventral hippocampal activity during a mnemonic delay, so it was previously unclear whether the ventral hippocampal units code time at any scale. Nonetheless, a range of experiments

implicate the vHPC in bridging the gap between temporally discontinuous events (Esclassan, Coutureau, Di Scala, & Marchand, 2009; Hunsaker & Kesner, 2008; Rogers et al., 2006). Studies examining the spatial firing characteristics of vHPC can be extrapolated to make strong predictions about its organization across time. The ventral hippocampus is thought to contain a less sparse code for space, wherein individual firing fields are active over larger proportions of the environment (Jung et al., 1994; Royer et al., 2010). This may suggest that vHPC ensembles may code time via larger time fields. Incongruent with this model, evidence from previous studies, including Chapter 3, suggest that dHPC units vary with time across a wide spectrum of scales, from seconds, to minutes and even hours (Mankin et al., 2012; Manns et al., 2007; Mau et al., 2018; Chapter 3). These conflicting data points result in an unclear prediction of how the vHPC codes time.

The time code we observed in the vHPC resembled that in LEC with individual units exhibiting slowly changing firing rates across the delay. Units in vHPC had a significantly higher mean firing rate during the delay than either dHPC or LEC, which may indicate a denser representation of time. Accordingly, the sparsity of vHPC was significantly less than that in the dHPC (Jung et al., 1994; Komorowski et al., 2013). Together these data points might indicate that individual units in the vHPC code time on a broader scale. We hypothesize that the vHPC may contain a reliable time code across minutes or hours similar to the code observed in Chapter 3, or similar to that observed in the LEC (Tsao et al., 2018).

The connections between these regions suggest that the time code in some regions may inform that of others, but the direction of causality remains unclear. Modeling work hypothesizes that the pointer-like representations exemplified by time cells may receive temporal information from regions representing elapsed time via ensembles with rising and decaying firing rates (Howard et al., 2014; Y. Liu et al., 2019). These results predict that LEC or vHPC ensemble activity may contribute to the temporal specificity observed in individual dHPC units. However, the hippocampus and entorhinal cortex normally exist in a loop, so it may be difficult to ascribe the true source of temporal information in this anatomical system. The question of directionality may be resolved by observing the development of these temporal signals to discern which may develop first. Alternatively, chemogenetically or optogenetically severing either feedforward or feedback connections between the dHPC, vHPC and LEC may result in an uneven loss of temporal information across those regions. Other studies have already examined the dependence of the time code in some regions on the integrity of the others. Indeed one report already examining this question concluded that hippocampal time cells require organized input from the MEC (Robinson et al., 2017). Given the overlap in firing properties of MEC and LEC observed in chapter 2, we hypothesize that lesions of either MEC or LEC are sufficient to impair memory across a delay and to abolish time modulation in hippocampal units.

5.4 Concluding remarks

The studies above advance our understanding of memory and the neural mechanisms supporting it in two important ways. First, these studies observed information content related to the content of experience in memory related regions that were either thought not to, or that had yet to be interrogated. Primarily, the first study observed associative item-place representations previously thought to only exist within the hippocampus. This study revised the model of information flow into and out of the hippocampus by revealing that item and place information are merged outside of the hippocampus. Furthermore, these studies are the first to observe time coding in individual units in both the LEC and vHPC specifically during a mnemonic delay. In these regions we observed a time code different from the previously described 'time cells.' Finally, these studies broadened our understanding of how time is represented in the hippocampus by revealing a time code that encompassed, but was not impacted by boundaries imposed upon experience. This time code was comprised of individual units whose activity was conjunctively selective to objects, places and time. These units coded for time with a spectrum of sensitivities such that some coded for small time windows, and others more broadly.

We also observed striking evidence of convergence and divergence in the coding of episodic associations across different MTL regions. In Chapter 2 we observed convergence in the coding of items, places, and item-place associations in the single unit activity within MEC and LEC. Conversely, population analyses

revealed divergent organization of information such that overall the MEC prioritized space, whereas the LEC prioritized items. Interestingly, in chapter 4 we observed the inverse result when examining unit and population activity in LEC, vHPC, and dHPC. This study revealed divergence in how the dHPC, vHPC and LEC coded time on a single cell basis. While dHPC units exhibited firing fields centered on moments during the delay, vHPC and LEC units exhibited progressive rate changes throughout the delay. At the population level, however, we observed convergence via similar predictability of time from activity in all regions. The observations from the experiments above lay bare the advantage of complementary single unit and population level analyses to neural data analysis. Furthermore, they reveal novel coding features in a number of medial temporal lobe structures that are relevant the organization and coding of episodic memory.

BIBLIOGRAPHY

Abbas, A. I., Sundiang, M. J. M., Henoch, B., Morton, M. P., Bolkan, S. S., Park, A. J., … Gordon, J. A. (2018). Somatostatin Interneurons Facilitate Hippocampal-Prefrontal Synchrony and Prefrontal Spatial Encoding. *Neuron*, *100*(4), 926–939.e3. http://doi.org/10.1016/j.neuron.2018.09.029

Aggleton, J. P. (2012). Multiple anatomical systems embedded within the primate medial temporal lobe: implications for hippocampal function. *Neuroscience & Biobehavioral Reviews*, *36*(7), 1579–96. http://doi.org/10.1016/j.neubiorev.2011.09.005

Ahn, J.-R., & Lee, I. (2015). Neural Correlates of Object-Associated Choice Behavior in the Perirhinal Cortex of Rats. *Journal of Neuroscience*, *35*(4), 1692–1705. http://doi.org/10.1523/JNEUROSCI.3160-14.2015

Akers, K. G., Martinez-Canabal, A., Restivo, L., Yiu, A. P., De Cristofaro, A., Hsiang, H.-L. L., … Frankland, P. W. (2014). Hippocampal neurogenesis regulates forgetting during adulthood and infancy. *Science (New York, N.Y.)*, *344*(6184), 598–602. http://doi.org/10.1126/science.1248903

Allen, T. A., Salz, D. M., McKenzie, S., & Fortin, N. J. (2016). Nonspatial Sequence Coding in CA1 Neurons. *The Journal of Neuroscience*, *36*(5), 1547–1563. http://doi.org/10.1523/JNEUROSCI.2874-15.2016

Amaral, D. G. (1993). Emerging principles of intrinsic hippocampal organization. *Current Opinion in Neurobiology*, *3*(2), 225–229. http://doi.org/10.1016/0959-4388(93)90214-J

Amaral, D. G., Scharfman, H. E., & Lavenex, P. (2007). The dentate gyrus: fundamental neuroanatomical organization (dentate gyrus for dummies). *Progress in Brain Research*, *163*, 3–22. http://doi.org/10.1016/S0079-6123(07)63001-5

Amaral, D. G., & Witter, M. P. (1989). The Three-dimensional Organization of the Hippocampal Formation: A Review of Anatomical Data. *Neuroscience*. Retrieved from http://www.sciencedirect.com/science/article/pii/0306452289904247

Amilhon, B., Huh, C. Y. L., Manseau, F., Ducharme, G., Nichol, H., Adamantidis, A., & Williams, S. (2015). Parvalbumin Interneurons of Hippocampus Tune Population Activity at Theta Frequency. *Neuron*, *86*(5), 1277–1289. http://doi.org/10.1016/j.neuron.2015.05.027

Anagnostaras, S. G., Maren, S., & Fanselow, M. S. (1999). Temporally graded retrograde

amnesia of contextual fear after hippocampal damage in rats: within-subjects examination. *The Journal of Neuroscience*, *19*(3), 1106–14. Retrieved from http://www.ncbi.nlm.nih.gov/pubmed/9920672

Aronov, D., Nevers, R., & Tank, D. W. (2017). Mapping of a non-spatial dimension by the hippocampal–entorhinal circuit. *Nature*, *543*(7647), 719–722. http://doi.org/10.1038/nature21692

Attardo, A., Fitzgerald, J. E., & Schnitzer, M. J. (2015). Impermanence of dendritic spines in live adult CA1 hippocampus. *Nature*. http://doi.org/10.1038/nature14467

Attneave, F. B. M., & Hebb, D. O. (1950). The Organization of Behavior; A Neuropsychological Theory. *The American Journal of Psychology*, *63*(4), 633. http://doi.org/10.2307/1418888

Baldassano, C., Chen, J., Zadbood, A., Pillow, J. W., Hasson, U., & Norman, K. A. (2017). Discovering Event Structure in Continuous Narrative Perception and Memory. *Neuron*, *95*(3), 709–721.e5. http://doi.org/10.1016/j.neuron.2017.06.041

Bellmund, J. L. S., Gärdenfors, P., Moser, E. I., & Doeller, C. F. (2018). Navigating cognition: Spatial codes for human thinking. *Science*, *362*(6415), eaat6766. http://doi.org/10.1126/science.aat6766

Bittner, K. C., Grienberger, C., Vaidya, S. P., Milstein, A. D., Macklin, J. J., Suh, J., … Magee, J. C. (2015). Conjunctive input processing drives feature selectivity in hippocampal CA1 neurons. *Nature Neuroscience*, *18*(8), 1133–1142. http://doi.org/10.1038/nn.4062

Bittner, K. C., Milstein, A. D., Grienberger, C., Romani, S., & Magee, J. C. (2017). Behavioral time scale synaptic plasticity underlies CA1 place fields. *Science*, *357*(6355), 1033–1036. http://doi.org/10.1126/science.aan3846

Blatt, G. J., & Rosene, D. L. (1998). Organization of direct hippocampal efferent projections to the cerebral cortex of the rhesus monkey: projections from CA1, prosubiculum, and subiculum to the temporal lobe. *The Journal of Comparative Neurology*, *392*(1), 92–114. Retrieved from http://www.ncbi.nlm.nih.gov/pubmed/9482235

Bliss, T. V. P., & Lømo, T. (1973). Long-lasting potentiation of synaptic transmission in the dentate area of the anaesthetized rabbit following stimulation of the perforant path. *The Journal of Physiology*, *232*(2), 331–356. http://doi.org/10.1113/jphysiol.1973.sp010273

Bonnevie, T., Dunn, B., Fyhn, M., Hafting, T., Derdikman, D., Kubie, J. L., … Moser, M.-B. (2013). Grid cells require excitatory drive from the hippocampus. *Nature*

Neuroscience, *16*(3), 309–17. http://doi.org/10.1038/nn.3311

Bousfield, W. A. (1953). The Occurrence of Clustering in the Recall of Randomly Arranged Associates. *The Journal of General Psychology*, *49*(2), 229–240. http://doi.org/10.1080/00221309.1953.9710088

Bower, G. H. (1970). Organizational factors in memory. *Cognitive Psychology*, *1*(1), 18–46. http://doi.org/10.1016/0010-0285(70)90003-4

Bower, M. R. (2005). Sequential-Context-Dependent Hippocampal Activity Is Not Necessary to Learn Sequences with Repeated Elements. *Journal of Neuroscience*, *25*(6), 1313–1323. http://doi.org/10.1523/JNEUROSCI.2901-04.2005

Bowles, B., Crupi, C., Mirsattari, S. M., Pigott, S. E., Parrent, A. G., Pruessner, J. C., … Kohler, S. (2007). Impaired familiarity with preserved recollection after anterior temporal-lobe resection that spares the hippocampus. *Proceedings of the National Academy of Sciences*, *104*(41), 16382–16387. http://doi.org/10.1073/pnas.0705273104

Brandon, M. P., Bogaard, A. R., Libby, C. P., Connerney, M. A., Gupta, K., & Hasselmo, M. E. (2011). Reduction of theta rhythm dissociates grid cell spatial periodicity from directional tuning. *Science (New York, N.Y.)*, *332*(6029), 595–9. http://doi.org/10.1126/science.1201652

Brandon, M. P., Koenig, J., Leutgeb, J. K., & Leutgeb, S. (2014). New and Distinct Hippocampal Place Codes Are Generated in a New Environment during Septal Inactivation. *Neuron*, *82*(4), 789–796. http://doi.org/10.1016/j.neuron.2014.04.013

Breindl, A., Derrick, B. E., Rodriguez, S. B., & Martinez, J. L. (1994). Opioid receptor-dependent long-term potentiation at the lateral perforant path-CA3 synapse in rat hippocampus. *Brain Research Bulletin*, *33*(1), 17–24. http://doi.org/10.1016/0361-9230(94)90045-0

Brown, M. W., & Banks, P. J. (2015). In search of a recognition memory engram. *Neuroscience & Biobehavioral Reviews*, *50*, 12–28. http://doi.org/10.1016/j.neubiorev.2014.09.016

Brun, V. H., Leutgeb, S., Wu, H.-Q., Schwarcz, R., Witter, M. P., Moser, E. I., & Moser, M.-B. (2008). Impaired spatial representation in CA1 after lesion of direct input from entorhinal cortex. *Neuron*, *57*(2), 290–302. http://doi.org/10.1016/j.neuron.2007.11.034

Brunelli, M., Castellucci, V., & Kandel, E. (1976). Synaptic facilitation and behavioral sensitization in Aplysia: possible role of serotonin and cyclic AMP. *Science*, *194*(4270), 1178–1181. http://doi.org/10.1126/science.186870

Bulkin, D. A., Law, L. M., & Smith, D. M. (2016). Placing memories in context: Hippocampal representations promote retrieval of appropriate memories. *Hippocampus*, *00*(2016), n/a-n/a. http://doi.org/10.1002/hipo.22579

Bulkin, D. A., Sinclair, D. G., Law, L. M., & Smith, D. M. (2018). Hippocampal State Transitions at the Boundaries between Trial Epochs. *BioRxiv*, 1–11. http://doi.org/10.1101/443077

Bunsey, M., & Eichenbaum, H. B. (1996). Conservation of hippocampal memory function in rats and humans. *Nature*. http://doi.org/10.1038/379255a0

Burgalossi, A., Herfst, L., von Heimendahl, M., Förste, H., Haskic, K., Schmidt, M., & Brecht, M. (2011). Microcircuits of functionally identified neurons in the rat medial entorhinal cortex. *Neuron*, *70*(4), 773–86. http://doi.org/10.1016/j.neuron.2011.04.003

Burwell, R. D., & Amaral, D. G. (1998). Perirhinal and postrhinal cortices of the rat: interconnectivity and connections with the entorhinal cortex. *The Journal of Comparative Neurology*, *391*(3), 293–321. Retrieved from http://www.ncbi.nlm.nih.gov/pubmed/9492202

Burwell, R. D., Witter, M. P., & Amaral, D. G. (1995). Perirhinal and postrhinal cortices of the rat: a review of the neuroanatomical literature and comparison with findings from the monkey brain. *Hippocampus*, *5*(5), 390–408. http://doi.org/10.1002/hipo.450050503

Buzsáki, G. (2002). Theta Oscillations in the Hippocampus. *Neuron*, *33*(3), 325–340. http://doi.org/10.1016/S0896-6273(02)00586-X

Cai, D. J., Aharoni, D., Shuman, T., Shobe, J., Biane, J., Lou, J., … Silva, A. J. (2016). A shared neural ensemble links distinct contextual memories encoded close in time. *Nature*, *534*(7605), 115–118. http://doi.org/10.1038/nature17955

Canto, C. B., & Witter, M. P. (2012). Cellular properties of principal neurons in the rat entorhinal cortex. I. The lateral entorhinal cortex. *Hippocampus*, *22*(6), 1277–99. http://doi.org/10.1002/hipo.20993

Caparelli, E. ., Backus, W., Telang, F., Wang, G.-J., Maloney, T., Goldstein, R., & Henn, F. (2012). Is 1 Hz rTMS Always Inhibitory in Healthy Individuals? *The Open Neuroimaging Journal*, *6*, 69–74. http://doi.org/10.2174/1874440001206010069

Castellucci, V., & Kandel, E. R. (1976). Presynaptic facilitation as a mechanism for behavioral sensitization in Aplysia. *Science*, *194*(4270), 1176–1178. http://doi.org/10.1126/science.11560

Cheke, L. G., & Clayton, N. S. (2010). Mental time travel in animals. *Wiley Interdisciplinary Reviews: Cognitive Science*, *1*(6), 915–930. http://doi.org/10.1002/wcs.59

Clayton, N. S., & Dickinson, A. (1998). Episodic-like memory during cache recovery by scrub jays. *Nature*, *395*(6699), 272–274. http://doi.org/10.1038/26216

Cohen, N. J., Ryan, J., Hunt, C., Romine, L., Wszalek, T., & Nash, C. (1999). Hippocampal system and declarative (Relational) memory: Summarizing the data from functional neuroimaging studies. *Hippocampus*, *9*(1), 83–98. http://doi.org/10.1002/(SICI)1098-1063(1999)9:1<83::AID-HIPO9>3.0.CO;2-7

Cohen, N. J., & Squire, L. R. (1980). Preserved learning and retention of pattern-analyzing skill in amnesia: dissociation of knowing how and knowing that. *Science (New York, N.Y.)*, *210*(4466), 207–10. Retrieved from http://www.psychology.uiowa.edu/Faculty/Freeman/cohen1980.pdf

Collie, M. F., Vaaga, C. E., Perederiy, J. V., Adelson, J. D., Woods, N. I., Chatzi, C., … Tovar, K. R. (2018). Preferential Targeting of Lateral Entorhinal Inputs onto Newly Integrated Granule Cells. *The Journal of Neuroscience*, *38*(26), 5843–5853. http://doi.org/10.1523/jneurosci.1737-17.2018

Collins, A. M., & Quillian, M. R. (1969). Retrieval time from semantic memory. *Journal of Verbal Learning and Verbal Behavior*, *8*(2), 240–247. http://doi.org/10.1016/S0022-5371(69)80069-1

Cressant, A., Muller, R. U., & Poucet, B. (1997). Failure of Centrally Placed Objects to Control the Firing Fields of Hippocampal Place Cells, *17*(7), 2531–2542.

Danielson, N. B., Zaremba, J. D., Kaifosh, P., Bowler, J., Ladow, M., & Losonczy, A. (2016). Sublayer-Specific Coding Dynamics during Spatial Navigation and Learning in Hippocampal Area CA1. *Neuron*, *91*(3), 652–665. http://doi.org/10.1016/j.neuron.2016.06.020

Davachi, L. (2006). Item, context and relational episodic encoding in humans. *Current Opinion in Neurobiology*, *16*(6), 693–700. http://doi.org/10.1016/j.conb.2006.10.012

Davachi, L., Mitchell, J. P., & Wagner, A. D. (2003). Multiple routes to memory: distinct medial temporal lobe processes build item and source memories. *Proceedings of the National Academy of Sciences*, *100*(4), 2157–62. http://doi.org/10.1073/pnas.0337195100

de Lavilléon, G., Lacroix, M. M., Rondi-Reig, L., & Benchenane, K. (2015). Explicit memory creation during sleep demonstrates a causal role of place cells in navigation. *Nature Neuroscience*, *18*(4), 493–495. http://doi.org/10.1038/nn.3970

Dede, A. J. O., Frascino, J. C., Wixted, J. T., & Squire, L. R. (2016). Learning and remembering real-world events after medial temporal lobe damage. *Proceedings of the National Academy of Sciences*, *113*(47), 13480–13485. http://doi.org/10.1073/pnas.1617025113

DeLong, G. R., & Heinz, E. R. (1997). The clinical syndrome of early-life bilateral hippocampal sclerosis. *Annals of Neurology*, *42*(1), 11–17. http://doi.org/10.1002/ana.410420105

Deshmukh, S. S., Johnson, J. L., & Knierim, J. J. (2012). Perirhinal cortex represents nonspatial, but not spatial, information in rats foraging in the presence of objects: Comparison with lateral entorhinal cortex. *Hippocampus*, *22*(10), 2045–58. http://doi.org/10.1002/hipo.22046

Deshmukh, S. S., & Knierim, J. J. (2011). Representation of non-spatial and spatial information in the lateral entorhinal cortex. *Frontiers in Behavioral Neuroscience*, *5*(October), 69. http://doi.org/10.3389/fnbeh.2011.00069

Deshmukh, S. S., Yoganarasimha, D., Voicu, H., & Knierim, J. J. (2010). Theta modulation in the medial and the lateral entorhinal cortices. *Journal of Neurophysiology*, *104*(2), 994–1006. http://doi.org/10.1152/jn.01141.2009

Deuker, L., Bellmund, J. L. S., Navarro Schröder, T., & Doeller, C. F. (2016). An event map of memory space in the hippocampus. *ELife*, *5*, 1–26. http://doi.org/10.7554/eLife.16534

DeVito, L. M., Kanter, B. R., & Eichenbaum, H. B. (2009). The hippocampus contributes to memory expression during transitive inference in mice. *Hippocampus*, *20*(1), NA-NA. http://doi.org/10.1002/hipo.20610

Diana, R. a., Yonelinas, A. P., & Ranganath, C. (2007). Imaging recollection and familiarity in the medial temporal lobe: a three-component model. *Trends in Cognitive Sciences*, *11*(9), 379–386. http://doi.org/10.1016/j.tics.2007.08.001

Dieni, C. V., Chancey, J. H., & Overstreet-Wadiche, L. S. (2013). Dynamic functions of GABA signaling during granule cell maturation. *Frontiers in Neural Circuits*, *6*(January), 1–11. http://doi.org/10.3389/fncir.2012.00113

DuBrow, S., Rouhani, N., Niv, Y., & Norman, K. A. (2017). Does mental context drift or shift? *Current Opinion in Behavioral Sciences*, *17*, 141–146. http://doi.org/10.1016/j.cobeha.2017.08.003

Eacott, M. J., & Gaffan, E. A. (2011). The roles of perirhinal cortex, postrhinal cortex, and the fornix in memory for objects, contexts, and events in the rat. *The Quarterly Journal of Experimental Psychology. B, Comparative and Physiological*

Psychology, *58*(3–4), 202–17. http://doi.org/10.1080/02724990444000203

Eacott, M. J., Machin, P. E., & Gaffan, E. A. (2001). Elemental and configural visual discrimination learning following lesions to perirhinal cortex in the rat, *124*, 55–70.

Eacott, M. J., & Norman, G. (2004). Integrated memory for object, place, and context in rats: a possible model of episodic-like memory? *The Journal of Neuroscience*, *24*(8), 1948–53. http://doi.org/10.1523/JNEUROSCI.2975-03.2004

Eichenbaum, H. B. (1998). Amnesia, the hippocampus, and episodic memory. *Hippocampus*, *8*(3), 197. http://doi.org/10.1002/(SICI)1098-1063(1998)8:3<197::AID-HIPO1>3.0.CO;2-H

Eichenbaum, H. B. (2000). A cortical-hippocampal system for declarative memory. *Nature Reviews. Neuroscience*, *1*(1), 41–50. http://doi.org/10.1038/35036213

Eichenbaum, H. B. (2014). Time cells in the hippocampus: a new dimension for mapping memories. *Nature Reviews Neuroscience*, (October). http://doi.org/10.1038/nrn3827

Eichenbaum, H. B. (2017). On the Integration of Space, Time, and Memory. *Neuron*, *95*(5), 1007–1018. http://doi.org/10.1016/j.neuron.2017.06.036

Eichenbaum, H. B., & Cohen, N. J. (2014). Can We Reconcile the Declarative Memory and Spatial Navigation Views on Hippocampal Function? *Neuron*, *83*(4), 764–770. http://doi.org/10.1016/j.neuron.2014.07.032

Eichenbaum, H. B., Otto, T., & Cohen, N. J. (1994). Two functional components of the hippocampal memory system. *Behavioral and Brain Sciences*, *17*(03), 449–472. http://doi.org/10.1017/S0140525X00035391

Eichenbaum, H. B., Yonelinas, A. R., & Ranganath, C. (2007). The medial temporal lobe and recognition memory. *Annual Review of Neuroscience*, (30), 123–152. Retrieved from http://www.ncbi.nlm.nih.gov/pmc/articles/pmc2064941/

Ennaceur, A., & Delacour, J. (1988). A new one-trial test for neurobiological studies of memory in rats. 1: Behavioral data. *Behavioural Brain Research*, *31*(1), 47–59. http://doi.org/10.1016/0166-4328(88)90157-X

Esclassan, F., Coutureau, E., Di Scala, G., & Marchand, A. R. (2009). Differential contribution of dorsal and ventral hippocampus to trace and delay fear conditioning. *Hippocampus*, *19*(1), 33–44. http://doi.org/10.1002/hipo.20473

Ezzyat, Y., & Davachi, L. (2011). What Constitutes an Episode in Episodic Memory? *Psychological Science*, *22*(2), 243–252. http://doi.org/10.1177/0956797610393742

Fanselow, M. S., & Dong, H.-W. (2010). Are the dorsal and ventral hippocampus

functionally distinct structures? *Neuron*, *65*(1), 7–19. http://doi.org/10.1016/j.neuron.2009.11.031

Feldman, D. E. (2009). Synaptic Mechanisms for Plasticity in Neocortex. *Annual Review of Neuroscience*, *32*(1), 33–55. http://doi.org/10.1146/annurev.neuro.051508.135516

Feng, T., Silva, D., & Foster, D. J. (2015). Dissociation between the Experience-Dependent Development of Hippocampal Theta Sequences and Single-Trial Phase Precession. *Journal of Neuroscience*, *35*(12), 4890–4902. http://doi.org/10.1523/JNEUROSCI.2614-14.2015

Ferbinteanu, J., & Shapiro, M. L. (2003). Prospective and retrospective memory coding in the hippocampus. *Neuron*, *40*(6), 1227–1239. http://doi.org/10.1016/S0896-6273(03)00752-9

Folkerts, S., Rutishauser, U., & Howard, M. W. (2018). Human episodic memory retrieval is accompanied by a neural contiguity effect. *The Journal of Neuroscience*, 2312–17. http://doi.org/10.1523/JNEUROSCI.2312-17.2018

Fortin, N. J., Agster, K. L., & Eichenbaum, H. B. (2002). Critical role of the hippocampus in memory for sequences of events. *Nature Neuroscience*, *5*(5), 458–462. http://doi.org/10.1038/nn834

Fortin, N. J., Wright, S. P., & Eichenbaum, H. B. (2004). Recollection-like memory retrieval in rats is dependent on the hippocampus. *Nature*, *431*(7005), 188–191. http://doi.org/10.1038/nature02853

Foster, D. J., & Wilson, M. A. (2007). Hippocampal theta sequences. *Hippocampus*, *17*(11), 1093–1099. http://doi.org/10.1002/hipo.20345

Foster, J. D., Kitchen, I., Bettler, B., & Chen, Y. (2013). GABAB receptor subtypes differentially modulate synaptic inhibition in the dentate gyrus to enhance granule cell output. *British Journal of Pharmacology*, *168*(8), 1808–19. http://doi.org/10.1111/bph.12073

Gabrieli, J. D. E., Corkin, S., Mickel, S. F., & Growdon, J. H. (1993). Intact acquisition and long-term retention of mirror-tracing skill in Alzheimer's disease and in global amnesia. *Behavioral Neuroscience*, *107*(6), 899–910. http://doi.org/10.1037/0735-7044.107.6.899

Gaugler, J., James, B., Johnson, T., Scholz, K., & Weuve, J. (2016). 2016 Alzheimer's disease facts and figures. *Alzheimer's & Dementia*, *12*(4), 459–509. http://doi.org/10.1016/j.jalz.2016.03.001

Gershman, S. J., Monfils, M. H., Norman, K. A., & Niv, Y. (2017). The computational

nature of memory modification. *ELife*, *6*, 1–41. http://doi.org/10.7554/eLife.23763

Gershman, S. J., & Niv, Y. (2010). Learning latent structure: Carving nature at its joints. *Current Opinion in Neurobiology*, *20*(2), 251–256. http://doi.org/10.1016/j.conb.2010.02.008

Gill, P. R., Mizumori, S. J. Y., & Smith, D. M. (2011). Hippocampal episode fields develop with learning. *Hippocampus*, *21*(11), 1240–1249. http://doi.org/10.1002/hipo.20832

Goodman, T., Trouche, S., Massou, I., Verret, L., Zerwas, M., Roullet, P., & Rampon, C. (2010). Young hippocampal neurons are critical for recent and remote spatial memory in adult mice. *Neuroscience*, *171*(3), 769–78. http://doi.org/10.1016/j.neuroscience.2010.09.047

GoodSmith, D., Chen, X., Wang, C., Kim, S. H., Song, H., Burgalossi, A., … Knierim, J. J. (2017). Spatial Representations of Granule Cells and Mossy Cells of the Dentate Gyrus. *Neuron*, *93*(3), 677–690.e5. http://doi.org/10.1016/j.neuron.2016.12.026

Grienberger, C., Milstein, A. D., Bittner, K. C., Romani, S., & Magee, J. C. (2017). Inhibitory suppression of heterogeneously tuned excitation enhances spatial coding in CA1 place cells. *Nature Neuroscience*, (December 2016). http://doi.org/10.1038/nn.4486

Grieves, R. M., Jenkins, B. W., Harland, B. C., Wood, E. R., & Dudchenko, P. A. (2016). Place field repetition and spatial learning in a multicompartment environment. *Hippocampus*, *26*(1), 118–134. http://doi.org/10.1002/hipo.22496

Grieves, R. M., Wood, E. R., & Dudchenko, P. A. (2016). Place cells on a maze encode routes rather than destinations. *ELife*, *5*, e15986. http://doi.org/10.7554/eLife.15986

Griffiths, D., Dickinson, A., & Clayton, N. (1999). Episodic memory: what can animals remember about their past? *Trends in Cognitive Sciences*, *3*(2), 74–80. http://doi.org/10.1016/S1364-6613(98)01272-8

Haam, J., Zhou, J., Cui, G., & Yakel, J. L. (2018). Septal cholinergic neurons gate hippocampal output to entorhinal cortex via oriens lacunosum moleculare interneurons. *Proceedings of the National Academy of Sciences*, 201712538. http://doi.org/10.1073/pnas.1712538115

Hafting, T., Fyhn, M., Molden, S., Moser, M.-B., & Moser, E. I. (2005). Microstructure of a spatial map in the entorhinal cortex. *Nature*, *436*(7052), 801–6. http://doi.org/10.1038/nature03721

Hamam, B. N., Amaral, D. G., & Alonso, A. a. (2002). Morphological and

electrophysiological characteristics of layer V neurons of the rat lateral entorhinal cortex. *Journal of Comparative Neurology*, *451*(1), 45–61. http://doi.org/10.1002/cne.10335

Hargreaves, E. L., Rao, G., Lee, I., & Knierim, J. J. (2005). Major dissociation between medial and lateral entorhinal input to dorsal hippocampus. *Science (New York, N.Y.)*, *308*(5729), 1792–4. http://doi.org/10.1126/science.1110449

Harvey, C. D., Collman, F., Dombeck, D. A., & Tank, D. W. (2009). Intracellular dynamics of hippocampal place cells during virtual navigation. *Nature*, *461*(7266), 941–946. http://doi.org/10.1038/nature08499

Hasselmo, M. E. (1999). Neuromodulation: acetylcholine and memory consolidation. *Trends in Cognitive Sciences*, *3*(9), 351–359. Retrieved from http://www.ncbi.nlm.nih.gov/pubmed/10461198

Hasselmo, M. E., & Schnell, E. (1994). Laminar selectivity of the cholinergic suppression of synaptic transmission in rat hippocampal region CA1: computational modeling and brain slice physiology. *The Journal of Neuroscience*, *14*(6), 3898–914. Retrieved from http://www.ncbi.nlm.nih.gov/pubmed/8207494

Hasselmo, M. E., Schnell, E., & Barkai, E. (1995). Dynamics of learning and recall at excitatory recurrent synapses and cholinergic modulation in rat hippocampal region CA3. *The Journal of Neuroscience*, *15*(7), 5249–5262. http://doi.org/10.1523/JNEUROSCI.15-07-05249.1995

Hasselmo, M. E., & Stern, C. E. (2006). Mechanisms underlying working memory for novel information. *Trends in Cognitive Sciences*, *10*(11), 487–493. Retrieved from http://www.sciencedirect.com/science/article/pii/S1364661306002427

Hasselmo, M. E., & Stern, C. E. (2014). Theta rhythm and the encoding and retrieval of space and time. *NeuroImage*, *85*, 656–666. http://doi.org/10.1016/j.neuroimage.2013.06.022

Henze, D. A., Wittner, L., & Buzsáki, G. (2002). Single granule cells reliably discharge targets in the hippocampal CA3 network in vivo. *Nature Neuroscience*, *5*(8), 790–795. http://doi.org/10.1038/nn887

Herzog, L. E., Pascual, L. M., Scott, S. J., Mathieson, E. R., Katz, D. B., & Jadhav, S. P. (2019). Interaction of taste and place coding in the hippocampus. *The Journal of Neuroscience*, 2478–18. http://doi.org/10.1523/JNEUROSCI.2478-18.2019

Heys, J. G., & Dombeck, D. A. (2018). Evidence for a subcircuit in medial entorhinal cortex representing elapsed time during immobility. *Nature Neuroscience*, *21*(November), 1. http://doi.org/10.1038/s41593-018-0252-8

Holt, R. R., Reiff, R., & Scheerer, M. (1961). Memory and Hypnotic Age Regression. Developmental aspects of cognitive function explored through hypnosis. *The Journal of Nervous and Mental Disease*, *132*(6), 545–547. http://doi.org/10.1097/00005053-196106000-00014

Holtmaat, A. J. G. D., Trachtenberg, J. T., Wilbrecht, L., Shepherd, G. M., Zhang, X., Knott, G. W., & Svoboda, K. (2005). Transient and persistent dendritic spines in the neocortex in vivo. *Neuron*, *45*(2), 279–91. http://doi.org/10.1016/j.neuron.2005.01.003

Hopfield, J. J. (1995). Pattern recognition computation using action potential timing for stimulus representation. *Nature*, *376*(6535), 33–36. http://doi.org/10.1038/376033a0

Howard, M. W., & Eichenbaum, H. B. (2013). The Hippocampus, Time, and Memory Across Scales. *Journal of Experimental Psychology. General*, *1058937*, 1–20. http://doi.org/10.1037/a0033621

Howard, M. W., Fotedar, M. S., Datey, A. V, & Hasselmo, M. E. (2005). The Temporal Context Model in Spatial Navigation and Relational Learning: Toward a Common Explanation of Medial Temporal Lobe Function Across Domains. *Psychological Review*, *112*(1), 75–116. http://doi.org/10.1037/0033-295X.112.1.75

Howard, M. W., Macdonald, C. J., Tiganj, Z., Shankar, K. H., Du, Q., Hasselmo, M. E., & Eichenbaum, H. B. (2014). A Unified Mathematical Framework for Coding Time, Space, and Sequences in the Hippocampal Region. *Journal of Neuroscience*, *34*(13), 4692–4707. http://doi.org/10.1523/JNEUROSCI.5808-12.2014

Howard, M. W., Youker, T. E., & Venkatadass, V. S. (2008). The persistence of memory: contiguity effects across hundreds of seconds. *Psychonomic Bulletin & Review*, *15*(1), 58–63. Retrieved from http://www.ncbi.nlm.nih.gov/pubmed/18605480

Hsiao, S., & Isaacson, R. L. (1971). Learning of food and water positions by hippocampus damaged rats. *Physiology and Behavior*, *6*(1), 81–83. http://doi.org/10.1016/0031-9384(71)90020-5

Hsieh, L. T., Gruber, M. J., Jenkins, L. J., & Ranganath, C. (2014). Hippocampal Activity Patterns Carry Information about Objects in Temporal Context. *Neuron*, *81*(5), 1165–1178. http://doi.org/10.1016/j.neuron.2014.01.015

Hunsaker, M. R., & Kesner, R. P. (2008). Dissociations across the dorsal–ventral axis of CA3 and CA1 for encoding and retrieval of contextual and auditory-cued fear. *Neurobiology of Learning and Memory*, *89*(1), 61–69. http://doi.org/10.1016/j.nlm.2007.08.016

Huth, A. G., Nishimoto, S., Vu, A. T., & Gallant, J. L. (2012). A continuous semantic

space describes the representation of thousands of object and action categories across the human brain. *Neuron*, *76*(6), 1210–24. http://doi.org/10.1016/j.neuron.2012.10.014

Igarashi, K. M., Lu, L., Colgin, L. L., Moser, M.-B., & Moser, E. I. (2014). Coordination of entorhinal-hippocampal ensemble activity during associative learning. *Nature*. http://doi.org/10.1038/nature13162

Jenkins, L. J., & Ranganath, C. (2016). Distinct neural mechanisms for remembering when an event occurred. *Hippocampus*, *26*(5), 554–559. http://doi.org/10.1002/hipo.22571

Jimenez, J. C., Su, K., Goldberg, A. R., Luna, V. M., Biane, J. S., Ordek, G., … Kheirbek, M. A. (2018). Anxiety Cells in a Hippocampal-Hypothalamic Circuit. *Neuron*, *0*(0), 1–14. http://doi.org/10.1016/j.neuron.2018.01.016

Jones, M. W., & Wilson, M. A. (2005). Theta rhythms coordinate hippocampal-prefrontal interactions in a spatial memory task. *PLoS Biology*, *3*(12), 1–13. http://doi.org/10.1371/journal.pbio.0030402

Jung, M., Wiener, S., & McNaughton, B. L. (1994). Comparison of spatial firing characteristics of units in dorsal and ventral hippocampus of the rat. *The Journal of Neuroscience*, *14*(12), 7347–7356. http://doi.org/10.1523/JNEUROSCI.14-12-07347.1994

Kahana, M. J. (1996). Associative retrieval processes in free recall. *Memory & Cognition*, *24*(1), 103–109. http://doi.org/10.3758/BF03197276

Kahle, J. S., & Cotman, C. W. (1989). Carbachol depresses synaptic responses in the medial but not the lateral perforant path. *Brain Research*, *482*(1), 159–163. http://doi.org/10.1016/0006-8993(89)90554-4

Keene, C. S., Bladon, J., McKenzie, S., Liu, C. D., O'Keefe, J., & Eichenbaum, H. B. (2016). Complementary Functional Organization of Neuronal Activity Patterns in the Perirhinal, Lateral Entorhinal, and Medial Entorhinal Cortices. *The Journal of Neuroscience*, *36*(13), 3660–3675. http://doi.org/10.1523/JNEUROSCI.4368-15.2016

Keinath, A. T., Julian, J. B., Epstein, R. A., & Muzzio, I. A. (2017). Environmental Geometry Aligns the Hippocampal Map during Spatial Reorientation. *Current Biology*, *27*(3), 309–317. http://doi.org/10.1016/j.cub.2016.11.046

Kempermann, G., Jessberger, S., Steiner, B., & Kronenberg, G. (2004). Milestones of neuronal development in the adult hippocampus. *Trends in Neurosciences*, *27*(8), 447–52. http://doi.org/10.1016/j.tins.2004.05.013

Kentros, C. (1998). Abolition of Long-Term Stability of New Hippocampal Place Cell Maps by NMDA Receptor Blockade. *Science*, *280*(5372), 2121–2126. http://doi.org/10.1126/science.280.5372.2121

Kerr, K. M., Agster, K. L., Furtak, S. C., & Burwell, R. D. (2007). Functional neuroanatomy of the parahippocampal region: the lateral and medial entorhinal areas. *Hippocampus*, *17*(9), 697–708. http://doi.org/10.1002/hipo.20315

Kesner, R. P., Crutcher, K., & Beers, D. R. (1988). Serial position curves for item (spatial location) information: role of the dorsal hippocampal formation and medial septum. *Brain Research*, *454*(1–2), 219–226. http://doi.org/10.1016/0006-8993(88)90821-9

Kesner, R. P., Hunsaker, M. R., & Gilbert, P. E. (2005). The role of CA1 in the acquisition of an object-trace-odor paired associate task. *Behavioral Neuroscience*, *119*(3), 781–786. http://doi.org/10.1037/0735-7044.119.3.781

Kheirbek, M. a, Drew, L. J., Burghardt, N. S., Costantini, D. O., Tannenholz, L., Ahmari, S. E., … Hen, R. (2013). Differential control of learning and anxiety along the dorsoventral axis of the dentate gyrus. *Neuron*, *77*(5), 955–68. http://doi.org/10.1016/j.neuron.2012.12.038

Kimble, D. P., & Kimble, R. J. (1965). Hippocampectomy and response perseveration in the rat. *Journal of Comparative and Physiological Psychology*, *60*(3), 474–476. http://doi.org/10.1037/h0022550

Kinsky, N. R., Sullivan, D. W., Mau, W., Hasselmo, M. E., & Eichenbaum, H. B. (2018). Hippocampal Place Fields Maintain a Coherent and Flexible Map across Long Timescales. *Current Biology*, *28*(22), 3578–3588.e6. http://doi.org/10.1016/J.CUB.2018.09.037

Kitamura, T., Macdonald, C. J., & Tonegawa, S. (2015). Entorhinal – hippocampal neuronal circuits bridge temporally discontiguous events.

Kitamura, T., Ogawa, S. K., Roy, D. S., Okuyama, T., Morrissey, M. D., Smith, L. M., … Tonegawa, S. (2017). Engrams and circuits crucial for systems consolidation of a memory. *Science*, *356*(6333), 73–78. http://doi.org/10.1126/science.aam6808

Kitamura, T., Saitoh, Y., Takashima, N., Murayama, A., Niibori, Y., Ageta, H., … Inokuchi, K. (2009). Adult neurogenesis modulates the hippocampus-dependent period of associative fear memory. *Cell*, *139*(4), 814–27. http://doi.org/10.1016/j.cell.2009.10.020

Kjelstrup, K. B., Solstad, T., Brun, V. H., Hafting, T., Leutgeb, S., Witter, M. P., … Moser, M.-B. (2008). Finite Scale of Spatial Representation in the Hippocampus. *Science*, *321*(5885), 140–143. http://doi.org/10.1126/science.1157086

Knierim, J. J. (2002). Dynamic Interactions between Local Surface Cues, Distal Landmarks, and Intrinsic Circuitry in Hippocampal Place Cells. *The Journal of Neuroscience*, *22*(14), 6254–6264. http://doi.org/10.1523/JNEUROSCI.22-14-06254.2002

Knierim, J. J., McNaughton, B. L., & Poe, G. R. (2000). Three-dimensional spatial selectivity of hippocampal neurons during space flight. *Nature Neuroscience*, *3*(3), 209–210. http://doi.org/10.1038/72910

Knierim, J. J., Neunuebel, J. P., & Deshmukh, S. S. (2013). Functional correlates of the lateral and medial entorhinal cortex: objects, path integration and local-global reference frames. *Philosophical Transactions of the Royal Society B: Biological Sciences*, *369*(1635), 20130369–20130369. http://doi.org/10.1098/rstb.2013.0369

Kobayashi, T., Nishijo, H., Fukuda, M., Bures, J., & Ono, T. (1997). Task-dependent representations in rat hippocampal place neurons. *Journal of Neurophysiology*, *78*(2), 597–613. Retrieved from http://jn.physiology.org/content/78/2/597.short

Komorowski, R. W., Garcia, C. G., Wilson, A., Hattori, S., Howard, M. W., & Eichenbaum, H. B. (2013). Ventral Hippocampal Neurons Are Shaped by Experience to Represent Behaviorally Relevant Contexts. *The Journal of Neuroscience*, *33*(18), 8079–8087. http://doi.org/10.1523/JNEUROSCI.5458-12.2013

Komorowski, R. W., Manns, J. R., & Eichenbaum, H. B. (2009). Robust conjunctive item-place coding by hippocampal neurons parallels learning what happens where. *The Journal of Neuroscience*, *29*(31), 9918–29. http://doi.org/10.1523/JNEUROSCI.1378-09.2009

Konkel, A., Warren, david E., Duff, M. C., Tranel, D., & Cohen, N. J. (2008). Hippocampal Amnesia Impairs All Manner of Relational Memory. *Frontiers in Human Neuroscience*, *2*(October). http://doi.org/10.3389/neuro.09.015.2008

Kosaki, Y., & Watanabe, S. (2012). Dissociable roles of the medial prefrontal cortex, the anterior cingulate cortex, and the hippocampus in behavioural flexibility revealed by serial reversal of three-choice discrimination in rats. *Behavioural Brain Research*, *227*(1), 81–90. http://doi.org/10.1016/j.bbr.2011.10.039

Kraus, B. J., Brandon, M. P., Robinson, R. J., Connerney, M. A., Hasselmo, M. E., & Eichenbaum, H. B. (2015). During Running in Place, Grid Cells Integrate Elapsed Time and Distance Run. *Neuron*, *88*(3), 578–589. http://doi.org/10.1016/j.neuron.2015.09.031

Kraus, B. J., Robinson, R. J., White, J. A., Eichenbaum, H. B., & Hasselmo, M. E. (2013). Hippocampal “Time Cells”: Time versus Path Integration. *Neuron*, *78*(6),

1090–1101. http://doi.org/10.1016/j.neuron.2013.04.015

Kriegeskorte, N. (2008). Representational similarity analysis – connecting the branches of systems neuroscience. *Frontiers in Systems Neuroscience*, *2*(November), 1–28. http://doi.org/10.3389/neuro.06.004.2008

Kurczek, J., Brown-Schmidt, S., & Duff, M. (2013). Hippocampal contributions to language: Evidence of referential processing deficits in amnesia. *Journal of Experimental Psychology: General*, *142*(4), 1346–1354. http://doi.org/10.1037/a0034026

Kyd, R. J., & Bilkey, D. K. (2005). Hippocampal Place Cells Show Increased Sensitivity to Changes in the Local Environment Following Prefrontal Cortex Lesions. *Cerebral Cortex*, *15*(6), 720–731. http://doi.org/10.1093/cercor/bhh173

LaRocque, K. F., Smith, M. E., Carr, V. A., Witthoft, N., Grill-Spector, K., & Wagner, A. D. (2013). Global similarity and pattern separation in the human medial temporal lobe predict subsequent memory. *Journal of Neuroscience*, *33*(13), 5466–5474. http://doi.org/10.1523/JNEUROSCI.4293-12.2013

Lashley, K. S. (1929). *Brain mechanisms and intelligence: A quantitative study of injuries to the brain.* Chicago: University of Chicago Press. http://doi.org/10.1037/10017-000

Lee, I., & Park, S.-B. (2013). Perirhinal cortical inactivation impairs object-in-place memory and disrupts task-dependent firing in hippocampal CA1, but not in CA3. *Frontiers in Neural Circuits*, *7*(August), 1–10. http://doi.org/10.3389/fncir.2013.00134

Leutgeb, J. K., Leutgeb, S., Moser, M.-B., & Moser, E. I. (2007). Pattern Separation in the Dentate Gyrus and CA3 of the Hippocampus. *Science*, *315*(5814), 961–966. http://doi.org/10.1126/science.1135801

Leutgeb, J. K., Leutgeb, S., Treves, A., Meyer, R., Barnes, C. A., McNaughton, B. L., … Moser, E. I. (2005). Progressive transformation of hippocampal neuronal representations in “morphed” environments. *Neuron*, *48*(2), 345–348. http://doi.org/10.1016/j.neuron.2005.09.007

Leutgeb, S. (2004). Distinct Ensemble Codes in Hippocampal Areas CA3 and CA1. *Science*, *305*(5688), 1295–1298. http://doi.org/10.1126/science.1100265

Leutgeb, S., & Leutgeb, J. K. (2007). Pattern separation, pattern completion, and new neuronal codes within a continuous CA3 map. *Learning & Memory*, *14*(11), 745–757. http://doi.org/10.1101/lm.703907

Leutgeb, S., Leutgeb, J. K., Moser, M.-B., & Moser, E. I. (2005). Place cells, spatial maps and the population code for memory. *Current Opinion in Neurobiology*, *15*(6), 738–46. http://doi.org/10.1016/j.conb.2005.10.002

Leutgeb, S., & Mizumori, S. J. Y. (1999). Excitotoxic Septal Lesions Result in Spatial Memory Deficits and Altered Flexibility of Hippocampal Single-Unit Representations. *The Journal of Neuroscience*, *19*(15), 6661–6672. http://doi.org/10.1523/JNEUROSCI.19-15-06661.1999

Liang, F., Paulo, R., Molina, G., Clyde, M. A., & Berger, J. O. (2008). Mixtures of g priors for Bayesian variable selection. *Journal of the American Statistical Association*, *103*(481), 410–423. http://doi.org/10.1198/016214507000001337

Lipton, P. A., White, J. A., & Eichenbaum, H. B. (2007). Disambiguation of overlapping experiences by neurons in the medial entorhinal cortex. *The Journal of Neuroscience*, *27*(21), 5787–95. http://doi.org/10.1523/JNEUROSCI.1063-07.2007

Liu, X., Ramirez, S., Pang, P. T., Puryear, C. B., Govindarajan, A., Deisseroth, K., & Tonegawa, S. (2012). Optogenetic stimulation of a hippocampal engram activates fear memory recall. *Nature*, *484*(7394), 381–5. http://doi.org/10.1038/nature11028

Liu, Y., Tiganj, Z., Hasselmo, M. E., & Howard, M. W. (2019). A neural microcircuit model for a scalable scale-invariant representation of time. *Hippocampus*, *29*(3), 260–274. http://doi.org/10.1002/hipo.22994

Lovett-Barron, M., Turi, G. F., Kaifosh, P., Lee, P. H., Bolze, F., Sun, X.-H., … Losonczy, A. (2012). Regulation of neuronal input transformations by tunable dendritic inhibition. *Nature Neuroscience*, *15*(3), 423–30, S1-3. http://doi.org/10.1038/nn.3024

Lu, L., Leutgeb, J. K., Tsao, A., Henriksen, E. J., Leutgeb, S., Barnes, C. A., … Moser, E. I. (2013). Impaired hippocampal rate coding after lesions of the lateral entorhinal cortex. *Nature Neuroscience*, *16*(July), 1085–93. http://doi.org/10.1038/nn.3462

Lu, X., & Bilkey, D. K. (2010). The velocity-related firing property of hippocampal place cells is dependent on self-movement. *Hippocampus*, *20*(5), 573–583. http://doi.org/10.1002/hipo.20666

Macdonald, C. J., Carrow, S., Place, R., & Eichenbaum, H. B. (2013). Distinct Hippocampal Time Cell Sequences Represent Odor Memories in Immobilized Rats. *Journal of Neuroscience*, *33*(36), 14607–14616. http://doi.org/10.1523/JNEUROSCI.1537-13.2013

Macdonald, C. J., Lepage, K. Q., Eden, U., & Eichenbaum, H. B. (2011). Hippocampal "time cells" bridge the gap in memory for discontiguous events. *Neuron*, *71*(4),

737–749. http://doi.org/10.1016/j.neuron.2011.07.012.

Mack, M. L., Love, B. C., & Preston, A. R. (2016). Dynamic updating of hippocampal object representations reflects new conceptual knowledge. *Proceedings of the National Academy of Sciences*, *113*(46), 13203–13208. http://doi.org/10.1073/pnas.1614048113

Mankin, E. A., Diehl, G. W., Sparks, F. T., Leutgeb, S., & Leutgeb, J. K. (2015). Hippocampal CA2 Activity Patterns Change over Time to a Larger Extent than between Spatial Contexts. *Neuron*, *85*(1), 190–201. http://doi.org/10.1016/j.neuron.2014.12.001

Mankin, E. A., Sparks, F. T., Slayyeh, B., Sutherland, R. J., Leutgeb, S., & Leutgeb, J. K. (2012). Neuronal code for extended time in the hippocampus. *Proceedings of the National Academy of Sciences*, *109*(47), 19462–19467. http://doi.org/10.1073/pnas.1214107109

Manning, J. R., Polyn, S. M., Baltuch, G. H., Litt, B., & Kahana, M. J. (2011). Oscillatory patterns in temporal lobe reveal context reinstatement during memory search. *Proceedings of the National Academy of Sciences*, *108*(31), 12893–12897. http://doi.org/10.1073/pnas.1015174108

Manns, J. R., Howard, M. W., & Eichenbaum, H. B. (2007). Gradual changes in hippocampal activity support remembering the order of events. *Neuron*, *56*(3), 530–40. http://doi.org/10.1016/j.neuron.2007.08.017

Markus, E. J., Barnes, C. A., McNaughton, B. L., Gladden, V. L., & Skaggs, W. E. (1994). Spatial information content and reliability of hippocampal CA1 neurons: Effects of visual input. *Hippocampus*, *4*(4), 410–421. http://doi.org/10.1002/hipo.450040404

Markus, E. J., Qin, Y. L., Leonard, B., Skaggs, W. E., McNaughton, B. L., & Barnes, C. A. (1995). Interactions between location and task affect the spatial and directional firing of hippocampal neurons. *The Journal of Neuroscience*, *15*(11), 7079–94. Retrieved from http://www.ncbi.nlm.nih.gov/pubmed/7472463

Masurkar, A. V, Srinivas, K. V, Brann, D. H., Warren, R., Lowes, D. C., & Siegelbaum, S. A. (2017). Medial and Lateral Entorhinal Cortex Differentially Excite Deep versus Superficial CA1 Pyramidal Neurons. *Cell Reports*, *18*(1), 148–160. http://doi.org/10.1016/j.celrep.2016.12.012

Mau, W., Sullivan, D. W., Kinsky, N. R., Hasselmo, M. E., Howard, M. W., Correspondence, H. E., & Eichenbaum, H. B. (2018). The Same Hippocampal CA1 Population Simultaneously Codes Temporal Information over Multiple Timescales. *Current Biology*, 1–10. http://doi.org/10.1016/j.cub.2018.03.051

McGaugh, J. L. (1999). The perseveration-consolidation hypothesis: Mueller and Pilzecker, 1900. *Brain Research Bulletin*, *50*(5–6), 445–446. http://doi.org/10.1016/S0361-9230(99)00126-4

McKenzie, S., Frank, A. J., Kinsky, N. R., Porter, B., Rivière, P. D., & Eichenbaum, H. B. (2014). Hippocampal representation of related and opposing memories develop within distinct, hierarchically organized neural schemas. *Neuron*, *83*(1), 202–215. http://doi.org/10.1016/j.neuron.2014.05.019

McNaughton, B. L., Barnes, C. A., Gerrard, J. L., Gothard, K., Jung, M. W., Knierim, J. J., … Weaver, K. L. (1996). Deciphering the hippocampal polyglot: the hippocampus as a path integration system. *The Journal of Experimental Biology*, *199*(Pt 1), 173–85. Retrieved from http://www.ncbi.nlm.nih.gov/pubmed/8576689

McNaughton, B. L., Barnes, C. A., & O'Keefe, J. (1984). The contributions of position, direction, and velocity to single unit activity in the hippocampus of freely-moving rats. *Experimental Brain Research*, *54*(1), 41–49. http://doi.org/10.1007/BF00235832

Miller, V. M., & Best, P. J. (1980). Spatial correlates of hippocampal unit activity are altered by lesions of the fornix and entorhinal cortex. *Brain Research*, *194*(2), 311–323. http://doi.org/10.1016/0006-8993(80)91214-7

Mishkin, M. (1978). Memory in monkeys severely impaired by combined but not by separate removal of amygdala and hippocampus. *Nature*. http://doi.org/10.1038/273297a0

Mizuseki, K., Sirota, A., Pastalkova, E., & Buzsáki, G. (2009). Theta oscillations provide temporal windows for local circuit computation in the entorhinal-hippocampal loop. *Neuron*, *64*(2), 267–80. http://doi.org/10.1016/j.neuron.2009.08.037

Monaco, J. D., Rao, G., Roth, E. D., & Knierim, J. J. (2014). Attentive scanning behavior drives one-trial potentiation of hippocampal place fields. *Nature Neuroscience*, *17*(5), 725–31. http://doi.org/10.1038/nn.3687

Morgan, J. I., & Curran, T. (1989). Stimulus-transcription coupling in neurons: role of cellular immediate-early genes. *Trends in Neurosciences*, *12*(11), 459–462. http://doi.org/10.1016/0166-2236(89)90096-9

Morris, R. G., Garrud, P., Rawlins, J. N., & O'Keefe, J. (1982, June 24). Place navigation impaired in rats with hippocampal lesions. *Nature*. Retrieved from http://www.ncbi.nlm.nih.gov/pubmed/7088155

Morrissey, M. D., & Takehara-Nishiuchi, K. (2014). Diversity of mnemonic function within the entorhinal cortex: A meta-analysis of rodent behavioral studies.

Neurobiology of Learning and Memory, *115*(August), 95–107. http://doi.org/10.1016/j.nlm.2014.08.006

Moser, E. I., Roudi, Y., Witter, M. P., Kentros, C., Bonhoeffer, T., & Moser, M.-B. (2014). Grid cells and cortical representation. *Nature Reviews Neuroscience*, 1–16. http://doi.org/10.1038/nrn3766

Muller, R. U., & Kubie, J. L. (1987). The effects of changes in the environment on the spatial firing of hippocampal complex-spike cells. *Journal of Neuroscience*, *7*(7), 1951–1968.

Murdock, B. B. J. (1962). The serial position effect of free recall. *Journal of Experimental Psychology*, *64*(5), 482–488. http://doi.org/10.1037/h0045106

Murray, E. a, & Mishkin, M. (1998). Object recognition and location memory in monkeys with excitotoxic lesions of the amygdala and hippocampus. *The Journal of Neuroscience*, *18*(16), 6568–82. Retrieved from http://www.ncbi.nlm.nih.gov/pubmed/9698344

Nakashiba, T., Young, J. Z., McHugh, T. J., Buhl, D. L., & Tonegawa, S. (2008). Transgenic Inhibition of Synaptic Transmission Reveals Role of CA3 Output in Hippocampal Learning. *Science*, *319*(5867), 1260–1264. http://doi.org/10.1126/science.1151120

Neunuebel, J. P., & Knierim, J. J. (2014). CA3 retrieves coherent representations from degraded input: direct evidence for CA3 pattern completion and dentate gyrus pattern separation. *Neuron*, *81*(2), 416–27. http://doi.org/10.1016/j.neuron.2013.11.017

Neunuebel, J. P., Yoganarasimha, D., Rao, G., & Knierim, J. J. (2013). Conflicts between local and global spatial frameworks dissociate neural representations of the lateral and medial entorhinal cortex. *The Journal of Neuroscience*, *33*(22), 9246–58. http://doi.org/10.1523/JNEUROSCI.0946-13.2013

Neves, G., Cooke, S. F., & Bliss, T. V. P. (2008). Synaptic plasticity, memory and the hippocampus: a neural network approach to causality. *Nature Reviews Neuroscience*, *9*(1), 65–75. http://doi.org/10.1038/nrn2303

Nielson, D. M., Smith, T. A., Sreekumar, V., Dennis, S., & Sederberg, P. B. (2015). Human hippocampus represents space and time during retrieval of real-world memories. *Proceedings of the National Academy of Sciences*, *112*(35), 11078–11083. http://doi.org/10.1073/pnas.1507104112

Norman, G., & Eacott, M. J. (2005). Dissociable effects of lesions to the perirhinal cortex and the postrhinal cortex on memory for context and objects in rats. *Behavioral*

Neuroscience, *119*(2), 557–66. http://doi.org/10.1037/0735-7044.119.2.557

O'Keefe, J. (1976). Place units in the hippocampus of the freely moving rat. *Experimental Neurology*, *51*(1), 78–109. http://doi.org/10.1016/0014-4886(76)90055-8

O'Keefe, J., & Burgess, N. (1996). Geometric determinants of the place fields of hippocampal neurons. *Nature*, *381*(6581), 425–428. http://doi.org/10.1038/381425a0

O'Keefe, J., & Dostrovsky, J. (1971). The hippocampus as a spatial map. Preliminary evidence from unit activity in the freely-moving rat. *Brain Research*, *34*(1), 171–175. http://doi.org/10.1016/0006-8993(71)90358-1

O'Keefe, J., & Nadel, L. (1978). *The Hippocampus as a Cognitive Map*. (Intergovernmental Panel on Climate Change, Ed.)*Oxford University Press* (Vol. 53). Cambridge: Cambridge University Press. Retrieved from http://ebooks.cambridge.org/ref/id/CBO9781107415324A009

O'Keefe, J., & Recce, M. L. (1993). Phase relationship between hippocampal place units and the EEG theta rhythm. *Hippocampus*, *3*(3), 317–330. http://doi.org/10.1002/hipo.450030307

Otto, T., & Eichenbaum, H. B. (1992). Neuronal activity in the hippocampus during delayed non-match to sample performance in rats: Evidence for hippocampal processing in recognition memory. *Hippocampus*, *2*(3), 323–334. http://doi.org/10.1002/hipo.450020310

Parkinson, J. K., Murray, E. A., & Mishkin, M. (1988). A selective mnemonic role for the hippocampus in monkeys: memory for the location of objects. *The Journal of Neuroscience*, *8*(11), 4159–4167.

Pastalkova, E., Itskov, V., Amarasingham, A., & Buzsáki, G. (2008). Internally Generated Cell Assembly Sequences in the Rat Hippocampus. *Science*, *321*(5894), 1322–1327. http://doi.org/10.1126/science.1159775

Patel, J., Fujisawa, S., Berényi, A., Royer, S., & Buzsáki, G. (2012). Traveling Theta Waves along the Entire Septotemporal Axis of the Hippocampus. *Neuron*, *75*(3), 410–417. http://doi.org/10.1016/j.neuron.2012.07.015

Paxinos, G., & Watson, C. (1997). *The rat brain in stereotaxic coordinates (2nd edn)*. *Academic Press* (2nd ed.). San Diego, CA: Academic Press. Retrieved from http://linkinghub.elsevier.com/retrieve/pii/0166223687900178

Paz, R., Gelbard-Sagiv, H., Mukamel, R., Harel, M., Malach, R., & Fried, I. (2010). A

neural substrate in the human hippocampus for linking successive events. *Proceedings of the National Academy of Sciences*, *107*(13), 6046–6051. http://doi.org/10.1073/pnas.0910834107

Penfield, W., & Rasmussen, T. (1950). *The cerebral cortex of man; a clinical study of localization of function. The cerebral cortex of man; a clinical study of localization of function.* Oxford, England: Macmillan.

Piaget, J. (1952). When thinking begins. In *The origins of intelligence in children.* (pp. 25–36).

Place, R., Farovik, A., Brockmann, M., & Eichenbaum, H. B. (2016). Bidirectional prefrontal-hippocampal interactions support context-guided memory. *Nature Neuroscience*, (November 2015), 1–5. http://doi.org/10.1038/nn.4327

Preston, A. R., Shrager, Y., Dudukovic, N. M., & Gabrieli, J. D. E. (2004). Hippocampal contribution to the novel use of relational information in declarative memory. *Hippocampus*, *14*(2), 148–152. http://doi.org/10.1002/hipo.20009

Rangel, L. M., Alexander, A. S., Aimone, J. B., Wiles, J., Gage, F. H., Chiba, A. A., & Quinn, L. K. (2014). Temporally selective contextual encoding in the dentate gyrus of the hippocampus. *Nature Communications*, *5*, 1–9. http://doi.org/10.1038/ncomms4181

Redondo, R. L., Kim, J., Arons, A. L., Ramirez, S., Liu, X., & Tonegawa, S. (2014). Bidirectional switch of the valence associated with a hippocampal contextual memory engram. *Nature*. http://doi.org/10.1038/nature13725

Robinson, N. T. M., Priestley, J. B., Rueckemann, J. W., Garcia, A. D., Smeglin, V. A., Marino, F. A., & Eichenbaum, H. B. (2017). Medial Entorhinal Cortex Selectively Supports Temporal Coding by Hippocampal Neurons. *Neuron*, *94*(3), 677–688.e6. http://doi.org/10.1016/j.neuron.2017.04.003

Rogers, J. L., Hunsaker, M. R., & Kesner, R. P. (2006). Effects of ventral and dorsal CA1 subregional lesions on trace fear conditioning. *Neurobiology of Learning and Memory*, *86*(1), 72–81. http://doi.org/10.1016/j.nlm.2006.01.002

Rosenbaum, R. S., Köhler, S., Schacter, D. L., Moscovitch, M., Westmacott, R., Black, S. E., … Tulving, E. (2005). The case of K.C.: contributions of a memory-impaired person to memory theory. *Neuropsychologia*, *43*(7), 989–1021. http://doi.org/10.1016/j.neuropsychologia.2004.10.007

Rosenbaum, R. S., Priselac, S., Köhler, S., Black, S. E., Gao, F., Nadel, L., & Moscovitch, M. (2000). Remote spatial memory in an amnesic person with extensive bilateral hippocampal lesions, *3*(10).

Ross, R. S., Brown, T. I., & Stern, C. E. (2009). The retrieval of learned sequences engages the hippocampus: Evidence from fMRI. *Hippocampus*, *19*(9), 790–799. http://doi.org/10.1002/hipo.20558

Roth, E. D., Yu, X., Rao, G., & Knierim, J. J. (2012). Functional differences in the backward shifts of ca1 and ca3 place fields in novel and familiar environments. *PLoS ONE*, *7*(4), 1–10. http://doi.org/10.1371/journal.pone.0036035

Royer, S., Sirota, A., Patel, J., & Buzsáki, G. (2010). Distinct representations and theta dynamics in dorsal and ventral hippocampus. *The Journal of Neuroscience*, *30*(5), 1777–87. http://doi.org/10.1523/JNEUROSCI.4681-09.2010

Royer, S., Zemelman, B. V, Losonczy, A., Kim, J., Chance, F., Magee, J. C., & Buzsáki, G. (2012). Control of timing, rate and bursts of hippocampal place cells by dendritic and somatic inhibition. *Nature Neuroscience*, *15*(5), 769–75. http://doi.org/10.1038/nn.3077

Rubin, A., Geva, N., Sheintuch, L., & Ziv, Y. (2015). Hippocampal ensemble dynamics timestamp events in long-term memory. *ELife*, *4*. http://doi.org/10.7554/eLife.12247

Salz, D. M., Tiganj, Z., Khasnabish, S., Kohley, A., Sheehan, D., Howard, M. W., & Eichenbaum, H. B. (2016). Time Cells in Hippocampal Area CA3, *36*(28), 7476–7484. http://doi.org/10.1523/JNEUROSCI.0087-16.2016

Sargolini, F., Fyhn, M., Hafting, T., McNaughton, B. L., Witter, M. P., Moser, M., & Moser, E. I. (2006). Conjunctive Representation of Position, Direction, and Velocity in Entorhinal Cortex. *Science*, *312*(May), 758–762.

Sasaki, T., Leutgeb, S., & Leutgeb, J. K. (2015). Spatial and memory circuits in the medial entorhinal cortex. *Current Opinion in Neurobiology*, *32*, 16–23. http://doi.org/10.1016/j.conb.2014.10.008

Save, E., Cressant, A., Thinus-Blanc, C., & Poucet, B. (1998). Spatial Firing of Hippocampal Place Cells in Blind Rats. *The Journal of Neuroscience*, *18*(5), 1818–1826. http://doi.org/10.1523/JNEUROSCI.18-05-01818.1998

Save, E., Nerad, L., & Poucet, B. (2000). Contribution of Multiple Sensory Information to Place Field Stability in Hippocampal Place Cells, *76*, 64–76.

Schacter, D. L., Eich, J. E., & Tulving, E. (1978). Richard Semon's theory of memory. *Journal of Verbal Learning and Verbal Behavior*, *17*(6), 721–743. http://doi.org/10.1016/S0022-5371(78)90443-7

Schapiro, A. C., Kustner, L. V., & Turk-Browne, N. B. (2012). Shaping of object representations in the human medial temporal lobe based on temporal regularities.

Current Biology, *22*(17), 1622–1627. http://doi.org/10.1016/j.cub.2012.06.056

Schapiro, A. C., Turk-Browne, N. B., Norman, K. A., & Botvinick, M. M. (2016). Statistical learning of temporal community structure in the hippocampus. *Hippocampus*, *26*(1), 3–8. http://doi.org/10.1002/hipo.22523

Scharfman, H. E., & Myers, C. E. (2013). Hilar mossy cells of the dentate gyrus: a historical perspective. *Frontiers in Neural Circuits*, *6*(January), 1–17. http://doi.org/10.3389/fncir.2012.00106

Schmitzer-Torbert, N., Jackson, J., Henze, D., Harris, K., & Redish, A. D. (2005). Quantitative measures of cluster quality for use in extracellular recordings. *Neuroscience*, *131*(1), 1–11. http://doi.org/10.1016/j.neuroscience.2004.09.066

Schomburg, E. W., Fernández-Ruiz, A., Mizuseki, K., Berényi, A., Anastassiou, C. A., Koch, C., & Buzsáki, G. (2014). Theta Phase Segregation of Input-Specific Gamma Patterns in Entorhinal-Hippocampal Networks. *Neuron*, *84*(2), 470–485. http://doi.org/10.1016/j.neuron.2014.08.051

Senzai, Y., & Buzsáki, G. (2017). Physiological Properties and Behavioral Correlates of Hippocampal Granule Cells and Mossy Cells. *Neuron*, *93*(3), 691–704.e5. http://doi.org/10.1016/j.neuron.2016.12.011

Sharp, P. E., & Koester, K. (2008). Lesions of the mammillary body region severely disrupt the cortical head direction, but not place cell signal. *Hippocampus*, *18*(8), 766–784. http://doi.org/10.1002/hipo.20436

Sheffield, M. E. J., Adoff, M. D., & Dombeck, D. A. (2017). Increased Prevalence of Calcium Transients across the Dendritic Arbor during Place Field Formation. *Neuron*, *96*(2), 490–504.e5. http://doi.org/10.1016/j.neuron.2017.09.029

Shen, M., & Greenberg, M. (1990). The Regulation and Function of c-fos and Other Immediate in the Nervous System. *Cell*, *4*, 477–485.

Skaggs, W. E., & McNaughton, B. L. (1998). Spatial firing properties of hippocampal CA1 populations in an environment containing two visually identical regions. *The Journal of Neuroscience*, *18*(20), 8455–66. Retrieved from http://www.ncbi.nlm.nih.gov/pubmed/9763488

Skaggs, W. E., McNaughton, B. L., Wilson, M. A., & Barnes, C. A. (1996). Theta phase precession in hippocampal neuronal populations and the compression of temporal sequences. *Hippocampus*, *6*(2), 149–172. http://doi.org/10.1002/(SICI)1098-1063(1996)6:2<149::AID-HIPO6>3.0.CO;2-K

Sloviter, R. S., & Lømo, T. (2012). Updating the lamellar hypothesis of hippocampal

organization. *Frontiers in Neural Circuits*, *6*(December), 102. http://doi.org/10.3389/fncir.2012.00102

Smith, D. M., & Bulkin, D. A. (2014). The form and function of hippocampal context representations. *Neuroscience & Biobehavioral Reviews*, *40*, 52–61. http://doi.org/10.1016/j.neubiorev.2014.01.005

Smith, D. M., & Mizumori, S. J. Y. (2006). Hippocampal place cells, context, and episodic memory. *Hippocampus*, *16*(9), 716–729. http://doi.org/10.1002/hipo.20208

Sols, I., Dubrow, S., Davachi, L., & Fuentemilla, L. (2017). Event Boundaries Trigger Rapid Memory Reinstatement of the Prior Events to Promote Their Representation in Long-Term Memory, 1–6. http://doi.org/10.1016/j.cub.2017.09.057

Solstad, T., Boccara, C. N., Kropff, E., Moser, M.-B., & Moser, E. I. (2008). Representation of geometric borders in the entorhinal cortex. *Science*, *322*(December), 1865–1868. http://doi.org/10.1126/science.1166466

Solstad, T., Moser, E. I., & Einevoll, G. T. (2006). From Grid Cells to Place Cells : A Mathematical Model. *Hippocampus*, *1031*, 1026–1031. http://doi.org/10.1002/hipo

Squire, L. R. (1992). Memory and the Hippocampuss: A Synthesis From Findings With Rats, Monkeys, and Humans. *Psychological Review*, *99*(2), 195–231. http://doi.org/10.1037/0033-295X.99.2.195

Squire, L. R., & Zola, S. M. (1998). COMMENTARY Episodic Memory, Semantic Memory, and Amnesia. *Neuroanatomy*, *211*(March), 205–211.

Stark, S. M., Reagh, Z. M., Yassa, M. A., & Stark, C. E. L. (2018). What's in a context? Cautions, limitations, and potential paths forward. *Neuroscience Letters*, *680*, 77–87. http://doi.org/10.1016/j.neulet.2017.05.022

Stensola, H., Stensola, T., Solstad, T., Frøland, K., Moser, M.-B., & Moser, E. I. (2012). The entorhinal grid map is discretized. *Nature*, *492*(7427), 72–8. http://doi.org/10.1038/nature11649

Stern, C. E., Corkin, S., González, R. G., Guimaraes, a R., Baker, J. R., Jennings, P. J., … Rosen, B. R. (1996). The hippocampal formation participates in novel picture encoding: evidence from functional magnetic resonance imaging. *Proceedings of the National Academy of Sciences*, *93*(16), 8660–5. Retrieved from http://www.pubmedcentral.nih.gov/articlerender.fcgi?artid=38729&tool=pmcentrez&rendertype=abstract

Strange, B. a., Witter, M. P., Lein, E. S., & Moser, E. I. (2014). Functional organization of the hippocampal longitudinal axis. *Nature Reviews Neuroscience*, *15*(10), 655–

669. http://doi.org/10.1038/nrn3785

Suzuki, W. A., Miller, E. K., & Desimone, R. (1997). Object and place memory in the macaque entorhinal cortex. *Journal of Neurophysiology*, *78*(2), 1062–1081.

Suzuki, W. A., Zola-Morgan, S., Squire, L. R., & Amaral, D. G. (1993). Lesions of the perirhinal and parahippocampal cortices in the monkey produce long-lasting memory impairment in the visual and tactual modalities. *The Journal of Neuroscience*, *13*(6), 2430–51. Retrieved from http://www.ncbi.nlm.nih.gov/pubmed/8501516

Swallow, K. M., Barch, D. M., Head, D., Maley, C. J., Holder, D., & Zacks, J. M. (2011). Changes in Events Alter How People Remember Recent Information. *Journal of Cognitive Neuroscience*, *23*(5), 1052–1064. http://doi.org/10.1162/jocn.2010.21524

Tanninen, S. E., Morrissey, M. D., & Takehara-Nishiuchi, K. (2013). Unilateral lateral entorhinal inactivation impairs memory expression in trace eyeblink conditioning. *PloS One*, *8*(12), e84543. http://doi.org/10.1371/journal.pone.0084543

Teles-Grilo Ruivo, L. M., & Mellor, J. R. (2013). Cholinergic modulation of hippocampal network function. *Frontiers in Synaptic Neuroscience*, *5*(JUL), 1–15. http://doi.org/10.3389/fnsyn.2013.00002

Terada, S., Sakurai, Y., Nakahara, H., & Fujisawa, S. (2017). Temporal and Rate Coding for Discrete Event Sequences in the Hippocampus Article Temporal and Rate Coding for Discrete Event Sequences in the Hippocampus. *Neuron*, 1–15. http://doi.org/10.1016/j.neuron.2017.05.024

Terrace, H. S., & Metcalfe, J. (2005). *The Missing Link in Cognition Origins of self-reflective consciousness*. *Episodic Memory and Autonoesis: Uniquely Human?* (Vol. 21). Oxford University Press. http://doi.org/10.1093/acprof:oso/9780195161564.001.0001

Teyler, T. J., & DiScenna, P. (1986). The hippocampal memory indexing theory. *Behavioral Neuroscience*. US: American Psychological Association. http://doi.org/10.1037/0735-7044.100.2.147

Thompson, L. T., & Best, P. J. (1990). Long-term stability of the place-field activity of single units recorded from the dorsal hippocampus of freely behaving rats. *Brain Research*, *509*(2), 299–308. http://doi.org/10.1016/0006-8993(90)90555-P

Todorova, R., & Zugaro, M. (2018). Hippocampal ripples as a mode of communication with cortical and subcortical areas. *Hippocampus*, (May), 1–11. http://doi.org/10.1002/hipo.22997

Tsao, A., Moser, M.-B., & Moser, E. I. (2013). Traces of experience in the lateral entorhinal cortex. *Current Biology : CB*, *23*(5), 399–405. http://doi.org/10.1016/j.cub.2013.01.036

Tsao, A., Sugar, J., Lu, L., Wang, C., Knierim, J. J., Moser, M.-B., & Moser, E. I. (2018). Integrating time from experience in the lateral entorhinal cortex. *Nature*. http://doi.org/10.1038/s41586-018-0459-6

Tulving, E. (1972). 10 Episodic and Semantic Memory. *Organization of Memory*. Retrieved from http://web.media.mit.edu/~jorkin/generals/papers/Tulving_memory.pdf

Tulving, E. (1985). How many memory systems are there? American Psychologist, 40(4), 385–398. Retrieved from http://psycnet.apa.org/journals/amp/40/4/385/y memory systems are there? *American Psychologist*, *40*(4), 385–398. Retrieved from http://psycnet.apa.org/journals/amp/40/4/385/

Tulving, E. (2001). Episodic memory and common sense: How far apart? *Philosophical Transactions of the Royal Society B: Biological Sciences*, *356*(1413), 1505–1515. http://doi.org/10.1098/rstb.2001.0937

Tulving, E., & Madigan, S. A. (1970). Memory and Verbal Learning. *Annual Review of Psychology*, *21*(1), 437–484. http://doi.org/10.1146/annurev.ps.21.020170.002253

Tulving, E., & Markowitsch, H. J. (1998). Episodic and declarative memory: role of the hippocampus. *Hippocampus*, *8*(3), 198–204. http://doi.org/10.1002/(sici)1098-1063(1998)8:3%3C198::aid-hipo2%3E3.0.co;2-g

Van Cauter, T., Camon, J., Alvernhe, A., Elduayen, C., Sargolini, F., & Save, E. (2013). Distinct roles of medial and lateral entorhinal cortex in spatial cognition. *Cerebral Cortex (New York, N.Y. : 1991)*, *23*(2), 451–9. http://doi.org/10.1093/cercor/bhs033

Van Cauter, T., Poucet, B., & Save, E. (2008). Unstable CA1 place cell representation in rats with entorhinal cortex lesions. *European Journal of Neuroscience*, *27*(8), 1933–1946. http://doi.org/10.1111/j.1460-9568.2008.06158.x

van Groen, T., Miettinen, P., & Kadish, I. (2003). The entorhinal cortex of the mouse: Organization of the projection to the hippocampal formation. *Hippocampus*, *13*(1), 133–149. http://doi.org/10.1002/hipo.10037

van Strien, N. M., Cappaert, N. L. M., & Witter, M. P. (2009). The anatomy of memory: an interactive overview of the parahippocampal-hippocampal network. *Nature Reviews. Neuroscience*, *10*(4), 272–82. http://doi.org/10.1038/nrn2614

Vann, S. D. (2013). Dismantling the Papez circuit for memory in rats. *ELife*, *2*, e00736.

http://doi.org/10.7554/eLife.00736

Vargha-Khadem, F., Gadian, D., Watkins, K., Connelly, A., Van Paesschen, W., & Mishkin, M. (1997). Differential Effects of Early Hippocampal Pathology on Episodic and Semantic Memory. *Science*, *277*(5324), 376–380. http://doi.org/10.1126/science.277.5324.376

Villette, V., Malvache, A., Tressard, T., Dupuy, N., & Cossart, R. (2015). Internally Recurring Hippocampal Sequences as a Population Template of Spatiotemporal Information. *Neuron*, *88*(2), 357–366. http://doi.org/10.1016/j.neuron.2015.09.052

Villette, V., Poindessous-Jazat, F., Simon, A., Lena, C., Roullot, E., Bellessort, B., … Stephan, A. (2010). Decreased Rhythmic GABAergic Septal Activity and Memory-Associated Oscillations after Hippocampal Amyloid- Pathology in the Rat. *Journal of Neuroscience*, *30*(33), 10991–11003. http://doi.org/10.1523/JNEUROSCI.6284-09.2010

Wagatsuma, A., Okuyama, T., Sun, C., Smith, L. M., Abe, K., & Tonegawa, S. (2017). Locus coeruleus input to hippocampal CA3 drives single-trial learning of a novel context. *Proceedings of the National Academy of Sciences*, 201714082. http://doi.org/10.1073/pnas.1714082115

Wang, C., Chen, X., Lee, H., Deshmukh, S. S., Yoganarasimha, D., Savelli, F., & Knierim, J. J. (2018). Egocentric coding of external items in the lateral entorhinal cortex. *Science*, *362*(6417), 945–949. http://doi.org/10.1126/science.aau4940

Weis, S., Specht, K., Klaver, P., Tendolkar, I., Willmes, K., Ruhlman, J., … Fernandez, G. (2004). Process dissociation between contextual retrieval and item recognition. *Neuroreport*, *15*(18), 2729–2733.

Wiesel, T. N., & Hubel, D. N. (1979). Brain mechanisms of vision. *Scientific American*, *241*(3), 150–162. http://doi.org/10.1038/scientificamerican0979-150

Wills, T. J. (2005). Attractor Dynamics in the Hippocampal Representation of the Local Environment. *Science*, *308*(5723), 873–876. http://doi.org/10.1126/science.1108905

Wiltgen, B. J., Brown, R. a M., Talton, L. E., & Silva, A. J. (2004). New circuits for old memories: the role of the neocortex in consolidation. *Neuron*, *44*(1), 101–8. http://doi.org/10.1016/j.neuron.2004.09.015

Winson, J., & Abzug, C. (1978). Neuronal transmission through hippocampal pathways dependent on behavior. *Journal of Neurophysiology*, *41*(3), 716–732. http://doi.org/10.1152/jn.1978.41.3.716

Witter, M. P. (1993). Organization of the Entorhinal-Hippocampal System: A Review of

Current Anatomical Data. *Hippocampus*, *3*, 33–44. http://doi.org/10.1002/hipo.1993.4500030707

Witter, M. P. (2007). Intrinsic and extrinsic wiring of CA3: Indications for connectional heterogeneity. *Learning & Memory*, *14*(11), 705–713. http://doi.org/10.1101/lm.725207

Witter, M. P., Naber, P. A., Van Haeften, T., Machielsen, W. C. M., Rombouts, S. A. R. B., Barkhof, F., … Lopes Da Silva, F. H. (2000). Cortico-hippocampal communication by way of parallel parahippocampal-subicular pathways. *Hippocampus*, *10*(4), 398–410. http://doi.org/10.1002/1098-1063(2000)10:4<398::AID-HIPO6>3.0.CO;2-K

Wood, E. R., Dudchenko, P. A., Robitsek, R. J., & Eichenbaum, H. B. (2000). Hippocampal neurons encode information about different types of memory episodes occurring in the same location. *Neuron*, *27*(3), 623–633. http://doi.org/10.1016/S0896-6273(00)00071-4

Wyss, J. M., Swanson, L. W., & Cowan, W. M. (1979). A study of subcortical afferents to the hippocampal formation in the rat. *Neuroscience*, *4*(4), 463–476. http://doi.org/10.1016/0306-4522(79)90124-6

Xu, W., & Wilson, D. A. (2012). Odor-evoked activity in the mouse lateral entorhinal cortex. *Neuroscience*, *223*, 12–20. http://doi.org/10.1016/j.neuroscience.2012.07.067

Yonelinas, A. P. (2002). The nature of recollection and familiarity: A review of 30 years of research. *Journal of Memory and Language*, *46*(3), 441–517. http://doi.org/10.1006/jmla.2002.2864

Yonelinas, A. P., Kroll, N. E. A., Dobbins, I., Lazzara, M., & Knight, R. T. (1998). Recollection and familiarity deficits in amnesia: Convergence of remember-know, process dissociation, and receiver operating characteristic data. *Neuropsychology*, *12*(3), 323–339. http://doi.org/10.1037/0894-4105.12.3.323

Young, B. J., Otto, T., Fox, G. D., & Eichenbaum, H. B. (1997). Memory representation within the parahippocampal region. *The Journal of Neuroscience*, *17*(13), 5183–95. Retrieved from http://www.ncbi.nlm.nih.gov/pubmed/9185556

Zacks, J. M., Tversky, B., & Iyer, G. (2001). Perceiving, remembering, and communicating structure in events. *Journal of Experimental Psychology: General*, *130*(1), 29–58. http://doi.org/10.1037/0096-3445.130.1.29

Zaremba, J. D., Diamantopoulou, A., Danielson, N. B., Grosmark, A. D., Kaifosh, P. W., Bowler, J. C., … Losonczy, A. (2017). Impaired hippocampal place cell dynamics in a mouse model of the 22q11.2 deletion. *Nature Neuroscience*, *20*(11), 1612–1623.

http://doi.org/10.1038/nn.4634

Zaromb, F. M., Howard, M. W., Dolan, E. D., Sirotin, Y. B., Tully, M., Wingfield, A., & Kahana, M. J. (2006). Temporal associations and prior-list intrusions in free recall. *Journal of Experimental Psychology: Learning, Memory, and Cognition*, *32*(4), 792–804. http://doi.org/10.1037/0278-7393.32.4.792

Zeithamova, D., Schlichting, M. L., & Preston, A. R. (2012). The hippocampus and inferential reasoning: building memories to navigate future decisions. *Frontiers in Human Neuroscience*, *6*(March), 1–14. http://doi.org/10.3389/fnhum.2012.00070

Zhang, H., Fell, J., & Axmacher, N. (2018). Electrophysiological mechanisms of human memory consolidation. *Nature Communications*, *9*(1), 4103. http://doi.org/10.1038/s41467-018-06553-y

Ziv, Y., Burns, L. D., Cocker, E. D., Hamel, E. O., Ghosh, K. K., Kitch, L. J., … Schnitzer, M. J. (2013). Long-term dynamics of CA1 hippocampal place codes. *Nature Neuroscience*, *16*(3), 264–6. http://doi.org/10.1038/nn.3329

Zola-Morgan, S., Squire, L., Amaral, D., & Suzuki, W. (1989). Lesions of perirhinal and parahippocampal cortex that spare the amygdala and hippocampal formation produce severe memory impairment. *The Journal of Neuroscience*, *9*(12), 4355–4370. http://doi.org/10.1523/JNEUROSCI.09-12-04355.1989

CURRICULUM VITAE

[redacted]

[redacted]

[redacted]